DOCTOR OF PHILOSOPHY

GPR30: a role for a novel estrogen-sensing receptor in hippocampal function?

Alexander, Amy

Award date:
2013

DOCTOR OF PHILOSOPHY

GPR30: a role for a novel estrogen-sensing receptor in hippocampal function?

Amy Alexander

2014

University of Dundee

GPR30: A ROLE FOR A NOVEL ESTROGEN-SENSING RECEPTOR IN HIPPOCAMPAL FUNCTION?

By Amy Alexander

A thesis submitted to the University of Dundee for the Degree of Doctor of Philosophy,

October 2013

CONTENTS

LIST OF TABLES

LIST OF FIGURES

ACKNOWLEDGEMENTS

One cannot get through the PhD experience alone.

Thanks first go to my supervisors, Dr. Andrew Irving and Dr. Jenni Harvey, for their guidance in the development of this project, constant reassurance and for allowing me the opportunities to attend and present my data at national and international conferences. Thank you.

Special thanks go to Pete Moult for efficiently training me in such a short space of time and to Dayne Beccanno-Kelly, for providing such a positive and enjoyable atmosphere in the lab through the bulk of the data gathering phase. To Mary Cooper, thank you for never failing to be there when I sought your counsel, and importantly, for introducing me to Korfball! To Rob and Neal, thank you for providing light-hearted conversation, the occasional dinner, and cups of tea when the PhD blues kicked in. To everyone who has passed through the Irving and Harvey laboratory doors, it has been a pleasure knowing you – even if it was only for a brief period. To the people dear to me scattered across the globe, it is heart-warming to know that your support crossed oceans.

To Ashley Dorning and June Penman, the attempts to express my gratitude in writing have so far been unavailing. I have been so fortunate to have met and befriended you two extraordinary ladies. Having you along-side throughout my PhD was an essential factor in its completion. Thank you.

Finally, to my mother and father, without your infinite encouragement and emotional sustenance; I never would have been able to achieve this. Thank you.

This thesis is dedicated to my mother and father.

DECLARATIONS

Candidate Declaration

I declare that I am the author of this thesis and that results presented herein were performed by me, unless otherwise stated. All references have been consulted by myself and are cited correctly. This work has not been previously accepted for a higher degree.

Amy Alexander

Supervisor Declaration

I hereby confirm that Amy Alexander has fulfilled the conditions of Ordinance 39, University of Dundee and is eligible to submit the following thesis for the degree of Doctor of Philosophy.

Dr. Andrew Irving

ABSTRACT

17β-estradiol (E2), the most potent form of the steroid hormone class, the estrogens, is a known regulator of hippocampal function and is capable of being synthesised within hippocampal neurons. E2 can modulate glutamatergic synaptic transmission and hippocampal synaptic plasticity, as well as enhance hippocampal dependent learning in rodent models. However, not all effects of estradiol are mediated by the two canonical estrogen receptors, ERα and ERβ. Recently, a novel estrogen-sensing G protein coupled receptor (GPR30) was identified, and hippocampal expression of GPR30 indicates a potential role for this receptor in modulating hippocampal function.

Thus, the primary aims of this thesis were to clarify the effects of E2 on glutamatergic synaptic transmission and establish whether activation of GPR30 is involved. Using evoked population EPSP recordings within the dendritic field of hippocampal region CA1, we show that acute application of a physiologically relevant concentration of E2 modulates excitatory synaptic transmission in a bi-directional manner; the most consistent effect however was the induction of a novel form of LTD. Moreover, we show that the GPR30 agonist (G1) mimics the bi-directional effects of E2 on excitatory synaptic transmission. Subsequent characterisation of the E2 and G1 induced LTD revealed that both forms of agonist-induced plasticity are expressed post-synaptically, correlating with findings in hippocampal cultures in which treatment with these agonists resulted in a reduction in the relative density of GluA1-containing AMPA receptors expressed at synapses. In addition, further investigation into the pharmacology of the G1-induced LTD revealed that this effect was not prevented by selective antagonists for GPR30, ERα or ERβ, however could be attenuated by a selective estrogen receptor downregulator and putative ligand for GPR30, ICI 182 780. Furthermore, we establish that in hippocampal neurons, the G1-induced LTD and reduction in surface AMPA receptor expression is mediated via the ERK 1/2 signalling pathway.

In summary, the data presented here suggests that at CA3 to CA1 synapses, E2 and the GPR30 agonist can induce a novel form of LTD in adult hippocampal tissue. Considering the multifaceted role of estrogens in human physiology, pharmaceuticals which modulate this system in a site specific manner (either by influencing estrogen synthesis or targeting estrogen receptors) could be of benefit in hippocampal dependent learning and memory processes in health and disease.

ABBREVIATIONS

AMPA	α-Amino-3-hydroxy-5-methyl-4-isoxazolepropionic acid
AMPAR	AMPA Receptor
ANOVA	Analysis of Variance
$[Ca^{2+}]_i$	intracellular calcium
CA	*cornu ammonis*
CB_1R	Cannabinoid Receptor type 1
CAMKII	Calcium / calmodulin kinase II
cAMP	cyclic Adenosine Monophosphate
cDNA	complementary Deoxyribonucleic Acid
CREB	cAMP response element binding protein
CRHR1	Coritcotropin releasing hormone receptor-1
CNS	Central Nervous System
DG	Dentate gyrus
DHEA	Dehydroepiandrosterone
DIV	Days *in Vitro*
DMSO	Dimethyl Sulfoxide
E1	Estrone
E2	17β-estradiol
E3	Estriol
EAAT	Excitatory Amino Acid Transporter
EC	Entorhinal Cortex
EGFR	Epidermal Growth Factor Receptor
EPSP	Excitatory Post-Synaptic Potential
EPSC	Excitatory Post-Synaptic Current
ER	Estrogen Receptor
ERα	Estrogen receptor alpha
ERβ	Estrogen receptor beta

ERK1/2	Extracellular Receptor Kinase 1/2
fEPSP	field Excitatory Post-Synaptic Potential
GABA	Gamma-Aminobutyric Acid
GPCR	G-Protein Coupled Receptor
GPR30	G-Protein Coupled Receptor 30
GPR55	G-Protein Coupled Receptor 55
GnRH	Gonodotropin Releasing Hormone
GSK-3	Glycogen synthase kinase 3
HA	Human influenza hemagglutinin protein
HBS	HEPES Buffered Saline
HEK-293 Cells	Human Embryonic Kidney 293 Cells
HEPES	Hydroxyethyl piperazineethanesulfonic acid
HFS	High Frequency Stimulation
IEG	immediate early gene
iGluR	ionotropic Glutamate Receptor
IP_3	inositol triphosphate
LFS	Low frequency stimulation
LTD	Long-term depression
LTP	Long-term potentiation
MAP2	Microtubule Associated Protein 2
MAPK	Mitogen Activated Protein Kinase
MEK	Mitogen Activated Protein Kinase Kinase
mER	membrane Estrogen Receptor
mERX	membrane Estrogen Receptor-X
mGluR	metabotropic Glutamate Receptor
mRNA	messenger RNA
NMDA	*N*-Methyl-D-aspartate
NMDAR	NMDA Receptor
P450scc	P450 side-chain cleavage

PFA	Paraformaldehyde
PI3K	phoshoinositide 3-kinase
PKC	Protein Kinase C
PKA	Protein Kinase A
PLC	Phospholipase C
PMRβ	Progestin membrane receptor-β
PP1	Protein Phosphatase 1
PPR	Paired-Pulse Ratio
pp-LFS	paired-pulse low frequency stimulation
PREG	Pregnenolone
PSD	Post-synaptic density
PSD-95	Post-synaptic density-95
RAMP	Receptor activity modifying protein
RNA	Ribonucleic Acid
ROCK	Rho-associated protein kinase
RT-PCR	Reverse Transcriptase Polymerase Chain Reaction
SEM	Standard Error of the Mean
siRNA	short-interfering RNA
SNARE	Soluble *N*-ethylmaleimide-sensitive factor attachment protein receptor
StAR	steroidogenic acute regulatory protein
Sub.	Subiculum
TARP	Transmembrane AMPAR regulator protein
TGN	Trans-Golgi Network
OVX	Ovariectomised
vGluT	vesicular Glutamate Transporter
5-HT1aR	5-hydroxy-tryptophan-1a receptor

Chapter One

Introduction

1.1: The Hippocampus

The hippocampus is part of a group of structures within the limbic system, and is classically known as the structure associated with the formation of new memories and spatial learning. The cellular anatomy of the hippocampus was studied in great detail in the late 1800's by Santiago Ramòn y Cajal. However, the physiological role of this structure only became apparent in the late 1950's, when Scoville and Milner (1957) noted complete loss of new "declarative" (episodic) memory formation from patient H.M. following bilateral removal of the hippocampus, suggesting that the hippocampus is vital for new memory formation. The basic curved structure and organisation of the hippocampus is conserved between all mammals, it is formed by two interlocking sheets of cortex which consist of a single layer of tightly packed pyramidal neurons, 3 – 5 cells deep. The laminar structure of hippocampus makes the hippocampal slice preparation an ideal structure to study synaptic transmission as circuitry and synaptic contacts are largely preserved.

1.1.2: Circuitry of the hippocampus

The hippocampal formation is organised into distinct regions (Figure 1.1 A), *cornu ammonis* (CA) regions 1 – 3, the dentate gyrus (DG), subiculum (Sub.), and entorhinal cortex (EC). The primary input into the hippocampus occurs via the EC and follows a unidirectional flow of neuronal communication. This is often termed the tri-synaptic loop: EC -> DG via the perforant path, DG -> CA3 via mossy fibres and CA3 -> CA1 via schaffer collateral fibres. The main excitatory output from the hippocampus occurs via principal cells of the CA1, via the subiculum.

A single CA1 pyramidal neuron receives about 30,000 excitatory and 1,700 inhibitory synaptic inputs (Megías *et al*., 2001). The main excitatory inputs to CA1 pyramidal neurons arise from axons of CA3 neurons, which synapse on apical dendrites in the stratum radiutum layer. Excitatory inputs to CA1 also occur at the stratum lacunosum-molecular which receives direct inputs from EC and the thalamus. Local inhibition is provided by a host of interconnected GABAergic interneurons (Klausberger and

Somogyi, 2008). Integration of these excitatory and inhibitory signals determines the level of excitatory output.

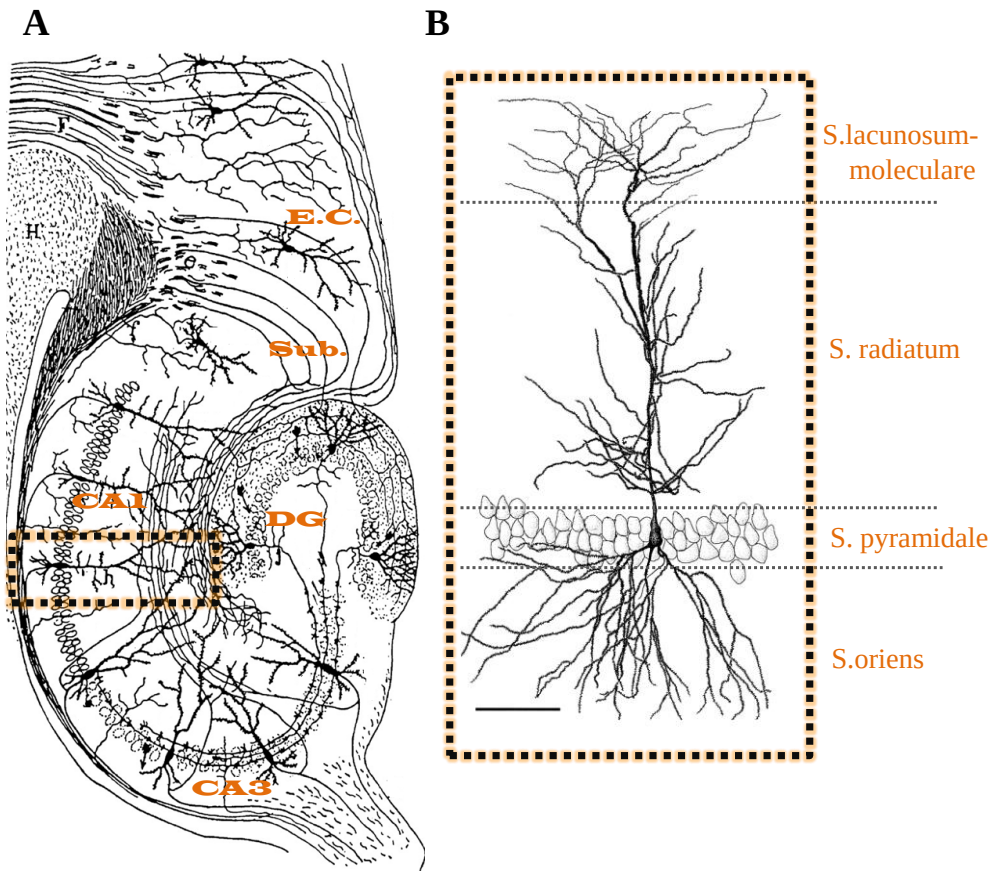

Figure 1.1: Neural circuitry of the rodent hippocampus and structure of a CA1 pyramidal neuron. ***A,*** Drawing by Santiago Ramón y Cajal, illustrating the tri-synaptic circuit and the laminar structure of the rodent hippocampus: E.C, entorhinal cortex; DG, dentate gyrus; CA1 and CA3, area *cornu ammonis* 1 and 3; Sub., subiculum. ***B,*** Drawing of an adult rat CA1 pyramidal neuron adapted from Megías *et al*., 2001; S., stratum; scale bar = 100µm.

A: *Original drawing published in:* Histologie du Système Nerveux de l'Homme et des Vertèbrès (Paris: Maloine, 1909-1911).

1.1.3: Glutamatergic Synaptic Transmission

The amino acid glutamate, is the primary excitatory neurotransmitter in the mammalian central nervous system (CNS). Glutamatergic synaptic transmission occurs primarily within the tripartite synapse (Fig 1.2). Briefly, calcium sensitive protein complexes (SNARE; Südhof and Rothman, 2009) facilitate the release of glutamate from the pre-synaptic terminal in response to a rise in intracellular calcium ($[Ca_{2+}]_i$). Once released within the synaptic cleft, glutamate then may activate ionotropic glutamate receptors (iGluR) and metabotropic glutamate receptors (mGluR) at synaptic or extrasynaptic sites on post-synaptic neurons to mediate post-synaptic responses (depolarisation, local protein synthesis, activation of intracellular signalling cascades etc.), or at pre-synaptic sites to mediate transmitter release. The concentration of glutamate within the synapse is tightly regulated such that after release, glutamate is rapidly removed from the synaptic cleft via excitatory amino acid transporters (EAAT) within glia, where glutamate is converted to glutamine by glutamine synthase. Glutamine is then transported out of the glia cell, and taken up by presynaptic neurons, where it is converted back into glutamate by glutaminase and packaged into vesicles by vesicular glutamate transporters (vGluTs) ready for release (Rousseaux *et al*., 2008).

Thus, modulation of glutamergic neurotransmission can occur at a number of sites within triparte synapse:

- Glutamate release
    - Influenced by the *probability* of vesicle release
    - Influenced the by the *number* of vesicles available for release (the ready releasable pool).
- Glutamate uptake (relative expression of EAAT)
- Glutamate metabolism – the rate at which glutamine/ glutamate cycle occurs.
- Expression levels of post-synaptic glutamate receptors

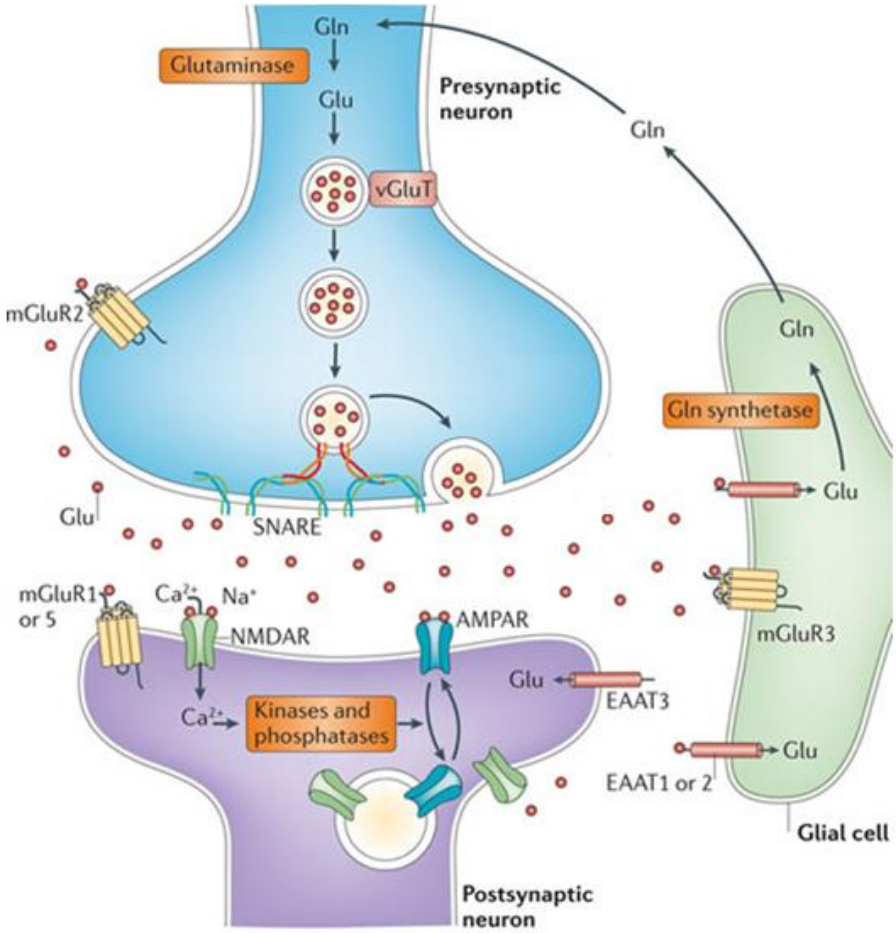

Figure 1.2: The Glutamatergic Synapse. Cartoon depicting glutamatergic synaptic transmission within the tripartite synapse. Glutamate is released from presynaptic terminals into the synaptic cleft and binds to post-synaptic NMDAR, AMPAR and mGluRs to mediate excitatory synaptic responses at the post-synaptic neuron. Glutamate is removed from the synaptic cleft by glia through glutamate transporters (EAAT).

Figure adapted from Popoli et al., (2012)

1.1.4: Ionotropic Glutamate Receptors

There are three classes of iGluR, named after the ligands they preferentially bind to: *N*-methyl-D-aspartate (NMDA), α-amino-3-hydroxy-5-methyl-4-isoxazolepropoinic acid (AMPA) and 2-carboxy-3-carboxymethyl-4-isopropenylpyrrolidine (Kainate). As well as a less-characterized class of δ receptors (delta: "orphan") (Traynelis *et al*., 2010). iGluR are tetrameric ligand gated ion channels, the individual subunits of which share similar architecture and several common features. Briefly, each subunit comprises of an extracellular amino terminal, three transmembrane domains (M1, M3 and M4), an extracellular ligand binding domain (formed from extracellular loops between M1 and M3), a cytoplasm facing re-entrant membrane loop (pore forming; M2) and an intracellular carboxyl terminal (as reviewed in: Dingledine *et al*., 1999; Traynelis *et al*., 2010). The general topology of an iGluR subunit is depicted below in Figure 1.3.

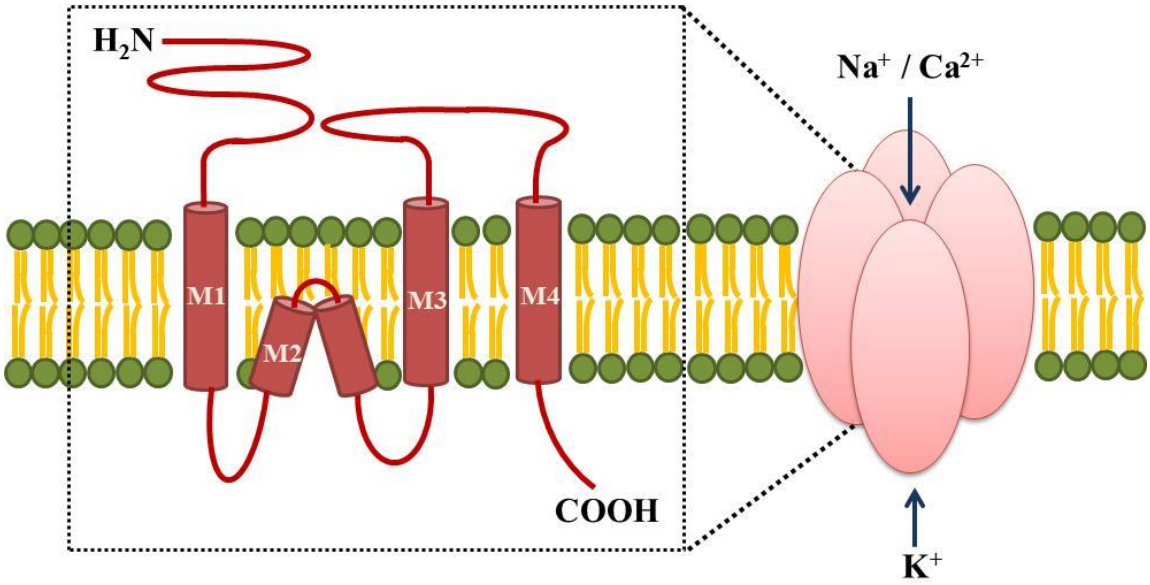

Figure 1.3: Cartoon depicting the general topology of ionotropic glutamate receptors. Ionotropic glutamate receptors are tetrameric ligand gated cation channels. Each subunit comprises of three membrane-spanning domains, a re-entrant pore forming domain and extracellular N-terminus, and an intracellular C-terminus.

1.1.4.1: AMPA Receptors

AMPAR are responsible for the majority of fast glutamatergic synaptic transmission in the mammalian CNS, and can be composed of homomeric or heteromeric combinations of subunits GluA1 – GluA4. In general, AMPAR channels display fast kinetics (fast activation and deactivation coupled with rapid desensitization) such that signalling via these ion channels occurs within milliseconds (Mosbacher *et al*., 1994; Jackson and Nicoll, 2011). AMPAR are permeable to sodium (Na^+), potassium (K^+) and calcium (Ca^{2+}); however calcium permeability is governed by incorporation of the GluA2 subunit (Hollmann *et al*., 1991; Jonas and Burnashev, 1995). The majority of GluA2-subunits are post-transcriptionally edited prior to mRNA splicing. This editing at the QRN site at the tip of the re-entrant pore loop (M2) results in a switching of an uncharged glutamine (Q) to a positively charged arginine (R) which renders GluA2-containing AMPAR impermeable to Ca^{2+} and favours heteromerization (Sommer *et al*., 1991; Greger *et al*., 2002, 2003). GluA2-containig AMPAR are characterised by a linear current-voltage relationship. In contrast, AMPAR lacking the GluA2 subunit (*ie*: homomeric or heteromeric combinations of GluA1, GluA3 or GluA4), which are permeable to Ca^{2+}, are sensitive to voltage-dependant block by intracellular polyamines, and are generally characterised by having an inwardly rectifying current-voltage relationship (as reviewed in: Traynelis *et al*., 2010). At CA3 - CA1 synapses, the majority of fast-glutatmatergic synaptic transmission is governed by activation GluA2/GluA1 heteromers (Na^+ influx; Lu *et al*., 2009), however recent evidence suggests that synaptic GluA2-lacking AMPAR may also contribute to basal synaptic responses (Rozov *et al*., 2012).

Contributing to desensitization characteristics of AMPAR is the capacity for all subunits to undergo alternative splicing. Alternative splicing yields two variants (*flip* and *flop*) and occurs at a region of the extracellular loop adjacent to the last transmembrane domain (M4). Flip variants desensitize more slowly and to a lesser extent than their flop counterparts, which can influence total AMPA current (Sommer *et al*., 1990; Dingledine *et al*., 1999). C-terminal phosphorylation (Boehm and Malinow, 2005; Lee, 2006) and association with auxiliary proteins, such as transmembrane AMPAR regulatory proteins (TARP's; Jackson and Nicoll, 2011) can also influence channel properties. Trafficking of AMPAR to and from excitatory synapses underlies long-term alterations in synaptic

strength (section 1.1.6.3 and for comprehensive reviews see: Malinow and Malenka, 2002; Henley *et al*., 2011).

1.1.4.2.: NMDA Receptors

NMDAR are permeable to Na^+, K^+ and importantly, readily permeable to Ca^{2+}. However, unlike AMPAR, binding of glutamate alone is insufficient for NMDAR channel opening and ion flux, as at resting membrane potential the channel pore is blocked by physiological concentrations of extracellular Mg^{2+} (Mayer *et al*., 1984). Only concurrent glutamate (and glycine / D-serine) binding, coupled with strong membrane depolarization can remove this voltage-dependant block, and permit cation flux. Thus NMDAR have a unique role as molecular coincidence detectors (Cull-Candy and Leszkiewicz, 2004; Traynelis *et al*., 2010; Sanz-Clemente *et al*., 2013). Three families of NMDAR subunits have been identified (GluN1; GluN2A –D and GluN3A and B). Functional NMDAR are composed of two obligatory GluN1 subunits (of which there are eight splice variants and which contain the co-agonist glycine / D-serine binding sites) and two regulatory subunits (GluN2A-D or GluN3A or B) and in most cases assemble as dimers of dimers. Glutamate binding occurs only at GluN2 subunits (Henson *et al*., 2010). In general, NMDARs channel kinetics are much slower than that of AMPARs, and like AMPARs, the subunit composition of NMDAR determines channel properties (Cull-Candy and Leszkiewicz, 2004).

Hippocampal neurons largely express GluN1 / GluN2 heteromers, with the current model suggesting that in adult, GluN2A containing NMDAR predominate at synaptic sites, whereas GluN2B containing NMDAR predominate at extrasynaptic sites (Groc *et al*., 2009). The activity of NMDAR at synaptic and extrasynaptic sites determines the level of Ca^{2+} influx and depending on levels of activity can initiate intracellular signalling cascades which may induce different forms of synaptic plasticity, changes in neuronal morphology or induce excitotoxicity.

1.1.5: Metabotropic Glutamate receptors

Metabotropic glutamate receptors are a family of class C G-protein coupled receptors (GPCRs), consisting of eight different receptor subtypes, categorised into three distinct groups (Groups I – III) which mediate synaptic transmission and plasticity (Niswender and Conn, 2010). Group I mGluRs ($mGluR_1$ and $mGluR_5$) are located predominantly at post-synaptic sites, they are coupled to G_q G-proteins and through phospholipase C (PLC) activation, inositol triphosphate (IP_3) generation and Ca^{2+} release from intracellular stores as well as activation of kinase signalling (PKC, MAPK), can influence the activity of voltage gated ion channels and effect neuronal excitability (Niswender and Conn, 2010). Whereas Group II ($mGluR_2$ and $mGluR_3$) and Group III ($mGluR_4$, $mGluR_6$, $mGluR_7$ and $mGluR_8$) mGluRs are located predominantly at pre-synaptic sites and modulate transmitter release by negatively coupling to adenylyl cyclase through $G_{i/o}$ G-proteins.

1.1.6: Synaptic Plasticity

Synaptic plasticity is defined as experience-dependent changes in synaptic connectivity. The idea that communication between two neurons could be strengthened if both neurons were active at the same time was first posed by Donald Hebb (Hebbian plasticity; (Hebb, 1949)). Bliss and Lomo (1973) experimentally illustrated this idea at the perforant path to granule cell synapse within the anaesthetised rabbit hippocampus. Brief trains of high-frequency stimulation at this synapse initiated a long-lasting (30 min – 10 hours) potentiation in the efficacy of excitatory synaptic transmission; a phenomenon which was termed long term potentiation (LTP; Bliss and Lomo, 1973).Since then, the cellular mechanisms underlying this type of plasticity and the converse (long lasting depression of synaptic transmission; LTD) have been extensively studied at many excitatory synapses. These long lasting changes in the efficacy of synaptic transmission are thought to be the cellular mechanisms for information storage (Bliss and Collingridge, 1993). Moreover, it is now recognised that a number of hormones including leptin (Moult and Harvey, 2011), insulin (Huang *et al.*, 2004), estrogen (Foy, 2001) and the glucocorticoids (Popoli *et al.*, 2012) can influence glutamatergic synaptic transmission and induce or regulate long lasting changes in synaptic efficacy.

1.1.6.1: Long term potentiation: CA3 – CA1 synapses

High frequency afferent stimulation at excitatory synapses triggers large quantities of glutamate release and subsequent depolarisation of the post-synaptic cell to a threshold which allows for the voltage dependent relief of the NMDAR Mg^{2+} block. A sufficient rise in dendritic calcium is required for the initiation of signalling cascades which leads to the induction (early phase) and maintenance (late phase) of LTP. Specifically, during the induction phase, calcium-dependent autophosphorylation of calcium / calmodulin-dependent kinase II (CAMKII) occurs; an event which is critical for LTP (except very early in postnatal development; Malenka and Bear, 2004). Subsequent activation of a host of other kinase signalling enzymes including extracellular signal-regulated kinase (ERK), protein kinase A (PKA), protein kinase C (PKC; specifically protein kinase M ζ), phosphoinositide-3kinase (PI3K), and the receptor tyrosine kinase Src, have all been implicated in mediating the expression and maintenance of LTP (Malenka and Bear, 2004). It is now generally accepted that expression of LTP requires the increase in conductance and number of synaptic AMPAR, driven by activation of protein kinases. For example PKC / CAMKII-dependent phosphorylation at Ser 831 of GluA1-containing receptors increases single channel conductance of these receptors (Kristensen *et al*., 2011), and PKA dependant phosphorylation of GluA1 at Ser 845 enhances surface delivery and incorporation of GluA1-containing AMPAR into synaptic sites (Man *et al*., 2007). Moreover incorporation of AMPAR into previously AMPA "silent" synapses (*i.e*: synapses which do not conduct current at resting membrane potential) contributes to enhancement of excitatory synaptic transmission during LTP (Liao *et al*., 1995; and reviewed in Kerchner and Nicoll, 2008). In addition, lateral diffusion of AMPAR into synapses may also play a role in the regulation of synaptic AMPAR content (as reviewed in Malinow and Malenka, 2002). The maintenance phase of LTP requires gene transcription and new protein synthesis which is mediated by the activation of transcription factor, cAMP response element binding protein (CREB) and transcription of immediate early genes (IEG) such as zif268, arc and c-fos. Activation of CREB (via PKA and indirectly through MAPK signalling) and the increase in IEG transcription results in the transcription of scaffolding proteins important for stabilization of synaptic AMPAR, enlargement of dendritic spines and cytoskeletal rearrangement; morphological changes that permit the sustained enhancement of excitatory synaptic transmission.

1.1.6.2: Long term depression

Long term depression of synaptic transmission is the activity dependent long lasting decrease in synaptic efficacy. Induction of *de-novo* LTD at hippocampal schaffer-collateral to CA1 synapses is age dependent and is more readily induced in slices from juvenile rodents. Although more difficult to induce in the adult hippocampus, LTD is thought to be important for certain types of learning. Two main types of LTD at these synapses have been identified, and are distinguished by their induction mechanisms; NMDAR-dependent and mGluR-dependent. As well as differing low frequency stimulation protocols, application of selective agonists for NMDAR (Lee *et al*., 1998) or Group I mGluR (Palmer *et al*., 1998; Fitzjohn *et al*., 1999, 2001; Moult *et al*., 2006), can induce these mechanistically distinct forms of LTD. For example, LTD induced by application of NMDA requires Ca^{2+} influx, as reducing the concentration of extracellular Ca^{2+} prevents expression of NMDA-induced LTD (Lee *et al*., 1998). Whereas, LTD induced by pharmacological activation of Group I mGluRs (by DHPG) is independent of Ca^{2+} signalling, such that LTD is still expressed when DHPG is applied in conditions where extracellular Ca^{2+} has been eliminated; after intracellular Ca^{2+} stores have been depleted and after intracellular incorporation of a calcium chelator (Fitzjohn *et al*., 2001). Despite this, both forms of LTD are expressed postsynaptically and involve a reduction in synaptic AMPAR (Collingridge *et al*., 2010).

Activation of serine/threonine protein phosphatases (protein phosphatase 2B and protein phosphatase 1), dephosphorylation of Ser 845 on GluA1-containing AMPAR and subsequent internalization of AMPAR has been implicated in NMDAR-dependent LTD. In addition, activation of tyrosine kinases, subsequent phosphorylation and internalisation of GluA2-containing AMPAR is also implicated in NMDAR-dependent LTD (Collingridge *et al*., 2010). Conversely, mGluR-dependent LTD is dependent on the activation of protein tyrosine phosphatases and tyrosine dephosphorylation of GluA2-containing AMPAR (Moult *et al*., 2006). Although dephosphorylation of AMPAR subunits appears to be an important common mechanism in the initiating AMPAR internalization, the exact downstream signalling events required for initiation and maintenance of NMDAR- and mGluR-LTD are still unclear. Moreover, studies utilizing inhibitors of protein kinases including p38 MAPK, PI3K, PKA, ERK1/2 and glycogen-synthase kinase-3 (GSK-3) have implicated all of these kinase signalling

pathways as important downstream effectors activated during the induction and required for the maintenance phases of LTD (Collingridge *et al*., 2010). In addition, rapid dendritic protein synthesis (Huber *et al.*, 2000), cytoskeletal rearrangement, spine shrinkage and alterations in the transcription of IEGs (such as arc (Plath *et al*., 2006)) are important for the maintenance of this form of synaptic plasticity (Hanley, 2008).

1.1.6.3: Trafficking of AMPAR

A key factor in determining the efficacy of glutamatergic synaptic transmission is the relative quantity and subtype composition of synaptic AMPAR. During basal states, AMPAR are continually trafficked into and out of the plasma membrane via constitutive rounds of clathrin-mediated endocytosis and through recycling endosomes, reinserted into the plasma membrane via SNARE-mediated exocytosis (Lüscher *et al*., 1999; Ehlers, 2000) at extrasynaptic sites. Moreover, AMPAR are highly mobile and can diffuse laterally into and out of synaptic sites (as reviewd in Shepherd and Huganir, 2007). These concepts have been validated experimentally as inhibition of SNARE-mediated membrane fusion events, inhibits LTP expression in hippocampal slices (Lledo *et al*., 1998) and in hippocampal cultures (Lu *et al*., 2001). Moreover, promoting membrane fusion potentiates synaptic transmission in hippocampal slices (Lledo *et al*., 1998) and importantly it has been demonstrated that AMPAR within recycling endosomes provide the source for the increase in AMPAR expression during LTP (Park *et al*., 2004). Similarly, agents which disrupt clathrin-mediated endocytosis inhibit LTD (Man *et al*., 2000), and chemical induction of LTD in hippocampal slices with DHPG, NMDA or insulin promotes the internalisation of AMPAR in culture (Beattie *et al*., 2000; Lin *et al*., 2000; Snyder *et al*., 2001). Thus, modulation of the trafficking of AMPAR and their stability at synaptic sites during activity dependent synaptic plasticity underlies the relative expression of AMPAR within the synapse.

1.2: Estrogen

17β-estradiol (E2) is the most potent and biologically prevalent steroid in a class of steroid compounds called the estrogens: which consists of E2, estrone (E1) and estriol (E3). Classically, E2 is regarded as the main female sex-hormone in mammals which is synthesised in the ovaries, and is primarily responsible for mediating the reproductive cycle. However, this is a highly simplified view of the actions of this incredibly diverse lipophilic compound.

Aside from contributing to CNS sexual dimorphism (notably within the hypothalamus) and female sexual reproduction, E2 (both peripheral and centrally derived) influences many other cognitive functions such as: mood (reviewed in Joffe and Cohen, 1998), executive function and stress (reviewed in Shansky and Lipps, 2013), learning and memory (below and reviewed in Luine and Frankfurt, 2012), as well as energy regulation and homeostasis (reviewed in Sinchak and Wagner, 2012).

Moreover, evidence for centrally derived (ie: synthesised from cholesterol *de novo* or by aromatisation of testosterone) non-genomic effects of estrogen in the CNS is growing rapidly, implicating this hormone as an important neuromodulator (Balthazart and Ball, 2006; Srivastava *et al*., 2011). Understanding the mechanisms by which E2 exerts its various effects within the CNS is vital in our attempt to understand its role in cognition.

1.2.1 Estrogen Biosynthesis and Metabolism

Unlike peptides, steroids are synthesised on demand and are not stored. Therefore, an essential part in understanding how E2 acts as a neuromodulator, is an appreciation of its biosynthesis (Fig 1.4) and metabolism. Factors which influence expression or activity of key enzymes in E2 biosynthesis and inactivation/metabolism would ultimately affect concentrations of available E2 and therefore, its actions.

Biosynthesis of all five classes of steroid hormones; glucocorticoids, mineralocorticoids, androgens, progestogens and estrogens, begin with the precursor, cholesterol. The key step for the synthesis of all steroid hormones is the conversion of cholesterol into pregnenolone (PREG), an event catalysed by the enzyme cytochrome

P450 side-chain cleavage (P450scc). However, P450scc is localised to the inner mitochondrial membrane and so the rate limiting step for all steroid synthesis is the delivery of cholesterol from the outer mitochondrial membrane to the inner membrane by the steroidogenic acute regulatory protein (StAR; Clark *et al*., 1994). Once synthesised, PREG leaves the mitochondria and can be converted into a host of steroidal end products. Illustrated are the key enzymatic steps for estrogen synthesis (Fig 1.4). The key enzymes involved in the conversion of PREG to 17β-E2 (enzymes which are located in the smooth endoplasmic reticulum) are 3β-hydroxysteroid dehydrogenase (3β-HSD), P450-C17, 17β-hydroxysteroid dehydrogenase (17β-HSD) and P450-aromatase (aromatase) (Do Rego *et al*., 2009).

The metabolism and excretion of plasma E2 into less active, water-soluble metabolites involves multiple and complex oxidative and conjugation pathways, and occurs primarily in the liver (Zhu and Conney, 1998). Briefly, E2 and estrone can be hydroxylated by numerous P450 enzymes and the 2- and 4- hydroxylated catechol estrogen metabolites can be *O*-methylated by catechol-*O*-methylstransferase. Moreover, esterification by estrogen acyltransferase or conjugation by β-glucuronidase or sulfatase of E2 and its hydroxyl metabolites may also occur (Zhu and Conney, 1998).

Classically, the synthesis of steroids was thought to be restricted to endocrine organs such as the adrenals, testis and ovaries. Due to their lipophilic nature, steroids were thought to reach the brain exclusively via circulation and act as neuromodulators via this mechanism (covered in, McEwen, 2001). However, in last 30 or so years, evidence has built to suggest that the brain itself is a steroidogenic organ and can synthesis steroids *in situ* (extensively reviewd in: Baulieu, 1998; Plassart-Schiess and Baulieu, 2001; Do Rego *et al*., 2009).

The term ‘neurosteroids’ was first proposed by Etienne-Emile Baulieu’s group in 1981, to describe steroids synthesised *de novo* (from cholesterol) within the central nervous system, independently (at least in part) from peripheral endocrine sources (Corpéchot *et al*., 1981). Over the past decade, evidence has built to suggest that E2 may indeed be classified as a neurosteroid. Supporting this, is that maximum ovarian derived circulating levels of E2 in the adult female rat reaches only approximately 100 pM (Smith *et al*., 1975; Woolley, 2007), whereas basal levels of E2 in acute freshly isolated

hippocampal slices reaches approximately 8 nM (Hojo *et al*., 2009), suggesting the hippocampus may be a site for E2 biosynthesis.

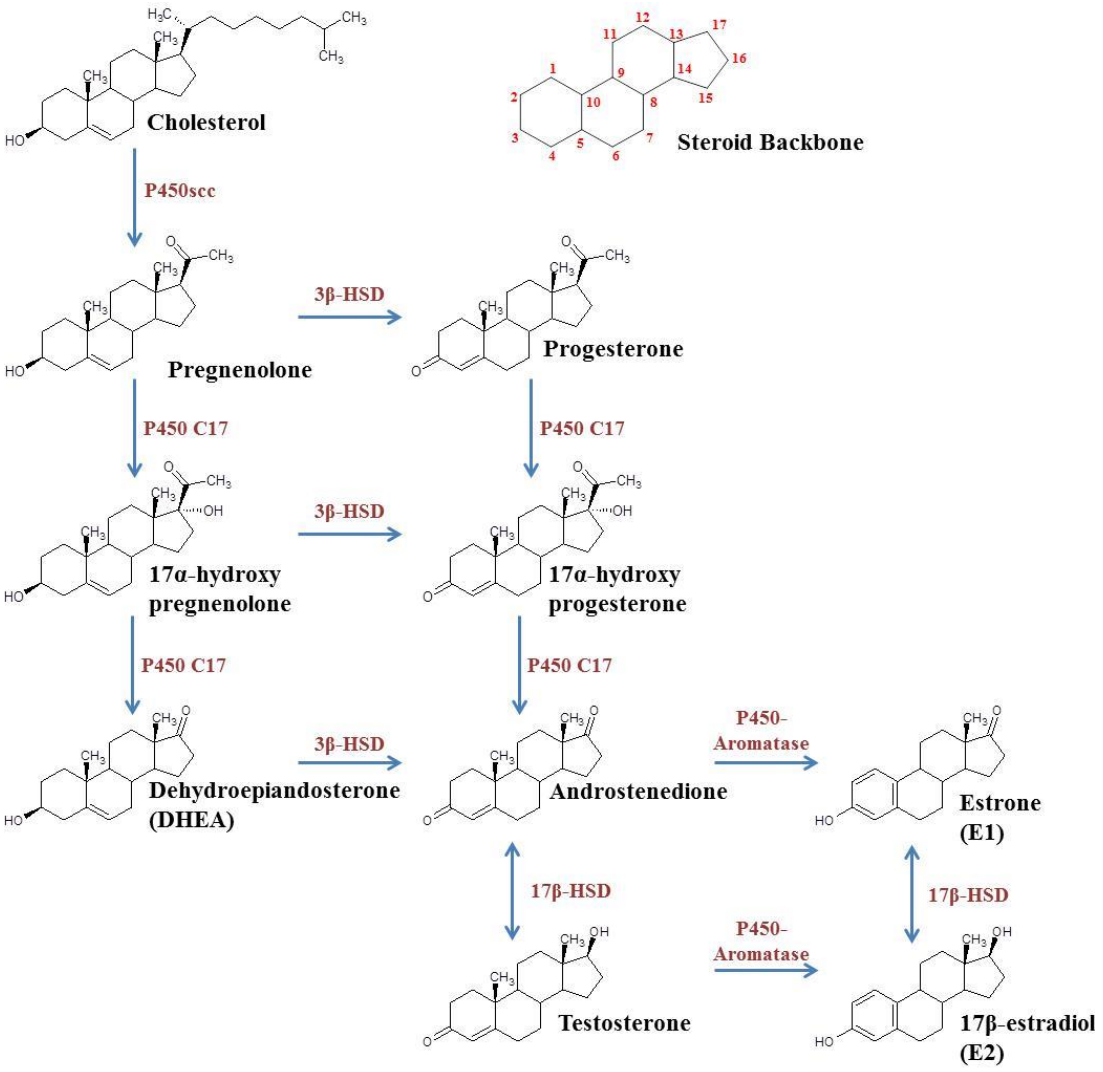

Figure 1.4: Estrogen Biosynthesis pathway.

1.2.2: Estrogen synthesis in the Hippocampus:

Expression of enzymes responsible for estrogen biosynthesis are expressed within hippocampal principal neurons (reviewed in Hojo *et al*., 2011) and importantly StAR colocalises with aromatase within the rat hippocampus (Wehrenberg *et al*., 2001). This suggests that principal cells within the hippocampus have the necessary machinery for

de novo E2 biosynthesis, which would allow newly synthesised hippocampal derived E2 to act in a local autocrine or paracrine manner to modulate hippocampal function.

Direct evidence of E2 synthesis from cholesterol *ex vivo* was established by Hojo *et al*., in 2004. In this study they elegantly show the conversion from [^{3}H]-PREG to [^{3}H]-DHEA, from [^{3}H]-DHEA to [^{3}H]-testosterone and to [^{3}H]-E2 via HPLC analysis in adult (12week) male rats. Moreover, specifically blocking P45017α and aromatase, abolished the conversion of [^{3}H]-PREG to [^{3}H]-DHEA and from [^{3}H]-DHEA to [^{3}H]-E2, respectively. Supporting this, Prange-Kiel *et al*. (2003) provided evidence for *de novo* synthesis of E2 in cultured hippocampal neurons. Using pure neuronal hippocampal cultures from adult hippocampi in serum- and steroid-free conditions, they established that estrogens were released into the culture media over a period of 11 days. Moreover, estrogen synthesis under these conditions was inhibited by the aromatase inhibitor, letrozol, and subsequent studies found this to be a dose dependent effect (Kretz *et al*., 2004).

Importantly, P450-C17 and aromatase expression is found within pre- and post-synaptic compartments of principal neurons within CA1 area of the hippocampus (Hojo *et al*., 2004). Interestingly, stimulation of hippocampal slices with NMDA increases levels of hippocampal derived E2 two fold (Hojo *et al*., 2004) and aromatase activity can be influenced by calcium dependent phosphorylation events, at least in the quail brain (Balthazart *et al*., 2003), thus suggesting not only that synaptic estrogen biosynthesis may occur but that this also may occur in an activity dependent manner. Therefore, the concentration of E2 within the hippocampus may be influenced not only via circulating estrogens but via local E2 biosynthesis as well.

How local concentrations of E2 are regulated within the brain is less well understood. However catabolic enzymes have been detected in brain regions of the male African catfish (Timmers *et al*., 1988) and the quail (Balthazart *et al*., 1994). Due to the high lipophilicity of E2, rapid diffusion into surrounding neurons, glia and blood vessels may be the mechanism by which effective local concentrations are lowered.

1.2.3: Estrogenic effects within the hippocampus

E2, via a plethora of genomic and non-genomic mechanisms can elicit a multitude of effects within the hippocampus. The focus here will be on the propensity for E2 to mediate changes in hippocampal dendritic morphology, neuronal excitability and glutamatergic synaptic transmission, which ultimately lends this hormone to influence hippocampal synaptic plasticity and hippocampal dependent learning tasks.

The ability for E2 to modulate dendritic morphology has been known for a number of years. For example, ovariectomy reduces dendritic spine number in the CA1 region of the adult rodent hippocampus, an effect which is reversed by treatment with E2 (Gould *et al*., 1990; Woolley *et al*., 1997). The density and shape of dendritic spines in female rodents also fluctuates over the course of the 4 – 5 day rat estrus cycle, as during proestrus the number of spines and the percentage of thin and mushroom type spines is significantly greater than during estrus (González-Burgos *et al*., 2005). Moreover, the effects of E2 on spine morphology are not limited to female rodents as exogenous E2 treatment increases the number of spines by approximately 1.6 – 1.7 fold in hippocampal slices from adult male rodents (Mukai *et al*., 2007), and in primary hippocampal cultures (Murphy and Segal, 1996). This suggests that both peripheral and local (brain derived) sources may contribute to E2-induced modulation of spine morphology. Furthermore, acute treatment with E2 influences the expression of synaptic proteins (spinophillin and PSD-95) in the adult male and female rodent hippocampus, and in hippocampal cultures (Akama and McEwen, 2003; Lee *et al*., 2004; Zhao *et al*., 2005). E2 signalling through RhoA and ROCK also regulates actin dynamics in hippocampal slices (Kramár *et al*., 2009).

In correlation with changes in synaptic proteins and synapse number; it is well established that E2 influences the excitability of hippocampal neurons and modulates glutamatergic synaptic transmission, presumably via membrane initiated signalling events. Acute E2 effects on hippocampal excitability were first demonstrated by Teyler *et al*., (1980), who found that 100 pM E2 could rapidly (5-10min) potentiate the amplitude of the CA1 population spike in hippocampal slices from adult male rodents. Since this study, many groups have also observed that E2 rapidly potentiates intracellularly recorded excitatory post-synaptic potentials (EPSPs) and excitatory post-synaptic currents (EPSCs) in hippocampal neurons (Wong and Moss, 1992; Foy *et al*., 1999; Rudick and Woolley, 2003; Smejkalova and Woolley, 2010), and increases the

magnitude of dendritic fEPSP in CA1 of male (Fugger *et al*., 2001; Kramár *et al*., 2009; Zadran *et al*., 2009) and female (Fugger *et al*., 2001; Sharrow *et al*., 2002; Lebesgue *et al*., 2009) rodents. The E2-induced increase in fEPSP magnitude has also recently been extended to other hippocampal regions, the CA3 and DG (Kim *et al*., 2006).

Not surprisingly, E2 can influence activity dependent hippocampal plasticity. For example, the stage of estrus cycle in adult rats influences the magnitude of high frequency stimulation (HFS)-induced LTP such that the magnitude of LTP is greater in rats at proestrus than at diestrus (Bi *et al*., 2001). Acute E2 administration can also enhance the magnitude of HFS-induced hippocampal LTP (Foy *et al*., 1999) and chronic E2 treatment facilitates the induction of LTP in OVX awake rats (Córdoba Montoya and Carrer, 1997). Conversely, acute application of E2 can influence the magnitude of chemically-induced hippocampal LTD in adult male rats (Shiroma *et al*., 2005; Mukai *et al*., 2007) and alter the frequency threshold for LTD induction in OVX adult female rats (Zamani *et al*., 2000). Moreover, E2 can attenuate the magnitude of low-frequency stimulation (LFS) induced LTD in hippocampal slices from aged (18 – 24 months) males.

Considering the influence of E2 on hippocampal synaptic plasticity, the cellular correlates for learning and memory, it is not surprising that hippocampal dependent learning tasks are also influenced by this steroid. Indeed, OVX rats perform less well in object recognition memory tasks compared to control animals (Luine *et al*., 2003; Wallace *et al*., 2006), and the deficits in performance can be corrected by E2 replacement (Luine *et al*., 2003; Sandstrom and Williams, 2004; Luine and Frankfurt, 2012). Moreover, administration of estradiol immediately after training for hippocampal-dependent tasks (for example the Morris water maze task and novel object recognition) enhances memory consolidation (as reviewed in Frick, 2013). Thus there is unequivocal evidence suggesting that estradiol is a key modulator of hippocampal function.

1.2.4: Estrogen receptors

Within the CNS, E2 exerts its cornucopia of effects through two distinct mechanisms, namely genomic (nuclear-initiated) or non-genomic (membrane or non-nuclear initiated). The classical genomic mechanism is mediated via two distinct nuclear

estrogen receptors; estrogen receptor α (ERα; White *et al*., 1987) and estrogen receptor β (ERβ; Kuiper *et al*., 1996). These receptors are ligand-activated transcription factors which upon ligand binding, dimerization and translocation to the nucleus, bind to estrogen response elements (EREs) at the promoter region of target genes, resulting in the modulation (enhancement or suppression) of estrogen-responsive genes.

However, signalling via E2 also occurs via "non-genomic" mechanisms which involve the activation of a number of different intracellular signalling cascades resulting in alterations in cellular function, including the transcription of genes without an upstream ERE site. Non-genomic effects of E2 have been attributed to plasma-membrane associated variants of ERα and ERβ (mERα/β; Levin, 2009), mER-X (Toran-Allerand, 2005), a G_q coupled mER (Roepke *et al*., 2009), and the recently identified G-protein coupled receptor, GPR30 (Revankar *et al*., 2005; Thomas *et al*., 2005). It should be noted that mER-X and the G_q coupled mER have not yet been cloned. Signalling via these non-nuclear ER includes: accumulation of second messengers such as 3'-5'-cyclic adenosine monophosphate (cAMP) and Ca^{2+} ; activation of kinase signalling pathways such as phosphatidylinositol 3-kinase (PI3K) and extracellular signal-regulated kinase (ERK); regulation of transcription factors (cAMP response binding protein; CREB); and immediate early gene transcription (c-Fos) (Vasudevan and Pfaff, 2007).

1.2.5: Expression of estrogen receptors within the hippocampus

Classic *in situ* hybridisation studies of the rat CNS revealed expression of both ERα and ERβ transcripts within the adult rat hippocampal formation (Shughrue *et al*., 1997), moreover, immunohistochemical studies in murine hippocampal tissue revealed expression of nuclear and extra-nuclear estrogen receptors within all regions of the hippocampus (Mitra, 2003).

ERα immunoreactivity was thought to be exclusively within nuclei of a select population of interneurons within the dentate gyrus and *stratum radiatum* of the CA1 region (Weiland *et al*., 1997). However expression of ERα within the hippocampus extends to extra-nuclear sites of principal neurons (such as at dendritic spines) and also within glia cells (Milner *et al*., 2001; Towart *et al*., 2003). Moreover, electron microscopy (EM) reveals that ERα is expressed in both pre- and post-synaptic compartments of principal cells at the *stratum radiatum* layer at the CA1 (Mukai *et al*.,

2007). The pattern of ERβ expression within the hippocampus is generally similar to that of ERα in that it is localised at both nuclear and extra-nuclear sites (Milner *et al*., 2005). However in contrast to ERα, the relative distribution of ERβ is predominantly extranuclear, more widespread and can be observed at axon terminals at the CA3 (Milner *et al*., 2005).

GPR30 immunoreactivity has also been detected within the rodent hippocampal formation. Specifically, in the cell body layer of the CA3-CA1 regions and granule cells of the dentate gyrus (Brailoiu *et al*., 2007; Matsuda *et al*., 2008; Hazell *et al*., 2009; Hammond *et al*., 2011), suggesting an abundant expression within principal cells across the different subregions of the hippocampus. Moreover, recent evidence revealed GPR30 expression in synaptosomes from whole hippocampal lysates of rats, and using electron microscopy, GPR30 labelling was observed in various types of spines profiles (thin, mushroom-shaped and concaved spines) within the *stratum radiutum* layer of the CA1 region (Akama *et al*., 2013).

The expression and distribution of these estrogen receptors within the hippocampal formation suggests that E2 has an important role in both mediating the transcription of estrogen responsive genes and inducing non-nuclear initiated cellular responses. This expression pattern also correlates well with the ability of E2 to acutely modulate neuronal excitability and excitatory synaptic transmission as well as its ability to modulate dendritic structural plasticity and influence the number of synaptic proteins.

By which receptors E2 is mediating effects on hippocampal synaptic transmission is unclear. In both ERα knockout (Fugger *et al*., 2001; Foster *et al*., 2008) and ERβ knockout (Foster, 2012) mice, the magnitude of acute E2-responses are reduced, but not eliminated, suggesting additional estrogen sensitive receptor/s are responsible for mediating the acute effects E2 on hippocampal synaptic transmission. The focus of this thesis will be on GPR30.

1.3: GPR30

GPR30 is a member of the class A rhodopsin-like G-Protein coupled receptor (GPCR) superfamily. Human GPR30 has five transcripts, four of which encode a 375 amino acid protein, and one which encodes a truncated 73 amino acid version (Ensembl; gene ID: ENSG00000164850). Since it was cloned between 1996 and 1998 (Owman *et al*., 1996, Carmeci *et al*., 1997, Feng and Gregor, 1997, Takada *et al*., 1997 and O'Dowd *et al*., 1998), it has been given a number of different names, for example: CEPR, GPCR-Br, CMKRL2, DRY12, FEG-1, LERGU, GPR30, GPER-1 and GPER.

For the purposes of this thesis, the receptor will be referred to as GPR30; however the International Union of Basic and Clinical Pharmacology (IUPHAR) has renamed and classified GPR30 as "G-protein coupled estrogen receptor" (GPER; http://www.iuphar-db.org/DATABASE/ObjectDisplayForward?objectId=221).

1.3.1: Discovery

During the late 1990's, several independent groups reported and cloned a novel GPCR, the gene for which is mapped to chromosome 7p22 in human and encodes a protein of 375 amino acids and a predicted molecular mass of 42 kDa (Owman *et al*., 1996; Carmeci *et al*., 1997; Feng and Gregor, 1997; Takada *et al*., 1997; O'Dowd *et al*., 1998). GPR30 was found to have highest homology (~30%) to the chemokine receptor CXCR1 (Owman *et al*., 1996 and O'Dowd *et al*., 1998) and the angiotensin II receptor (Feng and Gregor., 1997 and Takada *et al*., 1997), suggesting that GPR30 was a member of the chemokine GPCR family. However, Feng and Gregor, (1997) found negligible binding with both [I^{125}] angiotensin II and [I^{125}] angiotensin IV in COS-7 cells transiently expressing GPR30. Moreover, Owman *et al*, (1996) found that GPR30 did not respond to a variety of chemotactic peptides (concentrations up to 100μM) in both cAMP and intracellular calcium mobilization assays. Thus, these studies imply that GPR30 is not a member of the chemokine receptor family, despite its significant homology.

Carmeci *et al*. (1997), one of the first groups to clone GPR30, used differential cDNA library screening and identified and isolated a cDNA clone (GPR30) that was over

expressed in the MCF-7 (ERα +VE breast cancer cell line) but not expressed in the MDA-MB-231 (ERα -VE breast cancer cell line). The authors found a pattern of expression where three out of four ERα +VE breast cancer cell lines expressed GPR30 mRNA (MCF-7, T-47D and MDA-MB-361), whereas there was no evidence of expression in the ERα -VE cell lines (BT-20, MDA-MB-231 and HBL-100) or in normal human mammary epithelial cells (HMEC). The authors suggest from this expression pattern one could speculate that this receptor may contribute to physiological responses in tissues that are modulated by hormones, specifically, estrogen (Carmeci *et al*., 1997).

Thus, opening up the possibility of a G-protein coupled estrogen receptor.

1.3.2: GPR30, an estrogen-sensing receptor?

The first evidence to suggest that GPR30 may be involved in E2-mediated signalling was presented by Filardo and colleagues (2000). This group observed ERK1/2 phosphorylation in response to E2 in SKBr3 breast cancer cells, a cell line which does not express ERα or ERβ, but does express GPR30 (Filardo *et al*., 2000). This group postulated that stimulation of this signalling pathway occurred via E2-induced activation of GPR30 and subsequent transactivation of EGFR.

However, it was not until 2005 that specific binding of E2 to GPR30 was reported. Evidence for this came from two independent groups (Thomas *et al*., 2005; Revankar *et al*., 2005). In the first study from Edward Fildardo's group, specific, saturable binding of tritium labelled E2 ([H^3]-E2) was observed in SKBr3 breast cancer cells and in HEK-293 cells stably transfected with untagged GPR30 (hGPR30-HEK293). Dissociation constants were calculated as approximately 2.7 nM in SKBr3 cells and 3.3 nM in the hGPR30-HEK293 cells. Moreover, untransfected HEK293 cells and SKBr3 cells treated with GPR30 small interfering RNA (siRNA), showed negligible [H^3]-E2 binding. In addition, binding was specific for E2, as other steroids (testosterone, cortisol and progesterone) were unable to compete with [H^3]-E2 (Thomas *et al*., 2005). In the second study, the Prossnitz group used a novel approach to demonstrate binding, rather than radioactive E2, this group utilised membrane impermeable Alexa-fluoro 546 or 633 conjugated estadiol (E2-Alexa 546/633). In COS-7 cells stably transfected with GFP-

tagged GPR30 and permeabilized with saponin, specific intracellular co-localisation of GPR30 and E2-Alexa 546 fluorescent signals, and a direct-linear relationship between E2-Alexa 633 binding and GPR30-GFP expression was observed. Moreover, using intracellular fluorescence as a readout, unconjugated E2 competed with E2-Alexa 633 (2 nM) in these cells, with a K_i of 6.6 nM (Revankar *et al*., 2005).

These binding studies stemmed an explosion of research into the putative role for GPR30 in non-genomic E2 signalling mediated via this receptor (See section 1.3.3). However, not long after these initial studies, independent groups began to question the above studies and conflicting reports began to emerge.

In studies using endothelial cells expressing GPR30 from ERα/ERβ double knockout mice, Pedram and colleagues (2006) demonstrated that E2 failed to activate non-genomic E2 mediated cAMP accumulation, ERK phosphorylation and phosphatidylinositol (3,4,5)-triphosphate (PIP3) accumulation (Pedram *et al*., 2006). This group was also unable to detect saturable binding of radio-labelled E2 in SKBr3 cells, which directly contradicted the work by Edward Filardos group (Thomas *et al*., 2005). In addition, E2-induced signalling in MCF-7 cells could not be prevented by knockdown of GPR30, whereas silencing ERα gene expression prevented rapid signalling, suggesting that membrane ERα was responsible for rapid E2-induced signalling events and that GPR30 was not an estrogen-sensing receptor (Pedram *et al*., 2006). These data were later supported by Madak-Erdogan and co-workers (2008) who found membrane-initiated signalling in MCF-7 cells were exclusively mediated via ERα (Madak-Erdogan *et al*., 2008). Similarly, in a study comparing [H^3]-E2 binding in COS-7 cells transiently overexpressing ERα or GPR30 it was found that specific saturable binding only occurred in cells expressing ERα (Otto *et al*., 2008). Importantly, this group could not reproduce rapid E2-induced intracellular signalling responses such as cAMP accumulation and mobilization of intracellular calcium, demonstrated by others to be mediated via GPR30 (Otto *et al*., 2008).

Furthermore, GPR30 knockout animals exhibit no detrimental effects in classically estrogen-responsive tissue (Isensee *et al*., 2009; Mårtensson *et al.*, 2009; Otto *et al*., 2009), supporting evidence that GPR30 may not be an estrogen-sensing receptor. Moreover, non-classical E2 signalling in breast cancer cells and heterologous GPR30-

expressing cells has been attributed to an ERα splice variant (ERα-36; see section 1.3.5) rather than GPR30 (Kang *et al*., 2010).

Again challenging the estrogen-sensitivity of GPR30 is the recent evidence presented by Gros and coworkers (2011, 2013). This group show that the endogenous ligand for GPR30 may be the steroid aldosterone and action of this steroid at GPR30 may be more physiologically relevant than E2, at least in vasculature (Gros *et al*., 2011, 2013). Indeed, in freshly isolated aortic ring segments from rats, both aldosterone and the GPR30 agonist, G1, can stimulate ERK phosphorylation and importantly, the effects of aldosterone are blocked by the GPR30 antagonist, G15 (Gros *et al*., 2011). Moreover in vascular endothelial cells devoid of mineralocorticoid receptors, aldosterone mediates pro-apoptotic and anti-proliferative effects via GPR30 (Gros *et al*., 2013). However, in both report specific binding studies of aldosterone to GPR30 are missing.

Despite the apparent controversies in the field, the majority of studies support the concept that GPR30 acts as a G-protein coupled estrogen-sensing receptor (Reviewed in :Prossnitz *et al*., 2008a; Prossnitz and Barton, 2011; Filardo and Thomas, 2012).

1.3.3: GPR30 mediated signalling

GPR30-induced signalling has been extensively studied in breast cancer cells and recombinant cell lines (Prossnitz *et al*., 2008b). In the original studies from Filardo and colleagues (2000), E2 induced ERK1/2 signalling via GPR30 in SKBr3 cells was found to be initiated via the transactivation of epidermal growth factor receptor (EGFR) (Filardo *et al*., 2000). Specifically, stimulation of GPR30 results in the activation of Src tyrosine kinases through G-protein Gβγ-mediated mechanisms. Src activation promotes the formation of α5β1 integrin complexes with signalling adaptor protein Shc which enables the metalloproteinase (MMP)-dependant cleavage and release of heparin bound epidermal growth factor (HB-EGF) which subsequently binds to and activates EGFR (Filardo *et al*., 2000, 2002; Quinn *et al*., 2009). Transactivation of EGFR and subsequent initiation of ERK1/2 signalling is considered the primary mechanism by which GPR30 signals in breast cancer cell lines. In addition, activation of GPR30 results in the accumulation of cAMP through $G\alpha_s$-mediated stimulation of adenylyl cyclase in SKBr3 breast cancer cells and heterologously expressing HEK-293 cells (Filardo *et al*., 2002; Thomas *et al*., 2005), as well as activation of PI3K and subsequent

accumulation of PIP3, initiation of Akt signalling has also been reported (Revankar *et al*., 2005; Bologa *et al*., 2006; Blasko *et al*., 2009). Activation of GPR30 by both E2 and the GPR30 agonist (G1) can also stimulate a rise in intracellular Ca^{2+} in a number of different cell types (Revankar *et al*., 2005; Bologa *et al*., 2006; Filardo *et al*., 2007; Dennis *et al*., 2009; Noel *et al*., 2009), however the mechanisms by which GPR30 does this are not well understood. GPR30 signal transduction can also stimulate gene transcription, for example in SKBr3 cells, E2-induced MAPK signalling through GPR30 stimulates the expression of c-fos (Maggiolini *et al*., 2004).

1.3.4: GPR30 selective and non-selective ligands

Until recently, studying the function of GPR30 was problematic, as it was difficult to pharmacologically isolate GPR30 from other estrogen-sensing receptors, due to the lack of selective GPR30 ligands. However, in 2006, Bologa *et al*., identified a potent selective agonist for GPR30 (G1; (±)-1-[(3a*R**,4*S**,9b*S**)-4-(6-Bromo-1,3-benzodioxol-5-yl)-3a,4,5,9b-tetrahydro-3*H*-cyclopenta[*c*]quinolin-8-yl]-ethanone). Competitive binding assays with fluorescent-E2 revealed a K_i of 11 nM for G1 at GPR30 and in intracellular calcium mobilization assays, an EC_{50} of 2 nM (Bologa *et al*., 2006). Moreover, G1 (at a concentration of 10 μM) was unable to bind to a panel of 25 known GPCRs or nuclear ERα and ERβ, supporting the specificity of this compound for GPR30 (Blasko *et al*., 2009). Study of GPR30 function intensified when a selective antagonist, G15 (3a*S**,4*R**,9b*R**)-4-(6-Bromo-1,3-benzodioxol-5-yl)-3a,4,5,9b-3*H*-cyclopenta[*c*]quinolone), was developed (Dennis *et al*., 2009). However, at high concentrations (> 1 μM), weak ERα mediated estrogenic activity was reported, and subsequently an antagonist with improved GPR30 selectivity (G36; (±)-(3a*R**,4*S**,9b*S**)-4-(6-Bromo-1,3-benzodioxol-5-yl)-3a,4,5,9b-tetrahydro-8-(1-methyle-thyl)-3*H* cyclopenta[*c*]quinoline) was developed (Dennis *et al*., 2011).

GPR30 pharmacology is not simple, and according to numerous reports, this receptor appears to be quite promiscuous. For example, both Tamoxifen and ICI 182,780 two classical synthetic estrogen receptor antagonists have been identified as having agonist activity at GPR30. Specifically, Tamoxifen (or rather more accurately the active metabolite of Tamoxifen; 4-hydroxytamoxifen [4-OHT]) was originally developed as an estrogen receptor antagonist however has now been classified as a selective estrogen

receptor modulator (SERM) as it binds to nuclear estrogen receptors (ERα and ERβ) however has the properties of an antagonist and the properties of a transcription promoter in a tissue specific manner (Shiau *et al*., 1998). 4-OHT also competes with E2 at GPR30 (Thomas *et al*., 2005) and stimulates PI3K and MAPK signalling via GPR30 (Revankar *et al.,* 2005; Vivacqua *et al*., 2006). Whereas ICI 182,780 (Fulvestrant) which was originally developed as a selective estrogen receptor down-regulator (SERD) interacts with nuclear ERα and ERβ, prevents dimerization, inhibits nucleocytoplasmic shuffling, destabilises the receptors and promotes estrogen receptor degradation (Osborne *et al*., 2004). ICI 182,780 also competes with E2 at GPR30 (Thomas *et al*., 2005) and stimulates cAMP production via GPR30 (Filardo *et al*., 2002). Moreover, the E2 metabolite, estriol (E3) has antagonist properties at GPR30 (Lappano *et al.,* 2010), and a panel of xenoestrogens have also been shown to bind to GPR30 (Thomas and Dong, 2006). Moreover, agonist activity of these environmental estrogens has also been reported, most notably from the phytoestrogens; genistein and quercetin (Maggiolini *et al*., 2004), and synthetic xenoestrogen; Bisophenol A (BPA; Dong *et al*., 2011). Thus the potential for mediating GPR30 activity *in vivo* is not only limited to compounds that regulate the synthesis and metabolism of its (putative) endogenous ligand, E2 (eg: aromatase inhibitors), but also extends to estrogen receptor ligands currently being used as therapeutics (Tamoxifen and Fulvestrant) as well as exogenous estrogens found in the environment.

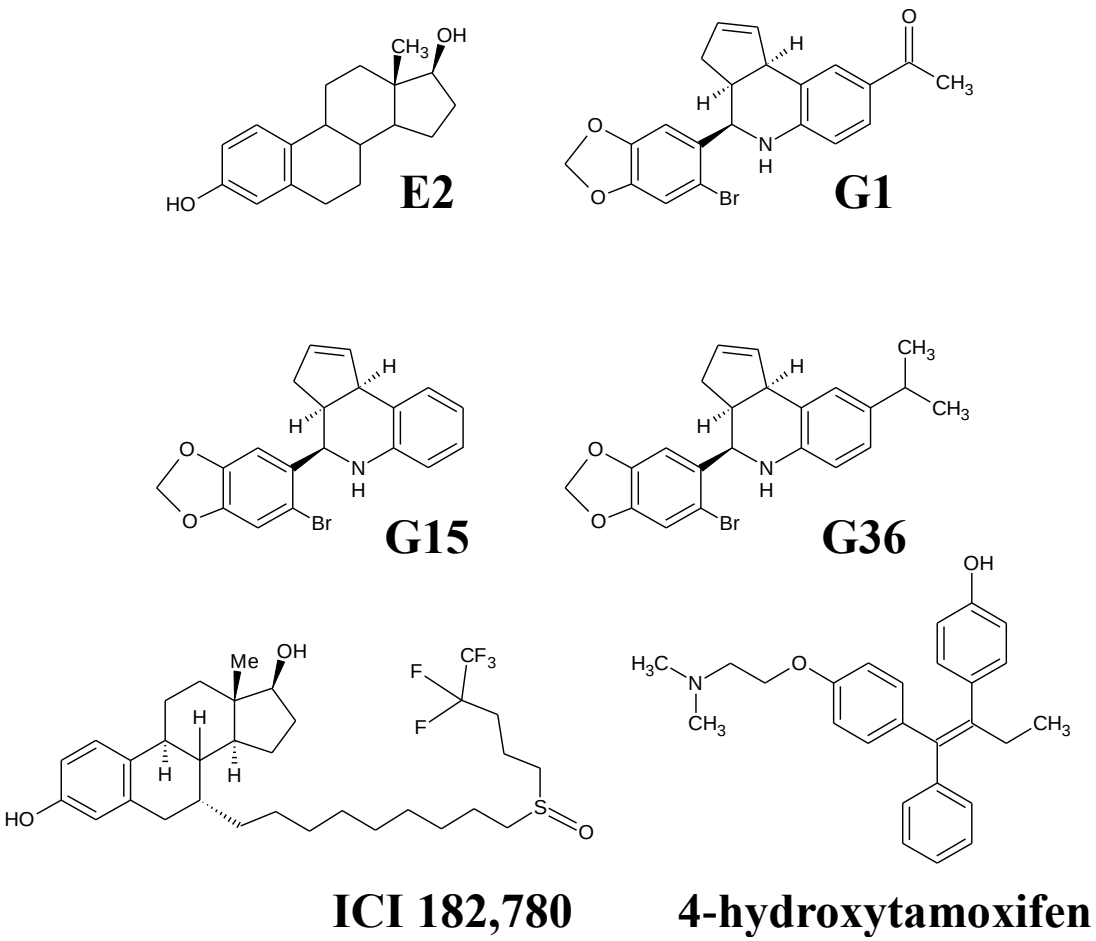

Figure 1.5: Structure of GPR30 ligands. The selective synthetic GPR30 ligands (G1, G15 and G36) are all modelled on the structure of the proposed endogenous agonist at GPR30, the steroid hormone E2. G1, ICI 182,780 and 4-hydroxytamoxifen are GPR30 agonists, whereas G15 and G36 are GPR30 antagonists.

1.3.5: A potential role for ERα-36?

ERα-36 is a 36kDa variant of the classical ERα, generated from a promoter located in the first intron of the ERα66 gene (Wang *et al*., 2005; Zou *et al*., 2009). This variant lacks the AF-1 and AF-2 transcription activation domains of the classical 66kDa ERα and has the capacity to reach the plasma membrane and mediate rapid E2 induced ERK1/2 phosphorylation (Wang *et al*., 2005, 2006). Moreover, this variant possesses a truncated ligand binding domain, suggesting a different ligand binding spectrum from the classic ERα-66 (Wang *et al*., 2005).

In 2010, Kang and co-workers suggested that this novel 36kDa variant of ERα was responsible for rapid non-genomic effects of E2, and that the selective GPR30 agonist, G1, activated signalling via this ERα variant rather than GPR30 itself (Kang *et al*., 2010). This study provided compelling evidence which suggests that heterologous expression of GPR30 promoted the expression of ERα-36 in HEK-293 and COS-7 cells. Importantly, inhibiting the binding capacity of ERα-36 with an antibody specific for the ligand binding domain of this protein, inhibited G1- and E2- induced activation of the MAPK/ERK1/2 pathway in SKBr3 cells (GPR30 and ERα-36 positive, ERα/β negative). In addition, the E2- and G1- induced effects could be inhibited via specific knockdown of ERα-36; although this effect could also be inhibited by GPR30 siRNA, it was found that knockdown of native GPR30 subsequently inhibited ERα-36 expression as well.

However, MCF-7 cells, (which express GPR30, but which do not strongly express ERα-36 (Zou *et al.*, 2009)), still respond to G1 (1 μM) as demonstrated in an intracellular calcium assay by Ariazi *et al*., (2010), and selective knockdown of GPR30 can abolish this effect. Moreover, G1-induced effects on oocyte maturation are observed in zebrafish, a species which does not possess a truncated variant of ERα, homologous to ERα-36 (Peyton and Thomas, 2011). Thus the role in which ERα-36 plays in G1 stimulated- or GPR30 mediated effects, is controversial.

1.3.6: GPR30 Knockout Mice

In the quest for establishing a physiological role for GPR30, transgenic GPR30 deficient mouse models have been developed and there are currently four which have been described (Wang *et al*., 2008; Isensee *et al.*, 2009; Mårtensson *et al*., 2009; Otto *et al*., 2009). Each group used different targeting strategies, mice of genetic backgrounds and mating schemes for the development of the GPR30 deficient mice. However, the observed phenotypes of the four knockouts only partially overlap, with a potential role for GPR30 in the vascular system and immune cell functions suggested. In the strain described by Wang *et al*., (2008) vasodilatory effects of G1 were absent in mutant mice and in the model described by Mårtensson *et al*., (2009) an elevated mean arterial blood pressure was observed in female knockout mice; these effects overlap with the strong reporter expression in vasculature seen in the GPR30-LacZ strain by Isensee *et al*.,

(2009). With respect to immune function, the GPR30 knockout mice described by Wang *et al*., (2008) exhibit impaired E2-induced thymic atrophy which relates to the impaired production of T-cells in the model described by Isensee *et al*., (2009). However in the model described by Otto *et al*., (2009) no change in T-cell production was observed.

Although the different approaches used to generate the mouse models could account for the differences in the observed phenotypes, due to lack of specific antibodies for murine GPR30, true knockdown of the gene has not been verified in these transgenic mice. Overall, general health of the four knockout strains is maintained, with two strains presenting changes in body weight (Wang *et al*., 2008; Mårtensson *et al*., 2009), and one strain exhibiting impaired glucose tolerance (Mårtensson *et al*., 2009). Unlike ERα knockout strains, all four GPR30 knockout strains remain fertile, and estrogen stimulated responses in mammary and uterus are still maintained (Otto *et al*., 2009) suggesting that GPR30 does not play a vital role in the classical estrogen responsive tissues in mice (Langer *et al*., 2010).

1.3.7: GPR30 tissue distribution and potential roles in the periphery

The mRNA expression profile of this receptor was first reported when GPR30 was initially cloned, using both northern blotting and RT-PCR, GPR30 expression was seen in a wide variety of human and rodent tissues, including: brain, lung, heart, placenta, liver, skeletal muscle, kidney and pancreas (Feng and Gregor 1997, Owman *et al*., 1996 and Carmeci *et al*., 1997).

However, due to the inconsistencies with knockout models, establishing physiological roles for GPR30 within the periphery have relied on pharmacological tools and gene silencing. GPR30 has been implicated in many physiological processes in the periphery (see Fig 1.6) including having roles in inflammation, cardiovascular and renal function as well as having roles in pancreatic-β cell function and glucose metabolism (as reviewed in Prossnitz and Barton, 2011). Thus, targeting GPR30 may have benefits in pathophysiological conditions such as multiple sclerosis (Blasko *et al*., 2009), cardiac ischemia/reperfusion injury (Nilsson *et al*., 2011), insulin resistance and type II diabetes (Tiano and Mauvais-Jarvis, 2012) and in hypertension associated renal injury (Lindsey and Chappell, 2011; Lindsey *et al*., 2011). Moreover, GPR30 is expressed in many cancer cell lines and primary tumours of breast, endometrium, ovaries, lung and

prostate, and has a role in cancer cell growth and metastasis (Prossnitz and Barton, 2011). However, a detailed overview of this literature is beyond the scope of this thesis. For comprehensive reviews of the putative *in vivo* roles see: Olde and Leeb-Lundberg, 2009, Prossnitz and Barton, 2011 or Barton, 2012.

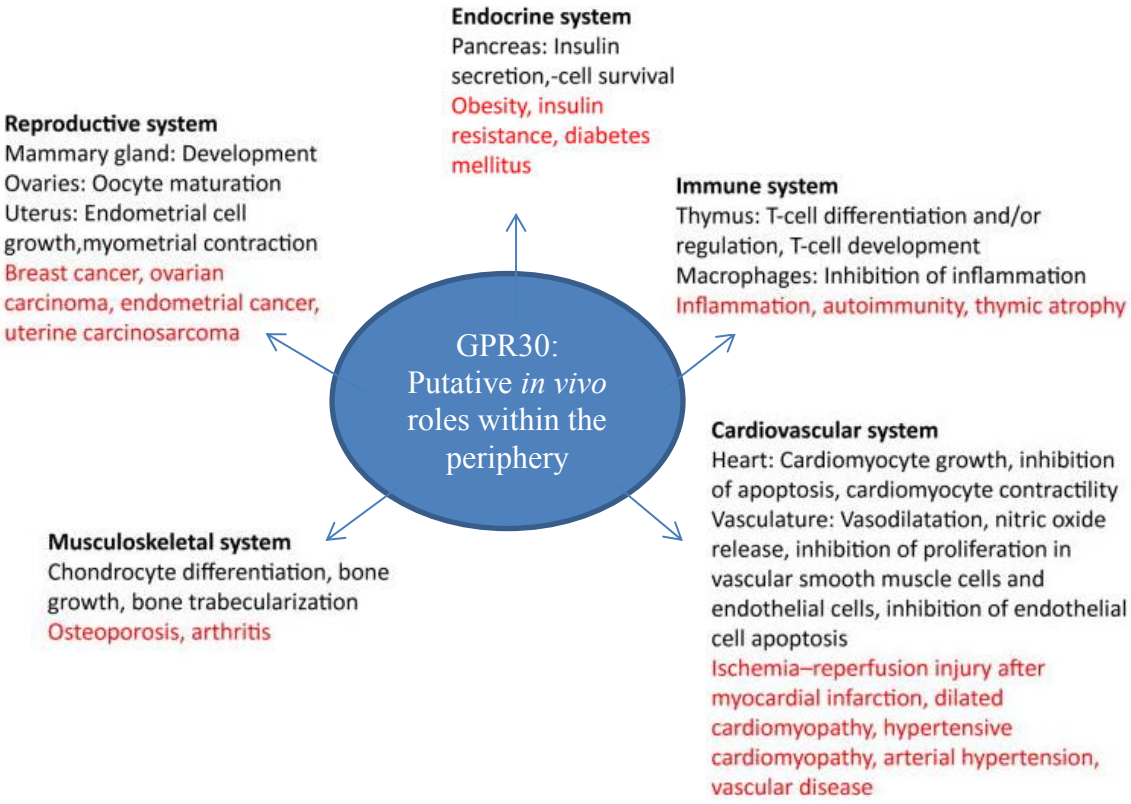

Figure 1.6: GPR30: Putative *in vivo* roles within the periphery. In black, general overview of physiological responses potentially mediated by GPR30. In red, potential diseases for which GPR30 could be used as a therapeutic target.

Figure adapted from Prossnitz and Barton, (2011): *The G-protein coupled estrogen receptor GPER in health and disease*

1.3.8: Expression of GPR30 within the nervous system

In addition to its expression in peripheral tissues GPR30 mRNA has been detected in many areas of human CNS tissue including: cerebellum, medulla, spinal cord, hypothalamus, hippocampus, thalamus, frontal cortex, amygdala, caudate nucleus and putamen (Owman *et al*., 1996; Feng and Gregor, 1997; O'Dowd *et al*., 1998), indicating a diverse role for this receptor within the nervous system.

Since then, GPR30 immunoreactivity has been detected in many regions of the rodent nervous system including: magnocellular neurons within the paraventricular nucleus and supraoptic nucleus of the hypothalamus (Brailoiu *et al*., 2007; Xu *et al*., 2009), Purkinje cells and granule cells of the cerebellum (Hazell *et al*., 2009), in both large and small diameter cells of rat dorsal root ganglion (Dun *et al.*, 2009), neurons in the pars reticular and pars compacta of the Substantia nigra (Brailoiu *et al*., 2007; Hazell *et al*., 2009), cholinergic neurons within the striatum and medial septum (Hammond *et al*., 2011), and within principal cells from all regions of the hippocampus (Brailoiu *et al*., 2007; Hazell *et al*., 2009; Hammond *et al*., 2011).

1.3.9: GPR30 may be implicated in Estrogen-mediated CNS physiology

Considering the almost omnipresent expression of GPR30 within the CNS and despite the controversies surrounding GPR30, it is not surprising that evidence has been rapidly accumulating to suggest that this receptor may have multiple roles in E2-mediated physiology.

In brief, GPR30 has been implicated in:

- *E2-induced pain sensitivity*. For example G1 increases cytosolic calcium and induces reactive oxygen species (ROS) accumulation in cultured spinal sensory neurons (Deliu *et al*., 2012). G1 administration can also mimic E2-mediated PKCε dependant mechanical hyperglasia in adult male rats (Kuhn *et al*., 2008).

- *E2 modulation of the serotonin system.* For example, GPR30 knockdown inhibits, and G1 mimics, E2-induced desensitisation of 5-HT_{1a}R signalling in the paraventricular nucleus in rats (Xu *et al*., 2009; Rossi *et al*., 2010; McAllister *et al*., 2012).

- *E2-induced modulation of gonadotropin releasing hormone (GnRH) secretion.* For example, G1 stimulates $[Ca^{2+}]_i$ oscillations and GnRH secretion in primate GnRH neurons in a manner similar to E2, an effect which can be abolished by siRNA knockdown of GPR30 (Noel *et al*., 2009; Terasawa and Kenealy, 2012).

- *E2 modulation of cholinergic inputs into the hippocampus*. Specifically, G1 can mimic the E2-induced enhancement of K^+ stimulated acetylcholine release in the hippocampus and the rate of acquisition in spatial learning tasks in female rats (Hammond *et al*., 2009, 2011). Moreover, the vast majority of cholinergic neurons which send afferents to the hippocampus, express GPR30 (Hammond *et al*., 2011).

- *Neuroprotective effects of E2.* For example, G1 mimics the E2-mediated protection against glutamate toxicity in immortalised murine hippocampal cultures (Gingerich *et al*., 2010), in cortical cultures G1 and E2 attenuate NMDA-induced excitotoxicity and knockdown of GPR30 reduces the E2- and G1-induced neuroprotection (Liu *et al*., 2012, however see Bryant and Dorsa, 2010). Chronic administration of G1 can also improve neuronal survival in murine models of experimental stroke (Zhang *et al*., 2010) and global ischemia following cardiac arrest (Kosaka *et al*., 2012). Moreover, in adult rats, a single infusion of G1 after induction of transient global ischemia can rescue CA1 pyramidal neurons from cell death to a similar degree as E2 (Lebesgue *et al*., 2009, 2010; Etgen *et al*., 2011).

1.3.10: Could GPR30 have a role in mediating the estrogenic effects on glutamatergic synaptic transmission in the hippocampus?

For over 40 years it has been known that E2 can modulate glutamatergic synaptic transmission and yet the mechanisms by which E2 exerts its actions, and the roles for the receptors responsible still have not been fully described or elucidated.

If GPR30 is involved in the E2-induced effects on excitatory hippocampal synaptic transmission then there should be evidence which suggests:

1) Estrogenic effects involve G-protein signalling:
    - The classic study by Gu and Moss (1996) elegantly demonstrates that E2-induced enhancement of kainate induced-currents (predominately AMPAR-mediated) in CA1 neurons requires a G-protein dependant cAMP-mediated phosphorylation event.

2) Estrogenic effects cannot be explained purely via activation of extra-nuclear / synaptic ERα and/or ERβ:
    - Rapid estrogenic effects are still observed in hippocampi of ERα (Gu *et al*., 1999; Fugger *et al*., 2001) and ERβ (reviewed in Foster, 2012) knockout mice.
3) GPR30 is expressed in the hippocampus
    - See section 1.2.5

Thus, it is highly feasible that this receptor may be involved in estrogenic effects on glutamateric synaptic transmission.

1.4: Aims

Thus the aims of this study were to:

1) Firstly, clarify the cellular localisation of GPR30 in hippocampal neurons and glia from rodents;
2) Establish a model for examining effects of the GPR30 agonist (G1) on CA3 - CA1 glutamatergic synaptic transmission;
3) Characterise the G1-induced effects and compare them with E2;
4) Use pharmacological tools and genetic manipulation to validate the receptor/s responsible for G1-induced effects.

Chapter Two

Materials and Methods

2.1: Materials

2.1.1: Reagents

Calcium chloride ($CaCl_2$), D-(+)-Glucose, dimethyl sulphoxide (DMSO), glycine, 4-(2-hydroxyethyl) piperazine-1-ethanesulfonic acid (HEPES), papain (from papaya latex), paraformaldehyde, potassium chloride (KCl), sodium bicarbonate ($NaHCO_3$), sodium phosphate monobasic monohydrate (NaH_2PO_4) and sucrose were obtained from Sigma Aldrich Company Ltd (Dorset, United Kingdom). Magnesium chloride ($MgCl_2$) was obtained from VWR International Ltd (Leicestershire, United Kingdom). Magnesium sulphate ($MgSO_4$) and sodium chloride (NaCl) were obtained from Fisher Scientific UK Ltd (Loughborough, United Kingdom). Triton X-100 was obtained from BDH laboratory supplies (Poole, United Kingdom).

Table 2.1: Pharmacological Tools

Compound	Source	Vehicle	Stock concentration
17β-Estradiol (E2)	Sigma Aldrich	DMSO	10 mM
Adenosine	Sigma Aldrich	aCSF	N/A
Brefeldin A	Sigma Aldrich	DMSO	10 mM
D-AP5	Ascent Scientific	dH_2O	50 mM
G1	Tocris Bioscience	DMSO	10 mM
G15	Tocris Bioscience	DMSO	10 mM
G36	Kind gift from Prof. JB Arterburn, University of New Mexico Heath Sciences Centre, Alburquerque, USA	DMSO	10 mM
ICI 182,780	Ascent Scientific	DMSO	10 mM
LY 341495	Tocris Bioscience	DMSO	10 mM
LY 294002	Ascent Scientific	DMSO	10 mM
MPP Dihydrochloride	Tocris Bioscience	dH_2O	5 mM
PD98059	Tocris Bioscience	DMSO	25 mM

PHTPP	Tocris Bioscience	DMSO	10 mM
U0124	Calbiochem	DMSO	5 mM
U0126	Abcam	DMSO	5 mM
Wortmannin	Calbiochem	DMSO	500 µM

Table 2.2: Primary antibodies for immunocytochemistry

Antibody	**Species (clone)**	**Source**	**Dilution**
Anti-rGluA1	Sheep (polyclonal)	In house	1:100
Anti-hGPR30	Goat (polyconal)	R&D Systems	1:500
Anti-hGPR30	Rabbit (polyclonal)	Abcam	1:300 or 1:1000
Anti-KDEL	Mouse (monoclonal)	Abcam	1:200
Anti-MAP2	Mouse (monoclonal)	Sigma-Aldrich	1:1000
Anti-c-Myc	Sheep (polyclonal)	In house	1:1000
Anti-synapsin1	Rabbit (polyclonal)	Sigma-Aldrich	1:250
Anti-TGN-46	Mouse (monoclonal)	Abcam	1:200

Table 2.3: Secondary antibodies for immunocytochemistry

Antibody	**Source**	**Dilution**
Alexa Fluor 488-conjugated donkey anti sheep	Invitrogen	1:250–1:500
Alexa Fluor 488-conjugated donkey anti mouse	Invitrogen	1:500
Alexa Fluor 488-conjugated donkey anti rabbit	Invitrogen	1:500
Alexa Fluor 555-conjugated donkey anti mouse	Invitrogen	1:500
Alexa Fluor 555-conjugated donkey anti rabbit	Invitrogen	1:500

Cy3-conjugated donkey anti goat	Jackson Immuno Research	1:500
Alexa Fluor 546-conjugated phalloidin	Intvitrogen	1:250

2.1.2: Cell culture material

Dulbecco's Modified Eagle's Medium: Nutrient Mixture F-12 (1:1 DMEM-F12), Dulbecco's Phosphate-Buffered Saline (DPBS), Neurobasal-A Medium and B-27 supplement were obtained from Gibco, Life Technologies Ltd. (Paisly, United Kingdom). Trypsin-EDTA solution, L-glutamine solution, and poly-d-lysine were obtained from Sigma Aldrich Company Ltd. (Dorset, United Kingdom). Sterile, heat inactivated EU-approved Foetal Bovine Serum (FBS) was obtained from Sera Laboratories (West Sussex, United Kingdom). Glass coverslips 9mm and 13mm diameter were obtained from VWR International Ltd. (Leicestershire, United Kingdom). Lipofectamine 2000 transfection reagent and Opti-MEM reduced serum media were obtained from Invitrogen, Life Technologies Ltd. (Paisly, United Kingdom).

2.1.3: Genetic Material

The OriGene Myc-DDK-tagged ORF clone of *Rattus norvegicus* G protein-coupled estrogen receptor 1 (rGPR30-myc) cloned into a pCMV6 vector was obtained from Insight Biotechnology Ltd. (RR201182; Middlesex, United Kingdom). ON-TARGET plus SMART pool rat GPER (GPR30) siRNA (L-093123-02-0005), rat Gria-1 (GluA1) siRNA (L-097755-02-0005) and human GPR55 siRNA (L-005581-00-0005) were obtained from Thermo Fisher Scientific, Inc. (Waltham, United States).

2.1.4: siRNA target sequences

hGPR55 siRNA SMARTpool:

Target sequence: J-005581-09	GCUACUACUUUGUCAUCAA
Target sequence: J-005581-08	AAGAACAGGUGGCCCGAUU
Target sequence: J-005581-07	GAGAAACAGCUUUAUCGUA
Target sequence: J-005581-06	GAAUUCCGCAUGAACAUCA

rGPER siRNA SMARTpool:

Target sequence: J-093123-08	GCAGUCAGAUGUCAAGUUC
Target sequence: J-093123-07	GACGAGCAGUAUUACGAUA
Target sequence: J-093123-06	GGGACAAGCUCAGGCUGUA
Target sequence: J-093123-05	GGAUGAGCUUCGACAGGUA

rGria-1 siRNA SMARTpool:

Target sequence: J-097755-12	GCAGUCAGAUGUCAAGUUC
Target sequence: J-097755-11	GACGAGCAGUAUUACGAUA
Target sequence: J-097755-10	GGGACAAGCUCAGGCUGUA
Target sequence: J-097755-09	GGAUGAGCUUCGACAGGUA

2.2: Methods

2.2.1: Cell maintenance and generation of primary cultures

2.2.1.1: HEK-293 cell maintenance

Human embryonic kidney 293 (HEK-293) cells were maintained in DMEM-F12 media, supplemented with 10 % FBS and 2 mM L-glutamine in 25 cm^2 cell culture treated flasks (Greiner Bio-One Ltd., Stonehouse, UK) at 37°C and 95 % O_2 / 5 % CO_2. Once cells had reached 80 – 90 % confluency, they were rinsed twice with calcium and magnesium free DPBS and exposed to 0.5 – 1 ml Trypsin-EDTA solution. Once cells

had detached, 3 ml of maintenance media was added and cells were passaged at a v/v ratio of 1:5. For experimental purposes, cells were plated onto sterile glass coverslips (9 mm diameter) coated with poly-d-lysine (20 µg/ml in sterile dH_2O for 1 hour) in sterile vented cell culture dishes (35 mm or 145 mm diameter; Greiner Bio-One Ltd., Stonehouse, UK) and left overnight at 37°C and 95 % O_2 / 5 % CO_2 in maintenance media, before transfection.

2.2.1.2: Primary culture of rat hippocampal neurons

Neonatal Sprague-Dawley rats (postnatal days (P) 1 - 2) were sacrificed by cervical dislocation in accordance with Schedule 1 of the UK Scientific Procedures Act, 1986. After decapitation, hippocampi were dissected out and washed with ice-cold HEPES buffered saline (HBS) containing (in mM): NaCl 135; KCl 5; $CaCl_2$ 1; $MgCl_2$ 1; HEPES 10; D-glucose 25, at pH 7.4. Tissue was finely chopped, suspended in HBS supplemented with 1.5 mg/ml papain and incubated at 37ºC for 20 min. Tissue was then transferred into 1 ml fresh HBS and triturated with a series of flame-polished glass pasture pipettes of decreasing diameter, until cells were dissociated. The cell suspension was then centrifuged at 1,200 x g for 3 min, supernatant was discarded and the remaining cell pellet was resuspended in neuronal culture medium consisting of: Neurobasal-A culture medium supplemented with 2 % (v/v) B-27 and 2 mM L-glutamine, at a density of 5 x 10^5 cells/ml. Cells were then plated onto sterilized glass coverslips (13 mm diameter) coated with poly-d-lysine (20 µg/ml in sterile dH_2O; for at least 1 hour) at a density of 3.76 x 10^4 cells/cm^2 in sterile vented cell culture dishes (35 mm diameter; Greiner Bio-One Ltd., Stonehouse, UK). Cultures were incubated at 37ºC in a humidified atmosphere of 5% CO_2 and 95% O_2 for one hour to allow the cells to settle onto the coverslips. After settling, cultures were removed from the incubator, and 2 ml of neuronal culture medium (as above) was added. Cultures were then returned to the incubator for up to 3 weeks. It is worth noting here that neurobasal culture medium is a serum- and estrogen- free media containing inorganic slats, glucose, HEPES, vitamins and amino-acids and supplementation with B-27 supports the growth and survival of neurons without the need for addition of serum (Brewer *et al*., 1993). Moreover, B-27 supplementation inhibits the proliferation of glia, thus the use of the Neurobasal/B-27 combination should, in theory, enable an almost pure neuronal culture (Brewer *et al*., 1993).

2.2.2: Incorporation of genetic material

2.2.2.1: Transient Transfection of HEK-293 cells

Adhered HEK-293 cells on coverslips were transferred into serum free media (DMEM-F12 media supplemented with 2 mM L-glutamine) and transiently transfected using Lipofectamine 2000. Briefly, 2 µl Lipofectamine 2000 reagent was diluted in 48 µl Opti-MEM, and ~2 µg of hGPR30-SEP or rGPR30-myc cDNA was diluted in Opti-MEM (final volume 50 µl) and left for 5 min at room temperature. The lipofectamine 2000 - Opti-MEM and cDNA- Opti-MEM solutions were then combined (total volume 100 µl), mixed gently and incubated for 20 min at room temperature to allow the DNA-lipofectamine 2000 complexes to form. 100 µl of the transfection complex was added to the HEK-293 cells in serum free media, mixed gently and incubated at 37 °C and 95 % O_2 / 5 % CO_2 for 12 - 24 hours to allow for protein expression.

2.2.2.2: siRNA treatment of hGPR55-HEK-293 cells

The hGPR55-HEK-293 cell line are a stable cell line expressing hGPR55 with a triple hemagglutinin epitope (HA) at the N-terminus, generated as described in Henstridge *et al*., (2009). Adhered cells on coverslips were transferred into serum free media (DMEM-F12 media supplemented with 2 mM L-glutamine) and transfected with On-TARGETplus SMARTpool hGPR55 or rGPR30 siRNA (100 nM) using Dharmafect 1 (Thermo Fisher Scientific, Inc). Briefly, 3 µl Dharmafect 1 was diluted in 97 µl serum free media and 5 µl siRNA was diluted in 95 µl serum free media (from a 20 µM stock concentration, to a final concentration of 100 nM in a total 1 ml serum free media) and left for 15 min at room temperature. The Dharmafect 1 solution and the siRNA solution were then combined and gently mixed (200 µl), and left for 20 min at room temperature to allow for Dharmafect 1 and siRNA complexes to form. Coverslips were placed into 800 µl serum free media and the Dharmafect 1 and siRNA complex solution was added to hGRP55-HEK cells in a drop wise manner and gently mixed. Cells were incubated at 37 °C and 95 % O_2 / 5 % CO_2 for 68 – 72 hours to allow for efficient knockdown.

2.2.2.3: siRNA treatment of primary cultured rat hippocampal neurons

Primary cultures of rat hippocampal neurons 5 days *in vitro* (DIV) were transfected using with On-TARGETplus SMARTpool hGPR55, rGPER or rGria1 siRNA (100 nM) using Dharmafect 1 (Thermo Fisher Scientific, Inc), as described above (2.2.2.2). However, with the following modification: in place of serum free media, cells were transfected in and maintained in fresh maintenance media (Neurobasal-A culture medium supplemented with 2 % (v/v) B-27 and 2 mM L-glutamine). Cells were then incubated at 37°C and 95 % O_2 / 5 % CO_2 for 46 – 96 hours.

2.2.3: Immunocytochemistry

2.2.3.1: HEK-293 Cells: GPR30 localisation and co-staining

Transfected HEK-293 cells were removed from the incubator and washed three times in 2 ml pre-warmed HBS (37ºC) containing (in mM): NaCl 135; KCl 5; $CaCl_2$ 1; $MgCl_2$ 1; HEPES 10; D-glucose 10, at pH 7.4. Cells were fixed with 4% paraformaldehyde (PFA) containing 200 mM sucrose, and permeabilized with 0.2% Triton X-100 in HBS (5 - 10min) at room temperature. To validate antibodies against the tagged receptor, cells were washed and labelled with either anti-hGPR30 (R+D systems; 1:500 in HBS for 1 hour at room temperature) or anti-hGPR30 (Abcam; 1:300 or 1:1000 in HBS for 3 hours or overnight, respectively at 4 ºC). GPR30 antibody staining was visualised by addition of Alexa-555-conjugated donkey anti-rabbit secondary antibody or Cy3-conjugated donkey anti-goat secondary antibody (1:500 in HBS for 30min at room temperature). For cells transiently transfected with rGPR30-myc, localisation of the tagged protein was determined by labelling with a primary antibody directed against the c-terminus-myc tag (sheep anti-myc; in house antibody against synthetic peptide AEEQKLISEEDLL; 1:1000 in HBS for 1 hour at room temperature) and visualised by addition of Alexa-488-conjugated donkey anti-sheep secondary antibody (1:500 in HBS for 30min at room temperature). In some cases, GPR30 localisation in transfected cells was determined using intracellular markers; mouse anti-KDEL (1:200 in HBS for 3 hours at 4 ºC) and visualised by addition of Alexa-555-conjugated donkey anti-mouse secondary antibody (1:500 in HBS for 30 min at room temperature) or Alexa-fluor 546 conjugated phalloidin (1:250 in HBS for 30 min at room temperature) . In some cases

transfected HEK-293 cells were subjected to drug treatment (30min – 2 hours at 37 ºC in HBS) before fixation, permeabilization and staining.

2.2.3.2: Total hGPR55 staining of hGRP55-HEK-293 cells after siRNA treatment

Knockdown of hGPR55 protein expression using the same protocol and target siRNA sequences has been previously described in our laboratory (Henstridge, *unpublished*), therefore this protocol was utilised as a positive control, to validate efficiency of siRNA. After 68 – 72 hours siRNA treatment, hGPR55-HEK-293 cells were fixed with 4 % PFA containing 200 mM sucrose (10 min, room temperature) and permeabilized with 0.2% Triton X-100 in HBS (5 - 10min, room temperature). Cells were then labelled with a primary antibody against HA (1:1000 in HBS; 1 hour; room temperature) followed by Alexa-488-conjugated donkey anti-mouse secondary antibody (1:500; 30 min; room temperature). Cells were imaged as detailed below (see section 2.2.7.6). Efficient protein knockdown was confirmed as whole cell HA-staining was dramatically reduced in hGPR55 siRNA treated cells (Fig 2.1)

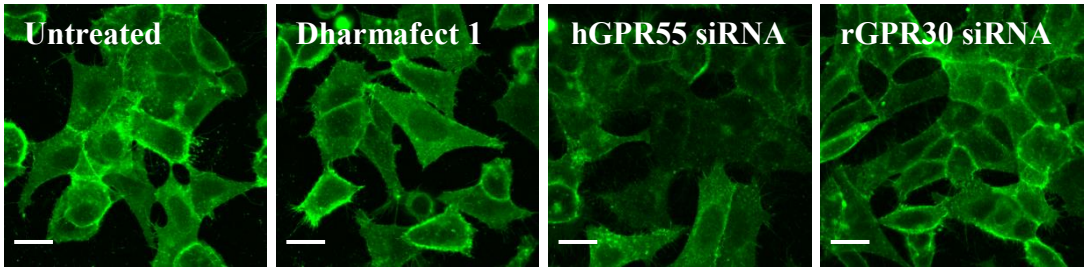

Figure 2.1: siRNA against hGPR55 reduces total hGPR55 expression in hGPR55-HEK-293 cells. Cells were treated with siRNA for hGPR55, rGPR30 or Dharmafect-1 alone for 68 – 72 hours in serum-free media, scale bars 20 µM. Images represent 3 individual experiments, *conducted in collaboration with June Penman.*

2.2.3.4: Primary cultured rat hippocampal neurons: GPR30 localisation and co-staining

Primary hippocampal neurons (DIV 8 – 16) were removed from the incubator and washed three times in 2 ml HBS containing glycine (0.01mM; room temperature). Cells were fixed with 4% PFA containing 200 mM sucrose, and permeabilized with 0.2 % Triton X-100 in HBS (5 - 10min) at room temperature. Neurons were washed and labelled with anti-hGPR30 (Abcam; 1:300 or 1:1000 in HBS for 3 hours or overnight, respectively, at 4 ºC), followed by intracellular markers; mouse anti-KDEL, mouse anti-TGN-46 (1:200 in HBS for 3 hours at 4 ºC), Alexa-fluor 546 conjugated phalloidin (1:500 in HBS for 30 min at room temperature) or rabbit anti synapsin-1 (1:250 in HBS for 30 min at room temperature). GPR30 staining was visualised by addition of Alexa-488-conjugated donkey anti-rabbit secondary antibody (1:500 in HBS for 30min at room temperature) and staining of the intracellular markers was visualised by addition of Alexa-555-conjugated donkey anti-mouse or donkey anti-rabbit secondary antibody (1:500 in HBS for 30min at room temperature). In some cases neurons were subjected to drug treatment (30min – 2 hours at 37 ºC in HBS) before fixation, permeabilization and staining. A marker for microtubule-associated protein 2 (mouse anti-MAP2; 1:1000 in HBS for 1 hour at room temperature) was utilized to distinguish between neuronal and non-neuronal cells (Izant and McIntosh, 1980; Dehmelt and Halpain, 2005) and visualised by the addition of Alexa-555-conjugated donkey anti-mouse secondary antibody (1:500 in HBS for 30 min at room temperature).

2.2.3.5: Primary cultured rat hippocampal neurons: Surface GluA1 staining after drug treatment

Primary hippocampal neurons (DIV 8 – 16) were removed from the incubator and washed three times in 2 ml HBS containing glycine (0.01 mM). Neurons in HBS were allowed to equilibrate to room temperature (10 min) and then subjected to drug treatment (21 - 23 ºC). As most agents, including E2 and G1, were solubilised in DMSO (see table 2.1), control cultures (vehicle treated) were always treated with an equivalent volume of DMSO (either 0.01 % or 0.1 % of the final volume, as indicated). For inhibitor/antagonist experiments, neurons were pre-treated for the indicated times before addition of E2 or G1. After drug treatment, living neurons were gently washed with HBS and labelled with primary antibody directed against the N-terminal region of the

GluA1 subunit of cell surface AMPA-receptors (Sheep anti-GluA1; in house antibody against synthetic peptide RTSDSRDHTRVDWKR corresponding to 253 - 267 residues of rat GluA1; Pickard *et al*., 2001) 1:100 in HBS for 30 minutes at 4ºC. Cells were then washed with HBS and fixed with 4 % PFA containing 200 mM sucrose for 5 - 10 min at room temperature. Surface GluA1 staining was visualized by addition of Alexa 488-conjugated donkey anti-sheep secondary antibody (1:250 in HBS for 30 min at room temperature). To compare surface GluA1 expression relative to synapsin-1 labelling, after fixation, cells were permeablized with 0.2% Triton X-100 in HBS (5 – 10 min) and labelled with primary antibody against synapsin-1 (rabbit anti-synapsin-1; 1:250 in HBS for 30 min at room temperature). Synapsin-1 is phosphoprotein which associates with the cytoplasmic surface of synaptic vesicles, the synapsin family has a role in the formation and maintenance of synaptic contacts, thus antibodies directed against this protein can be used as a marker for synapse location (Südhof, 1990; Ferreira and Rapoport, 2002). Synapsin-1 labelling was visualised by addition of Alexa-555 conjugated donkey anti-rabbit secondary antibody (1:500 in HBS for 30 min at room temperature). No staining was observed after incubation with either secondary antibody alone (30 min).

2.2.3.6: Image Acquisition for immunocytochemistry

Cells were imaged using a Zeiss LSM510 laser scanning confocal microscope. Laser lines (488 and 543 nm) were used to excite the Alexa-488 and Alexa-555/ Alexa-546 / Cy3 fluorphores, respectively. Dual labelling images were obtained in multi-tracking mode using a 15 s scan speed. Images of at least four randomly selected cells for each condition were collected. For surface GluA1 staining of hippocampal neurons, all data were obtained from at least three different cultures from different animals. For GPR30 localisation studies, data from hippocampal neurons and HEK-293 cells were obtained from at least two different cultures from different animals or cell passages. Within a given experiment, all imaging conditions were kept constant; including illumination intensity and photomultiplier gains.

2.2.3.7: A note about phenol red containing media

Media used for all cell culture in this thesis contained phenol red, a pH indicator. Phenol red has putative estrogenic activity in estrogen responsive cancer cell lines, particularly in MCF-7's (a breast cancer cell line that is GPR30 positive), and competes with estradiol in binding studies of cytosolic estrogen receptor (Welshons *et al*., 1988). Therefore, to ensure that the presence of phenol red does not affect GPR30 expression in our studies, hGPR30-SEP and rGPR30-myc were transfected into HEK-293 cells and plated in phenol red or phenol red free media. Fig. 2.1 illustrates that the intracellular distribution of human and rat GPR30 is not affected by the presence of phenol red.

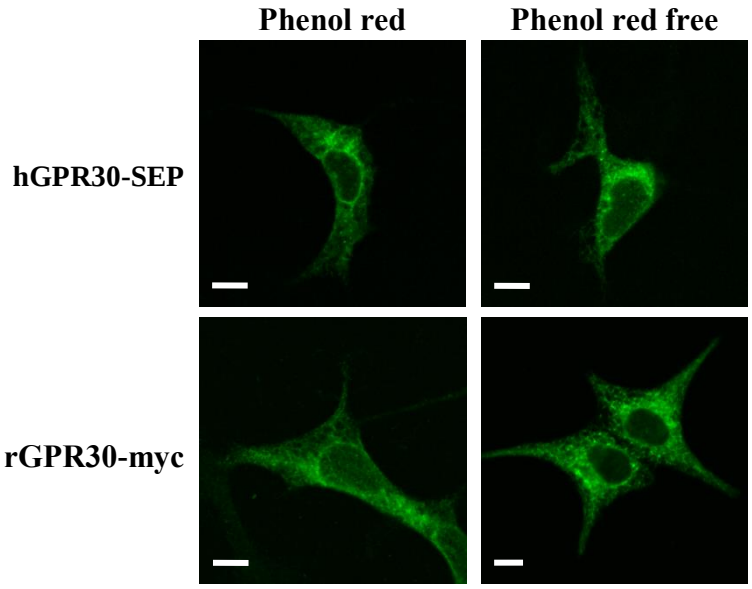

Figure 2.2: The presence of phenol red in cell culture media does not affect the intracellular expression pattern of GPR30. *Images represent at least 2 individual experiments, scale bars 10 µm.*

2.2.4: Electrophysiology

2.2.4.1: Animal care

Sprague-Dawley rats were housed under a 12 hour light/dark cycle and had access to food and water *ad libitum.* After weaning, male rats were caged with male litter mates (3-4 animals per cage). All efforts were made to minimise the number of animals used and their suffering.

2.2.4.2: Hippocampal slice preparation

Male Sprague-Dawley rats aged P11 - 18 or three to five months (12 -20 weeks) were either sacrificed by cervical dislocation (P11-18) or anaesthetized with isoflurane until unconscious and then sacrificed by decapitation (12-20 weeks) in accordance with the UK Scientific Procedures Act, 1986. Following decapitation, the brain was carefully removed and placed into oxygenated (95 % O_2/ 5% CO_2 ; pH 7.4) ice-cold modified high-sucrose artificial cerebral spinal fluid (aCSF) containing (in mM): Sucrose 75; NaCl 87; KCl 2.5; $NaHCO_3$ 26; NaH_2PO_4 1.25; $MgSO_4$ 7; $CaCl_2$ 0.5 and D-glucose 10. The brain was then placed onto filter paper soaked in the above solution and the cerebellum, olfactory bulbs and a small portion of the lateral sides of the cortex were removed. The brain was cut down the intrahemispheric fissure and parasagittal hippocampal slices (350 µm) were cut using a Campden Instruments 7000 smz vibrating microtome (Campden Instruments Ltd., Loughborough, UK). Slices were allowed to recover in a holding chamber containing aCSF (in mM): NaCl 124; KCl 3; $NaHCO_3$ 26; NaH_2PO_4 1.25; $MgSO_4$ 1; $CaCl_2$ 2 and D-glucose 10, oxygentated (95 % O_2/ 5% CO_2 ; pH7.4) and at 33-34 ºC for at least one hour.

2.2.4.3: Basal synaptic transmission

Hippocampal slices were transferred to a submerged recording chamber perfused with oxygenated (95% O_2/ 5% CO_2; pH7.4) aCSF (5 - 6ml.min^{-1}; 31-32 ºC). Extracellular field excitatory postsynaptic potentials (fEPSPs) were recorded from dendrites of pyramidal neurons of the *stratum radiatum* layer in area CA1 using glass microelectrodes (Harvard Apparatus Ltd, Kent, UK) filled with aCSF (resistance = ~1MΩ). Responses were evoked by stimulation of the Schaffer collateral-commissural (Scc) pathway using a handmade bi-polar electrode (twisted nickel-chromium wire) at a frequency of 0.0333 Hz from a constant voltage isolated stimulator (DS2A-MKII, Digitimer Ltd., Hertfordshire, UK) at a stimulus intensity that produced a 40 - 60% maximal response. Figure 2.3 depicts the positioning of electrodes in hippocampal slices and Figure 2.4 illustrates an example fEPSP, and the parameters of which were recorded. Recordings were made using an Axopatch 200B patch clamp amplifier (Molecular Devices, Sunnyvale, CA, USA), and data were low pass filtered at 2 kHz. Electrical signals were recorded and monitored using the WinLTP software (courtesy of Dr. Bill Anderson, University of Bristol, Bristol, UK: Anderson and Collingridge,

2001). Both the peak amplitude and initial slope of the fEPSP were monitored; stable responses for at least 20 min were required before application of any agents. A baseline was considered stable when response amplitude and slope were neither ramping up, ramping down nor varying drastically between two consecutive stimuli, this was determined by eye. If the responses from a slice were not stabilising after one hour of recording, then the slice was discarded. Using these criteria for determining stability, the magnitude of the fEPSP slope and amplitude can remain stable for up to 3 hours (the longest recording made without application of any agents).For experiments conducted in low Mg^{2+} aCSF (0.1 mM), a stable baseline was generated in normal aCSF for at least 10 min before low Mg^{2+} aCSF was perfused over the slice. Perfusion of low Mg^{2+} aCSF greatly enhanced fEPSP slope and amplitude measurements compared to baseline transmission and so in response to this enhancement, stimulus voltage was decreased in order to prevent hyper excitability, and population-spike generation. Stimulus intensity was reduced to a level approximating 50% maximal response amplitude under normal conditions. A 20 min stable baseline in these conditions was required before application of any agents. Pharmacological agents were diluted from stock solutions (Table 2.1) into oxygenated aCSF immediately before perfusion over the slice. For each set of experiments, each *n* value was obtained from a slice from a different animal.

2.2.4.4: Paired-pulse facilitation

For experiments using the paired-pulse stimulation protocol, a stable baseline was recorded for at least 10min before the stimulation protocol was initiated. The protocol consisted of two identical stimuli separated by a 50ms inter-stimulus interval at a frequency of 0.0333 Hz and was maintained throughout the duration of the experiment.

Paired-pulse facilitation is a type of short term, activity-dependant synaptic plasticity and is manifested by an enhancement of a second post-synaptic response, when shortly (20 – 200 ms) preceded by a first. It is classically accounted for by the residual calcium hypothesis of Katz and Miledi, (1968). The paired-pulse facilitation ratio (PPR) can be used to quantify this effect, and is determined by the amplitude of the second response divided by the first (see section 2.2.5.2). Changes in the PPR traditionally reflect changes in presynaptic neurotransmitter release probability (where the PPR is inversely proportional to the initial release probability).

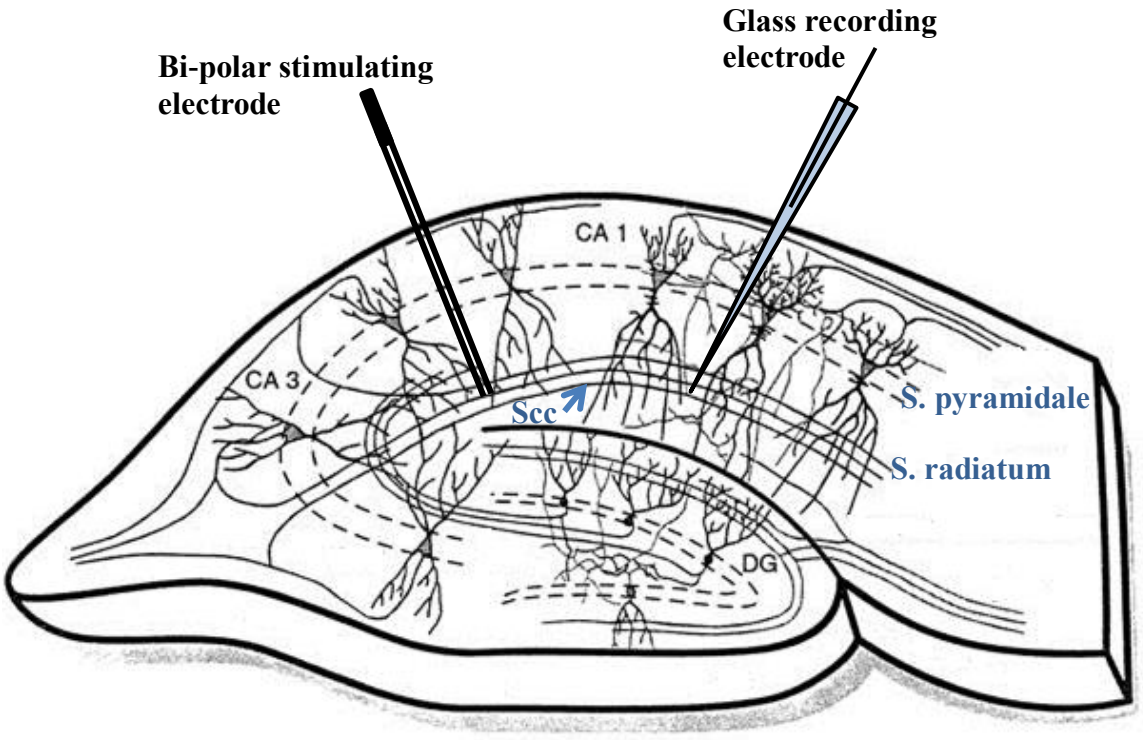

Figure 2.3: Cartoon of a parasagittal hippocampal slice from rat. The cartoon depicts the positioning of the bi-polar stimulating electrode and glass recording electrode within the rat hippocampal slice. The Schaffer collateral-commissural (Scc) pathway from CA3 provides glutamatergic synaptic input to dendrites of pyramidal and inhibitory neurons in area CA1.

Figure modified from Nishikawa and MacIver (2000)

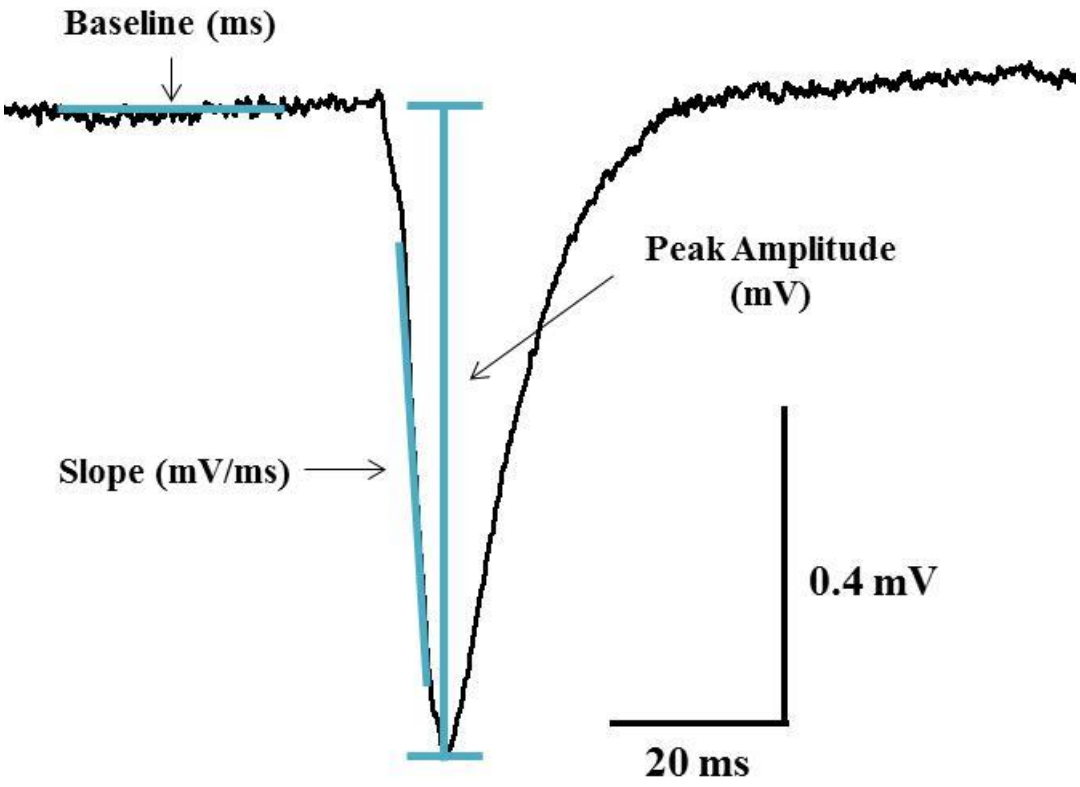

Figure 2.4: Example of an extracellular field excitatory post-synaptic potential (fEPSP) recorded from hippocampal region CA1. The fEPSP is generated from simultaneous depolarisation of the dendritic field from a population of CA1 pyramidal neurons. A negative potential is recorded, as positive ions flow into post-synaptic membranes away from the extracellular recording electrode. The peak amplitude of the fEPSP and the initial slope of the fEPSP are measured. However, the peak amplitude of the fEPSP can be contaminated with population spikes or population inhibitory post-synaptic potentials (pIPSPs). Therefore, the slope of the response is used for analysis as this is a more accurate representation of excitatory synaptic transmission.

2.2.5 Data Analysis

2.2.5.1 : Surface GluA1 expression and Synapsin-1 co-localisation

For surface GluA1 expression, fluorescence intensity of staining was determined offline using LSM Image Browser software, where three analysis lines of 50 µm were drawn along randomly selected dendritic regions from each cell image. Data was transferred to SigmaPlot11.0 (Systat Software Inc.) and mean fluorescence intensity was calculated. In order to quantify experimental data from separate experiments, data were normalized relative to mean fluorescence intensity of vehicle treated neurons. For co-localisation studies, surface GluA1 staining was compared with synapsin-1 staining. Percentage of surface GluA1 at synapses was calculated as number of GluA1-positive puncta that co-localised with synapsin-1-positive puncta and expressed as a percentage relative to the total amount of synapsin-1-positive puncta (Moult *et al*., 2010). To quantify synapse number across treatments, the number of synapsin-1-positive puncta were counted along each 50 µm analysis line and normalised relative to vehicle treated neurons. All statistical analyses were carried out using SigmaPlot 11.0 (Systat Software Inc.). A one-way Analysis of Variance (ANOVA) was performed to test for significance between treatment groups. Tukey *post-hoc* analyses were done only in the case of a significant ANOVA. If data failed normality or equal variance tests then a Kruskal-Wallis one-way ANOVA on ranks was performed, followed by a Dunn's *post-hoc* analysis, as noted. All data are expressed as mean ± standard error of mean (SEM) and $p < 0.05$ was considered statistically significant. *n* represents the total number of neurites assessed in each treatment group.

2.2.5.2: Electrophysiology analysis

Data were analysed off-line using the WinLTP reanalysis software (Anderson and Collingridge, 2001). Data was transferred to SigmaPlot 11.0 (Systat Software Inc.) and a mean of the raw fEPSP slope measurements ($mVms^{-1}$) from the 20min baseline were obtained. Data were transformed to a per cent of mean baseline measurements. Transformed data were then averaged with corresponding experiments and plotted against time, each data point represents mean ± standard error mean (SEM) for a given set of experiments. The paired-pulse facilitation ratio (PPR) was calculated as a ratio of

the amplitude of the second fEPSP relative to the amplitude of the first fEPSP (PPR = $_{amp}$fEPSP2/$_{amp}$fEPSP1).

All statistical analyses were carried out using SigmaPlot 11.0 (Systat Software Inc.) The degree of potentiation or depression was calculated as a mean of normalised fEPSP slope measurements from a 5 min period at a given time point and compared with baseline values. The time points taken and averaged for each slices were as follows: baseline values were taken as the 5 min period before the addition of any agents; antagonist values as the 5 min before the addition of any further agents; values for agonist effect were taken as the 5 min period before agonist washout; washout effects were taken as the 5 min period before termination of the experiment. Using these values, the effects of agents on normalised fEPSP slope or the PPR were analysed using a one-way repeated measures ANOVA or paired t-test, where appropriate. Thus, the data used for statistical comparisons were the means of each of the 5 min time periods (as above) for each slice. In this respect, data was analysed as "raw data". With respect to the data subjected to one-way repeated measures ANOVA, baseline, post-drug and washout values were included in the analyses.

Pairwise Tukey *post-hoc* tests were used in the case of a significant ANOVA. For comparison between means of different experimental groups, a one-way ANOVA was performed, followed by pairwise Tukey *post-hoc* analysis. If data failed normality or equal variance tests then a Kruskal-Wallis one-way ANOVA on ranks was performed, followed by pairwise Dunn's *post-hoc* analysis, as noted.

2.2.5.3: Stratification of fEPSP recordings

It was noted that G1 and E2 elicited different response profiles during ligand application and washout (see Chapter 4). For each slice, data was subsequently separated into one of three different response types, biphasic, depression only and sustained potentiation, according to the following criteria:

Biphasic: the normalised mean of the 5 min period during agonist application before washout (*ie:* 15 – 20 min of agonist application) was at least 4 % greater than baseline and the mean final 20 min of the washout phase (*ie:* 40 – 60 min after agonist washout) was below at least 4 % below baseline. Depression only: the normalised mean of the 5

min period during agonist application before washout (*ie:* 15 – 20 min of agonist application) was < 4 % of baseline (100 %), a lack of potentiation during agonist application and washout, and the mean final 20 min of the washout phase (*ie:* 40 – 60 min after agonist washout) was at least 4 % below baseline. Sustained potentiation: the normalised mean of the 5 min period during agonist application before washout (*ie:* 15 – 20 min of agonist application) was at least 4 % greater than baseline and the mean final 20 min of the washout phase was also at least 4 % greater than baseline.

2.2.5.4: Relative GPR30 and total GluA1 fluorescence after siRNA treatment

Fluorescence intensity of GPR30 staining or total GluA1 staining in primary hippocampal neurons after siRNA treatment were analysed using ImageJ, image analysis software. A region of interest (ROI) for analysis was selected for each neuron and the following parameters were recorded: area, mean grey value (mean fluorescence intensity) and integrated density. Corrected fluorescence intensity was calculated using the following equation:

Corrected fluorescence intensity = integrated density value for the ROI – (area of ROI x mean fluorescence value of background)

This type of analysis takes into consideration the fluorescent intensity of the ROI with respect to its area. See: *http://sciencetechblog.com/2011/05/24/measuring-cell-fluorescence-using-imagej/*. This method for quantifying fluorescence intensity has been used previously by the following authors: Burgess *et al*., 2010; Gavet and Pines, 2010; Potapova *et al*., 2011.

In order to quantify experimental data from separate experiments, data were normalized relative to the mean corrected fluorescence values from neurons which were not subjected to siRNA treatment.

Chapter Three

GPR30 localisation

3.1: Introduction

GPCRs represent the largest family of integral membrane proteins, with over 800 GPCR genes identified within the human genome. GPCRs are a target for approximately 40 – 50% of clinically marketed drugs and so are of great commercial value to the pharmaceutical industry (Wheatley *et al*., 2012). As worldwide life-expectancy rises, so does the incidence of age-related neurological disorders, such as dementia and Alzheimer's disease (Gao *et al*., 1998). Estrogen has a diverse role in CNS; moreover animal studies show that estrogen has many beneficial effects within the brain (as reviewed in Frick, 2012). However, large randomized clinical trials in humans (such as the Women's Health Initiative Memory Study; WHIMS) suggest that estrogen therapy initiated later in life has no beneficial effect on cognition but rather increases the risk for dementia, stroke and mild cognitive decline (Shumaker *et al*., 2004). Therefore targeting novel estrogen-sensitive GPCRs, such as GPR30, may provide new therapeutics for these age-related disorders, without deleterious effects associated with hormone therapy.

Since the discovery of GPR30 as a putative estrogen-sensing receptor in 2005, the field has expanded rapidly, now with over 350 published articles examining its function. However, there is currently considerable debate over the cellular localisation, endogenous expression and even whether GPR30 functions as an estrogen receptor (for reviews see Langer *et al*., 2010; Maggiolini and Picard, 2010; Levin, 2011). Thus in order to investigate the function of this receptor and its potential as a therapeutic target, experimental models that best mirror the endogenous environment are employed. Rodent models present an invaluable tool in assessing GPCR function within the CNS, however species orthologs may have pronounced differences in expression profiles and pharmacology and hence overall function (for a review on this matter, see Strasser *et al*., 2013).

The cellular localisation of human GPR30 has long been a topic of controversy. Some groups report that GPR30 localisation is restricted to the endoplasmic reticulum and Golgi in heterologous (Revankar *et al*., 2005; Matsuda *et al*., 2008; Otto *et al*., 2008) and endogenously expressing cells (Brailoiu *et al*., 2007; Revankar *et al*., 2007; Sakamoto *et al*., 2007; Matsuda *et al*., 2008; Otto *et al*., 2008; Lin *et al*., 2009;

Takanami *et al*., 2010), and thus functions as an intracellular GPCR. Whereas others detect plasma membrane association in heterologous (Funakoshi *et al*., 2006; Filardo *et al*., 2007; Cheng *et al*., 2011a, 2011b; Sandén *et al*., 2011) and endogenously expressing cells (Funakoshi *et al*., 2006; Pang *et al*., 2008; Gao *et al*., 2011; Lindsey *et al*., 2011; Maiti *et al*., 2011), and functions as a classical plasma-membrane associated GPCR.

Although there is significant overall homology between human and rat GPR30 (see 3.2.1 and Pang *et al*., 2008), the N-terminus sequence (residues 1 – 62) between the two species differs dramatically (only 55% sequence identity). These differences could consequently direct the proteins to different cellular compartments, as there is evidence to suggest that, in addition to the C-terminus, the N-terminal region can also play a role in directing proteins to the plasma membrane (as reviewed in Dong *et al*., 2007).

Thus, as a prelude to investigating the role for GPR30 in modulating excitatory synaptic transmission in the rodent hippocampus, confocal imaging experiments were conducted in a heterologous expression system to compare the cellular localisation of human and rat GPR30. Furthermore, an antibody capable of recognising rat GPR30 was utilised to examine the endogenous cellular localisation of GPR30 in rat hippocampal neurons.

3.2: Results

3.2.1: Amino Acid sequence homology between human and rat GPR30

Amino acid sequences for hGPR30 and rGPR30 were aligned and compared. The predicted topological domains from hGPR30 (Q99527) and rGPR30 (O08878) were obtained from the protein knowledge database (UniprotKB; version 122 for hGPR30 and version 90 for rGPR30; modified on 3 April 2013).

Both hGPR30 and rGPR30 encode a 375 amino acid protein and share 86% sequence identity (Fig 3.1), with the N-terminus (residues 1 – 62) being the least conserved region with only 55% sequence identity. Three potential N-glycosylation sites (in red) were recognised in the N-terminal region for both rat and human GPR30 at residues 25, 32 and 44. Importantly, the DRY (Asp – Arg – Tyr) sequence (boxed) is conserved between rat and human. The DRY motif, located at the boundary between transmembrane domain 3 and intracellular loop 2, is typical of most Class A rhodopsin-like GPCRs (Rovati *et al*., 2007) and is thought to be involved in stabilising the inactive-state conformation (Rovati *et al*., 2007; Vogel *et al*., 2008; Rosenbaum *et al*., 2009). Conserved cysteine residues (130 and 207; purple) indicate a potential disulphide bond site. Disulphide bonds between extracellular loop 2 and the top of transmembrane 3 provide conformational constraint and are highly conserved in the majority of family A GPCRs (reviewed in Wheatley *et al*., 2012). Moreover, residues adjacent to the 207-cysteine in extracellular loop 2 are conserved between the two species and it is thought that this area is important for ligand binding in Class A receptors (reviewed in Wheatley *et al*., 2012).

These highly conserved structural defining regions suggest that both human and rat GPR30 share similar regions for potential post-translational modification, tertiary structure and ligand binding.

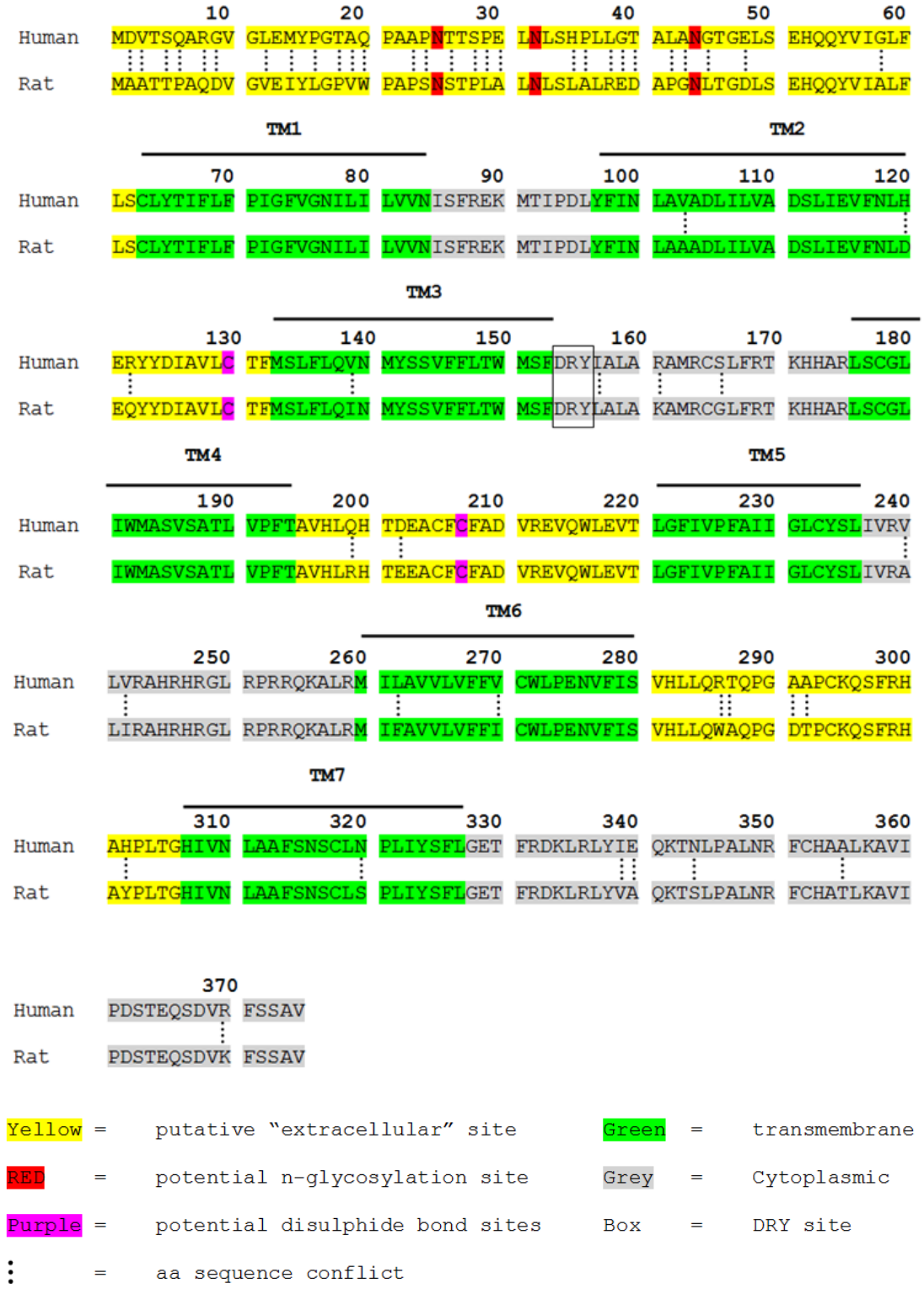

Figure 3.1: Amino acid sequence alignment of GPR30 from human and rat. Sequences were obtained from Uniprot Knowledge database and aligned. Both human and rat GPR30 gene products encode a 375 amino acid protein, and share 86% sequence identity.

3.2.2: Comparison of intracellular localisation

In order to investigate and compare the cellular localisations of hGPR30 and rGPR30, immortalised human embryonic kidney cells (HEK-293; Graham *et al*., 1977) were transiently transfected overnight with vectors containing hGPR30 with a C-terminus SEP tag or with rGPR30 with a C-terminus myc tag (see section 2.1.3) and examined using confocal microscopy. Preliminary confocal experiments revealed an intracellular localisation which resembled endoplasmic reticulum expression for both human and rat constructs. Dual-labelling studies were then employed to verify this expression pattern.

Dual labelling of hGPR30-SEP or rGPR30-myc (green) transfected HEK-293 cells, with an anti-KDEL antibody (red; an antibody specific for the ER retention signal sequence, Lys-Asp-Glu-Leu (KDEL); Munro and Pelham, 1987) revealed almost complete co-localisation (yellow) for both hGPR30-SEP and rGPR30-myc (Fig 3.2 A). In contrast, dual-labelling with a marker for polymerised F-actin (alexa-555 conjugated phalloidin; red) revealed no co-localisation (Fig 3.2 B). Conjugated phalloidin staining was used here to illustrate cell morphology (cytoskeleton) and to demonstrate the intracellular distribution of GPR30. Thus, these data suggest that when expressed in heterologous systems, both human and rat GPR30 localise to the endoplasmic reticulum. Moreover, the data presented here are in agreement with the reported distribution of hGPR30, heterologously expressed in either COS-7 cells (Revankar *et al*., 2005; Bologa *et al*., 2006; Otto *et al*., 2008; Dennis *et al*., 2009) or HEK-293 cells (Otto *et al*., 2008).

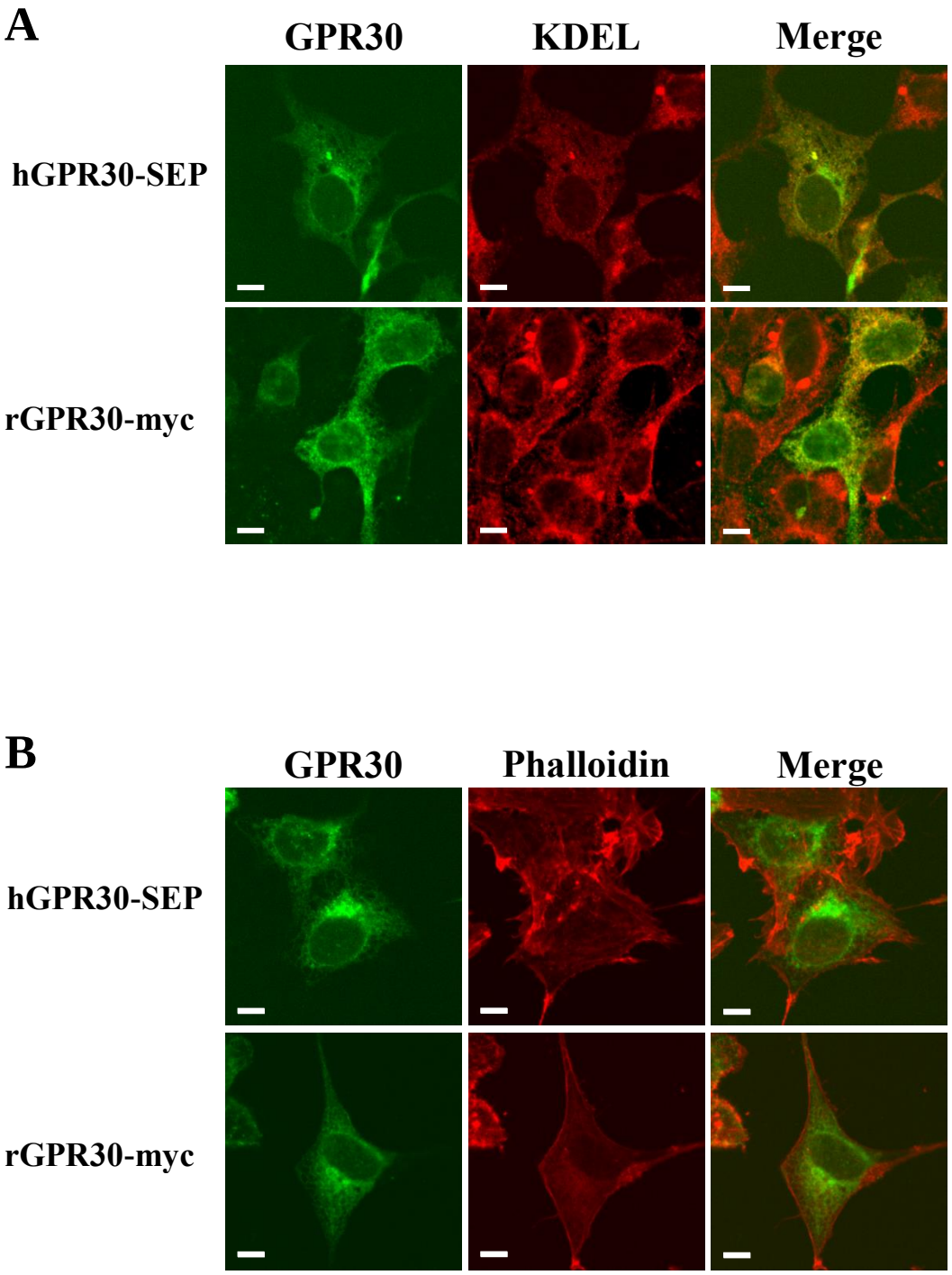

Figure 3.2: Intracellular expression of both human and rat GPR30 in transiently expressing HEK-293 cells. Representative confocal images illustrating HEK-293 cells transiently transfected with tagged human or rat GPR30 cDNA that were fixed and stained for GPR30 expression (green) and with organelle markers for endoplasmic reticulum (**A**; KDEL; red) and polymerised actin (**B**; F-actin; red), illustrating the cytoskeleton. Data are representative of at least two individual experiments. Scale bars, 10μm

3.2.3: Intracellular localisation of GPR30 is unaltered with specific agonists or antagonists

The localisation of a GPCR to intracellular compartments is atypical; however it is feasible that surface expression is very low and undetectable in our system, or it may be that GPR30 is functioning as an intracellular receptor. Cell surface expression of the human δ-opioid receptor (hδOR) is enhanced by pharmacological chaperones (agonists and antagonists of the hδOR), which stabilizes and releases newly synthesised receptors from the endoplasmic reticulum (Petäjä-Repo *et al*., 2002; Leskelä *et al*., 2007). Newly synthesised GPR30 may require pharmacological chaperones for expression at the cell surface. Due to the lipophilic nature of GPR30s' proposed endogenous ligand (E2; Muller *et al*., 1979), this is a reasonable hypothesis. Moreover, GPR30 may be constitutively active and require receptor inhibition to enhance cell surface expression and prevent constitutive endocytosis. For example, surface expression of heterologously expressed cannabinoid receptor type 1 (CB_1) is enhanced in cells treated with antagonists (Ellis *et al*., 2006).

In order to test this, hGPR30-SEP and rGPR30-myc were transiently transfected in HEK-293 cells and treated with GPR30 agonists (G1 and E2; 10 nM for both) or antagonists (G15 and G36; 1 μM for both) for 30 min or two hours. Confocal microscopy revealed that there was no detectable change in the intracellular localisation of hGPR30 or rGPR30 after 30 min (data not shown) or two hour (Fig 3.3 A and Fig 3.3 B) treatment with G1, E2, G15 or G36. Exposure of GPR30 agonists and antagonists to COS-7 cells expressing GPR30-GFP also fails to alter the intracellular localisation in studies presented from Eric Prossnitzs' group (Revankar *et al*., 2005; Bologa *et al*., 2006; Dennis *et al*., 2009), thereby supporting our findings.

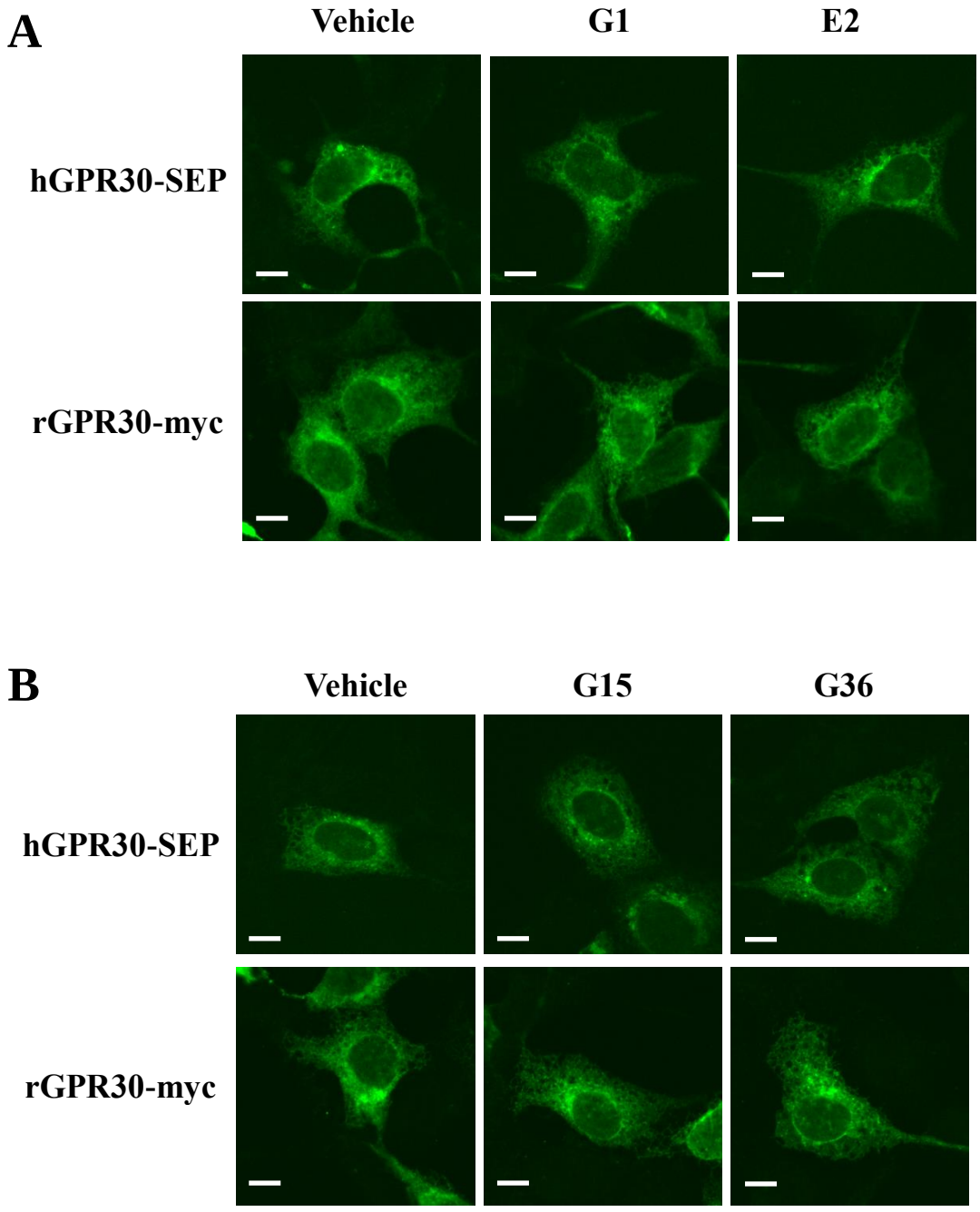

Figure 3.3: Exposure of GPR30 ligands does not alter its intracellular localisation in transiently expressing HEK-293 cells. Representative confocal images illustrating HEK-293 cells expressing either human or rat GPR30 (green) and were treated for 2 hours with **A)** vehicle (0.01% DMSO) or agonists (G1 or E2; 10nM) or **B)** vehicle (0.01% DMSO) or antagonists (G15 or G36; 1µM) for GPR30. Strong endoplasmic reticulum localisation persists after ligand exposure. Data are representative of at least two individual experiments. Scale bars, 10µm.

3.2.4: Identifying an antibody suitable for recognizing native rat GPR30

In order to establish the endogenous localisation of native GPR30 in rat hippocampal neurons, an antibody capable of recognising rGPR30 needed to be identified. Here, two commercially available polyclonal anti-human GPR30 antibodies were used. The first antibody (R + D systems; Catalogue no: AF5534) was derived from recombinant human GPR30 with the immunogen directed against residues 1-62 at the N-terminus of hGPR30. The second antibody (Abcam; Catalogue no: ab39742) was derived from human GPR30 with the immunogen directed against a sequence within residues 350 – 375, at the C-terminus of hGPR30. A cartoon illustrating their predicted binding sites for hGPR30 is shown in Fig 3.4.

As previously mentioned, the homology between the N-terminus of hGPR30 and rGPR30 is low (55% sequence identity; Fig 3.1). Whereas, sequence alignment of residues 350 – 375 revealed a 92% sequence identity between hGPR30 and rGPR30 (Fig 3.1). The specificity of the N-terminal and C-terminal anti-hGPR30 antibodies was tested by comparing their localisation against tagged hGPR30-SEP and rGRP30-myc, in transiently transfected HEK-293 cells (Fig 3.5).

Specific GPR30-immunostaining (anti-hGPR30 N-terminal antibody) was detected only in cells transfected with hGPR30-SEP, which almost completely co-localised with hGPR30-labelling. In contrast, anti-GPR30 immunostaining was absent in cells transfected with rGPR30-myc (Fig 3.5A). Conversely, in cells treated with the anti-GPR30 C-terminal antibody specific labelling was observed in cells transfected with either hGPR30-SEP or rGPR30-myc (Fig 3.5B). Importantly, anti-GPR30 C-terminal immunostaining completely co-localised with labelling from hGPR30-SEP (yellow; top panel) and rGPR30-myc (yellow; bottom panel).

These results suggest that the C-terminal anti-GPR30 antibody (Abcam) is more suitable for identifying endogenous GPR30 in rat tissue.

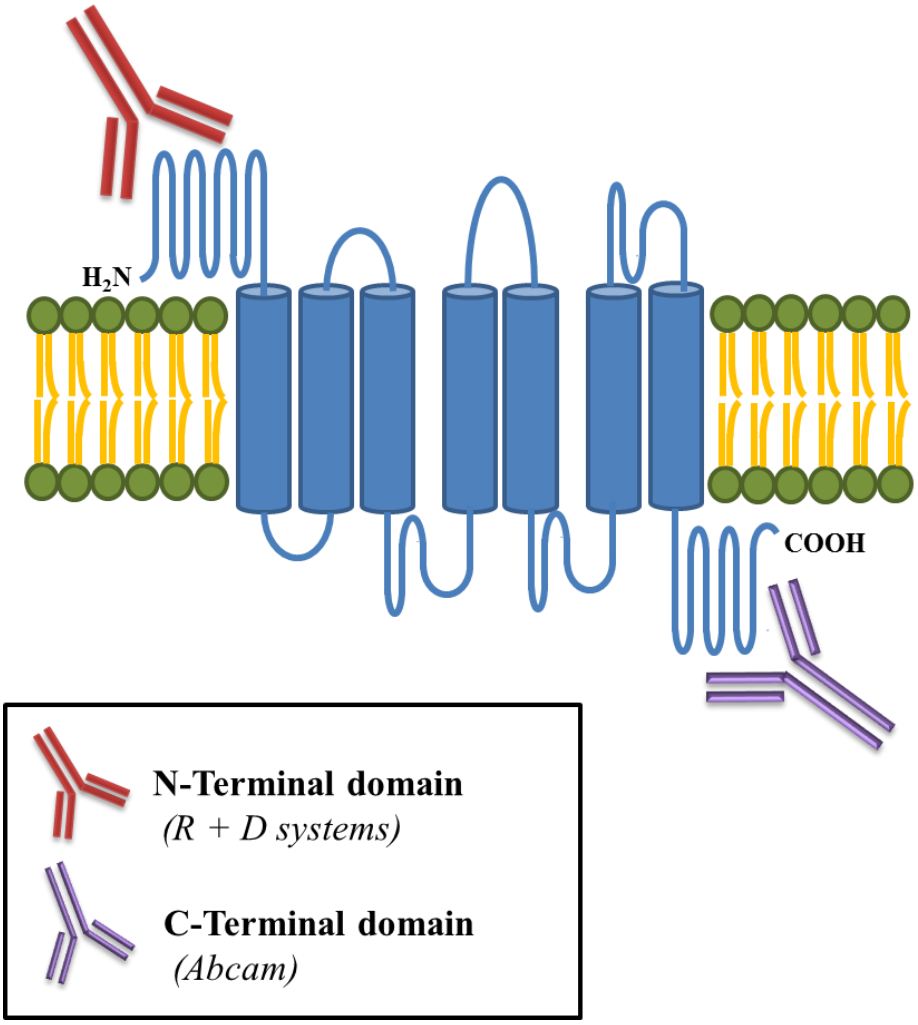

Figure 3.4: Cartoon representation of predicted binding sites for anti hGPR30 antibodies. The cartoon depicts the predicted binding sites of the two commercial anti-hGPR30 antibodies.

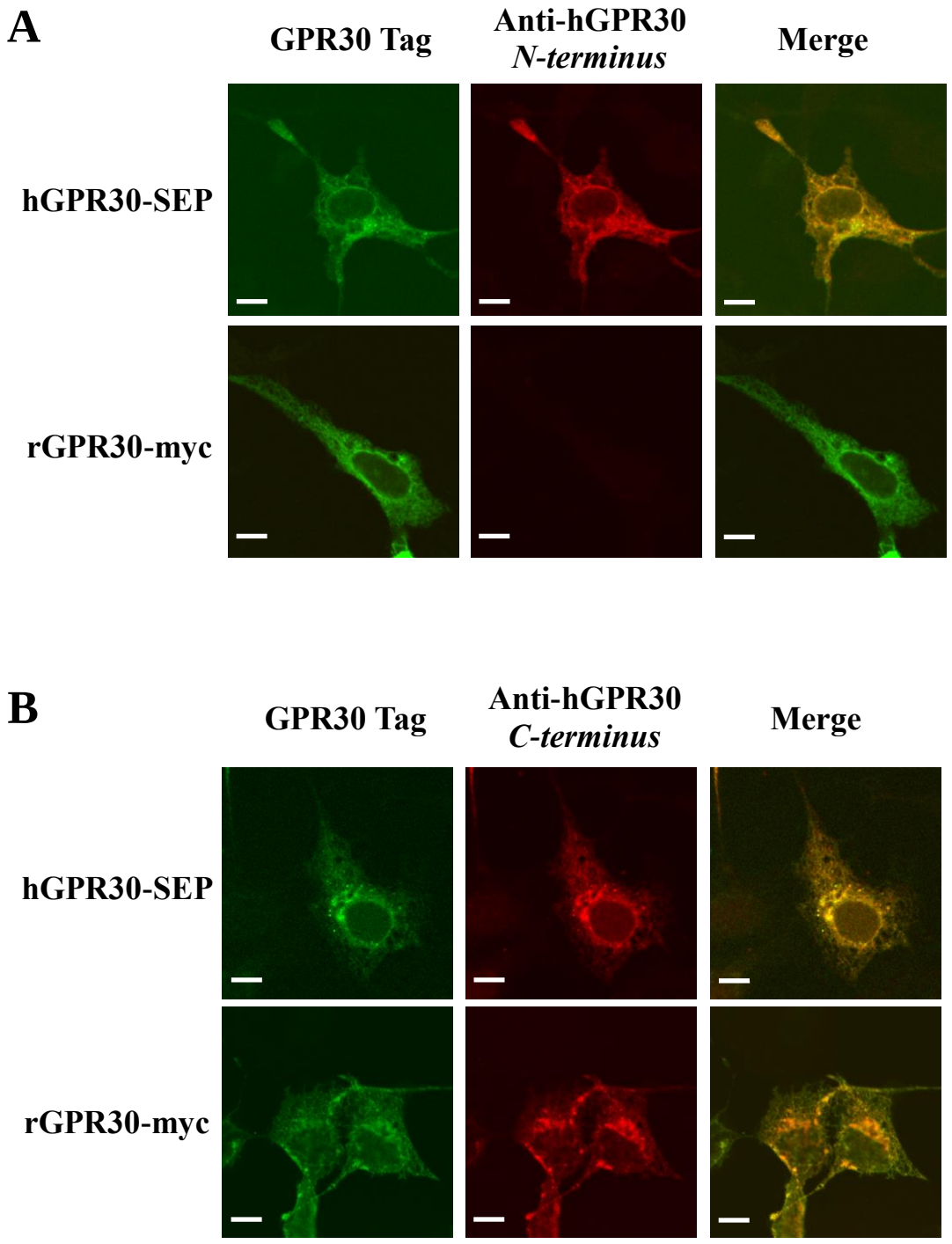

Figure 3.5: Characterisation of two commercial anti-hGPR30 antibodies. Representative confocal images illustrating HEK-293 cells expressing hGPR30-SEP or rGPR30-myc (green) and treated with anti-hGPR30 antibodies (red) directed against **A)** the *N*-terminus (R+D systems) or **B)** the C-terminus (Abcam). Only the C-terminus antibody was able to detect rGPR30. Data are representative of two individual experiments. Scale bars, 10µm.

3.2.5: GPR30 staining in primary rat hippocampal cultures.

Heterologous expression systems with tagged proteins of interest are useful in identifying potential endogenous function and localisation; however the environment of the host cell is not likely to represent the endogenous environment (intracellularly or extracellularly).

Previous studies using immunohistochemistry have identified GPR30 immunoreactivity in cells within the rat (Brailoiu *et al*., 2007) and mouse (Hazell *et al*., 2009) hippocampal formation. In order to confirm GPR30 expression in hippocampal tissue, the C-terminal anti-GPR30 antibody (Abcam) was utilised for staining in primary rat hippocampal cultures (DIV 8 – 14). In order to distinguish between neuronal and non-neuronal cells, co-staining with an antibody for microtubule associated protein-2 (MAP2; red; Izant and McIntosh, 1980; Dehmelt and Halpain, 2005) was utilised. In addition to being used to identify neurons, anti-MAP2 can be used as a soma / dendritic marker, thus giving insight into distribution of native GPR30 within different neuronal compartments.

Figure 3.6 illustrates GPR30 staining (green) in both neuronal (MAP2-positive; top panel) and non-neuronal (MAP2-negative; bottom panel) cell types. This is in agreement with other studies suggesting that GPR30 protein is expressed in rat hippocampal neurons (Funakoshi *et al*., 2006; Brailoiu *et al*., 2007; Matsuda *et al*., 2008; Akama *et al*., 2013) and in glia (Blasko *et al*., 2009; Hirahara *et al*., 2013).

The staining pattern for GPR30 appears to be intracellular, largely within the soma and perhaps associated with perinuclear organelles (Fig 3.6). Thus further co-staining studies were conducted to determine the exact intracellular localisation for GPR30 (see Fig 3.7).

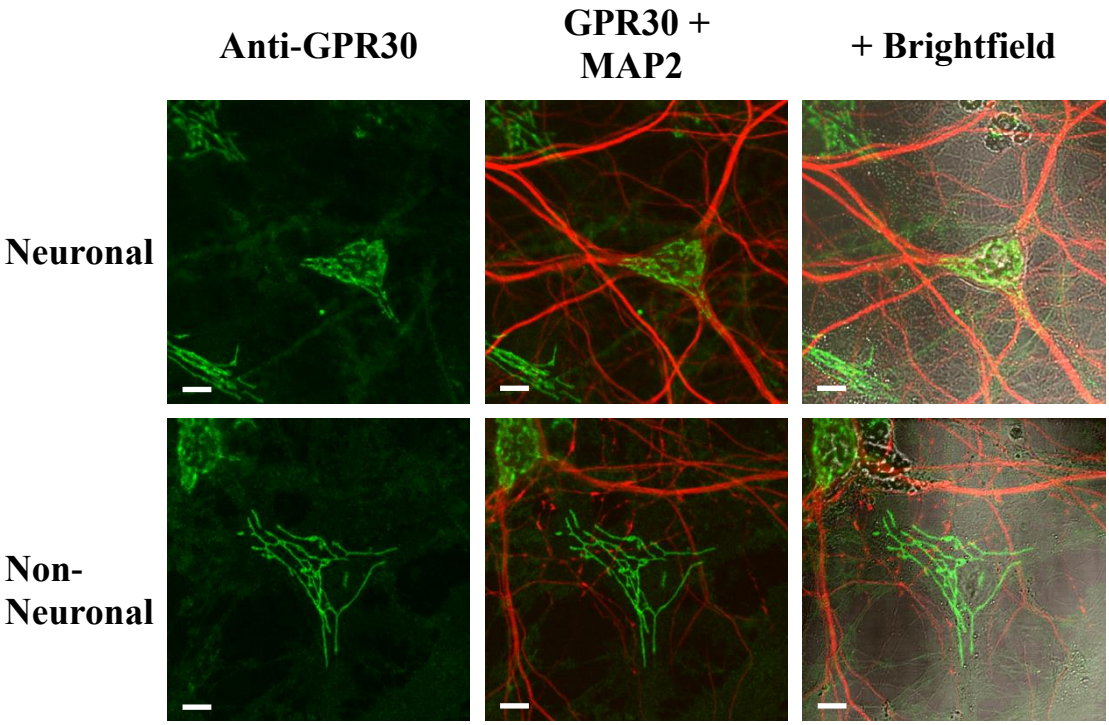

Figure 3.6: GPR30 expression in primary rat hippocampal cultures. Representative single plane confocal images illustrating GPR30 immunoreactivity (green) in DIV 14 hippocampal cultures. MAP2 immunostaining (red) was used to identify neuronal versus non-neuronal cells. The staining pattern of GPR30 staining in both neuronal and non-neuronal cells is intracellular and appears to be largely perinuclear. Data are representative of at least two individual experiments from cultures of different animals. Scale bars represent 10µm.

3.2.6: Cellular localisation of GPR30 in primary rat hippocampal cultures.

If GPR30 does have a role in mediating fast, non-genomic effects of estradiol on hippocampal synaptic transmission, one would speculate that cellular expression would be at or near synapses. However, previous studies using electron microscopy to establish the cellular localisation in hippocampal neurons yielded conflicting results. With groups reporting the localisation of GPR30 within intracellular compartments in CA3 pyramidal neurons (Matsuda *et al*., 2008) and conversely a plasma-membrane associated localisation in CA2 pyramidal neurons (Funakoshi *et al*., 2006).

Thus, to identify the specific localisation of GPR30 staining in hippocampal cultures, co-staining with cellular markers for the endoplasmic reticulum (anti-KDEL), trans-Golgi network (anti-TGN46), cytoskeleton (Alexa fluor-546 conjugated phalloidin) and synapses (anti-synapsin-1) were utilised (Fig 3.7). Hippocampal GPR30 staining did not co-localise with the markers for the endoplasmic reticulum (KDEL), cystoskeleton (F-actin) or synapses (synapsin-1). However, almost complete co-localisation was observed when co-stained with the trans-Golgi network marker (TGN46), a localisation which is in agreement with a report by Matsuda *et al*. (2008).

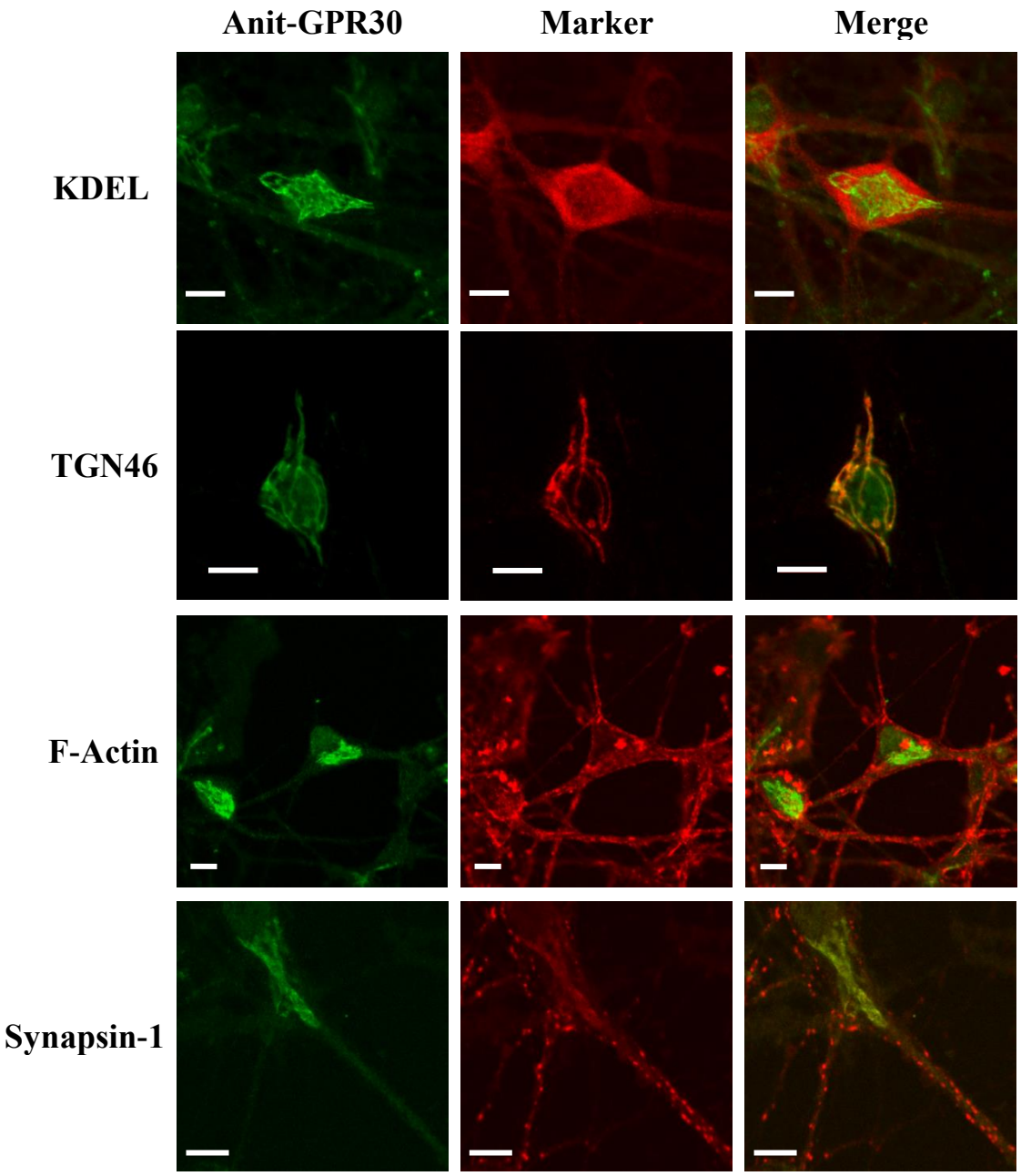

Figure 3.7: GPR30 co-localises with TGN46 in cultured hippocampal neurons. Representative single plane confocal images illustrating GPR30 immunoreactivity (green) and co-staining with the subcellular markers KDEL, TGN46, F-actin or synapsin-1 (red) in DIV 8 – 14 cultured hippocampal neurons. Almost complete co-localisation of GPR30 labelling is observed with TGN46 (a trans-Golgi network marker). Data are representative of at least three experiments from cultures of different animals. Scale bars represent 10µm.

3.2.7: GPR30 localisation in hippocampal neurons is not altered after treatment with specific GPR30 agonists and antagonists.

In order to establish whether endogenous neuronal rat GPR30 requires pharmacological chaperones for its surface expression, primary hippocampal cultures (DIV 8 – 12) were treated with GPR30 agonists (G1 and E2; both 10 nM) or antagonists (G15 and G36; both 1 µM) for 30 min or two hours. After fixation and permeabilisation the cultures were stained with the anti-MAP2 antibody (red) and the C-terminal anti-hGPR30 antibody (green). Confocal microscopy revealed that there was no detectable change in the intracellular localisation of GPR30 after 30min (data not shown) or two hours treatment with ligands (Fig 3.8 A and 3.8 B).

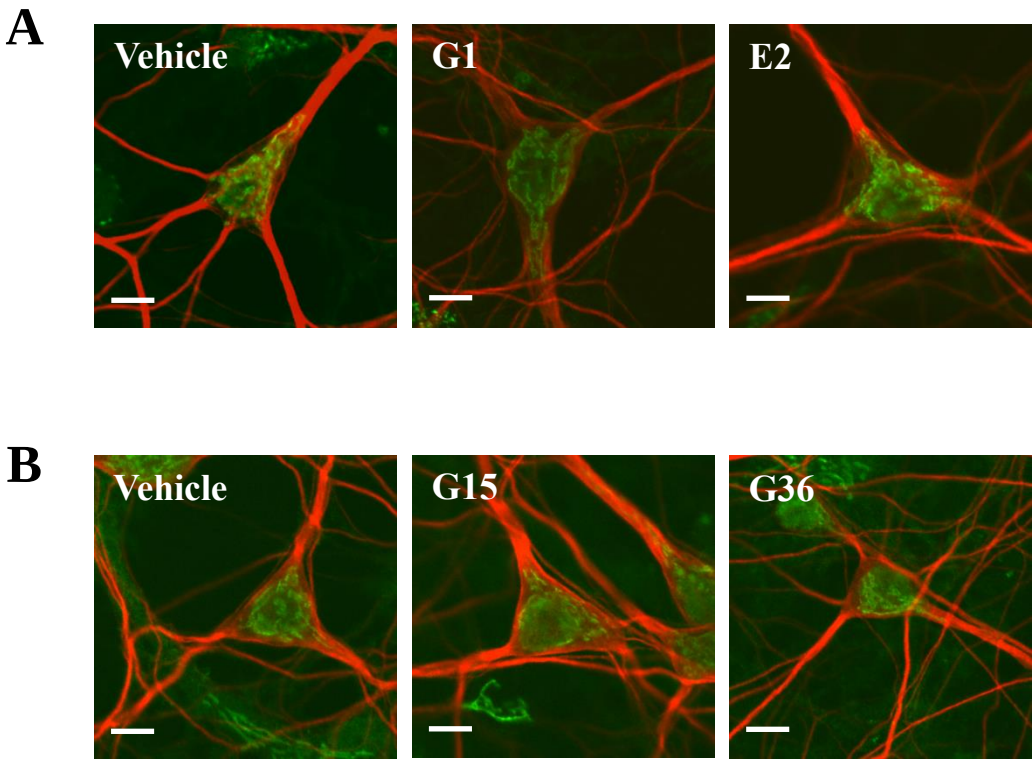

Figure 3.8: Treatment with ligands for GPR30 does not alter GPR30 localisation in hippocampal cultures. Representative confocal images of GPR30 expression (green) in hippocampal neurons that were treated for 2 hours with **A)** vehicle (0.01% DMSO) or agonists (G1 or E2; 10nM) or **B)** vehicle (0.01% DMSO) or antagonists (G15 or G36; 1µM) for GPR30. Staining for MAP2 is illustrated in red. Data are representative of at least two individual experiments. Scale bars, 10µm.

3.3: Discussion

These data indicate that when expressed in a heterologous system the localisation of hGPR30 and rGPR30 is associated with intracellular regions of the cell. Dual-labelling studies suggest that GPR30 expression is likely to be localised to the endoplasmic reticulum. Moreover, the localisation of hGPR30 and rGPR30 in this system is unaltered following exposure to specific GPR30 agonists or antagonists. Conversely in native hippocampal neurons, GPR30 localisation is restricted to the TGN, and this expression pattern is also unaltered following treatment with specific GPR30 agonists and antagonists.

The finding that GPR30 is expressed intracellulary contrasts with the more typical expression of Class A GPCRs at the plasma membrane (as reviewed in Vischer *et al*., 2011; Magalhaes *et al*., 2012). A predominantly intracellular localisation of GPR30 also contradicts the classic idea that GPCRs function to quickly relay information from extracellular signals. However, the putative endogenous ligand for GPR30 (E2) is lipophilic and can readily pass through the plasma membrane (Muller *et al*., 1979) and functional intracellular GPCRs can be expressed at intracellular sites (For reviews see: Gobeil *et al*., 2006; Boivin *et al*., 2008; Tadevosyan *et al*., 2012).

3.3.1: GPR30 intracellular localisation in heterologous expression systems.

This study is the first report to compare the localisations of hGPR30 and rGPR30 in a heterologous expression system. These data indicate that both hGPR30 and rGPR30 are expressed at the endoplasmic reticulum, suggesting that despite clear differences in N-terminal sequences, both species orthologs are directed to the same intracellular compartment in this expression system (Fig 3.2).

There are a number of possibilities why GPR30 expression is restricted to the endoplasmic reticulum in HEK-293 cells. Firstly, generation of fluorescently-tagged chimeric constructs (N- or C- terminal) can influence the surface expression and function of a native protein. For example, epitope or chimeric tagging of hGnRH receptors can misroute this receptor to the plasma membrane (Brothers *et al*., 2003) and

N-terminally tagged GFP-CB_1R chimeras are restricted to the endoplasmic reticulum (McDonald *et al*., 2007a). Thus, it is feasible that the C-terminal tags attached to hGPR30 and rGPR30 prevent delivery of GPR30 to the plasma membrane in our heterologous expression system. Moreover, the host cell type systems may also influence surface expression and function of a protein (Jiang *et al*., 2012). Indeed, these caveats have been attempted to be resolved by a number of groups. For example, Funakoshi and colleagues illustrated that GFP tagged GPR30 accumulates within the endoplasmic reticulum, whereas GPR30 was expressed at the surface when tagged with a smaller epitope (-FLAG) in HeLa cells (Funakoshi *et al*., 2006). However, using the same GPR30-FLAG construct in HeLa cells, Matsuda *et al*. (2008) failed to replicate the findings of Funakoshi and co-workers (2006), and only observed an intracellular expression profile for GPR30 (Matsuda *et al*., 2008). Moreover, Otto *et al*., (2008) consistently observed an intracellular localisation of GPR30 when comparing GFP N- and C- terminus tagged GPR30 with untagged GPR30 in COS-7 and HEK-293 cells, suggesting that an epitope tag or the host cell type, does not disrupt the intracellular localisation of GPR30 in heterologous expression systems (Otto *et al*., 2008).

Recent advances in the field suggest the redundancy of using the overexpressing heterologous system in assays attempting to determine plasma-membrane associated GPR30 function. Indeed, Cheng and colleagues demonstrated that only very low levels of N-terminal HA tagged GPR30 (HA-GPR30) are observed in the plasma membrane of stably expressing HEK-293 cells; that the receptor undergoes fast constitutive endocytosis (whereby surface GPR30 is internalised within 30 min without ligand stimulation) and surface (HA-tagged) GPR30 is subsequently degraded quickly (half-life < 30 min) (Cheng *et al*., 2011b). Their data suggest that the receptor does have the capacity to reach the surface; however levels are very low and are unstable. Thus, if GPR30 is a functional membrane associated estrogen-sensitive receptor, one would speculate that mechanisms would be put in place in order to conserve energy (*ie:* why would the cell expend energy producing and exporting the receptor to the cell surface, where it is not stable and is readily sent for degradation?). A consideration was perhaps the requirement for pharmacological chaperones; although results presented here suggest that this may not be the case (Fig 3.3), we cannot rule out the possibility that the ligands used here are not specific for GPR30. Indeed, the synthetic ligands developed for GPR30 have been suggested to specifically bind to the ERα variant, ERα-36, and not

GPR30 (Kang *et al*., 2010). In addition, it has been suggested that aldosterone is the endogenous agonist for GPR30 and that eplerenone (a minerocorticoid receptor antagonist) can act as a partial antagonist for GPR30-mediated effects (at least in vasculature) (Gros *et al.*, 2011).

Another consideration is that GPR30 contains an endoplasmic retention signal that restricts export for surface expression. Association with an interacting protein or another GPCR may mask such a sequence. Examination of both hGPR30 and rGPR30 sequences reveals that they have two conserved RXR endoplasmic reticulum retention motifs in the third cytoplasmic loop (at residues 246 – 248 and 251 – 253). Functional RXR signals can be found in a variety of cytosolic positions, including intracellular loops in transmembrane proteins (Zerangue *et al*., 1999). Endoplasmic reticulum retention sequences can be masked by interacting proteins, which conveys importance for function. For example mutating the RKR sequence in SUR1, a β subunit that forms part of the ATP-sensitive potassium ion channel that is not expressed at the cell surface as a monomer, results in surface expression (Zerangue *et al*., 1999). This holds true for GPCRs as well, as the surface expression of $GABA_{B1}$ is dependent on the masking of its RKR endoplasmic reticulum retention motif by interaction with $GABA_{B2}$ (Pagano *et al*., 2001).

GPR30 may indeed express a functional endoplasmic reticulum retention sequence, which would require masking before export. However, RXR-dependent ER retention machinery is sensitive to the length between the RXR signal and transmembrane domains (Shikano and Li, 2003). Although the third intracellular loop of GPR30 is the largest of the three, these RXR retention signals may not be functional in this respect. For example, in $GABA_{B1}$ receptors the RXR endoplasmic reticulum retention sequence was only functional within the cytoplasmic tail and not in any of the intracellular loops, when grafted to ectopic sites (Gassmann *et al*., 2005). Site directed mutagenesis of GPR30 at its RXR sites could resolve this and may also give insight as to whether a protein-protein interaction is needed for stable surface expression of GPR30.

To support this idea, evidence is emerging to suggest that GPR30 does indeed associate with other proteins, which may encourage surface expression or stabilise the receptor at the surface, depending on the endogenous setting. For example GPR30 can associate with RAMP-3 in heart tissue of female mice (Lenhart *et al*., 2013) and PSD-95 in

murine hippocampal neurons (Akama *et al*., 2013). Moreover, co-expression of murine PSD-95-FLAG and HA-GPR30 significantly increases the proportion of HA-GPR30 expressed at the cell surface in COS-7 cells (Akama *et al*., 2013).

It is worth noting that in breast cancer cells, endogenous expression of GPR30 is predominately intracellular (Revankar *et al*., 2005; Bologa *et al*., 2006; Filardo *et al*., 2006; Otto *et al*., 2008; Lin *et al*., 2009), whereas GPR30 expression is predominantly expressed at the plasma membrane in renal epithelia (Lindsey *et al*., 2011) and in Atlantic croaker oocytes (Pang *et al*., 2008). Thus, considering the evidence, it is plausible that the functional localisation of GPR30 (whether it be intracellular or plasma membrane associated), is determined by the endogenous cell type.

3.3.2: localisation of GPR30 in primary rat hippocampal neurons

However, as with the debate regarding the cellular distribution of hGPR30 in heterologous and endogenously expressing breast cell lines, there are also inconsistencies within the literature regarding the cellular localisation of GPR30 within the rodent central nervous system. For example, using electron microscopy and ultrastructure analysis, two independent groups published contradictory findings within hippocampal tissue. Funakoshi and co-workers reported GPR30 immunoreactivity at the plasma membrane (soma) of CA2 pyramidal neurons with no expression in the endoplasmic reticulum (Funakoshi *et al*., 2006). Whereas in a report from Matsuda and colleagues (2008), GPR30 immunoreactivity was absent at the plasma membrane in neurons of the CA3 and rather associated with membrane structures of the Golgi apparatus and endoplasmic reticulum (Matsuda *et al*., 2008). Thus, in order to attempt to resolve the issue and determine the distribution of GPR30 in our primary hippocampal cultures, an antibody capable of recognising rGPR30 was utilised (Fig 3.5).

In agreement with Mastuda *et al*. (2008), our data show GPR30 labelling in primary hippocampal cultures is associated with the intracellular TGN compartment as GPR30 positive staining co-localised with the TGN marker, TGN46 (Fig 3.7). Matsuda *et al.* (2008) also identified GPR30 immunoreactivity in membranes of vesicles localised in the dendritic shafts of CA3 neurons. However, as we only found evidence for GPR30 associated with TGN around the nucleus, this may reflect limitations of using confocal

microscopy to visualise very low levels of endogenous receptor expression, or limitations of the antibody used (see below).

Other groups who utilise confocal microscopy have also reported intracellular localisation of GPR30 in other neuronal cell types. For example, GPR30 co-localises with TGN38 in magnocellular oxytocin neurons in the paraventricular and supraoptic nuclei of the rat hypothalamus (Sakamoto *et al*., 2007), GPR30 is also detected within the cytoplasm of primary rat cortical cultures (Liu *et al*., 2012) and at the endoplasmic reticulum and Golgi in rat lumbar dorsal root ganglion (DRG) neurons (Takanami *et al*., 2010). In all studies detecting intracellular expression, antibodies directed against the C-terminal region of human GPR30 were used. Thus it is possible that these antibodies may be recognising a form of GPR30 (precursor or ubiquitnated) that is not functionally relevant. This is a feasible hypothesis as the endoplasmic reticulum is the site for protein translation and Cheng *et al*., (2011) demonstrated that the TGN serves as a checkpoint for GPR30 degradation. If this is the case, then true functional endogenous localisation is not able to be determined with these tools.

Nevertheless, an intracellular localization of GPR30 is consistent with its function as an estrogen receptor. Moreover, endogenous intracellular GPR30 is capable of cellular signalling (Revankar *et al*., 2007). Using a range of cell permeable and impermeable charged E2 derivatives, Revankar and co-workers (2007) observed that only with cell permeable E2 derivatives were SKBr3 cells (ERα/β –VE, GPR30 +VE) capable of PIP3 production.

Although an intracellular (particularly, perinuclear) localisation in hippocampal neurons is not consistent with the hypothesis that GPR30 may be involved in rapid non-genomic effects of estradiol at excitatory synapses, results from this chapter support evidence for hippocampal expression of GPR30, thus further investigation into the role GPR30 may have on hippocampal function is warranted. Interestingly, a very recent report illustrated using electron microscopy, GPR30 labelling in the peri-synaptic zone adjacent to the post-synaptic density (PSD) in a variety of different dendritic spine profiles in adult rat CA1 (Akama *et al*., 2013). Additionally, this group found that GPR30 directly associates with a PSD protein, PSD-95, *in vitro* and *in vivo*.

Chapter Four

Effects of E2 and a GPR30 agonist on hippocampal excitatory synaptic transmission

4.1: Introduction

There is overwhelming evidence suggesting that GPR30 is expressed within the hippocampus and results from the previous chapter support this (O'Dowd *et al*., 1998; Funakoshi *et al*., 2006; Brailoiu *et al*., 2007; Matsuda *et al*., 2008; Dun *et al*., 2009; Hazell *et al*., 2009; Isensee *et al*., 2009 and see section 3.2.5). Recent ultra-structural analysis indicating GPR30 localisation at CA1 synapses also suggests that this receptor is well positioned to mediate fast estrogenic effects on hippocampal excitatory synaptic transmission (Akama *et al*., 2013).

Ideally, in order to establish whether GPR30 has a role in the non-genomic actions of E2 on hippocampal excitatory synaptic transmission, knockout animals would be utilised. Although there are four GPR30 knockout animals already described (see section 1.3.6), a well-established mutant is not currently available for examining GPR30 function. Therefore, the GPR30 field relies on pharmacological tools in conjunction with receptor knockdown to examine function.

Nevertheless, since the generation of a selective agonist for GPR30 (G1; Bologa *et al*., 2006; see section 1.3.4), numerous groups have speculated roles for GPR30 as a mediator of a number of different estrogenic effects within the hippocampus (Hammond *et al*., 2009; Lebesgue *et al.*, 2009, 2010; Gingerich *et al*., 2010; Kajta *et al*., 2013; Ruiz-Palmero *et al*., 2013). However, a thorough examination of the effects of the GPR30 agonist (G1) on hippocampal excitatory synaptic transmission has not yet been conducted. Thus in order to characterise the effects of G1, extracellular field potential recordings (fEPSPs) were used to monitor excitatory synaptic transmission at Schaffer-collateral – CA1 synapses in hippocampal slices from male rodents.

4.2: Results

4.2.1: G1 induces LTD in juvenile male hippocampal slices under conditions of enhanced excitability.

G1 (1 µM; 20 min) was applied to juvenile (P11 – P18) hippocampal slices in order to establish whether activation of GPR30 had any effect on basal hippocampal excitatory synaptic transmission (Fig 4.1). During G1 application the magnitude of synaptic transmission was unaltered (100 ± 5.7% of baseline; n = 4), although a small depression of synaptic transmission was observed after 40 min of drug washout (to 92 ± 4.5 % of baseline), these effects were not significant ($p > 0.05$; one-way repeated measures ANOVA).

Under basal conditions, there is a strong voltage-dependent block of NMDAR by Mg^{2+} (Mayer *et al*., 1984; Ascher *et al*., 1988). Removing this blockade (by means of reducing extracellular Mg^{2+} content) enhances NMDAR-mediated events and increases overall excitability. Indeed, studies in our laboratory have established that under conditions of enhanced excitability, significant effects of hormonal modulators on synaptic transmission can be uncovered. Specifically, leptin can induce LTD in the CA1 region of P11 – P18 rats, when slices are perfused with Mg^{2+} free aCSF or the $GABA_A$ receptor antagonist, picrotoxin (Durakoglugil *et al*., 2005).

Therefore, hippocampal slices (P11 – 18) were perfused with low Mg^{2+} aCSF (0.1 mM; Fig 4.2). Within 10 min of G1 (1 µM) application, synaptic transmission quickly started to depress and significant depression of synaptic transmission (to 71 ± 3.7% of baseline; $p < 0.001$; n = 5; t = 7.461; 4 degrees of freedom) was reached 20 min post G1 washout and was sustained for the duration of recordings (a further 20 min). These data suggest that under conditions of increased excitability, G1 can induce LTD in juvenile hippocampal slices. However, it must be noted that there are caveats in using tissue from juvenile animals (P11 – P18). A large number of developmental changes in receptors mediating excitatory synaptic transmission, and estrogen-mediated physiology, are occurring during this time window. Moreover, mechanisms for inducing and maintaining synaptic plasticity differ in adult tissue.

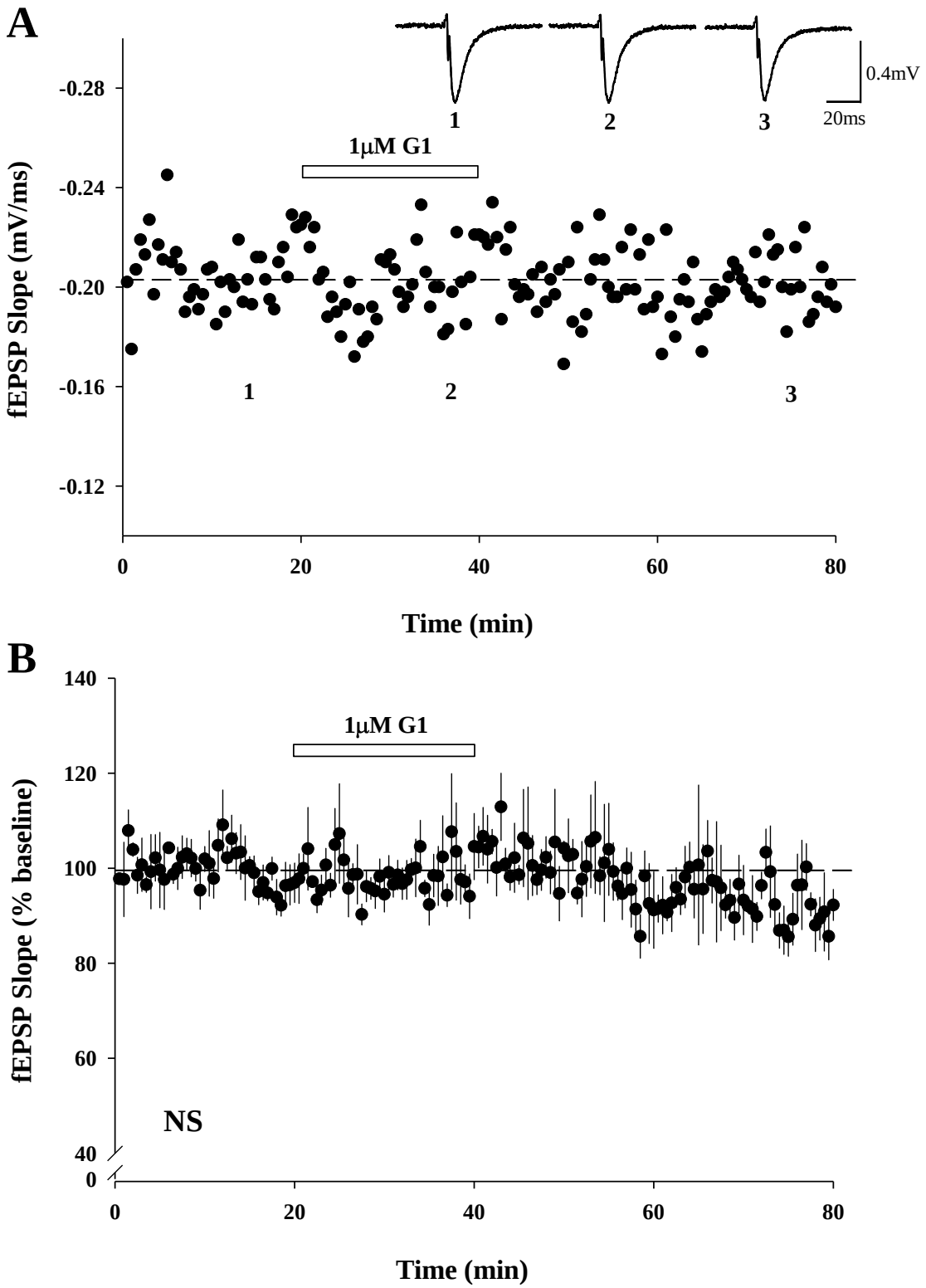

Figure 4.1: 1 μM G1 has no effect on basal excitatory synaptic transmission in juvenile male hippocampal slices. ***A,*** representative experiment showing G1 (1 μM; 20 min) application has no effect on basal excitatory synaptic transmission. Top, example traces from the experiment are shown at the time points indicated. ***B,*** data pooled (n = 4) and normalised with respect to baseline are expressed as mean ± SEM. NS represents $p > 0.05$ vs. baseline; one-way repeated measures ANOVA.

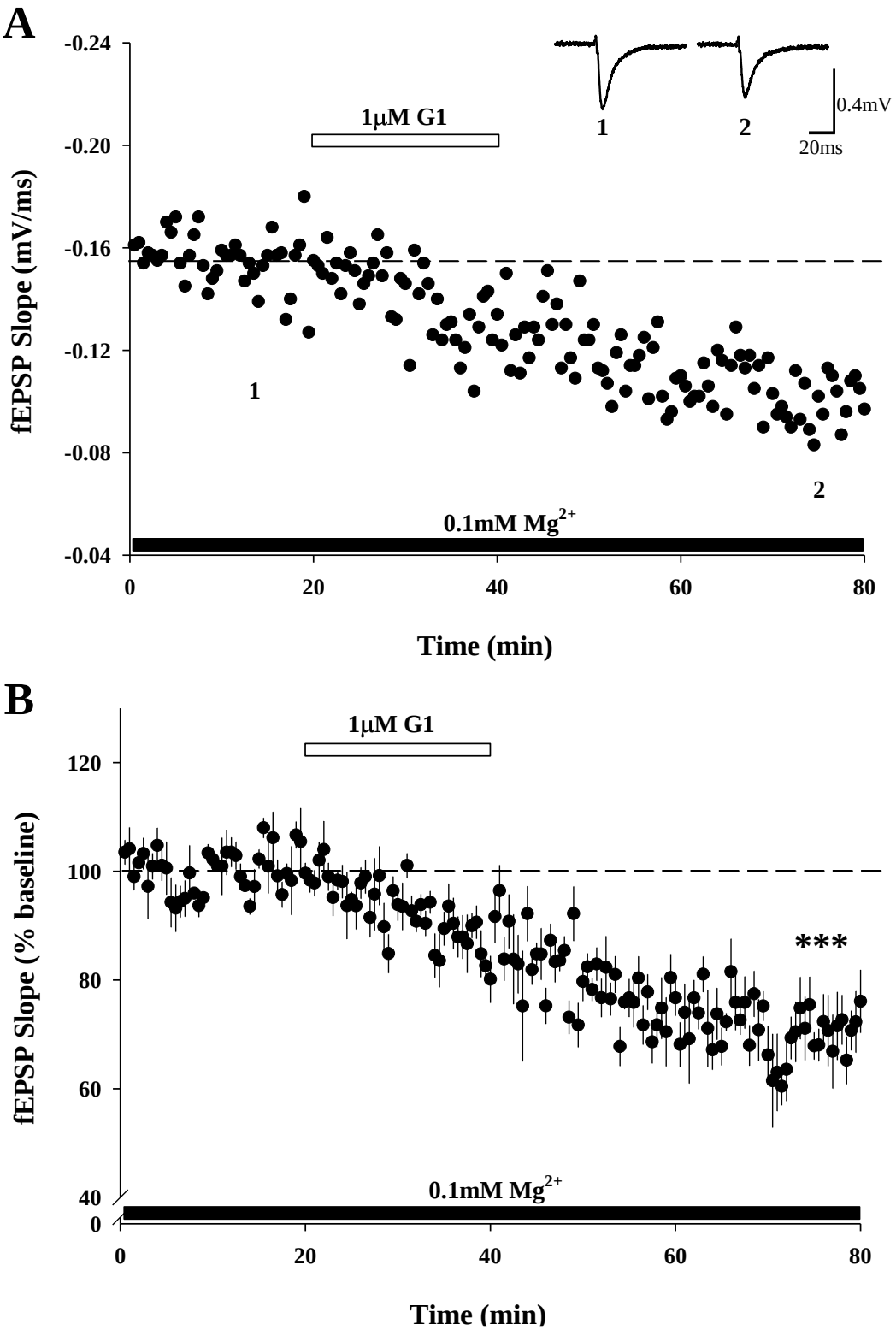

Figure 4.2: Under conditions of enhanced neuronal excitability, 1 μM G1 induces LTD in juvenile male hippocampal slices. ***A,*** representative experiment showing G1 (1 μM; 20 min) application induces LTD in low Mg^{2+} aCSF. Top, example traces from the experiment are shown at the time points indicated. ***B,*** data pooled (n = 5) and normalised with respect to baseline are expressed as mean ± SEM. *** represents $p < 0.001$ vs. baseline; paired t-test.

4.2.2: Estradiol has variable effects on basal excitatory post-synaptic transmission in adult male hippocampal slices.

Thus, in order to overcome the caveats of using juvenile tissue, hippocampal slices from adult (12 – 20 weeks) male rats were utilized in the following experiments (Fig 4.3 onwards). In the adult male model, hormonal systems are fully developed and stable (as reviewed in McCarthy, 2008), the influence of circulating estrogens is not an issue and acute effects of E2 have been described by others (Teyler *et al*., 1980; Foy *et al*., 1999; Kramár *et al*., 2009; Zadran *et al*., 2009). In this model, GPR30 expression has also been observed (Matsuda *et al*., 2008) and effects of G1 on basal hippocampal excitatory synaptic transmission have been revealed, albeit in adult OVX rats (Lebesgue *et al*., 2009, 2010).

Considering the general consensus is that GPR30 is an estrogen-sensitive receptor we wanted to establish the effects of its proposed endogenous agonist 17β-estradiol (E2) on hippocampal excitatory synaptic transmission. E2 can be synthesised *de novo* in the adult hippocampus, and in gonadally intact adult male rodents hippocampal derived E2 concentrations reach approximately 8 nM (Hojo *et al*., 2008, 2009). Thus, E2, at a physiologically relevant concentration of 10 nM, was bath applied to hippocampal slices from adult male rodents.

Bath application of E2 (10 nM; 20 min; Fig 4.3) resulted in a transient potentiation of synaptic transmission (to 105 ± 1.2 % of baseline after 15 min ligand application; $F[2,63] = 46.2$; $p < 0.01$; n = 22,). During the 60 min E2 washout phase the magnitude of synaptic transmission slowly reduced, where maximal depression of synaptic transmission was revealed at the end of washout (to 89 ± 1.6 % of baseline, $F[2,63] = 46.2$; $p < 0.001$, n = 22).

However, it was noted that not all of the slices exhibited a transient potentiation in synaptic transmission in response to E2 application (10 nM; 20 min). Moreover, in some cases where an E2-induced potentiation was observed a slow-onset depression of synaptic transmission following washout was not, but rather the E2-induced enhanced magnitude of synaptic transmission was sustained. Indeed, within the published literature it has been noted that the potentiating effect of E2 is (in some cases) only observed in a proportion of slices or cells tested (see Table A1 in Appendix). Thus, in

order to probe further the differing effects of E2 application, data was stratified to expose the different response profiles of this agonist (see 2.2.5.3 in Methods).

Out of 22 slices that were exposed to E2 (10 nM; 20 min), 12 slices (55%) showed a bi-phasic response profile (Fig 4.4). In this group, application of E2 induced an initial increase in excitatory synaptic transmission (to 107 ± 1.0% of baseline within 10 min of ligand application; $F[2,35] = 108.3$; $p < 0.001$; n = 12). Following E2 washout a slow-onset long-lasting depression of synaptic transmission was revealed, where maximal depression (87 ± 1.5 % of baseline; $F[2,35] = 108.3$; $p < 0.001$; n = 12) was obtained approximately 50 min after E2 removal. In 6 out of 22 slices (27%) application of E2 failed to induce an increase in synaptic transmission (98 ± 1.5 % of baseline after 15 min E2 application; $p > 0.05$; n = 6; Fig 4.5). However, following E2 removal a slow-onset but sustained depression of synaptic transmission was observed (to 89 ± 2.7% of baseline; $F[2,17] = 11.0$; $p < 0.05$; n = 6). This magnitude of E2-induced synaptic depression was not significantly different from the magnitude of synaptic depression elicited in slices which show a bi-phasic response profile ($p > 0.05$; Kruskal-Wallis One-way ANOVA on Ranks). In the remaining four slices (18%; Fig 4.6) an E2-induced increase in synaptic transmission was observed, which was sustained for up to 40 min following washout (to 110 ± 3.0 % of baseline; $F[2,11] = 6.3$; $p < 0.05$; n = 4; Fig 4.6).

These results suggest that treatment with E2 can induce bi-directional response profiles. The most consistent response observed was the induction of a slow-onset long lasting depression of synaptic transmission (E2-induced LTD). This effect was seen in 18 out of 22 slices (82 %) and correlates well with previous studies in the laboratory that also observed a novel form of LTD induced by E2 in adult hippocampal slices treated with 0.1mM Mg^{2+} (Moult and Findlay, *unpublished observation*).

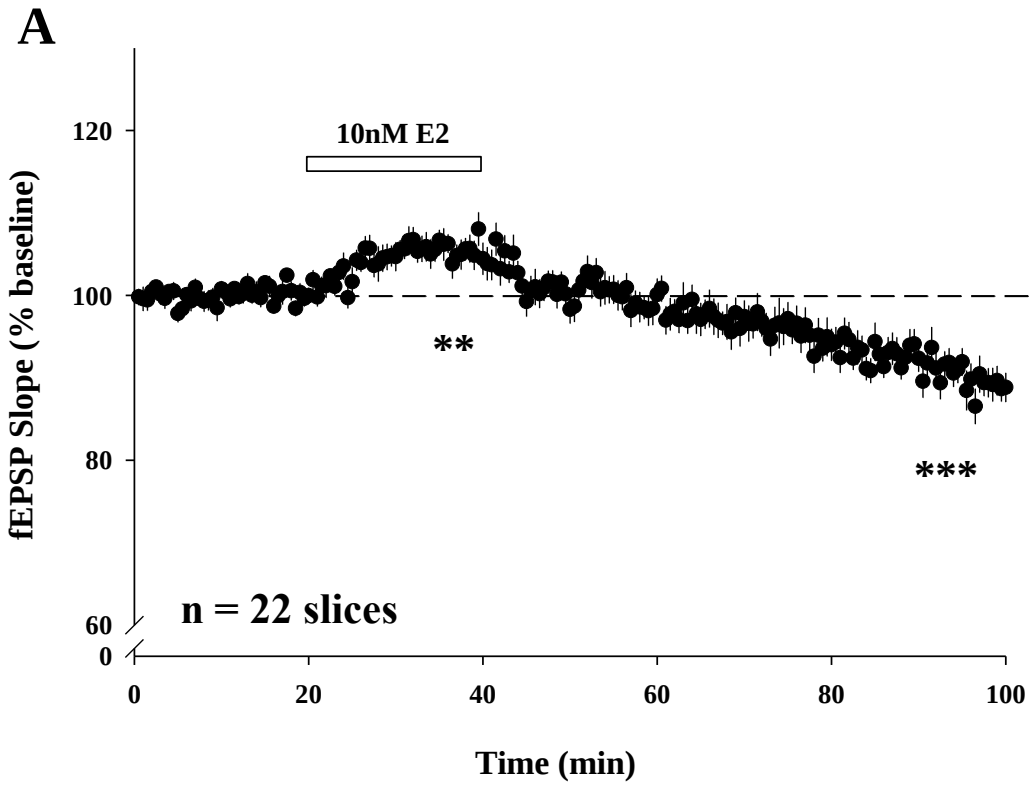

Figure 4.3: E2 evokes a bi-phasic effect on basal synaptic transmission in adult male hippocampal slices. ***A,*** E2 (10 nM; 20 min) application transiently potentiates synaptic transmission, followed by a slow onset reduction in synaptic transmission following washout. Data are pooled (n = 22 slices) and normalised with respect to baseline are expressed as mean ± SEM. ** represents $p < 0.01$ vs. baseline, *** represents $p < 0.001$ vs. baseline; one-way repeated measures ANOVA followed by tukey *post-hoc* analyses.

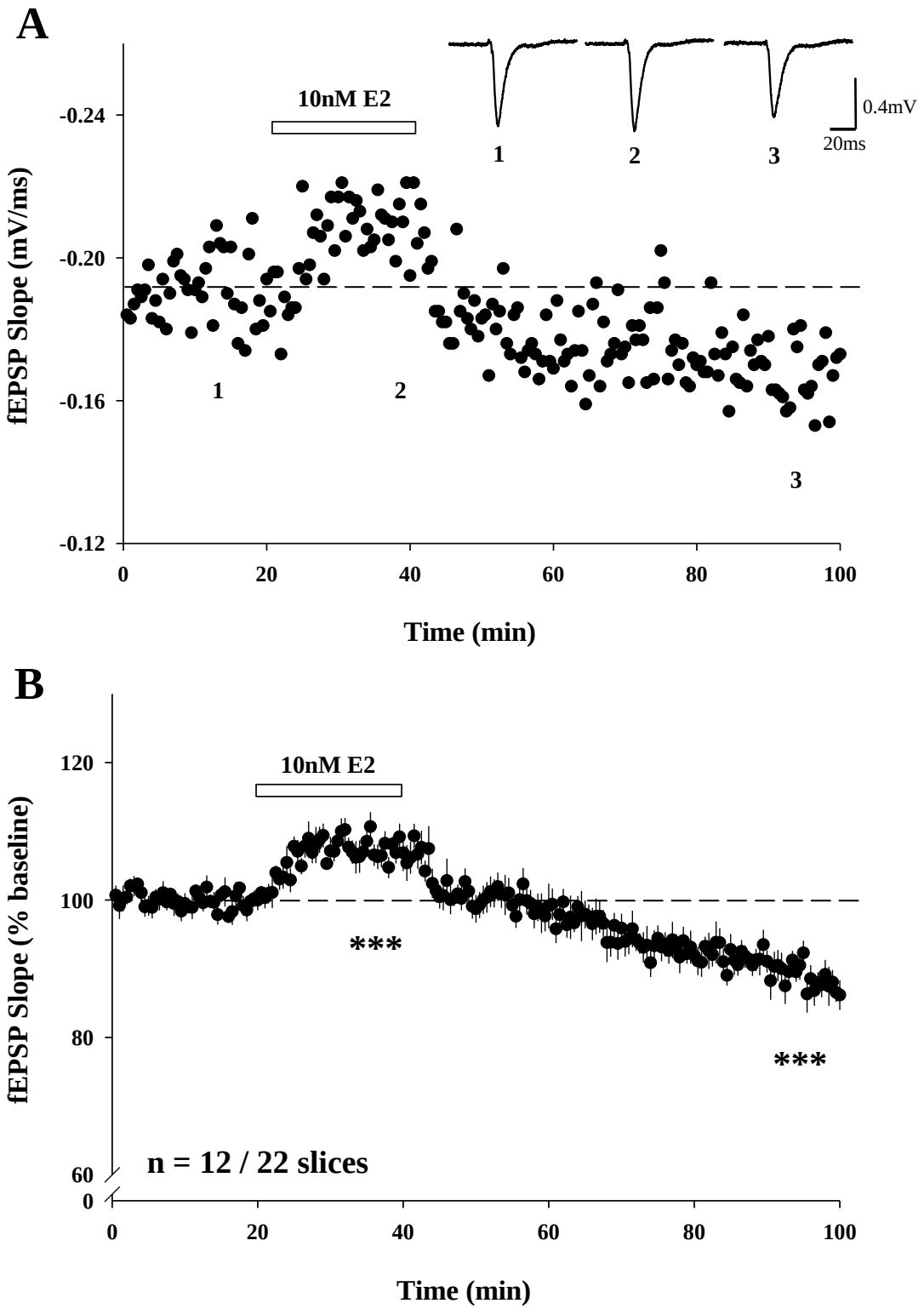

Figure 4.4: In a proportion of slices E2 evokes a bi-phasic effect on basal synaptic transmission. ***A,*** representative experiment showing E2 (10 nM; 20 min) application transiently potentiates synaptic transmission, followed by a long-lasting reduction in synaptic transmission upon E2 washout. Top, example traces from the experiment are shown at the time points indicated. ***B,*** data pooled (n = 12 out of 22 slices) and normalised with respect to baseline are expressed as mean ± SEM. *** represents $p < 0.001$ vs. baseline; one-way repeated measures ANOVA followed by tukey *post-hoc* analyses.

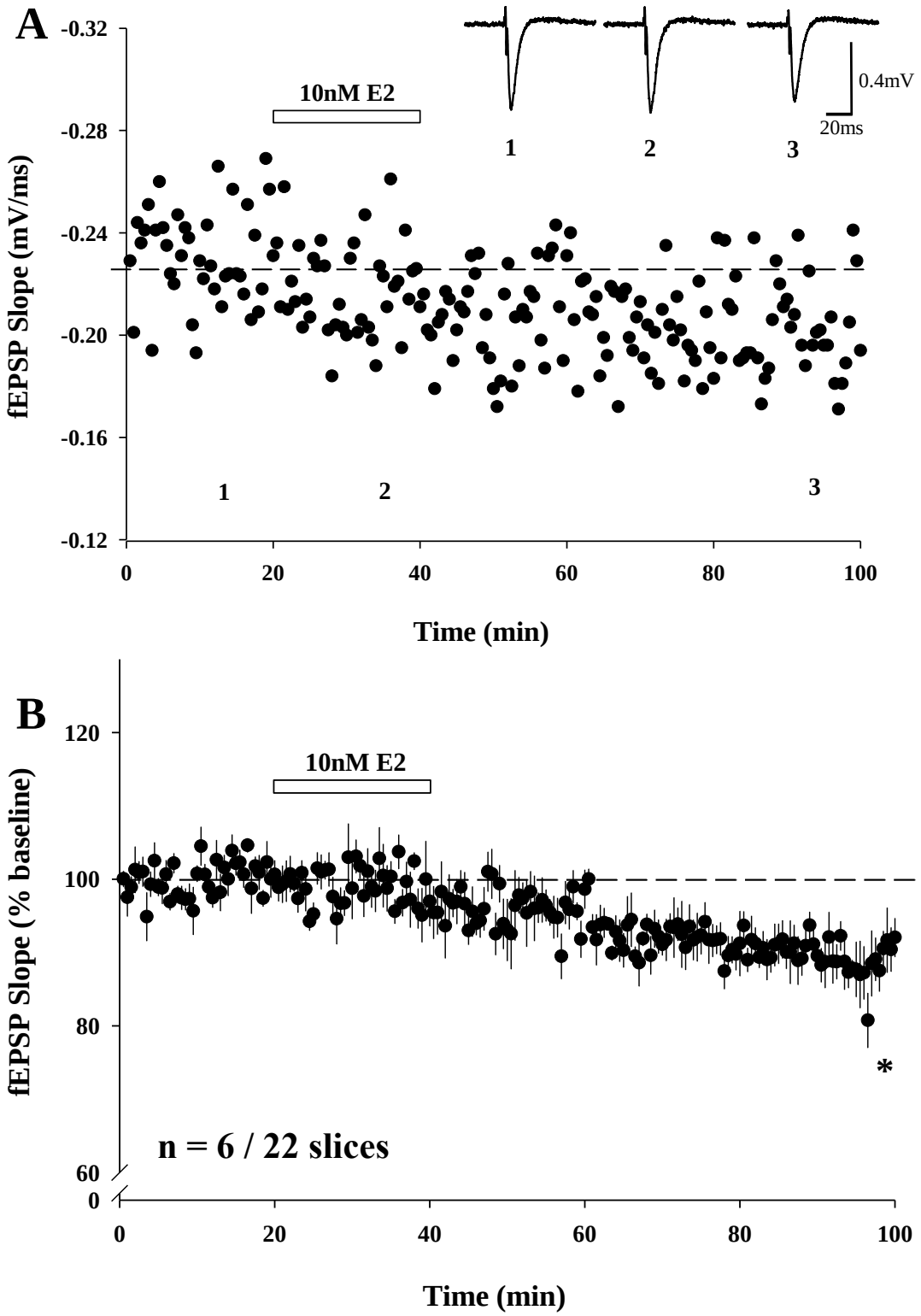

Figure 4.5: E2 induces LTD without a preceding potentiation of synaptic transmission in a subset of experiments. ***A,*** representative experiment showing E2 (10 nM; 20 min) application results in a slow onset long-lasting reduction in synaptic transmission. Top, example traces from the experiment are shown at the time points indicated. ***B,*** data pooled (n = 6 out of 22) and normalised with respect to baseline are expressed as mean ± SEM. * represents $p < 0.05$ vs. baseline; one-way repeated measures ANOVA followed by tukey *post-hoc* analyses.

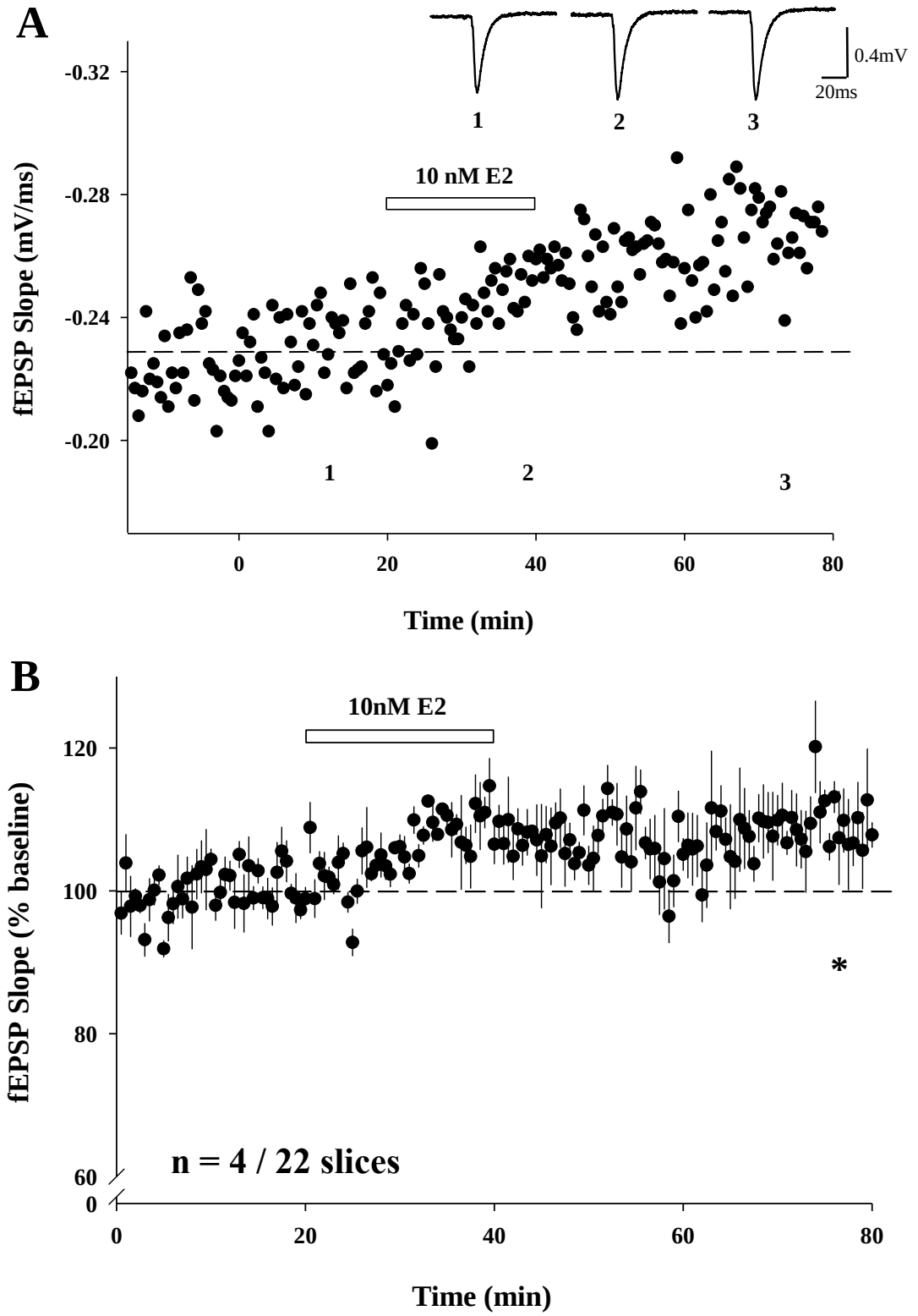

Figure 4.6: E2 induces a long-lasting potentiation of synaptic transmission in a subset of experiments. ***A,*** representative experiment showing E2 (10 nM; 20 min) application results in a sustained increase in synaptic transmission. Top, example traces from the experiment are shown at the time points indicated. ***B,*** data pooled (n = 4 out of 22) and normalised with respect to baseline are expressed as mean ± SEM. * represents $p < 0.05$ vs. baseline; one-way repeated measures ANOVA followed by tukey *post-hoc* analyses.

4.2.3: Effects of the GPR30 agonist on excitatory synaptic transmission in adult male hippocampal slices.

In the next series of experiments the effects of the selective GPR30 agonist (G1) on hippocampal excitatory synaptic transmission were examined in order to establish whether the effects of this agonist mimicked those of E2. Although G1 has a similar binding affinity for GPR30 as E2 (K_i ~ 6nM for E2 vs. K_i = 11nM for G1; Revankar *et al*., 2005; Bologa *et al*., 2006), initial studies examined the effects of applying a low concentration of G1 (1 nM; 20 min) to adult hippocampal slices. At this concentration however, G1 had no effect on basal excitatory synaptic transmission such that the magnitude of evoked synaptic responses remained unchanged during drug application (102 ± 1.1% of baseline; $p > 0.05$; n=5; Fig 4.7) and after 60 min of washout (98 ± 3.0% of baseline; $p > 0.05$; n = 5).

Due to the lack of effect at 1 nM, the concentration of G1 was increased. Application of G1 at 10 nM (20 min; Fig 4.8) elicited a transient but not significant potentiation in synaptic transmission (to 105 ± 2.3 % of baseline; $p = 0.078$; n = 27) followed by a slow-onset depression of synaptic transmission during G1 washout. The magnitude of the G1-induced depression peaked approximately 40 min after G1-washout (to 89 ± 2.5 % of baseline; $F[2,80] = 27.4$; $p < 0.001$; n = 27). In a manner similar to E2, it was noted that application of G1 at this concentration resulted in differing response profiles, thus data was stratified in order to further investigate these (see 2.2.5.3 in Methods).

Out of the 27 slices that were exposed to G1 at 10 nM (20 min), a bi-phasic response profile was evident in 12 slices (44%) (Fig 4.9). In this group, application of G1 induced an initial increase in excitatory synaptic transmission (to 110 ± 1.4% of baseline within 15 min of G1 application; $F[2,35] = 67.6$; $p < 0.001$; n = 12). Following G1 removal, synaptic transmission quickly began to decrease and a sustained depression of synaptic transmission was observed approximately 40 min after G1 washout (to 88 ± 2.0 % of baseline; $F[2,35] = 67.6$; $p < 0.001$; n = 12). Exposure to G1 (10 nM; 20 min) in another 12 out of 27 slices (44%), elicited only a slow-onset depression of excitatory synaptic transmission. Specifically, during G1 application there was no significant difference in the magnitude of synaptic transmission (95 ± 2.1 % of baseline during G1 application; $p > 0.05$; Fig 4.10), whereas by the end of the 60 min washout period, synaptic transmission was significantly reduced to 84 ± 2.8% of baseline ($F[2,35] = 21.4$; $p < 0.001$; n = 12). In a manner similar to E2, G1-induced an increase in synaptic

transmission in a subset of experiments (3 out of 27 slices; 11%); an effect that was sustained for up to 40 min following G1 washout, however due to variability and a low number of replicates, this effect was not significant (to 111 ± 6.0 % of baseline; $p > 0.05$; Fig 4.11).

In order to establish whether there are concentration-dependent effects of G1 at this synapse, a higher concentration (100 nM) of G1 was also examined. Here we find that exposure to 100 nM (20 min) results in a biphasic response profile (n = 6), exposure to 100 nM results in a rapid and significant potentiation of synaptic transmission (to 110 ± 2.8 % of baseline; $F[2,16] = 36.0$; $p < 0.05$; n = 6; Fig 4.12), followed by a slow onset depression of synaptic transmission which peaked 50 min after G1 washout (to 90 ± 1.3 % of baseline; $F[2,16] = 36.0$; $p < 0.05$; n = 6). After data was subjected to stratification, it was found that out of the 6 slices that were exposed to 100 nM G1 (20 min), 4 slices exhibited a bi-phasic response profile (67%). Application of 100 nM G1 induced a rapid and significant potentiation of synaptic transmission (to 112 ± 3.8 % of baseline; $F[2,11] = 32.1$; $p < 0.05$; n = 4; Fig 4.13); a magnitude which was not significantly different to that evoked at 10 nM G1 which induced a biphasic response profile (110 ± 1.4% of baseline for 10 nM G1; $p > 0.05$; n = 12; one-way ANOVA on ranks followed by Dunns' *post-hoc* analysis). The G1-induced enhancement was followed by a slowly developing reduction of synaptic transmission that peaked 40 min after G1 washout (to 90 ± 1.7 % of baseline; n = 4; $F[2,11] = 32.1$; $p < 0.05$). Moreover, the magnitude of the synaptic depression induced by 100 nM G1 was not significantly different to that observed in response to 10 nM G1 application which was preceded by an enhancement of synaptic transmission (88 ± 2.0 % of baseline for 10 nM G1; $p > 0.05$; one-way ANOVA on ranks followed by Dunns' *post-hoc* analysis). Of the two remaining slices examined, exposure to 100 nM G1 induced only a slow-onset sustained depression of synaptic transmission in one slice (Fig 4.14 A) and in the other, a long-lasting increase in synaptic transmission in response to 100nM G1 application was observed (Fig 4.14 B).

These results suggest that the GPR30 agonist, G1, like E2, can induce three different effects on hippocampal synaptic transmission: A transient potentiation followed by LTD; LTD in the absence of prior potentiation and a sustained increase in synaptic transmission. Moreover, the magnitude of the depression elicited by G1 (10 nM – 100 nM) was not significantly different between the different response profiles (Fig 4.15).

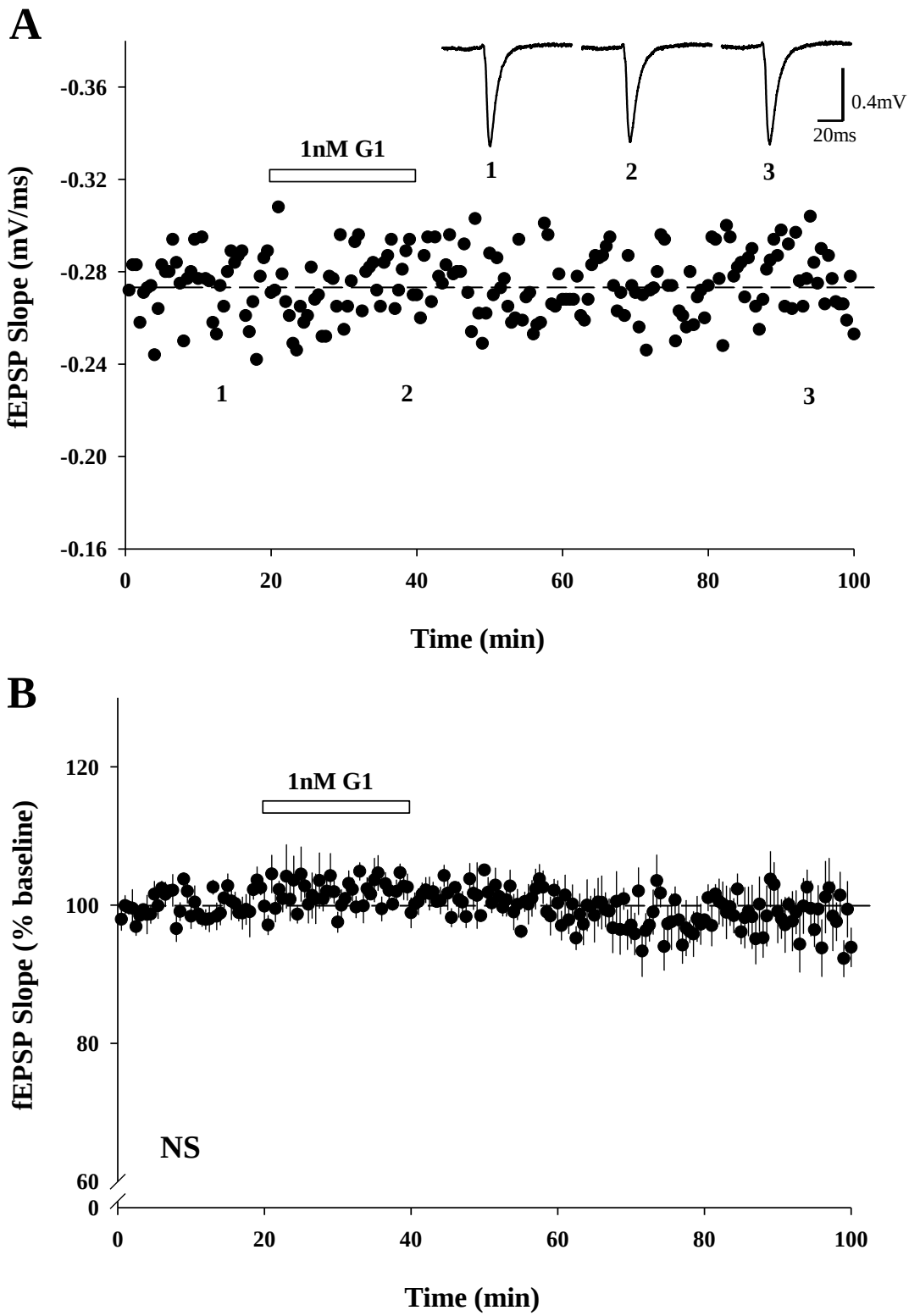

Figure 4.7: 1 nM G1 has no effect on basal synaptic transmission in adult male hippocampal slices. ***A,*** representative experiment showing G1 (1 nM; 20 min) application does not alter basal excitatory synaptic transmission. Top, example traces from the experiment are shown at the time points indicated. ***B,*** data pooled (n=5) and normalised with respect to baseline are expressed as mean ± SEM. NS represents a non-significant ANOVA ($p > 0.05$); One-way repeated measures ANOVA.

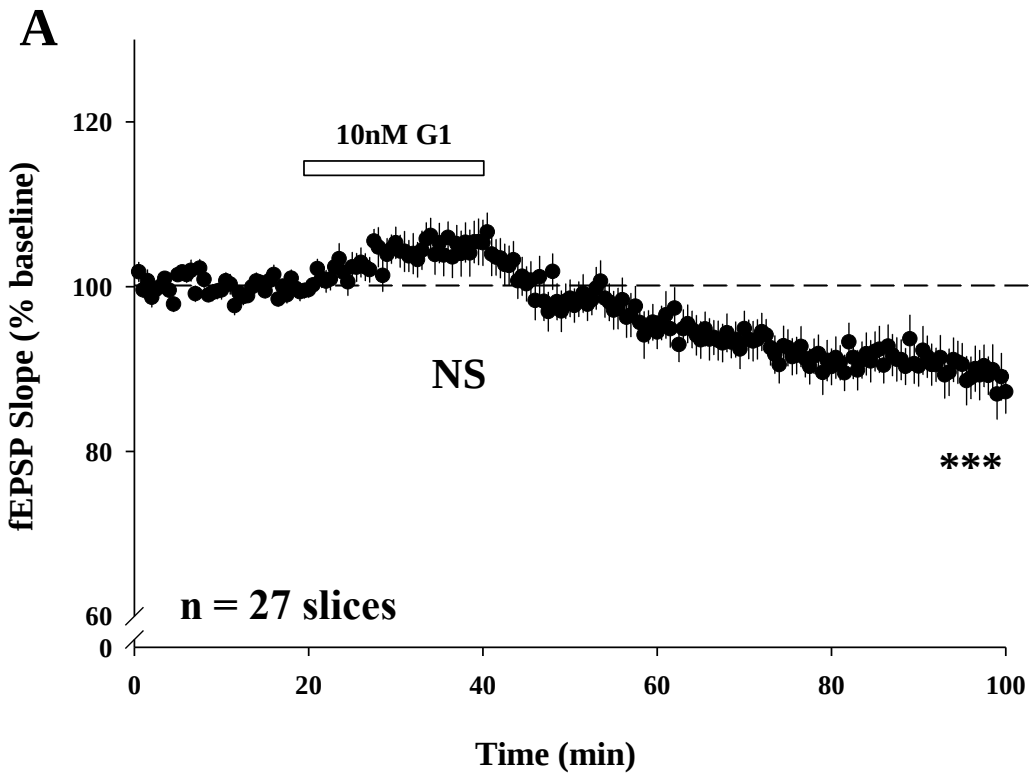

Figure 4.8: 10 nM G1 elicits a bi-phasic effect on basal synaptic transmission in adult male hippocampal slices. ***A,*** G1 (10 nM; 20 min) application transiently potentiates excitatory synaptic transmission, followed by a reduction in synaptic transmission after washout. Data are pooled (n = 27) and normalised with respect to baseline and are expressed as mean ± SEM. NS represents $p > 0.05$ vs. baseline; *** represents $p < 0.001$ vs. baseline; one-way repeated measures ANOVA and Tukey *post-hoc* analysis.

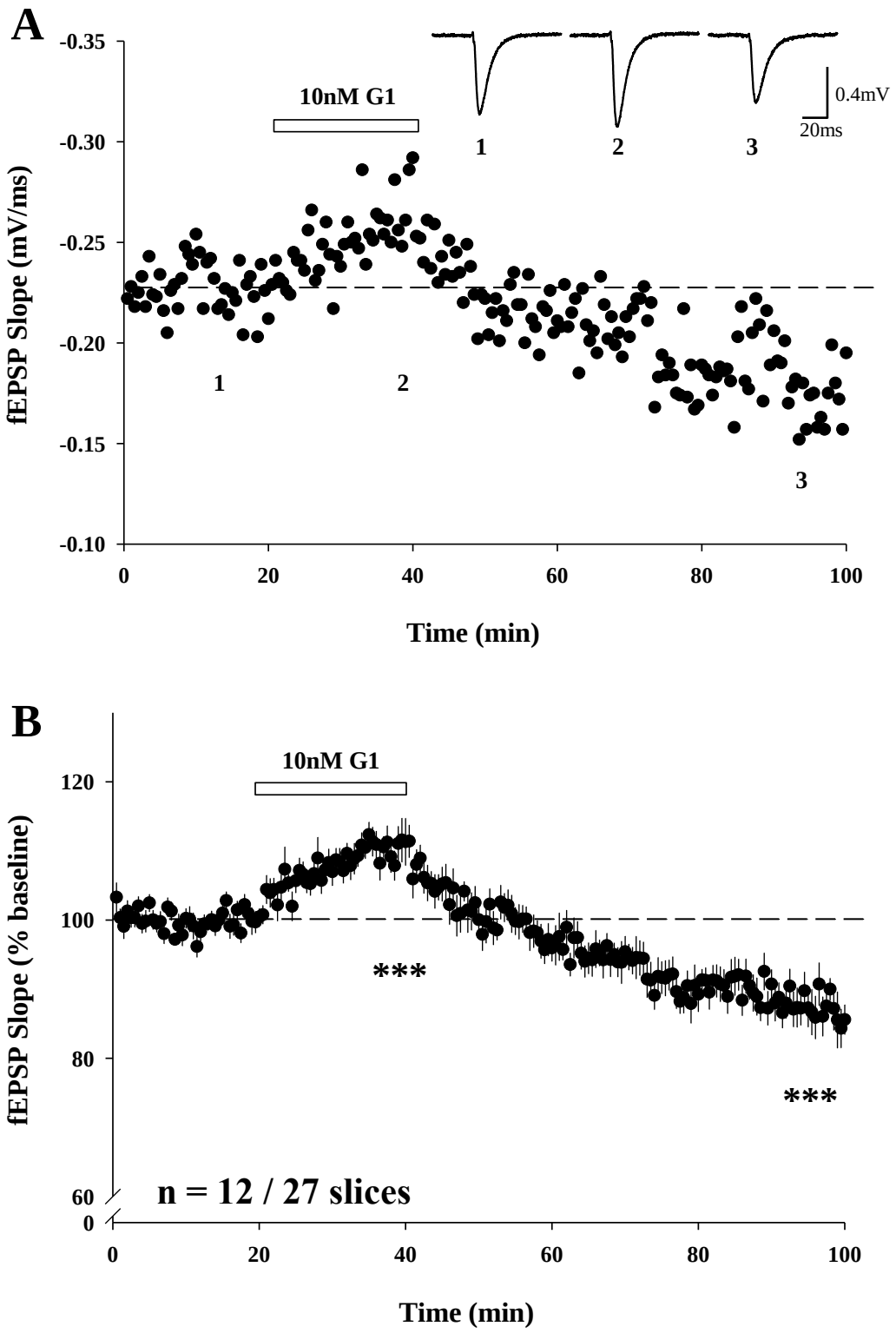

Figure 4.9: In a proportion of slices 10 nM G1 elicits a bi-phasic effect on basal synaptic transmission. ***A,*** representative experiment showing G1 (10 nM; 20 min) application transiently potentiates excitatory synaptic transmission, followed by a reduction in synaptic transmission after washout. Top, example traces from the experiment are shown at the time points indicated. ***B,*** data pooled (n = 12 out of 27) and normalised with respect to baseline are expressed as mean ± SEM. *** represents $p < 0.001$ vs. baseline; one-way repeated measures ANOVA and Tukey *post-hoc* analysis.

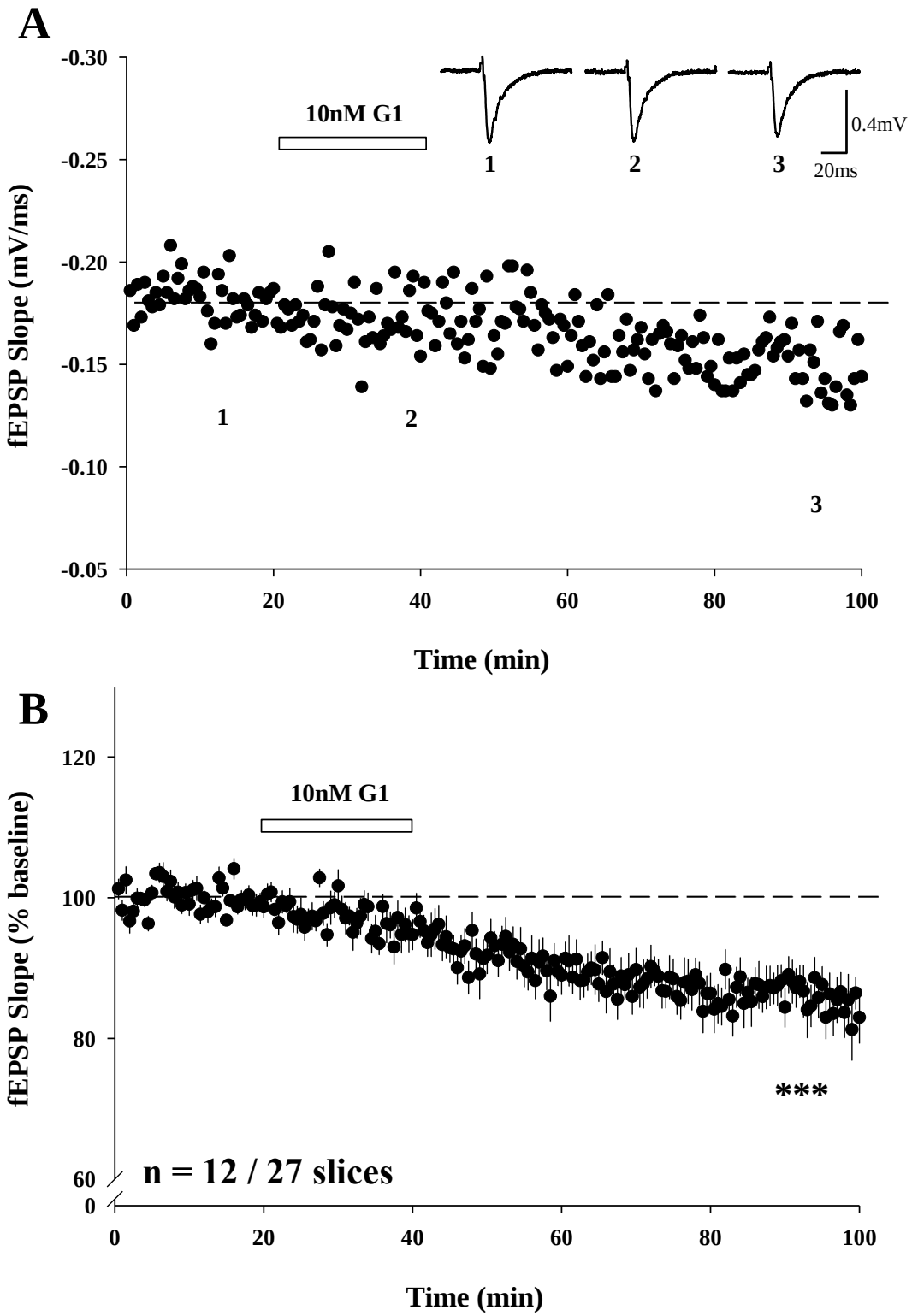

Figure 4.10: 10 nM G1 induces LTD without a preceding potentiation of synaptic transmission. ***A,*** representative experiment showing G1 (10 nM; 20 min) application results in a slow onset long-lasting reduction in synaptic transmission. Top, example traces from the experiment are shown at the time points indicated. ***B,*** data pooled (n = 12 out of 27) and normalised with respect to baseline are expressed as mean ± SEM. *** represents $p < 0.001$ vs. baseline; one-way repeated measures ANOVA and Tukey *post-hoc* analysis.

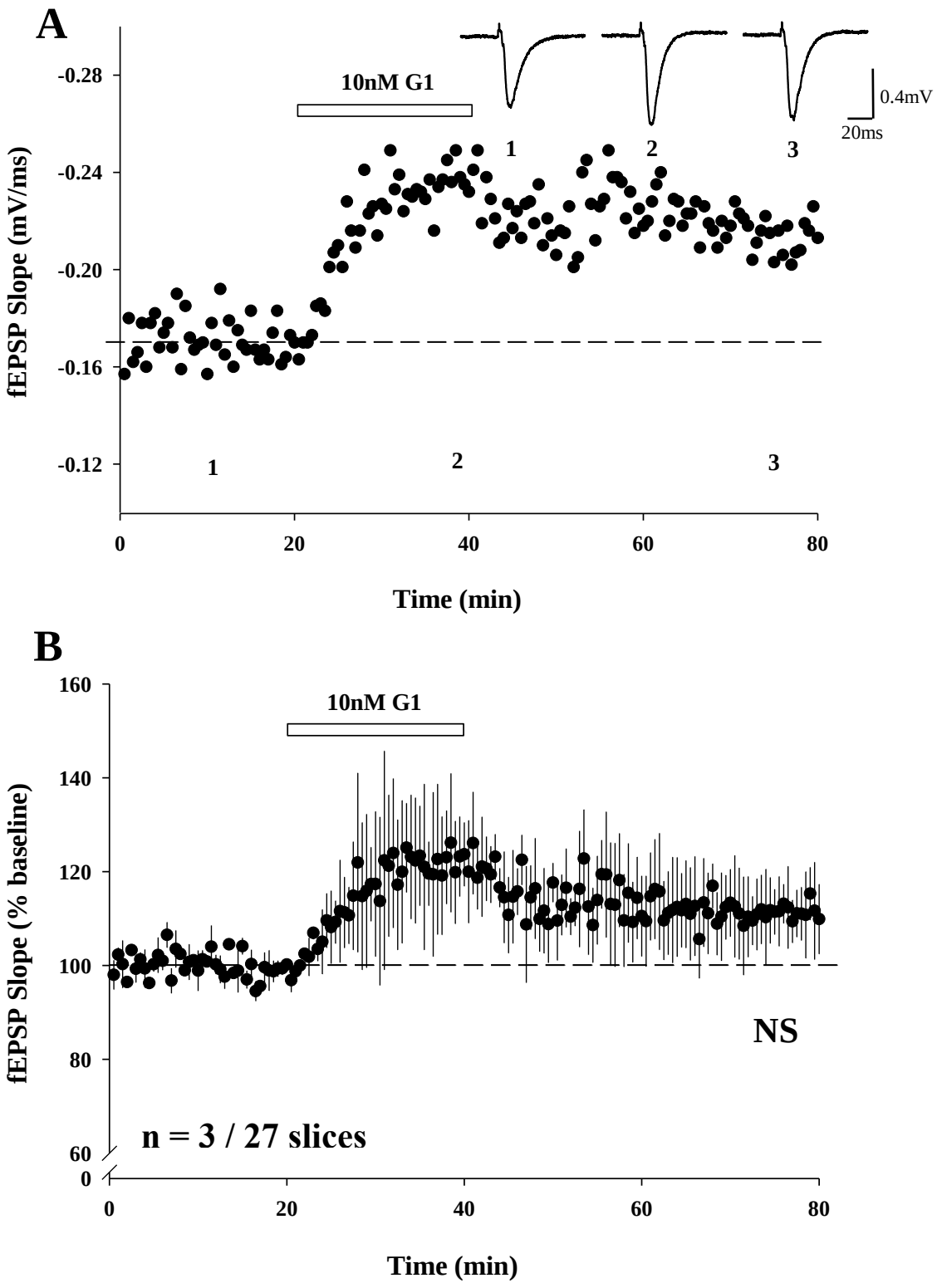

Figure 4.11: 10 nM G1 induces a long-lasting potentiation of synaptic transmission in a subset of experiments. ***A,*** representative experiment showing G1 (10 nM; 20 min) application results in a sustained increase in synaptic transmission. Top, example traces from the experiment are shown at the time points indicated. ***B,*** data pooled (n = 3 out of 27) and normalised with respect to baseline are expressed as mean ± SEM. NS represents $p > 0.05$; a non-significant ANOVA.

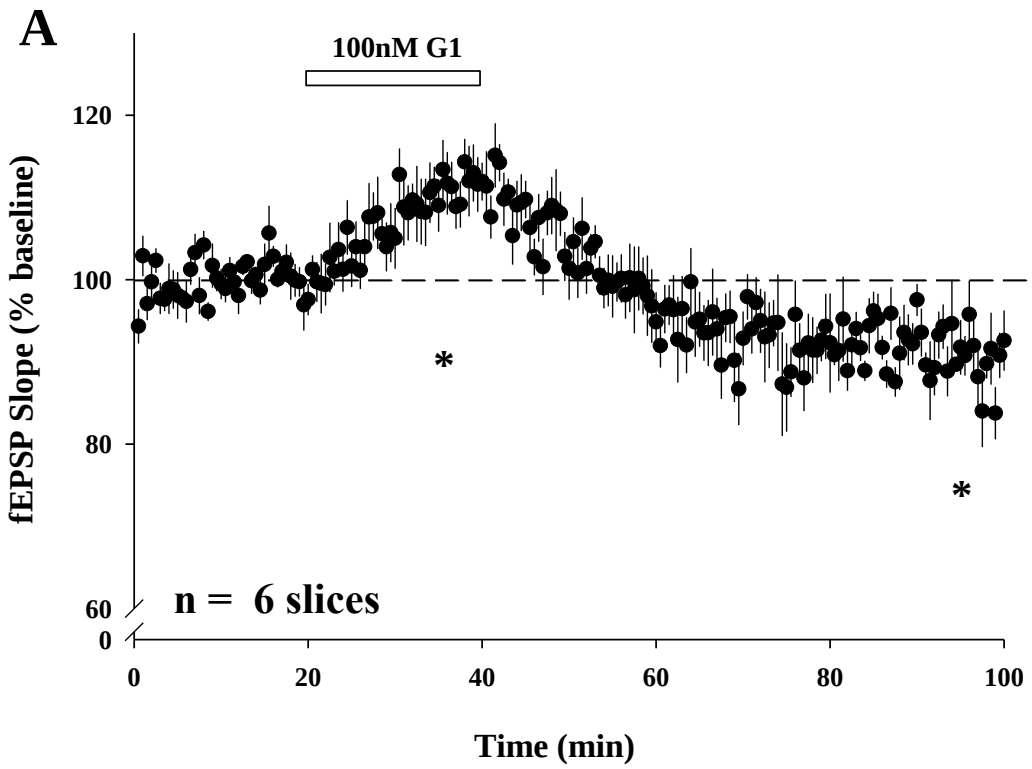

Figure 4.12: 100 nM G1 has a bi-phasic effect on basal synaptic transmission in adult male hippocampal slices. ***A,*** Data pooled (n = 6) and normalised with respect to baseline are expressed as mean ± SEM. * represents $p < 0.05$ vs. baseline; one-way repeated measures ANOVA followed by Tukey *post-hoc* analysis.

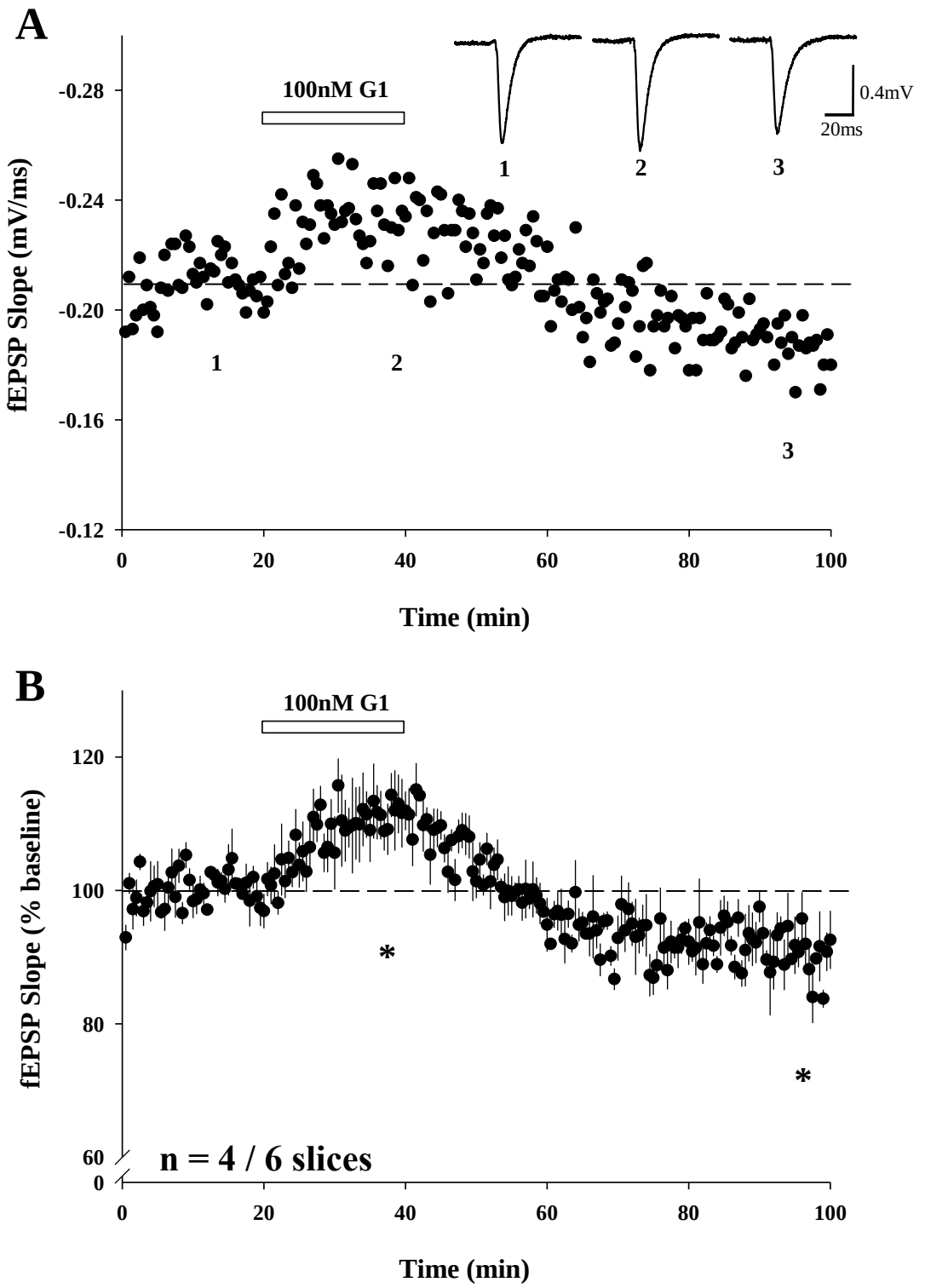

Figure 4.13: In a proportion of slices 100 nM G1 has a bi-phasic effect on basal synaptic transmission. ***A,*** representative experiment showing G1 (100 nM; 20 min) application transiently potentiates excitatory synaptic transmission, followed by a long-lasting reduction in synaptic transmission. Top, example traces from the experiment are shown at the time points indicated. ***B,*** data pooled (n = 4 out of 6) and normalised with respect to baseline are expressed as mean ± SEM. * represents $p < 0.05$ vs. baseline; one-way repeated measures ANOVA followed by Tukey *post-hoc* analysis.

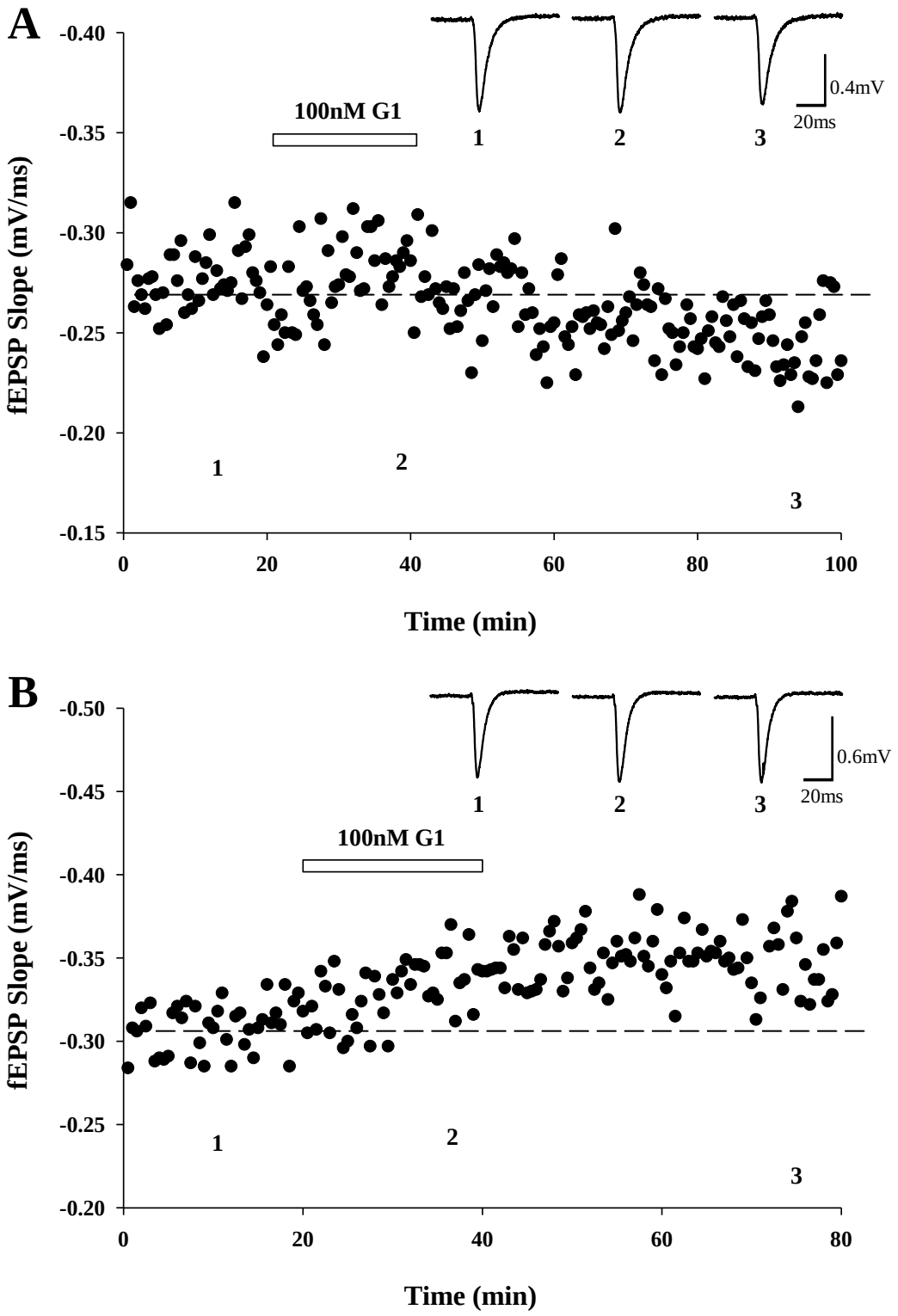

Figure 4.14: 100 nM G1 can also induce a sustained depression or a sustained potentiation of synaptic transmission in a proportion of slices. ***A,*** Experiment illustrating G1 (100 nM; 20 min) application induces a depression of synaptic transmission (1 out of 6 slices). ***B,*** Experiment illustrating (100 nM; 20 min) induces a sustained increase in synaptic transmission (1 out of 6 slices). Top, example traces from the experiments are shown at the time points indicated.

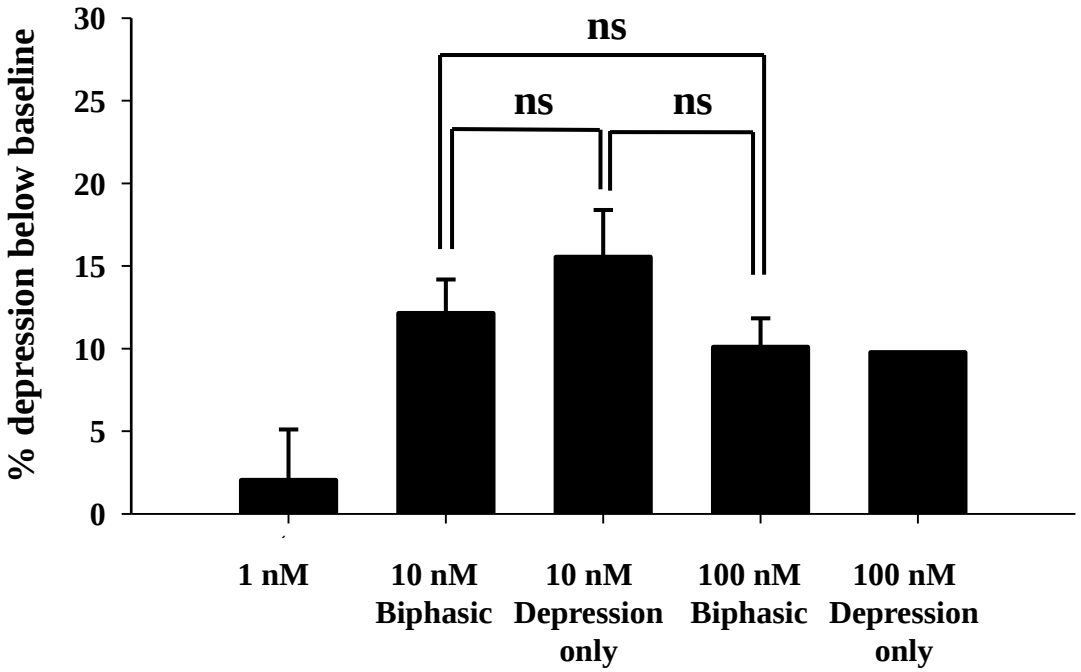

Figure 4.15: Comparison of the mean magnitudes of depression of synaptic transmission elicited by differing concentrations of G1. Histogram depicts the mean ± SEM % of depression of synaptic transmission 50 – 60 min post washout of G1 from the different response profiles. There is no significant difference between the magnitudes of depression elicited by 10 nM G1 from the biphasic response profile, 10 nM depression only profile and 100 nM Biphasic response profiles. NS represents $p > 0.05$ between the magnitudes of the G1-induced depression from differing response profiles and concentrations; One-Way ANOVA followed by Tukey *post-hoc* analysis.

4.2.4: Comparison of the two most prevalent response profiles of E2 and G1.

In order to compare the time course and magnitude of the effects of both E2 and G1 on synaptic transmission, the pooled data were overlayed. Figure 4.16 A illustrates that the time course and magnitudes of the bi-phasic response profiles for E2 and G1 are comparable. Specifically, the magnitudes of the agonist-induced transient potentiation of synaptic transmission are not significantly different from each other (E2: 107 ± 1.0 % of baseline, n = 12 / 22 slices; G1: 110 ± 1.4 % of baseline, n = 12 / 27 slices; $p > 0.05$; Kruskal-Wallis one-way ANOVA on ranks). In addition, the magnitudes of the slow-onset agonist-induced depression of synaptic transmission are not significantly different from each other (E2: 87 ± 1.5 % of baseline; n = 12 / 22 slices; G1: 88 ± 2.0 % of baseline, n = 12 /22 slices; $p > 0.05$; Kruskal-Wallis one-way ANOVA on ranks).

The time course and magnitudes of the slow-onset depression of synaptic transmission without a preceding potentiation of synaptic transmission between E2 and G1 are also very similar (Fig 4.16 B). Specifically, the magnitudes of the agonist-induced depression of synaptic transmission are not significantly different from each other (E2: 89 ± 2.7 % of baseline, n = 6 / 22; G1: 84 ± 2.8% of baseline, n = 12 / 27; $p > 0.05$; Kruskal-Wallis one-way ANOVA on ranks).Thus, these data would suggest that the GPR30 agonist (G1) can mimic the effects of E2 on excitatory synaptic transmission in adult male hippocampal slices.

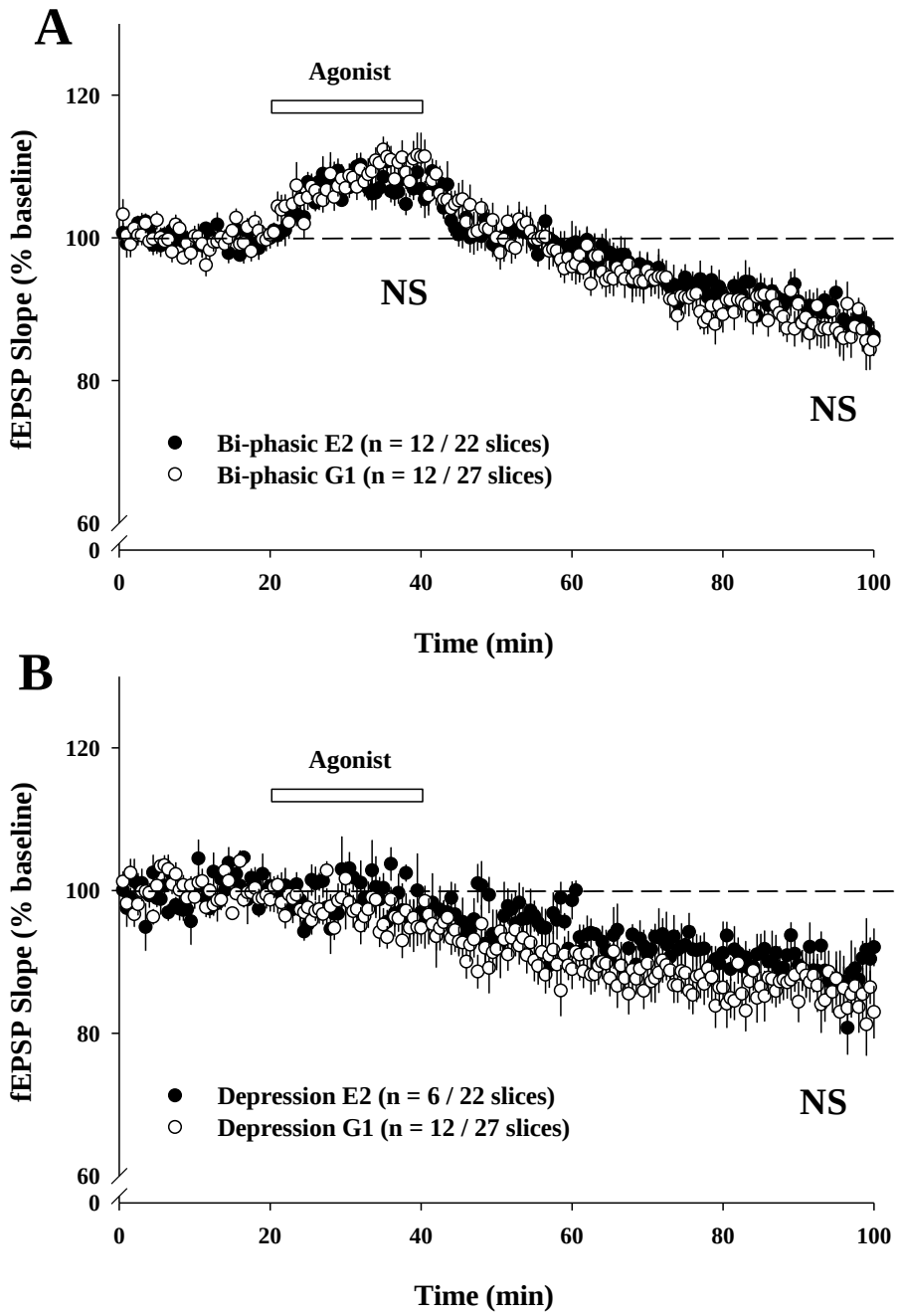

Figure 4.16: The GPR30 agonist mimics the effects of E2 on hippocampal excitatory synaptic transmission. ***A,*** Plot of pooled data from the preceding experiments illustrating the bi-phasic response profile of E2 and G1 (from Fig. 4.4 B and Fig. 4.9 B) ***B,*** Plot of pooled data from the preceding experiments illustrating the depression only response profile of E2 and G1 (from Fig. 4.5 B and Fig. 4.10 B). NS represents $p > 0.05$ between the magnitudes of the E2 and G1 effects on synaptic transmission at the time points shown, Kruskal-Wallis one-way ANOVA on ranks.

Summary of findings from Chapter 4, Part I:

1) In juvenile hippocampal slices, G1 induces a large depression of excitatory synaptic transmission under conditions of enhanced excitability (Fig. 4.2).
2) Acute administration of E2 induces three different response profiles in adult male hippocampal slices (Fig 4.4, 4.5 and 4.6). The predominant effect of which, is the induction of LTD
3) In a manner similar to E2, application of G1 evokes three distinct effects on synaptic transmission, with the induction of LTD the predominant response observed. Moreover, the time-courses and magnitudes of the two most prevalent response profiles of E2 are mimicked by the GPR30 agonist, G1 (Figure 4.16).

4.3: Discussion

4.3.1: Developmental differences in G1-mediated effects on hippocampal synaptic transmission.

We show here that there are differences in the effects of the GPR30 agonist, G1, on hippocampal excitatory synaptic transmission between slices from juvenile (P11 – P18) and adult (12 – 20 weeks) rodents. It is not uncommon for hormone modulators of hippocampal function to have differing effects across developmental time periods. For example exposure to leptin in juvenile hippocampal slices transiently depresses synaptic transmission under normal conditions and induces a novel form of LTD in conditions of enhanced excitability (Durakoglugil *et al*., 2005; Moult and Harvey, 2011). Whereas in adult tissue, leptin induces a long lasting potentiation of synaptic transmission (Moult *et al.*, 2010; Moult and Harvey, 2011). These leptin-induced effects on synaptic transmission in juvenile tissue parallel those which we see with G1, as we were unable to see significant effects in basal conditions; however in conditions of increased excitability a significant depression of synaptic transmission was observed.

Synaptic maturation at CA3 – CA1 synapses occurs during the first two weeks of post-natal development. Specifically, early in development, synapses are predominantly AMPA silent and express the slowly-deactivating GluN1/GluN2B NMDAR complexes, facilitating activity-dependant maturation of glutamatergic synapses (shifting from more AMPA-silent to un-silent; Pickard *et al*., 2000). This transition is also accompanied by a change in the expression ratio of NMDAR subunits at synapses from predominantly GluN1/GluN2B complexes to the more quickly deactivating GluN1/GluN2A complexes (Monyer *et al*., 1992, 1994; Sheng *et al*., 1994). Developing neurons also have a higher pre-synaptic glutamate release probability (Bolshakov and Siegelbaum, 1995; Wasling *et al*., 2004) and the magnitude and ease at which LTD is induced is significantly greater in rodents < 3 weeks old (Dudek and Bear, 1993; Milner *et al*., 2004; Strandberg *et al*., 2009; Strandberg and Gustafsson, 2011). In addition, there is evidence for a developmental switch in the mechanisms of mGluR mediated LTD between P8 – P15 and P21+ rodents (Nosyreva and Huber, 2005).

Considering we observe an LTD of synaptic transmission in response to G1 in tissue from P11 – P18 rodents only in conditions of enhanced NMDAR-mediated synaptic transmission, this may suggest that during development, G1-induced effects require enhanced NMDAR activity whereas at more mature synapses, G1-induced effects do not require enhanced NMDAR activity. This suggests a shift in the mechanisms by which G1 can effect glutamatergic synaptic transmission between juvenile and adult tissue, and may illustrate a potential role for GPR30 in mediating maturation of synapses.

Moreover, there is a wealth of evidence beginning to emerge suggesting that all aspects related to estrogen physiology within the hippocampus are developmentally regulated. For example, in rats, hippocampal derived E2 levels peak at birth and gradually decline over the first two weeks of postnatal life (Konkle and McCarthy, 2011). Expression of key enzymes required for the conversion of PREG to E2 are significantly higher in P10 male rodents compared to adult and the rate of metabolism from testosterone and E1 to E2 is significantly faster in P10 rodents compared to adult (Higo *et al*., 2009). Hippocampal expression levels of StAR, the protein responsible for the rate-limiting step or all steroidogenesis also increases throughout the first few weeks of post natal life (Kim *et al*., 2002; Sierra *et al*., 2003). In addition, expression levels of estrogen receptors fluctuate during development. For example there are significant differences in

cortical and hippocampal expression levels of the classical ERα between P10 and adult rodents (O'Keefe *et al*., 1995; Solum and Handa, 2001; Kimoto *et al*., 2010; Wilson *et al*., 2011). Specifically, in the male rodent hippocampus relative mRNA levels of ERα (Esr1) only stabilize to constant levels at 4 weeks of age, to around 70 – 80% of post-natal day 1 expression levels (Kimoto *et al*., 2010). However, it is also worth noting that hippocampal mRNA levels of ERβ (Esr2) remain relatively constant throughout development (from post-natal day 1 through to 12 week old rodents) (Kimoto *et al*., 2010). As GPR30 is generally considered an estrogen-sensitive receptor, it is feasible that expression of GPR30 is also developmentally regulated. Although the developmental profile of GPR30 expression has not been thoroughly examined in the rodent hippocampus, there is evidence for developmental changes in GPR30 expression in other animal models. For example, in the zebra finch songbird, telencephalon expression of GPR30 mRNA drastically increases from P3 to P30 and drops substantially in adult, for both male and female finches (Acharya and Veney, 2012). Songbirds are important animal models, often utilised to study behavioural sex-differences. Acharya and Veney (2012) postulated that GPR30 may contribute to the E2-induced organisation of circuits required for song production and memory in male finches, considering that expression of GPR30 significantly increased and was significantly different from female finches around P25, a time where vocalisation of song begins to occur. With respect to the rodent hippocampus, GPR30 has also been implicated in having a pivotal role in E2-induced enhancement of neurite outgrowth in developing (DIV 3) hippocampal neurons (Ruiz-Palmero *et al.*, 2013).

As estrogen receptor expression levels and concentrations of E2 within the CNS of juvenile rodents are substantially different compared to those in adult, it is likely that responses to exogenous application of estrogen receptor agonists will vary throughout different stages of development. Further work to characterise the acute effects of estrogen and synthetic estrogen receptor agonists across the developmental time period would be beneficial to our overall understanding of the role that this hormone has in hippocampal function.

4.3.2: E2 elicits different response profiles on basal hippocampal synaptic transmission, which are mimicked by the GPR30 agonist, G1.

Here we find that acute administration of E2 or G1 (10 – 100nM) on adult male hippocampal slices can elicit three different response profiles:

1) A bi-phasic response consisting of an initial increase in synaptic responses, followed by LTD.
2) An induction of LTD without prior potentiation of synaptic transmission.
3) And in a small proportion of slices, an agonist-induced long-lasting increase in synaptic transmission (LTP).

As we are recording synaptic responses from a population of dendrites at the *stratum radiatum,* the variable response profiles seen here for both E2 and G1 could be attributed to number of factors.

For example, estrogen receptor expression ratios in populations of synapses or in slices from different animals may vary. Indeed ERα, ERβ or GPR30 immunoreactivity is only observed in a subset of dendritic spine or shaft profiles in the *stratum radiatum* (specifically only ~30% of synapses in this layer are ERα positive) (Milner *et al*., 2001, 2005; Adams *et al*., 2002; Akama *et al*., 2013). Moreover, expression of estrogen receptors can also be influenced by external factors outside the level of control in this study, such as the level of maternal care rodents received as pups, which has been demonstrated to influence levels of ERα expression in the CNS (Champagne *et al*., 2003).

Between animal or between slice variations in levels of neuronal excitability and synaptic connectivity may also account for the variable response profiles. This is feasible considering effects of G1 in juvenile rodents is revealed in hyper-excitable conditions (Figure 4.2) and a novel form of E2-induced LTD in adult hippocampal tissue is observed in hyper-excitable conditions (Moult and Findlay, *unpublished findings*). Since recent or chronic exposure to corticosteroids can influence many aspects of hippocampal glutamatergic synaptic transmission in rodents (as reviewed in Popoli *et al*., 2012), it is reasonable to suggest that individual exposure to stress would impact the G1- and E2- induced effects observed here. Indeed acute exposure to corticosterone increases pre-synaptic glutamate release at CA3 – CA1 synapses (Karst *et al*., 2005) and influences the content and mobility of synaptic GluA2 containing

AMPARs in hippocampal cultures (Groc *et al*., 2008; Martin *et al*., 2009). In addition, chronic stress impairs the magnitude of LTP at CA1 – pre-frontal cortex connections (Cerqueira *et al*., 2007) and decreases dendritic spine density in CA3 (Magariños *et al*., 2011) and CA1 (Pawlak *et al*., 2005) neurons. Thus it is feasible that stress induced alterations in dendritic morphology, excitability and transmission at CA1 synapses may influence the effects of G1 and E2. In support of this, it is becoming increasingly evident that these two hormonal systems are closely related and integrate to influence hippocampal excitatory synaptic transmission and plasticity (Ooishi *et al*., 2012b; Wang *et al*., 2013).

There is a general consensus that E2 has the ability to acutely potentiate hippocampal excitatory synaptic transmission (or increase excitability) in a proportion (~50 – 80%) of experiments (whether it be population or single cell recordings), table A.1 in the appendix summarises this data. With respect to acute administration of G1, Lebesgue and colleagues (2010) illustrate that in young-adult OVX female rodents, a concentration of G1 (10 nM) can induce an acute potentiation of hippocampal CA1 excitability in 9 out of 14 slices tested (64 %) (Lebesgue *et al*., 2010) or (at 100 nM G1) in 4 out of 7 cells tested (57 %) (Lebesgue *et al*., 2009); a rate of response which is similar to our data (56% and 83 % of slices exhibited a potentiation upon 10 nM or 100 nM G1-application, respectively). However, others have shown in OVX and E2-primed rodents, the rate of G1-induced enhancement of synaptic responses is very low (2 out of 15 cells, 13 %; Smejkalova and Woolley, 2010). Moreover, the time course at which we see E2- and G1- induced potentiation (within 5 – 10 min of ligand application) equals the time course of these effects which others have observed at this synapse (Teyler *et al*., 1980; Foy *et al*., 1999; Gu *et al*., 1999; Sharrow *et al*., 2002; Kramár *et al*., 2009; Lebesgue *et al*., 2009, 2010; Zadran *et al*., 2009; Smejkalova and Woolley, 2010). Thus the rate at which we see the G1- or E2- induced enhancement of excitatory synaptic transmission, and the time course for which this occurs, parallels those which have been observed in other studies. However, the exact molecular mechanisms for the E2-induced enhancement of synaptic transmission and excitability within the hippocampus are not fully understood and may involve a number of mechanisms. Classic studies reported an E2-induced increase in AMPAR conductance (amplitude of kainate-induce currents) via a G-protein coupled and cAMP-dependant phosphorylation event (Gu and Moss, 1996, 1998; Gu *et al*., 1999). Whereas more recent studies indicate an E2-induced potentiation

of Ca^{2+} influx through L-type Ca^{2+} channels (Wu *et al*., 2005; Zhao *et al*., 2005) and a subsequent activation of the Src/MAPK/ERK signalling pathway leading to ERK-dependant phosphorylation and modulation NMDAR function (Bi *et al*., 2000, 2003). Conversely, the mechanism for rapid effects of E2 have been shown to be calcium independent and to involve rapid cytoskeletal arrangement and insertion of synaptic GluA1-containing AMPAR, effects which are thought to be mediated via activation of ERβ (Liu *et al*., 2008; Kramár *et al*., 2009; Zadran *et al*., 2009). It is also feasible that E2, by modulating glutamate and GABA release from presynaptic terminals, enhances synaptic transmission (Smejkalova and Woolley, 2010; Huang and Woolley, 2012).

Nevertheless, the important finding in this study is that following washout of E2 or G1, leads to in most cases (in 82% and 89% of slices for E2 and G1, respectively) the induction of a long-lasting depression of synaptic transmission. Previous electrophysiology studies examining the acute effects of E2 on basal hippocampal excitatory synaptic transmission using extracellular recording techniques at CA3 – CA1 synapses either concluded experiments after a 15 – 30min drug application (Teyler *et al*., 1980; Fugger *et al*., 2001; Sharrow *et al*., 2002; Zadran *et al*., 2009; Lebesgue *et al*., 2010) or continued E2 administration for an extended period of time (up to 100 min; Kim *et al*., 2006). Only one other study has followed experiments through a washout period, however the group did not observe any significant depression of synaptic transmission in response to E2 (Kramár *et al*., 2009). Although male rodents were used in that study (which may exclude the possibility a sex-specific effect) and a comparable concentration of E2 was used (1 nM) their washout period lasted only 30 min, which may account for this discrepancy (Kramár *et al*., 2009). Therefore, the data presented here demonstrates that long duration experiments with extended washout periods can uncover long-lasting changes in excitatory synaptic transmission induced by E2 and G1.

Although most studies have focused on the ability of E2 to enhance excitability and synaptic transmission as well as facilitate LTP (as reviewed in Woolley, 2007; Foy *et al*., 2008; Ogiue-Ikeda *et al*., 2008; Foy, 2011; Srivastava *et al*., 2011), our data indicate that this hormone also has the capacity to induce LTD at hippocampal CA3 – CA1 synapses. The slow-onset induction of long-lasting depression begins to occur ~15 min – 20 min after agonist washout when preceded by an enhancement of synaptic transmission (biphasic response profile) or ~15 – 20 min after agonist application in the cases where an enhancement of synaptic transmission was not observed (depression

only profile). Due to the time frame of these responses (< 1 hour), the data suggest that the induction of this type of LTD is likely to be attributed to a non-genomic mechanism of action (*ie*. activation of extra-nuclear estrogen receptors). Moreover, as the magnitude of the E2-induced long-lasting depression of synaptic transmission is not significantly different from the G1-induced effect, it is feasible that activation of GPR30 may be involved in this non-genomic action of E2.

In accordance with our data, previous studies have demonstrated that E2 (acute or chronic application) can enhance the magnitude or facilitate the induction of hippocampal LTD. For example, in hippocampal slices from adult male rats, acute application of E2 (1 – 10 nM) dose-dependently enhances the magnitude of NMDA-induced LTD at the CA1, CA3 and DG (Mukai *et al*., 2007). Interestingly, others have shown in the CA1 region that acute administration of E2 (1 nM) can also enhance DHPG-induced LTD (Shiroma *et al*., 2005). A genomic mechanism of E2-induced facilitation of LTD has also been observed. Specifically 2 day *in vivo* treatment of E2 in OVX female rats facilitated the induction of paired-pulse low frequency stimulation-induced LTD (Zamani *et al*., 2000). Together, these data would suggest an important role for E2 in mediating this type of synaptic plasticity.

LTD at CA1-synapses can also be induced by acute exposure to other hormonal modulators, such as leptin (albeit in juvenile rodents; (Durakoglugil *et al*., 2005)) and insulin (Huang *et al*., 2004; van der Heide *et al*., 2005). Moreover, acute exposure to another class of steroid hormones – the glucocorticoids (either by acute stress or application of corticosterone to slices) can enhance low frequency stimulation-(LFS), paired pulse-LFS- and DHPG-induced LTD in the hippocampus (Chaouloff *et al*., 2008; Huang *et al*., 2012; Popoli *et al*., 2012). Thus the ability for E2 to mediate hippocampal LTD is consistent with the body of literature suggesting that endocrine hormones influence hippocampal function.

LTD of excitatory synaptic transmission is a major form of synaptic plasticity in the mammalian CNS that (along with LTP) allows for the refinement of neuronal circuitry in response to external stimuli. The observation that E2 (in most cases) induces this form of plasticity, and this effect can be mimicked by a GPR30 agonist, is an important finding. Considering LTP and LTD of synaptic efficacy are considered the cellular correlates of learning and memory (Bliss and Collingridge, 1993), therapies which

target estrogen receptors and the synthesis of estradiol, may have long-lasting effects on cognition (Agrawal *et al*., 2010; Espeland *et al*., 2010; Frick, 2012).

4.3.3: Technical Considerations

In this study we have chosen to monitor basal synaptic transmission by recording evoked population EPSP's, as opposed to extracellular single unit or whole-cell recordings. This recording technique was chosen primarily due to the ease with which recordings could be made, moreover with this technique being far less invasive than whole-cell patch clamp it can be considered more physiologically relevant (compared to whole-cell recordings, as cells within slices remain intact and their intracellular constituents are not diluted with artificial intracellular solutions). Importantly, utilizing field EPSP recordings one can monitor synaptic transmission for extended periods of time more easily than with the patch-clamp technique.

Previously published literature had not fully investigated the long-lasting washout effects of neither estradiol nor the GPR30 agonist at the hippocampal CA3 – CA1 synapse. Thus, an electrophysiological recording technique which consistently enabled one to monitor synaptic transmission during extended agonist washout periods (1 hour) was employed, in order to probe for a washout effect. However, there are caveats of this technique. For example, unlike using the whole-cell patch clamp technique, one cannot manipulate the system as easily (for example, by including agents into the intracellular solution such as the calcium buffer BAPTA, or the non-hydrolysing GTPγS analogue, to delineate intracellular signalling mechanisms associated with agonist-induced effects). Nevertheless, using the extracellular fEPSP recordings, we are able to monitor the effects of ligands on a large population of cells, rather than at the single cell level, giving greater insight into the global effects of the agonists used.

Although we suggest here that the long-lasting washout effects of E2 and G1 are due to a decrease in synaptic transmission, we cannot exclude the possibility that these agonists may be inducing effects other than this. For example, application of these agonists may be causing a population of CA1 neurons to depolarise, an effect which is not reversed upon washout. If this were the case, then the electrochemical driving force for cation (Na^+ or Ca^{2+}) flux into the post-synaptic cell through activated ionotropic glutamate receptors in response to afferent stimulation, would be reduced. Thus, this

would manifest itself as a reduction in fEPSP slope measurements, like that which is observed here. This is a feasible explanation as it has been previously demonstrated that G1 (100 nM) can depolarise some (61 %) motor neurons in rat spinal cord slices by approximately 5 mV (Deliu *et al*., 2012) and in cultured spinal neurons by approximately 8 mV (Dun *et al*., 2009), however these groups demonstrated that this effect was readily reversible. In addition, in the seminal study by Wong and Moss (1991), it was observed that brief application of E2 (100 pM; 2 min) can depolarise a proportion (20 %) of CA1 pyramidal neurons in hippocampal slices from adult male and female rats by approximately 7 mV. However, like G1, this E2-induced depolarisation was readily reversible upon washout (Wong and Moss, 1991). If a sustained agonist-induced depolarisation accounts for the E2 and G1-induced reduction in fEPSP slope measurements in our study, then it would be worthwhile investigating this possibility by employing the whole-cell patch clamp technique in hippocampal slices in order to monitor membrane potential (by recording in current clamp mode) during agonist administration and importantly after agonist washout.

Moreover, another possible explanation for our G1- and E2- induced reduction in fEPSP slope measurements during washout could simply be due to toxic effects of these compounds. However, it should be noted that concentrations of 1 µM G1 failed to induce a significant change in fEPSP measurements in the juvenile model (Fig. 4.1) suggesting that this is not the case. Although unlikely, this does not exclude the possibility that G1 and E2 may have toxic effects in the adult model. In order to control for this, quantifying cell death (using propridium iodide staining for example) after exposure to these compounds and compared with vehicle controls would be useful in this respect.

4.4: Conclusion

The GPR30 agonist (G1) is likely to be inducing LTD in the juvenile hippocampus, an effect which requires enhanced NMDAR activity. In contrast, acute administration of E2 and G1 leads to (in most cases) the induction of a novel form of LTD in adult male hippocampal slices. Considering this novel form of LTD in adult tissue can be induced in basal conditions, this effect warranted further characterisation (see Chapter 5).

Chapter Five

Characterisation of the E2- and G1-induced LTD

5.1: Introduction

The novel and most consistent effect of E2 and G1 (10 nM) in our model is the slow-onset LTD of hippocampal excitatory synaptic transmission. LTD of hippocampal excitatory transmission can be expressed either pre- or post-synaptically (as reviewed in Malenka and Bear, 2004). Specifically, this may involve trafficking of post-synaptic AMPAR away from the synapse, changes in pre-synaptic glutamate release either directly (as reviewed in Collingridge *et al.*, 2010), or via retrograde messengers (such as cannabinoids (Péterfi *et al*., 2012) or NO (Reyes-Harde *et al*., 1999)).

Ultrastructure analysis in adult rodents has revealed localisation of ERα and ERβ in both pre- and post- synaptic compartments of CA1 pyramidal neurons (Milner *et al*., 2001, 2005; Mukai *et al*., 2007), and recently it has been reported that GPR30 is found at post-synaptic sites in a subset of CA1 dendritic spines (Akama *et al*., 2013). Although numerous studies have investigated the mechanisms of the E2 induced enhancement of excitability and synaptic transmission at CA3 – CA1 synapses, there are discrepancies regarding the locus of this effect, with groups reporting pre-synaptic (Smejkalova and Woolley, 2010) or post-synaptic (Wong and Moss, 1992; Foy *et al*., 1999; Kim *et al*., 2006) mechanisms. Considering the pre- and post-synaptic expression of extra-nuclear estrogen receptors' and as hippocampal LTD can be expressed pre- or post-synaptically, it is important to compare the locus of the novel E2- and G1-induced LTD in our model.

Excitatory synaptic transmission at CA3 – CA1 synapses primarily depends on activation of synaptic GluA2/GluA1 heteromeric AMPAR (Lu *et al*., 2009). Therefore, if E2- and G1- induced LTD involve a post-synaptic expression mechanism, then removal of synaptic AMPAR may contribute to the expression of LTD as this is generally considered a key event underlying activity-dependant post-synaptically expressed LTD (as reviewed in: Malenka, 2003; Shepherd and Huganir, 2007; Collingridge *et al*., 2010).

One mechanism by which LTD at CA3-CA1 synapses can be induced is dependent on the activity of NMDAR (Malenka and Bear, 2004; Collingridge *et al*., 2010). Previous studies have shown that some E2 induced effects in the rodent hippocampus are NMDAR-dependent, for example, E2 effects on dendritic spine density in the adult female (Woolley and McEwen, 1994; Woolley *et al*., 1997) and male (Mukai *et al*., 2007). Moreover, *in vivo* E2 replacement in OVX rats lowers the frequency threshold for hippocampal LTD induction in an NMDAR dependent manner (Zamani *et al*., 2000). Acute E2 exposure can also enhance LTD induced by exogenous NMDA administration (Mukai *et al*., 2007). In addition, acute application of E2 increases the amplitude of pharmacologically isolated NMDAR-mediated EPSPs of CA1 neurons (Foy *et al*., 1999). Thus it is feasible that the E2- and G1- induced depression of synaptic transmission may also involve an NMDAR-mediated component.

Thus, the aim of this chapter was to characterise further the cellular mechanisms underlying the novel forms of LTD induced by E2 and G1. We sought to establish the locus of the E2- and G1- induced LTD in the adult male hippocampal slice preparation and whether these agents could influence trafficking of AMPAR in primary hippocampal cultures. Furthermore, a role for NMDA receptors in the E2- and G1-induced effects was investigated.

5.2: Results

5.2.1: The effects of E2 and G1 on excitatory synaptic transmission are likely to be expressed post-synaptically.

To determine the locus of the E2- and G1-induced effects on hippocampal excitatory synaptic transmission a paired-pulse facilitation stimulation protocol was implemented, whereby slices were stimulated twice every 30s with an inter-stimulus interval of 50 ms. After establishing a 20 min stable baseline, E2 or G1 were bath applied to slices (10 nM; 20 min) followed by a 60 min washout period.

The E2-induced increase in excitatory synaptic transmission (which was observed in 3 out of the 4 slices) and LTD generation (observed in all 4 slices) were not accompanied by significant changes in pooled PPR (from 1.54 ± 0.02 during baseline, to 1.53 ± 0.01 during E2 application and 1.53 ± 0.02 during washout; $p > 0.05$; n = 4; Fig 5.1). Like E2, the G1-induced increase in synaptic transmission (observed in 2 out of the 3 slices) and LTD generation (observed in all 3 slices) were not accompanied by significant changes in the pooled PPR (from 1.49 ± 0.04 during baseline, to 1.49 ± 0.04 during G1 application and 1.50 ± 0.06 during washout; $p > 0.05$; n = 3; Fig 5.2).

It is well established that adenosine potently depresses synaptic transmission at CA3 - CA1 synapses and is a result of pre-synaptic activation of A_1 receptors resulting in a lowering of initial glutamate release probability (Wu and Saggau, 1994). For this reason, the effects of adenosine on the PPR were used as a control. As expected, application of adenosine (100 µM; 10 min) quickly depressed synaptic transmission (Fig 5.3), and this effect was accompanied by a significant increase in the PPR (from 1.45 ± 0.01 during baseline recordings to 2.08 ± 0.07 during adenosine application; t = -6.9, 2 degrees of freedom; $p < 0.05$; Fig 5.3; n = 3).

To illustrate the effects of adenonsine on the paired-pulse facilitation ratio, compared with E2 or G1, example traces from the different phases of the experiments were scaled (Fig 5.4). This figure shows an enhancement of the second response during adenosine-induced synaptic depression. Moreover, scaling shows that there is no change in the magnitude of the second response during E2- or G1- induced synaptic enhancement or depression (example traces for E2 and G1 are from experiments which show a bi-phasic response profile). These data suggest that both the E2- and G1-induced LTD of

hippocampal synaptic transmission are likely to be expressed post-synaptically and are not likely to involve alterations in glutamate release probability. Furthermore, these data support the hypothesis that GPR30 may be involved in E2 mediated effects on hippocampal synaptic transmission as similar expression mechanisms underlie the LTD induced by E2 and the GPR30 agonist.

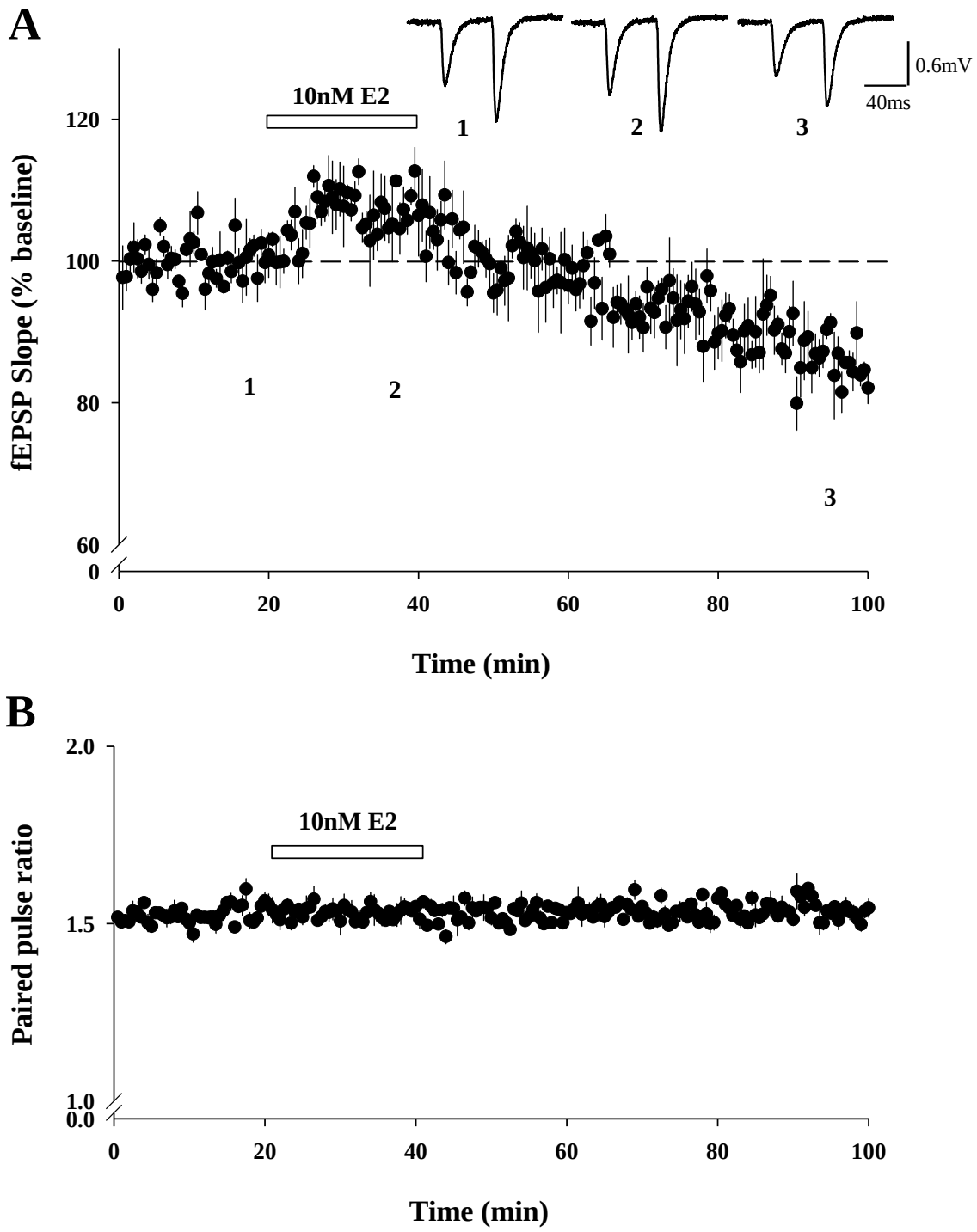

Figure 5.1: E2 has no effect on the paired pulse facilitation ratio. ***A,*** pooled data (n = 4) illustrating the effects of E2 (10 nM; 20 min); 3 out of 4 slices show a biphasic response and 1 of the 4 slices show LTD only. ***B,*** Corresponding PPR from (A). Top, example traces from a representative experiment that illustrated a bi-phasic response are shown at the time points indicated. There is no significant change in PPR $p > 0.05$ (one-way repeated measures ANOVA on ranks).

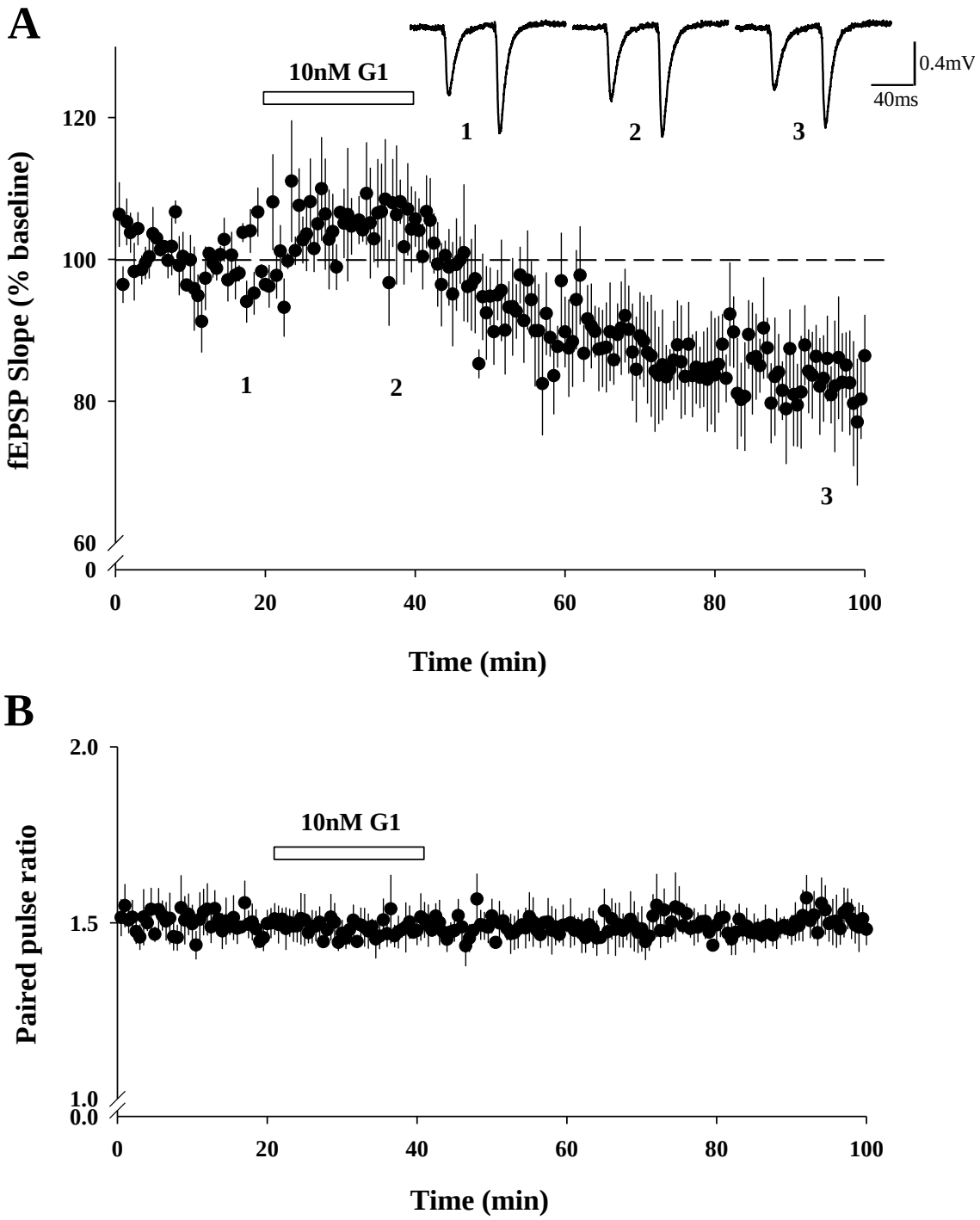

Figure 5.2: G1 has no effect on the paired pulse facilitation ratio. ***A,*** pooled data (n = 3) illustrating the effects of G1 (10 nM; 20 min); 2 out of 3 slices show a biphasic response and 1 out of 3 slices show LTD generation only. ***B,*** Corresponding PPR from (A). Top, example traces from a representative experiment that illustrated a bi-phasic response are shown at the time points indicated. There is no significant change in PPR $p > 0.05$ (one-way repeated measures ANOVA).

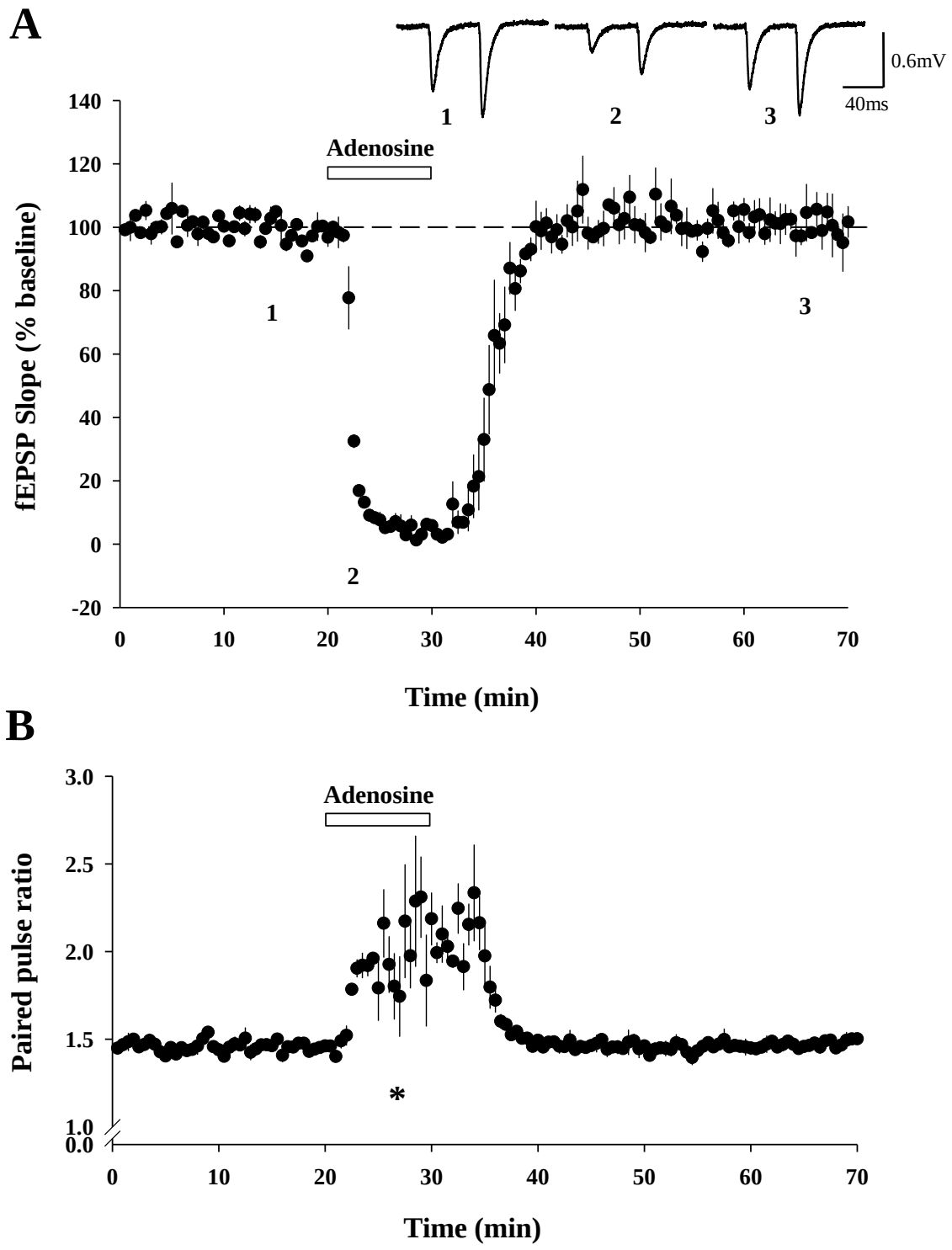

Figure 5.3: Adenosine depresses hippocampal excitatory synaptic transmission through a pre-synaptic mechanism. ***A,*** pooled data (n = 3) illustrating changes in average fEPSP slope after adenosine ***B,*** Corresponding PPR from (A) representing changes in PPR after adenosine (100 µM; 10 min) administration; Top, example traces from a representative experiment.. * represents $p < 0.05$ vs. baseline; paired t-test.

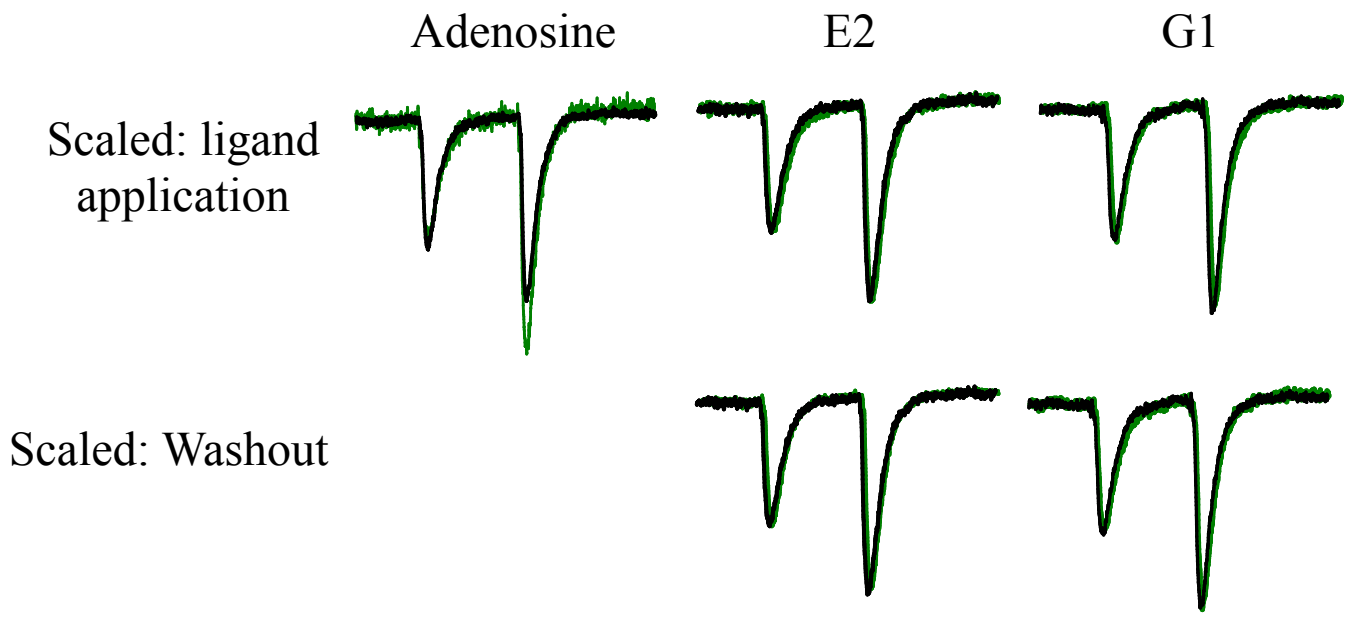

Figure 5.4: Scaled representation of paired fEPSP: *Black traces represent example traces from baseline and green traces represent traces from agonist application or washout and have been scaled to the first response from the respective baseline trace.* Scaling the responses illustrates that after adenosine (100 µM) application there is an increase in the magnitude of the second response, whereas there is no change in the magnitude of the second response during E2 (10 nM) or G1 (10 nM) application or washout.

5.2.2: The E2- and G1- induced LTD do not require afferent stimulation

The E2- and G1- induced LTD are likely to be expressed post-synaptically, however expression may require concurrent pre-synaptic activity (*ie:* post-synaptic AMPAR and/or NMDAR activation in conjunction with estrogen receptor activation). Therefore, in the following experiments (Fig 5.5), Schaffer-collateral stimulation was ceased 20 min during agonist application and resumed during the washout phase, to establish whether afferent stimulation was necessary for the induction of either E2- or G1-induced LTD.

Without stimulation during agonist application, the E2- and G1-induced depression of synaptic transmission was still observed (to 89 ± 3.1% of baseline after E2 washout; t = 3.5 with 4 degrees of freedom; $p < 0.05$; n = 5; and 91 ± 1.7% of baseline after G1 washout; t = 5.3 with 5 degrees of freedom; $p < 0.05$; n = 6; Fig 5.5). The magnitudes of the E2- and G1- induced depression in these experiments were not significantly different from each other ($p > 0.05$; Kruskal-Walls one-way ANOVA on ranks). Vehicle (0.01% DMSO) controls were conducted to ensure that these E2- and G1-induced effects were not a result of termination of electrical stimulation during agonist application. Once electrical stimulation resumed after vehicle application, an initial increase in fEPSP response size was seen, which matched those from E2 and G1 experiments, however responses declined to baseline levels after 60 min (to 102 ± 1% of baseline; $p > 0.05$; n = 6). These data suggest that E2- and G1- induced LTD do not require afferent stimulation.

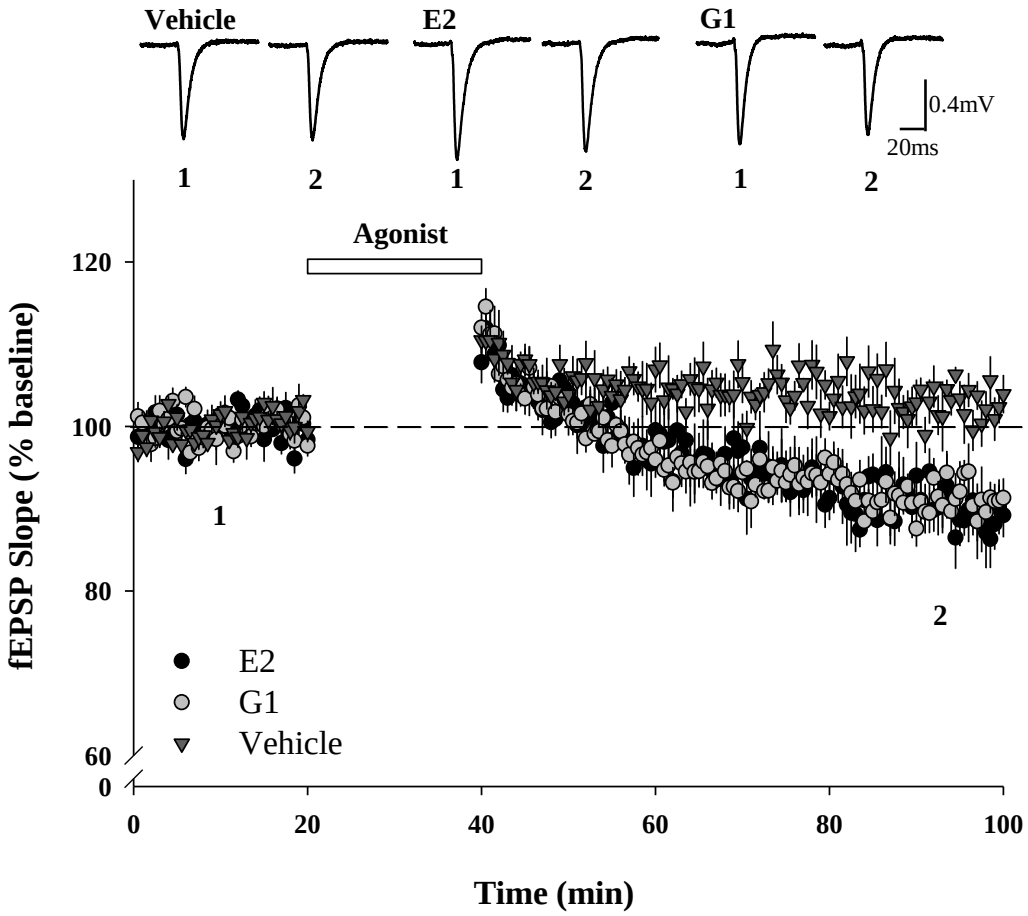

Figure 5.5: E2- and G1- induced LTD do not require presynaptic stimulation. Pooled data illustrating E2 (10 nM; 20 min; n = 5), G1 (10 nM; 20 min; n = 6) and vehicle (0.01% DMSO; 20 min; n = 6) effects on excitatory synaptic transmission after electrical stimulation is ceased during drug application. Top; representative traces from each set of experiments are shown for the time points indicated. E2 and G1 significantly reduced synaptic transmission ($p < 0.05$ vs. baseline; paired t-tests).

5.2.3: E2 and G1 modulate the surface expression of GluA1 containing AMPA receptors.

It is likely that the E2- and G2- induced LTD are post-synaptically expressed (section 5.2.2) thus we then sought to determine if these agonists altered the trafficking of AMPAR by monitoring their effects in primary cultured hippocampal neurons. Accordingly, we tested the concentration-dependent effects of E2 and G1 (0.01 – 1000 nM; Fig 5.6 and 5.7) using established immunocytochemical approaches to assay the surface expression of GluA1-containing AMPAR in living cultured hippocampal neurons (Moult *et al*., 2010).

Exposure of neurons to 1 nM and 10 nM E2 resulted in modest but significant reductions (to 84 ± 2.0 % and 90 ± 2.0 % of control, respectively; H = 110.9 with 6 degrees of freedom; $p < 0.05$ vs. vehicle treated; n = 48; Fig 5.6) in surface GluA1 expression. In contrast, 100 nM E2 significantly increased surface GluA1 staining (to 113 ± 2.0 % of control; $p < 0.05$ vs. vehicle treated; n = 48). Although 1 µM E2 increased surface GluA1 staining (to 110 ± 2.7 % of control; n = 48), this effect was not statistically significant compared to vehicle ($p > 0.05$ vs. vehicle treated). Exposure of neurons to G1 resulted in a similar concentration-response relationship, such that concentrations of 1 nM, 10 nM and 100 nM G1 significantly reduced surface GluA1 expression (to 80 ± 1.8%, n = 48; 81 ± 1.4%, n = 96 and 84 ± 1.5 % n = 84, of control respectively; H = 104.6 with 6 degrees of freedom; $p < 0.05$ vs. vehicle treated; Fig 5.7), whereas 1 µM G1 had no significant effect on surface GluA1 staining (98 ± 2.2% of control, n = 84; $p > 0.05$ vs. vehicle treated).

Although the concentration-dependent effects for G1 and E2 differ at higher concentrations, these data suggest that G1 can mimic the effects of E2 at low nanomolar concentrations. Taken together, the E2- and G1- induced decrease in surface GluA1 containing AMPAR is consistent with the electrophysiology data which suggests that the G1- and E2-induced LTD are likely to have a post-synaptic expression mechanism and thus may involve the removal of post-synaptic GluA1-containig AMPAR.

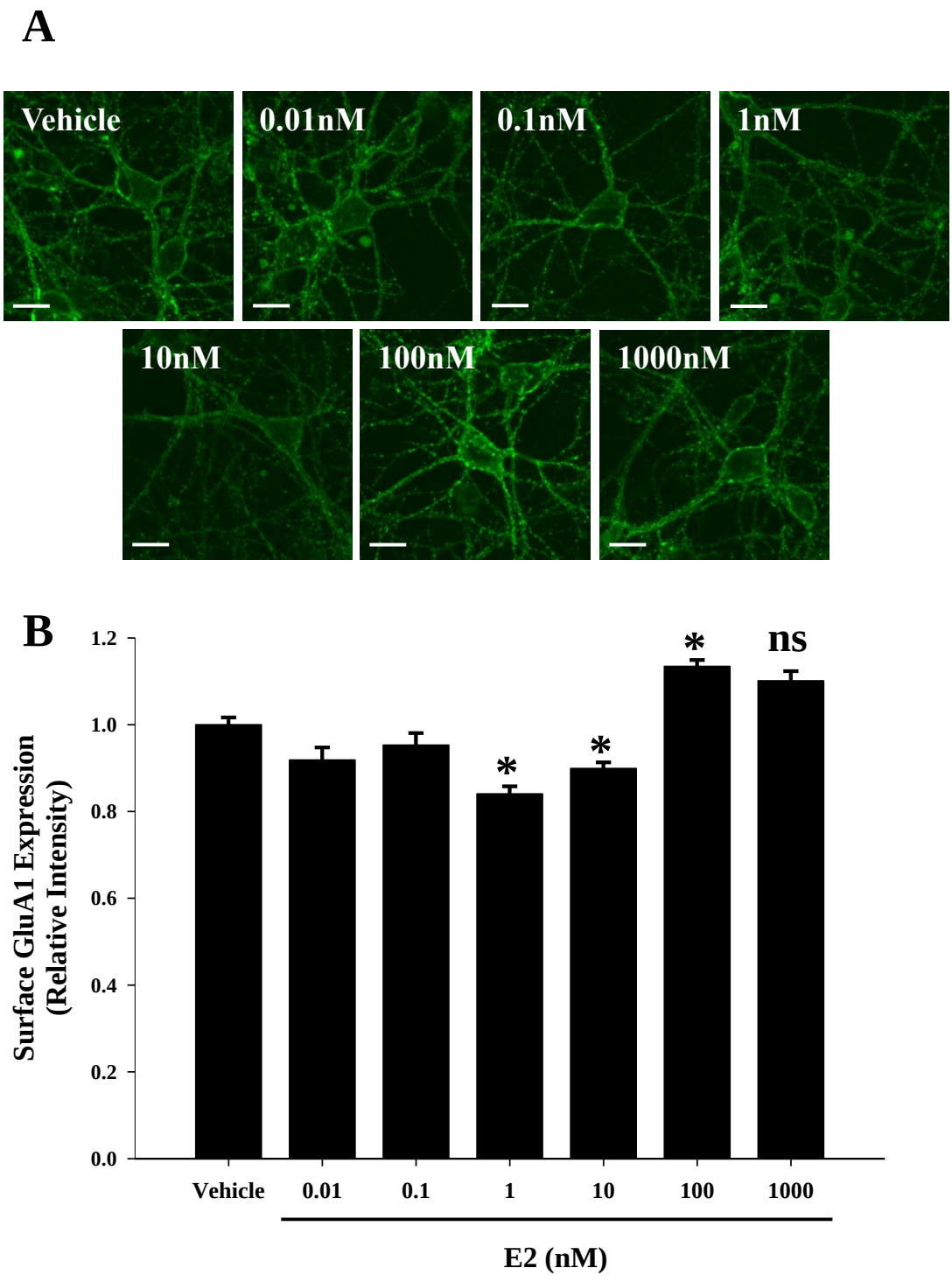

Figure 5.6: E2 effects surface GluA1 expression in a concentration-dependent manner. *Neurons (*DIV *8 -16) were treated with vehicle (0.1 % DMSO) or E2 (0.01 nM – 1000 nM; 30 min).* ***A,*** representative confocal images of surface GluA1 staining. ***B,*** pooled data (n = 48 neurites; n = 4 independent cultures from different animals) showing the concentration-dependant effects of E2 on surface GluA1. Scale bars, 20 µm. * represents $p < 0.05$ vs. vehicle treated, ns represents $p > 0.05$ vs. vehicle treated; Kruskill-Wallis one-way ANOVA on ranks, followed by Dunn's *post-hoc* analyses.

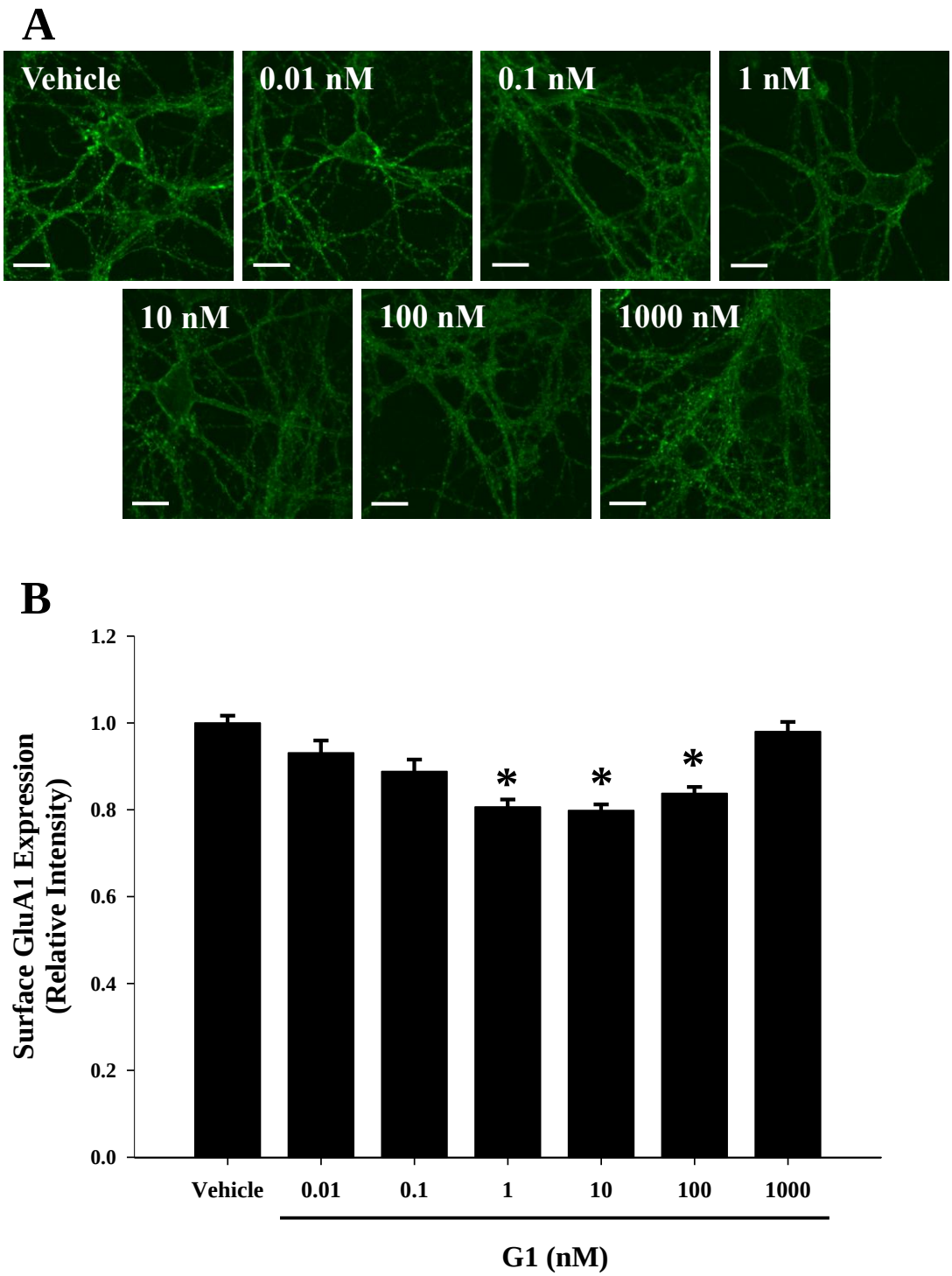

Figure 5.7: The selective GPR30 agonist effects surface GluA1 expression in a concentration-dependent manner. *Neurons (*DIV *8 – 16) were treated with vehicle (0.1 % DMSO) or G1 (0.01 nM – 1000 nM; 30min).* ***A,*** representative confocal images of surface GluA1 staining. ***B,*** pooled data (n= 48 – 96 neurites; n = 4 – 8 independent cultures from different animals) showing the concentration-dependant effects of G1 on surface GluA1. Scale bars, 20 µm. * represents $p < 0.05$ vs. vehicle treated; Kruskill-Wallis one-way ANOVA on ranks followed by Dunn's *post-hoc* analysis.

Internalisation of AMPAR from synaptic sites is necessary for the expression of many forms of LTD at the CA1 (Man *et al*., 2000; Kim *et al*., 2001; Snyder *et al*., 2001; Huang *et al*., 2004; Casimiro *et al*., 2011). Although these data indicate that surface AMPAR expression is decreased by low nM concentrations of E2 and G1, it is not clear if the agonists promote the removal of AMPAR from synaptic or extra-synaptic sites. Moreover, as E2 is a known modulator of spine and dendritic architecture *in vivo* (Woolley and McEwen, 1992), the effects of these agonists could induce morphological changes and alterations in spine density, which would manifest as a reduction in surface GluA1-containing AMPAR. It is worth noting that synapse loss is more likely to occur over a time-period greater than that which we see here (> 24 hours), and is more likely to be attributed to pathophysiological conditions (such as amyloid-β oligomer formation; repeated LTD stimulation, or chronic stress; (Shankar *et al*., 2007; Shinoda *et al*., 2010; Wei *et al*., 2010; Liston and Gan, 2011)). Nevertheless, in order to control for this and to address if synaptically-located GluA1-containing AMPAR were specifically removed from synapses in response to E2 and G1 treatment, we used dual-labelling immunocytochemical techniques to compare the co-localisation of the synaptic marker synapsin-1 and GluA1 (Moult *et al*., 2010; Doherty *et al*., 2013).

To determine the level of AMPAR associated with synapses, surface GluA1 expression relative to synapsin-1 staining was assessed in primary hippocampal neurons after exposure to vehicle (0.001 % DMSO), G1 (10 nM) or E2 (10 nM; 30 min; Fig 5.8). As expected, application of G1 or E2 significantly reduced surface GluA1 staining (to 86 ± 2% and 74 ± 1% of vehicle control, respectively; H = 78.9 with 2 degrees of freedom; $p < 0.05$ vs. vehicle treated; n = 45; Fig 5.8 D). The relative number of synapsin-1 positive puncta was not significantly affected by either agonist (G1: 107 ± 4.4 %, E2: 98 ± 4.3 %, of vehicle; n = 45; $p > 0.05$ vs. vehicle treated; Fig 5.8 B). However, exposure to either G1 or E2 decreased surface GluA1-staining that co-localized with synapsin-1 staining from 54 ± 1.6 % in vehicle treated neurons, to 47 ± 2.4 % and 39 ± 1.8 %, respectively (H = 24.6 with 2 degrees of freedom; $p < 0.05$ vs. vehicle treated; n = 45; Fig 5.8 C).

These data suggest that both G1 and E2 reduce the expression of synaptic GluA1 containing AMPAR, without affecting synapse number. The ability of G1 and E2 to promote the removal of GluA1 from hippocampal synapses may be an important step in the expression of G1- and E2-induced LTD at the CA3 – CA1 synapse.

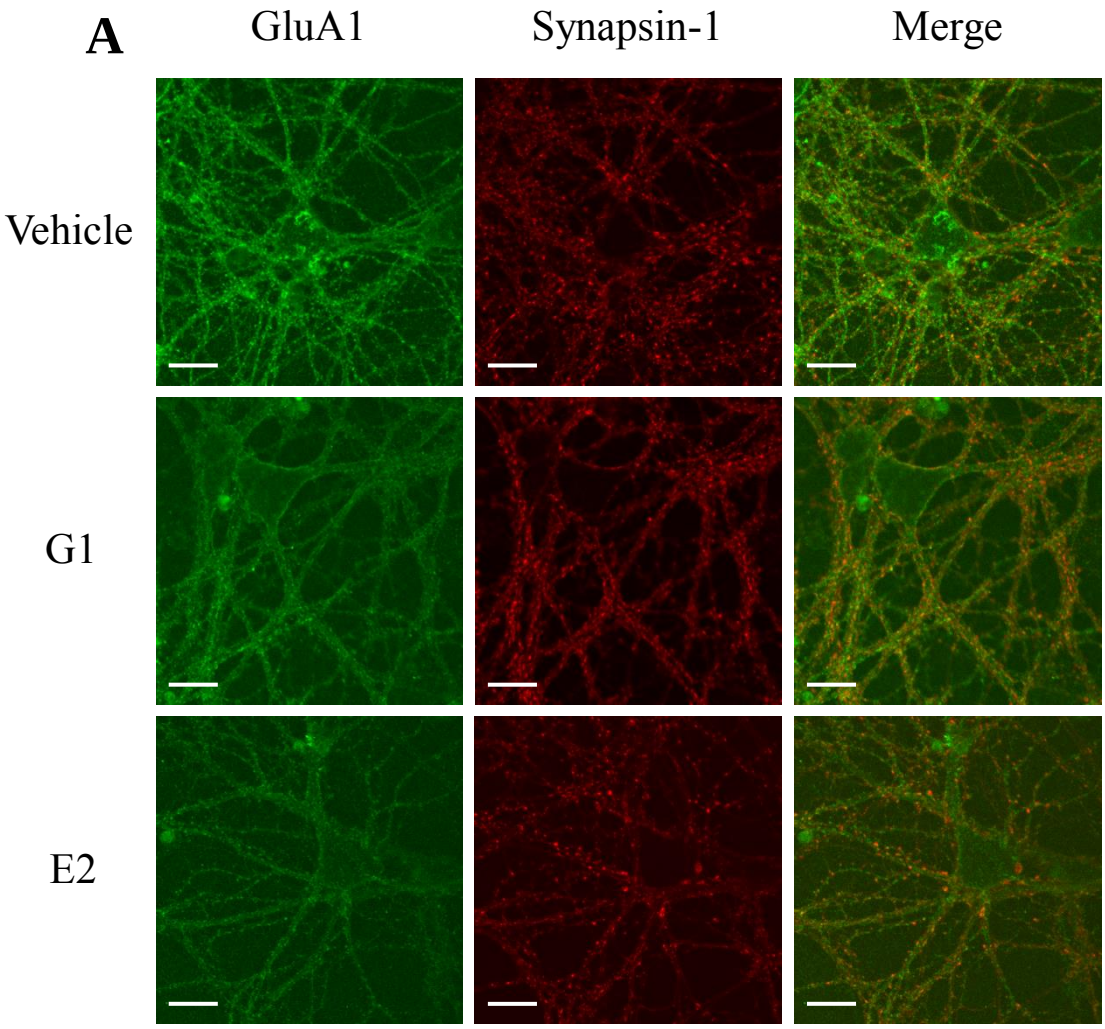
A
GluA1
Synapsin-1
Merge
Vehicle
G1
E2

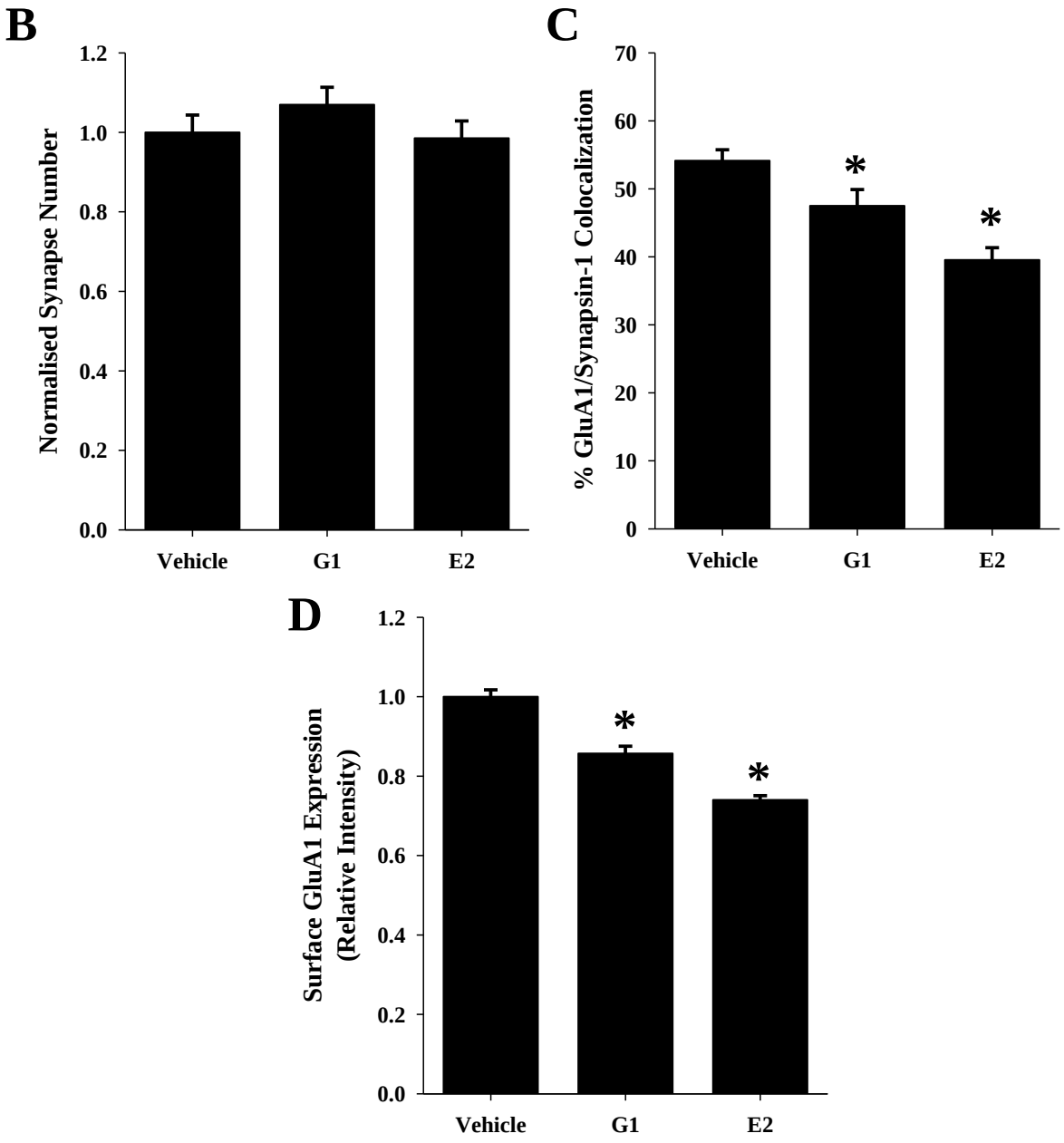

Figure 5.8: Both E2 and G1 promote removal of AMPAR from synapses. *Neurons were treated with vehicle (0.01 % DMSO), E2 or G1 (10 nM; 30 min).* ***A,*** representative confocal images of surface GluA1 staining (green) and synapsin-1 staining (red) after treatment, both E2 and G1 treatment reduced GluA1 staining, but did not affect number of synapsin-1 puncta. ***B,*** pooled data illustrating normalised number of synapses as determined by synapsin-1 staining after treatment. ***C,*** pooled data illustrating percentage GluA1 expression that colocalized with synapsin-1 staining after treatment. ***D,*** pooled data illustrating the relative expression of surface GluA1 labelling after treatment. Scale bars, 20 µm. * represents $p < 0.05$ vs. vehicle treated; Kruskill-Wallis-one way ANOVA followed by Dunn's *post-hoc* analyses; n = 45 neurites from 3 independent cultures from different animals.

5.2.4: G1- induced LTD is likely to be independent of NMDAR activation, whereas E2-induced LTD may involve an NMDAR mediated component

In order to test if the E2- or G1- induced LTD involved an NMDAR-mediated component, hippocampal slices were perfused with the competitive NMDAR antagonist, D-AP5 (50 µM) for 20 - 45 min before application of either E2 or G1 (both at 10 nM; 20 min).

In the presence of D-AP5, the magnitude of the E2-induced LTD was significantly attenuated (from 86 ± 2.4% of baseline in E2 treated slices, [F2,14] = 10.1; $p < 0.05$ vs. baseline; n = 5; to 93 ± 2.0 % of baseline in D-AP5 treated slices, n = 6, t = 2.3 with 9 degrees of freedom, $p < 0.05$ vs. E2 treated, Fig 5.9). However, the residual depression was still significant (F[2,17] = 11.1; $p < 0.01$ vs. baseline), suggesting that a component of the E2- induced LTD is NMDAR-mediated. The E2-induced increase in synaptic transmission was only observed in 2 out of 5 control slices, and was not observed in any of the slices treated with D-AP5. Therefore a definitive conclusion as to whether the initial E2- induced increase in excitability is dependent on NMDAR activity cannot be made.

In contrast to E2, the magnitude of the G1-induced depression in the presence of D-AP5 is not significantly different to that in G1 control experiments (Fig. 5.10 B) (G1: 84 ± 3.8 % of baseline, n = 5, F[2,14] = 14.4; $p < 0.05$ vs. baseline; G1 + D-AP5: 87 ± 1.9 % of baseline, n = 9, F[2,26] = 23.9; $p < 0.05$ vs. baseline, $p > 0.05$ vs. G1 alone, unpaired t-test).

Moreover, subsequent stratification of the data revealed that out of the nine slices that were exposed to G1 in the presence of D-AP5, four exhibited a bi-phasic response profile (Fig 5.11), four a depression-only response profile (Fig 5.12) and in one slice a sustained increase in synaptic transmission was observed (data not shown). Specifically, in the slices which exhibited a bi-phasic response profile, the magnitude of the G1-induced potentiation of synaptic transmission in the presence of D-AP5 was not significantly different from control slices (G1: 108 ± 2.3 % in of baseline, n = 3 /5; G1 + D-AP5: 109 ± 1.3 % of baseline, n = 4 / 9; F[2,11] = 110.7, $p < 0.05$ vs. baseline; $p > 0.05$ vs. G1 alone; Fig 5.11). In addition, the magnitude of the G1-induced depression of synaptic transmission in the presence of D-AP5 was not significantly different from control (G1: 87 ± 5.5 % of baseline, n = 3 / 5; G1 + D-AP5: 84 ± 2.3 % of baseline, n =

4 / 9; F[2,11] = 110.7, $p < 0.05$ vs. baseline; $p > 0.05$ vs. G1 alone; unpaired t-test; Fig 5.11). In slices where a G1-induced potentiation of synaptic transmission was not observed, the magnitude of the G1-induced LTD was not significantly different in slices treated with D-AP5 (G1: 80 ± 4.7 of baseline, n = 2 / 5; G1 + D-AP5: 87 ± 1 % of baseline D-AP5 treated slices, n = 4 / 9; F[2,11] = 35.9; $p < 0.05$ vs. baseline; $p > 0.05$ vs. G1 alone; unpaired t-test; Fig 5.12).

Taken together, these results suggest that the E2-induced depression of synaptic transmission may have a D-AP5-sensitive and a D-AP5-insensitive component, whereas the G1-induced effects are not sensitive to D-AP5.

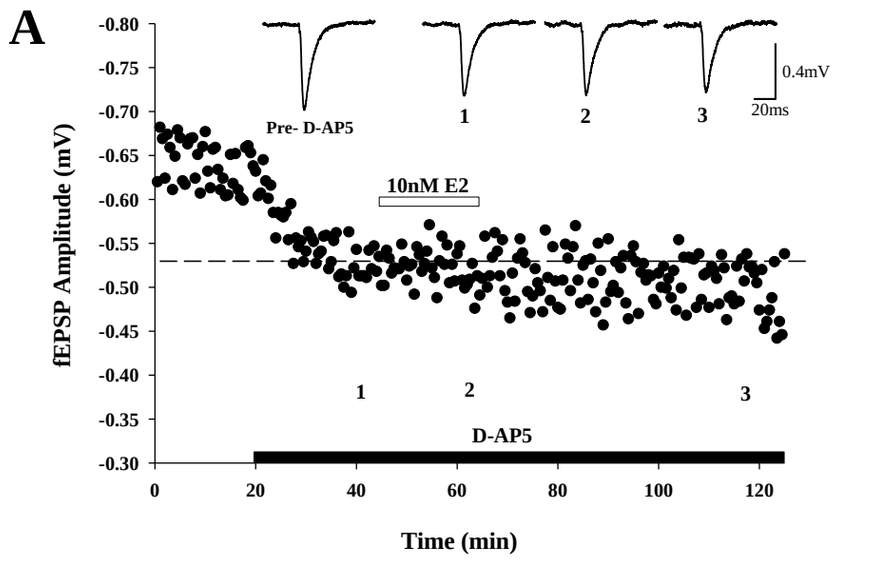

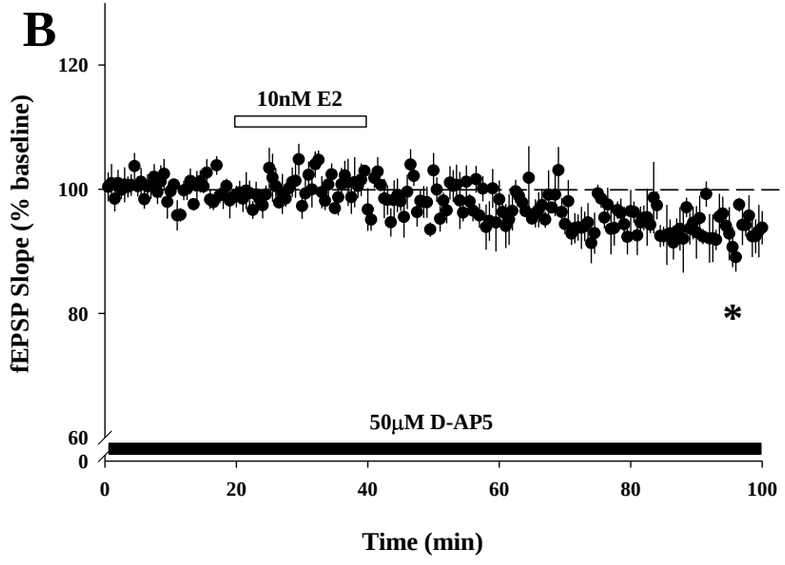

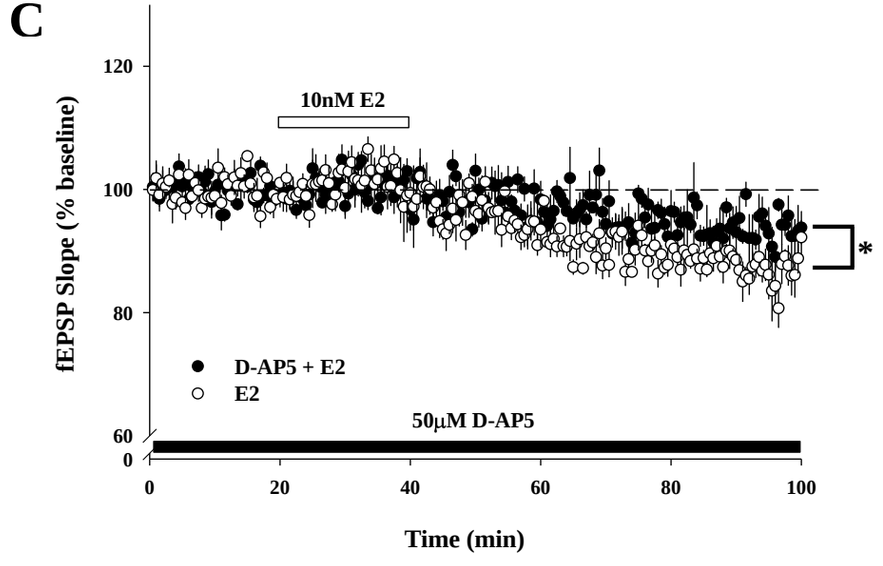

Figure 5.9: D-AP5 attenuates the E2- induced depression of synaptic transmission in adult male hippocampal slices. ***A,*** representative experiment showing effects of D-AP5 (50 μM) and E2 (10 nM; 20 min) on fEPSP amplitude. Top, example traces from the experiment are shown at the time points indicated. ***B,*** data pooled (n = 6) and normalised with respect to baseline are expressed as mean ± SEM; * represents $p < 0.05$ vs. baseline; one-way repeated measures ANOVA followed by Tukey *post-hoc* analyses. ***C,*** Data from ***B***, comparing the effects of E2 in the presence (filled circles) and absence (open circles) of D-AP5; * represents $p < 0.05$ vs. E2 alone; unpaired t-test.

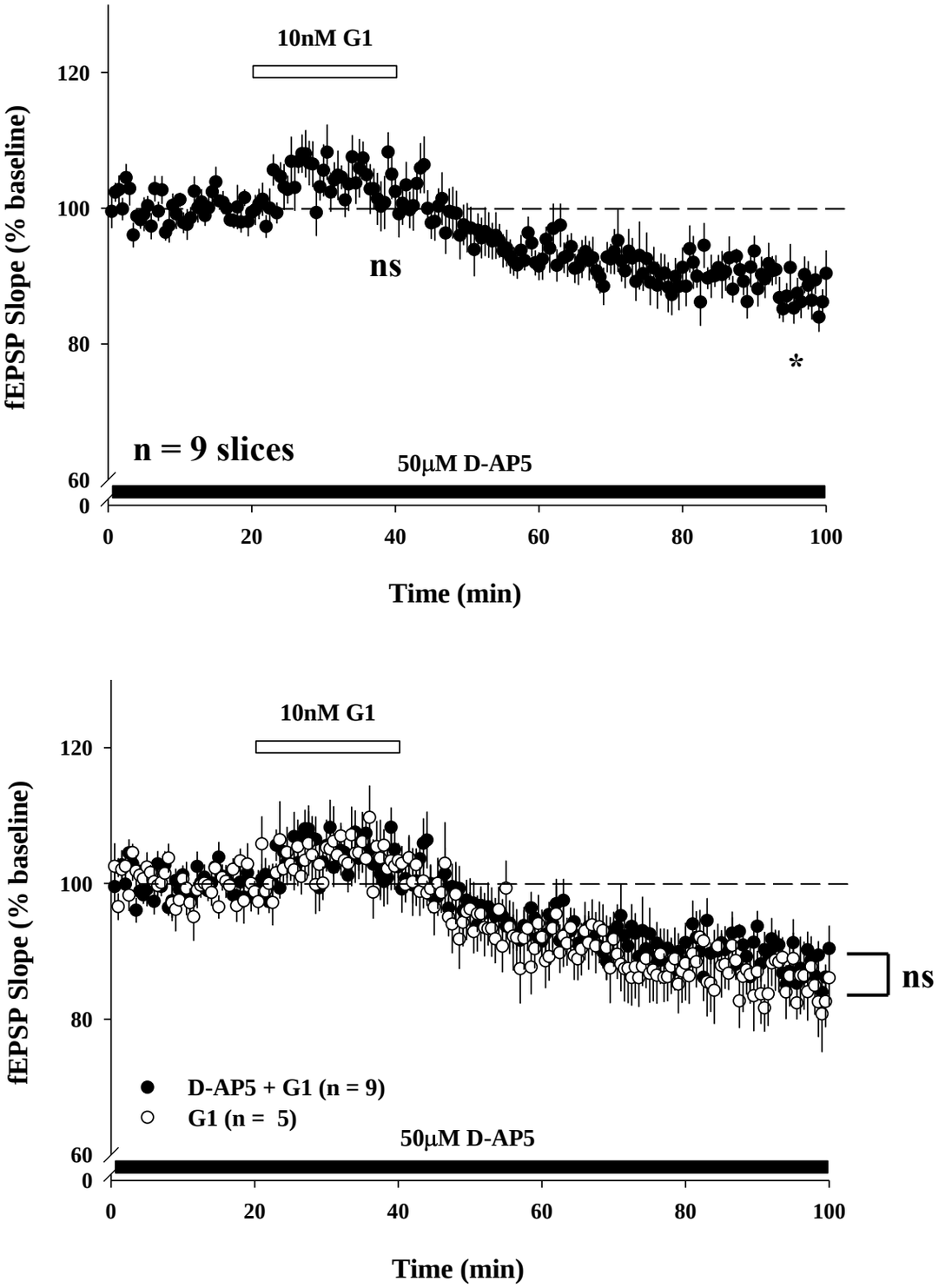

Figure 5.10: D-AP5 does not block the G1-induced effect on synaptic transmission in adult male hippocampal slices. ***A,*** Data pooled (n = 9) and normalised with respect to D-AP5 baseline, illustrating that in the presence of D-AP5 (50 μM), G1 (10 nM; 20 min) can still induce a slow-onset depression of synaptic transmission. ***B,*** comparing the effects of G1 in the presence (filled circles) and absence (open circles) of D-AP5. Data are expressed as mean ± SEM; * represents $p < 0.05$ vs. baseline (in figure ***A***); NS represents $p > 0.05$ vs. baseline (in figure ***A***), One-way repeated measures ANOVA followed by Tukey *post-hoc* analyses; NS represents $p > 0.05$ vs. the magnitude of G1-induced effects in control slices at the time point indicated; unpaired t-test (in figure ***B***).

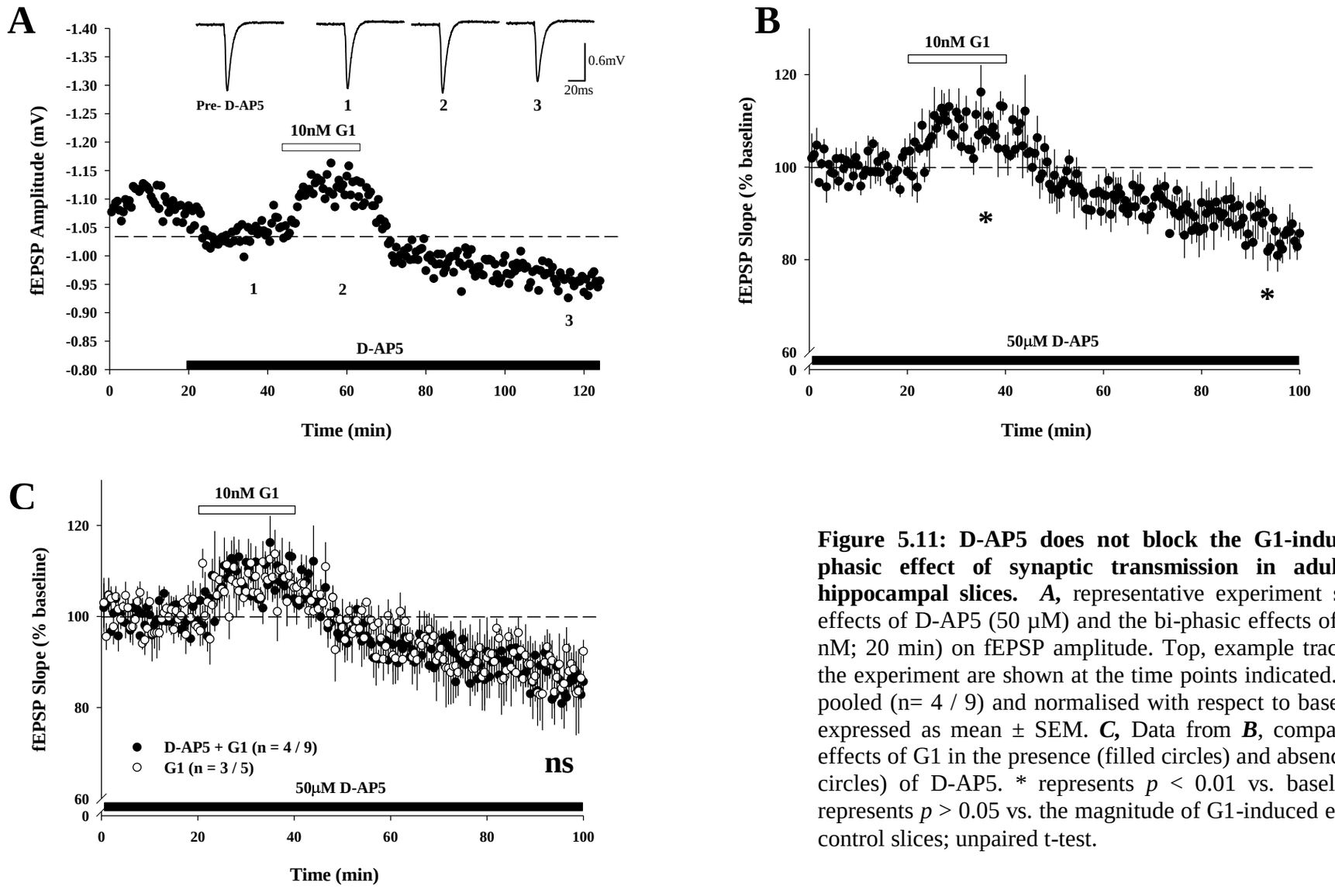

Figure 5.11: D-AP5 does not block the G1-induced bi-phasic effect of synaptic transmission in adult male hippocampal slices. ***A,*** representative experiment showing effects of D-AP5 (50 μM) and the bi-phasic effects of G1 (10 nM; 20 min) on fEPSP amplitude. Top, example traces from the experiment are shown at the time points indicated. ***B,*** data pooled (n= 4 / 9) and normalised with respect to baseline are expressed as mean ± SEM. ***C,*** Data from ***B***, comparing the effects of G1 in the presence (filled circles) and absence (open circles) of D-AP5. * represents $p < 0.01$ vs. baseline; NS represents $p > 0.05$ vs. the magnitude of G1-induced effects in control slices; unpaired t-test.

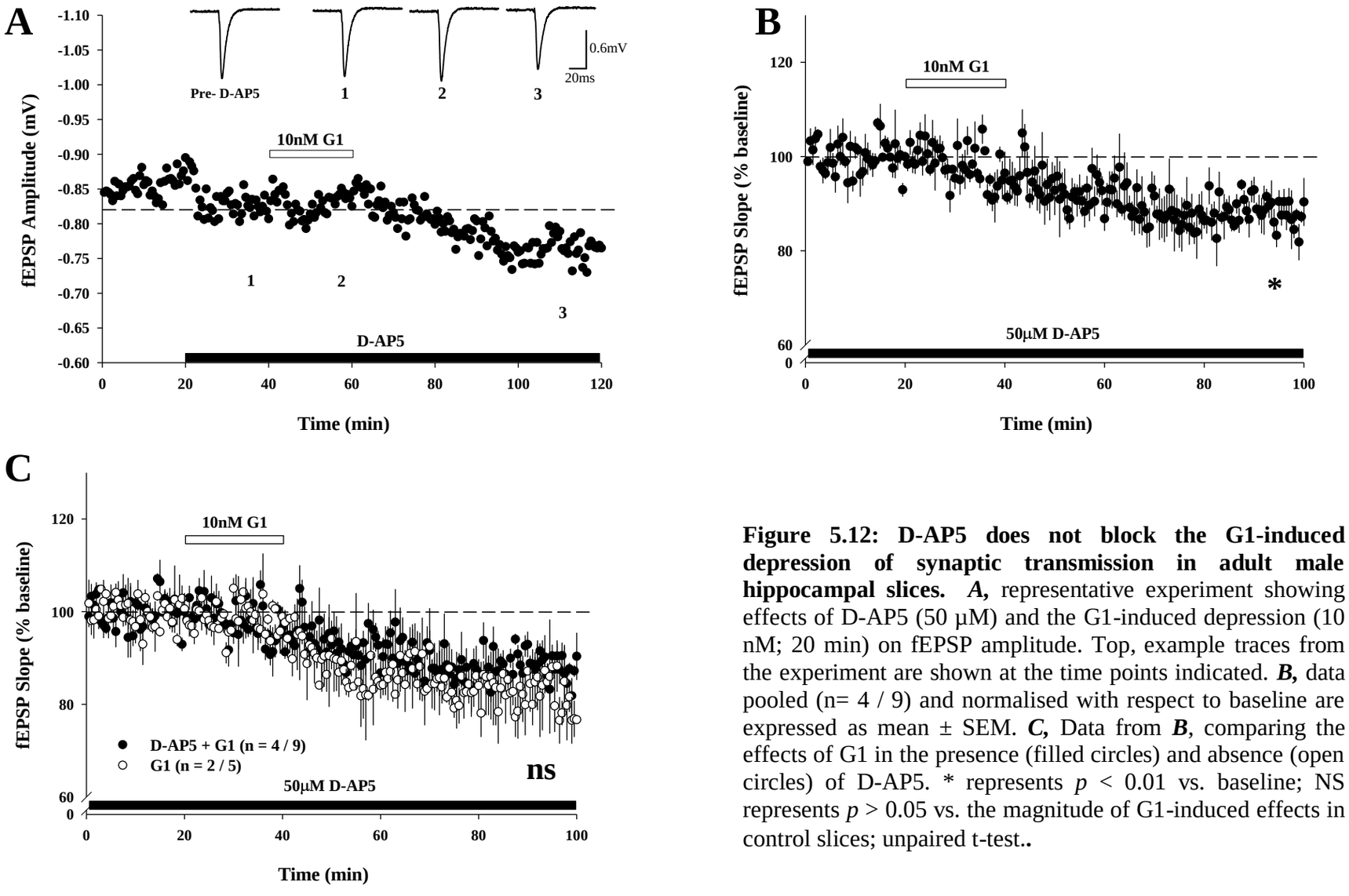

Figure 5.12: D-AP5 does not block the G1-induced depression of synaptic transmission in adult male hippocampal slices. ***A,*** representative experiment showing effects of D-AP5 (50 μM) and the G1-induced depression (10 nM; 20 min) on fEPSP amplitude. Top, example traces from the experiment are shown at the time points indicated. ***B,*** data pooled (n= 4 / 9) and normalised with respect to baseline are expressed as mean ± SEM. ***C,*** Data from ***B***, comparing the effects of G1 in the presence (filled circles) and absence (open circles) of D-AP5. * represents $p < 0.01$ vs. baseline; NS represents $p > 0.05$ vs. the magnitude of G1-induced effects in control slices; unpaired t-test..

5.2.5: The effects of G1 and E2 on AMPAR trafficking are NMDAR dependent

In contrast to the electrophysiology data, both the E2- and G1- induced reduction in surface AMPAR expression in hippocampal neurons were attenuated by D-AP5 (Fig 5.13). Specifically, the magnitude of the G1-induced reduction in surface AMPAR expression (from 84 ± 2.3 % of vehicle; $p < 0.05$ vs. vehicle treated) was significantly attenuated by D-AP5 (to 95 ± 1.7 % of vehicle; H = 63.4 with 5 degrees of freedom; $p < 0.05$ vs. G1 treated; n = 48). Furthermore, the E2-induced reduction in surface GluA1 expression (from 81 ± 2.5 % of vehicle; $p < 0.05$ vs. vehicle treated) was blocked in the presence of D-AP5 (to 98 ± 2.0 % of vehicle; H = 63.4 with 5 degrees of freedom; $p < 0.05$ vs. E2 treated; n = 48;). D-AP5 exposure (50 µM; 45 min) alone had no effect on surface AMPAR expression compared to vehicle treated neurons (100 ± 1.3%; $p > 0.05$ vs. vehicle treated; n = 60). These data suggest that in primary hippocampal cultures, the effects of G1 and E2 on surface GluA1 expression require NMDAR activity.

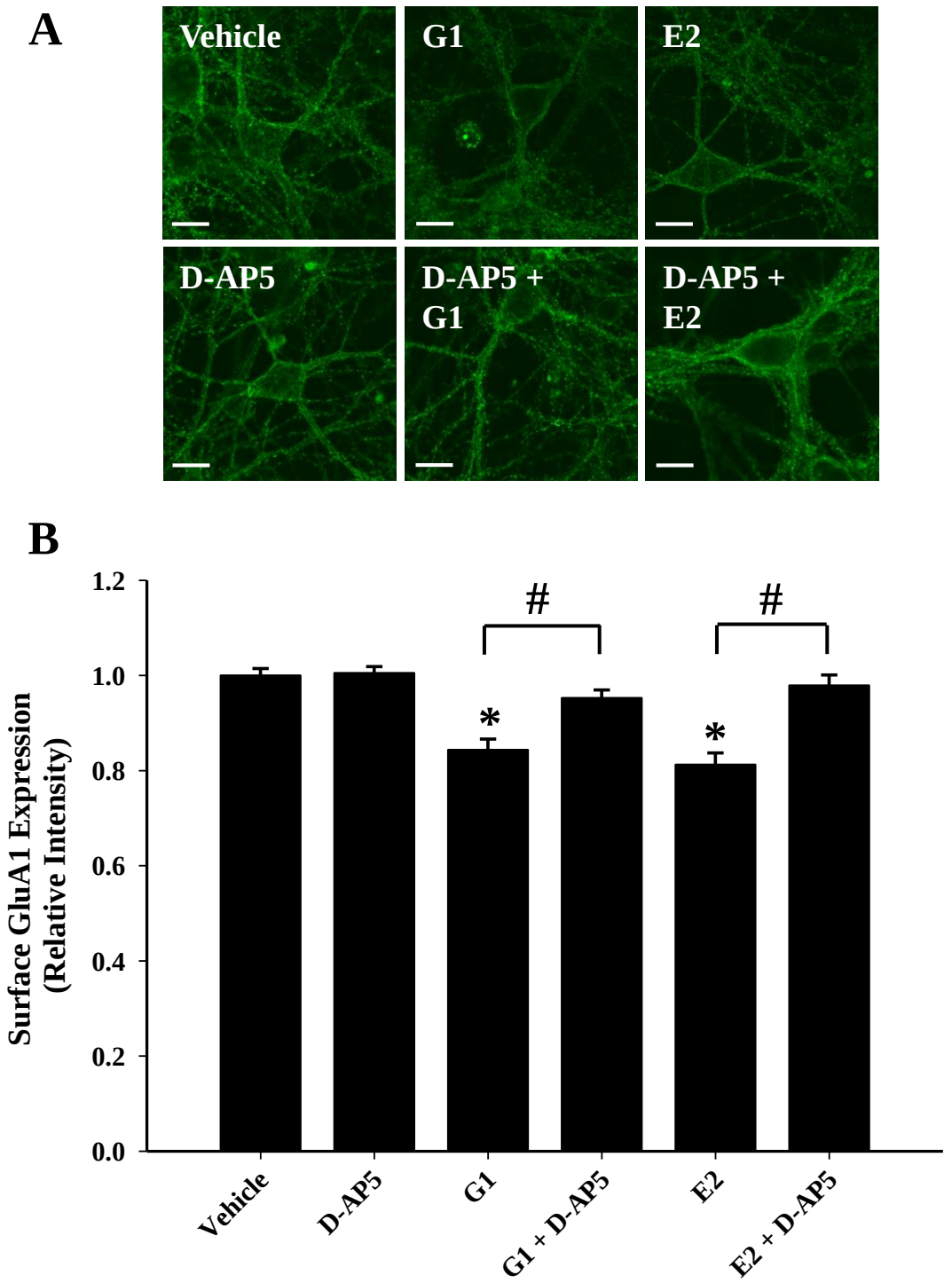

Figure 5.13: The G1- and E2- induced reduction in surface GluA1 expression is attenuated by D-AP5. DIV *8 –16 neurons were pre-treated with vehicle (0.01 % DMSO) or D-AP5 (50 µM; 15 min) and then G1 or E2 (10 nM) or vehicle, or in combination with D-AP5 (30 min).* ***A,*** representative confocal images of surface GluA1 staining. ***B,*** pooled data showing relative changes in surface GluA1 after exposure to D-AP5 alone and in the presence of G1 or E2. Scale bars, 20 µm. A Kruskal-Wallis one way ANOVA on ranks followed by Dunn's *post-hoc* analyses was performed. * Represents $p < 0.05$ vs. vehicle; # represents $p < 0.05$ between the indicated treatments; n = 48 – 60 neurites from 4 - 5 individual cultures from different animals.

5.2.6: An mGluR antagonist does not inhibit the G1-induced reduction in surface AMPAR expression

Although both NMDA- and mGluR- dependent LTD induce mechanistically distinct forms of LTD, both phenomena involve the internalization of surface AMPAR (Malenka and Bear, 2004; Moult *et al*., 2006; Collingridge *et al*., 2010; Casimiro *et al*., 2011).

Our results suggest that in hippocampal cultures the E2- and G1-induced reduction of surface AMPAR expression are via an NMDAR dependent mechanism, however recent studies indicate that extra-nuclear estrogen receptors can associate with and signal via mGluRs (Boulware *et al*., 2005, 2007; Boulware and Mermelstein, 2009; Meitzen *et al*., 2012). Therefore, it is plausible that the E2- or G1- induced effects on surface AMPAR expression may involve signalling via Group I or Group II mGluR's. In order to test this, we utilised LY 341495, a compound which selectively antagonises group II mGluRs (Kingston *et al*., 1998) and can inhibit group I mGluR at high concentrations (Fitzjohn *et al*., 1998). Application of LY 341495 (20 μM; 45 min) had no significant effect on surface AMPAR expression compared to vehicle (97 ± 2.4 % of vehicle; n = 36; $p > 0.05$ vs. vehicle treated, Fig 5.14), in hippocampal cultures. Moreover the ability of G1- and E2- (for both 10 nM; 30 min) to reduce surface GluA1-staining was not inhibited in the presence of LY 341495 (to 82 ± 2.8 % of vehicle and 88 ± 2.9 % of vehicle for G1 and E2, respectively; H = 42.9 with 5 degrees of freedom; $p < 0.05$ vs. vehicle treated; $p > 0.05$ vs. G1 or E2 treated, respectively; Fig 5.14). Thus, these data suggest that in hippocampal cultures, the E2- and G1- induced reduction in surface AMPAR expression is likely to be independent of mGluR–mediated signalling.

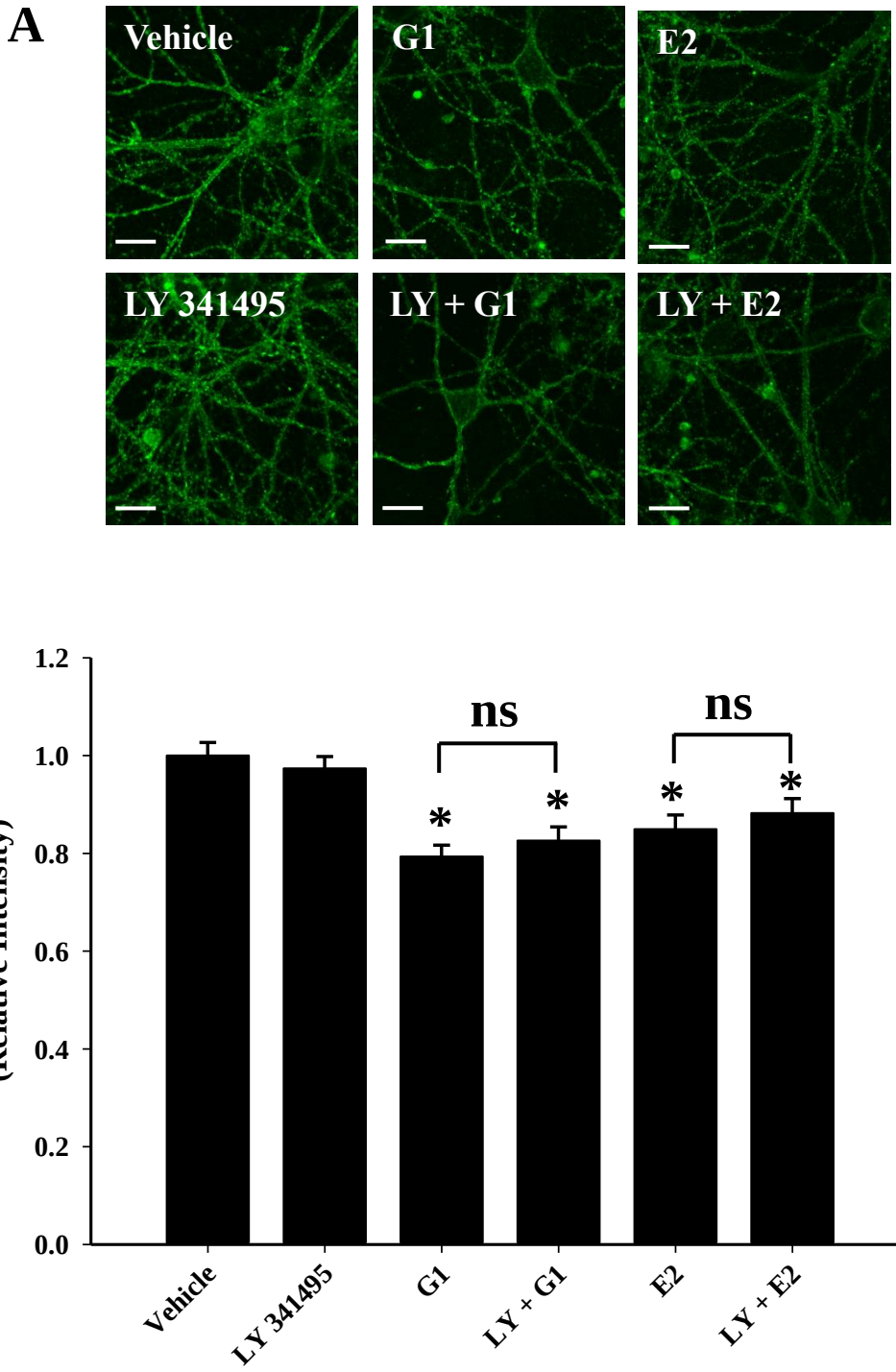

Figure 5.14: The G1- and E2- induced reduction in surface GluA1 expression is not effected by a Group I/II mGluR antagonist. DIV *8 –16 neurons were pre-treated with vehicle (0.01 % DMSO) or LY 341495 (20 µM; 15 min) and then G1 or E2 (10 nM) or vehicle, or in combination with LY 341495 (30 min).* ***A,*** representative confocal images of surface GluA1 staining. ***B,*** pooled data showing relative changes in surface GluA1 after exposure to LY341495 alone and in the presence of G1 or E2. Scale bars, 20 µm. A Kruskal-Wallis one way ANOVA on ranks followed by Dunn's *post-hoc* analysis was performed. * represents $p < 0.05$ vs. vehicle; ns represents $p > 0.05$ between the indicated treatments; n = 36 neurites from 3 individual cultures from different animals.

Summary of findings from Chapter 5:

1) Acute E2- and G1- induced LTD generation is not likely to be a consequence of an altered glutamate release probability and does not require afferent stimulation (Fig 5.1, 5.2 and 5.5).
2) E2 and G1 exposure leads to a reduction in synaptic GluA1-containing AMPAR expression in hippocampal cultures (Fig 5.8).
3) E2 induced LTD of synaptic transmission may (at least in part) involve NMDAR activation, whereas it is likely that the G1-induced LTD does not (Fig 5.9, Fig 5.10, Fig 5.11 and Fig 5.12).
4) The E2- and G1- induced reduction in surface AMPAR expression is NMDAR dependent (Fig 5.13).
5) It is likely that the E2- and G1-induced reduction in surface AMPAR expression does not involve mGluR signalling (Fig 5.14).

5.3: Discussion

5.3.1. E2- and G1- induced LTD at hippocampal synapses are likely to have a post-synaptic expression mechanism.

Here we demonstrate that the E2- and G1- induced LTD are not likely to be attributed to alterations in the probability of pre-synaptic glutamate release, as no alterations in PPR accompanied LTD induced by either E2 or G1. However in parallel control studies the synaptic depression induced by adenosine was coupled with a marked increase in the PPR, which is consistent with a presynaptic mechanism mediating synaptic depression at this synapse (Wu and Saggau, 1994).

In agreement with a possible post-synaptic expression mechanism for E2-induced LTD, acute E2-induced increases in excitability and potentiation of synaptic transmission at CA3 – CA1 synapses have previously been suggested to occur via post-synaptic mechanisms (Wong and Moss, 1992; Foy *et al*., 1999; Gu *et al.*, 1999; Kim *et al*., 2006). In contrast, recent data suggests pre-synaptic mechanisms for the potentiation of

synaptic transmission by E2, an effect which may be sex-specific (Smejkalova and Woolley, 2010; Huang and Woolley, 2012). Specifically, E2 acutely potentiates synaptically evoked EPSCs in slices from female rats through an ERβ-mediated increase in pre-synaptic glutamate release probability (Smejkalova and Woolley, 2010). Moreover, in slices from OVX and E2 primed rodents, acute E2 exposure enhances the excitability of CA1 neurons via an ERα mediated inhibition of GABA release, via a mechanism which involves retrograde signalling of anandamide and pre-synaptic CB_1R activation, an effect not present in male rodents (Huang and Woolley, 2012).

It should be noted that another possible explanation for the agonist induced depression of synaptic transmission is an agonist-induced reduction in the number of presynaptic fibres generating action potentials rather than effects which are expressed post-synaptically. We cannot exclude this possibility as the amplitude of the presynaptic fibre volley was not monitored throughout the duration of recordings (the amplitude of the fibre volley is a measure of the number of presynaptic fibres generating action potentials in response to electrical stimuli).

Nevertheless, recent evidence adds weight to the concept that the G1- and E2 induced LTD are expressed post-synaptically, as GPR30 associates with the dendritic scaffolding protein post-synaptic density-96 (PSD-95) in close proximity to the post-synaptic density (PSD) in a subset of dendritic spines in the rodent CA1 (Akama *et al*., 2013). In view of this and the fact that the response profiles of E2- and G1- are analogous, it is possible that E2 may be activating GPR30 located at post-synaptic sites on dendrites in the CA1 region, which culminates in the induction of LTD (in most cases).

5.3.2: The E2- and G1- induced LTD does not require afferent stimulation

The results presented here suggest that the E2- and G1- induced LTD do not require evoked glutamate release as LTD persisted even in the absence of synaptic stimulation (Fig 5.5). The protocol used here is primarily designed to test whether concurrent activation of post-synaptic AMPAR and NMDAR are required for agonist-induced effects on synaptic transmission. However, considering the CA3 is still intact in our preparations, spontaneous glutamate release from pre-synaptic inputs is likely to occur, therefore we cannot rule out this possibility. Other forms of chemically induced LTD at

the CA3 - CA1 synapse do not require stimulation of the presynaptic terminal, for example LTD induced by the mGluR agonist, DHPG (Fitzjohn *et al*., 1999; Huber *et al*., 2001) or the muscarinic agonist, carbachol (Kumar, 2010). Thus, the E2- and G1-induced LTD, like those mentioned above; involve mechanisms distinct from forms of chemically induced-LTD which involve afferent stimulation, including insulin-LTD (van der Heide *et al*., 2005) or LTD-induced by low-frequency stimulation (as reviewed in Collingridge *et al.*, 2010).

5.3.3: AMPAR trafficking

LTD that is expressed post-synaptically is most likely attributed to a reduction in synaptic GluA1-containing AMPAR (Malenka, 2003; Kessels and Malinow, 2009). The data here indicate that at physiological concentrations (1 – 10 nM) both E2 and G1 reduce the surface expression of GluA1-containig AMPAR in DIV 8 –16 primary hippocampal neurons, thus potentially providing a mechanism for the observed depression of synaptic transmission in response to these agonists. Moreover, the data presented here is directly supported by results from another group who show in cortical cultures, exposure to E2 (10 nM; 30 min) results in a reduction in surface GluA1-expression and in parallel, a reduction in the frequency of AMPAR-mediated mEPSC's (Srivastava *et al.*, 2008). However, contrary to these results, acute application of the same concentration of E2 (10 nM; 5 min) in adult male hippocampal slices can increase the surface expression of GluA1 in the CA1 region (Zadran *et al*., 2009). In this study, the authors did not examine GluA1 expression after longer time periods of E2 exposure and their assay was not sensitive to changes in synaptic GluA1, providing a reasonable explanation for this discrepancy. Their results may also suggest that the E2-induced effects on AMPAR-trafficking may occur in a time- dependant manner.

In our study, we chose to investigate the effects of G1 and E2 after 30 min ligand exposure, a time point where E2 has previously been demonstrated to have effects on surface GluA1 expression in primary cortical cultures (Srivastava *et al*., 2008) and primary hippocampal cultures (*unpublished observations by Farquharson and Moult, 2010*). This time point correlates with a point during electrophysiological recordings when GluA1 trafficking away from synaptic sites in response to agonist exposure may be occurring and may be observed at the level of the individual cell. However, in order

to fully correlate our findings from primary hippocampal cultures with the results from electrophysiological recordings, it would be worthwhile to subject slices exposed to E2 or G1, to GluA1 cell surface biotinylation assays at different experimental times points during ligand application and washout.

Nevertheless, supporting the hypothesis that E2 may be acting at GPR30 to effect surface AMPAR expression, were the characteristics of the concentration-response relationships between the two agonists (E2 and G1). Application of either agonist did not result in a linear nor a threshold concentration-response relationship, but rather an inverted-U shaped concentration response. Exposure to E2 resulted in what may be a hormetic concentration response relationship, characterised by an inverse-U shaped concentration response and the reversal of response at high concentrations (Kendig *et al*., 2010), as at a concentration of 100 nM E2, an increase in GluA1-staining was observed. This intriguing concentration-response relationship is not uncommon for E2 at different biological endpoints, although usually a response attributed to toxic-effects of high concentrations of E2 (Strom *et al*., 2011). The reversal of response seen here may be attributed to preferential signalling mediated by different estrogen receptor sub-types. This hypothesis is supported by unpublished observations from our laboratory, which suggests that exposure to selective ERα and ERβ agonists have opposing effects on surface GluA1 expression (*unpublished observations by Farquharson and Moult, 2010*). Specifically, a selective ERα agonist (0.2 – 20 nM PPT; 30 min) significantly reduces, whereas a selective ERβ agonist (50 – 100 nM DPN; 30 min) significantly increases, surface GluA1-expression in hippocampal neurons (*unpublished observations by Farquharson and Moult, 2010*). In addition, similar effects of selective estrogen receptor agonists on GluA1-trafficking within hippocampal neurons have been reported by others. For example, Liu and colleagues (2008) demonstrate that in hippocampal extracts from OVX rats dosed with a bolus subcutaneous injection of either selective ERα (PPT; 10 mg kg^{-1}) or ERβ (WAY-200070; 10 mg kg^{-1}) agonists, selective activation of ERβ significantly increases hippocampal GluA1 expression, whereas although not statistically significant, selective activation of ERα shows a trend towards reducing hippocampal GluA1 expression (Liu *et al*., 2008). Thus, we and others have demonstrated that trafficking of GluA1-containing AMPAR in response to estradiol, is differentially regulated depending on the estrogen receptor subtype activated.

Here we show that G1 did not result in a reversal of response (*ie*: an increase in surface GluA1-staining), however an inverted-U concentration relationship was observed, mimicking part of the effects of E2 at lower concentrations. As selective ERα agonists induced a decrease in surface GluA1-expression (*unpublished findings from Farquharson and Moult, 2010*) and considering signalling via GPR30 may require association with ERα (Levin, 2009a; Vivacqua *et al*., 2009) and/or G1 may be selectively activating a variant of ERα, ERα36 (Kang *et al*., 2010), the G1-induced concentration-response observed here may be a reflection of this.

Nevertheless, rapid effects of E2 in spatial recognition memory tasks (object-placement) have been recently reported to exhibit an inverted-U concentration-response (Luine and Frankfurt, 2012). This type of behavioural task is dependent on the intact hippocampus, which perhaps gives an *in vivo* role for the type of concentration-response relationship we see in our molecular assay.

5.3.4: NMDAR involvement

Another novel finding here is that the G1-induced LTD and a component of the E2-induced LTD are NMDAR-independent, as the competitive NMDAR antagonist D-AP5 failed to alter the magnitude of G1-induced LTD and failed to fully inhibit the E2-induced LTD. In agreement with the data presented here, unpublished findings from our laboratory suggest that in adult male rodents, the novel form of LTD induced by E2 in conditions of hyper excitability is not fully blocked by D-AP5 (*Findlay and Moult, unpublished findings, 2010*). However in contrast, E2-mediated alterations in CA1 dendritic morphology involve D-AP5 sensitive mechanisms (Woolley and McEwen, 1994; Woolley *et al*., 1997) and recent evidence in primary pre-frontal cortical cultures, suggest that GPR30 initiated signalling can modulate the phosphorylation state of NR2B subunits (Liu *et al*., 2012).

Another type of hormonally-induced LTD (insulin-induced LTD) is also NMDAR-independent (Huang *et al*., 2004) and is associated with a reduction in surface AMPAR expression in slices (Huang *et al*., 2004) and in DIV 21 – 28 hippocampal cultures (Man *et al*., 2000). Therefore, it is feasible that signalling induced by E2 and G1 in adult hippocampal slices, may lead to direct down-regulation of surface GluA1-containing AMPAR, without the requirement of NMDAR-dependant Ca^{2+} influx. The finding that

there is a component of the E2-induced LTD sensitive to D-AP5, may reflect the involvement of a multitude of estrogen receptors and differing mechanisms by which E2 induces its effects at these synapses. In support of this hypothesis, ERα-mediated reductions in surface GluA1-containing AMPAR in primary hippocampal cultures are NMDAR-dependant, whereas ERβ-mediated increases in surface GluA1 are NMDAR-independent (*unpublished findings from Farquharson and Moult, 2010*).

The immunocytochemistry data presented here however conflicts with the results from the electrophysiology experiments. The data here would suggest that in primary hippocampal cultures the G1- and E2-induced reduction in surface-AMPAR expression does indeed involve NMDAR activation. In our study, primary hippocampal cultures were used between 8 and 16 DIV, as in our laboratory, cultures older than 7 DIV are deemed mature (Shanley *et al*., 2002; McDonald *et al*., 2007b) and at this age, effects of neuromodulators (leptin) on surface GluA1 expression mimic those in adult slices (Moult *et al*., 2010). However, in a study by Srivastava *et al*., (2008), E2-induced reduction in surface GluA1 expression in cortical cultures occurred in the presence of D-AP5, yet the age of the cultures used in their study were DIV 28 (Srivastava *et al*., 2008). Considering the media we use in the AMPAR-trafficking assay contains glycine (co-agonist for NMDAR), and in juvenile slices effects of G1 were only uncovered in conditions of enhanced NMDAR activity (Fig 4.2) and there are likely to be developmental differences in estradiol-induced effects within the hippocampus (see section 4.3.1). The mechanisms by which estrogen receptor agonists affect GluA1-trafficking in primary hippocampal neurons may depend on basal NMDAR activity which may differ depending on the maturity of hippocampal cultures.

5.3.5: mGluR involvement

The immunocytochemistry results do not support a role for mGluRs in E2- or G1-mediated reduction in surface AMPAR-expression. However, it should be noted that estradiol-induced effects can be mediated via mGluRs. Indeed, the Mermelstein group have established that rapid effects of E2 in different brain regions can occur via association of membrane estrogen receptors (mERα or mERβ) and mGluR's (Group I and Group II/III; as reviewed in Meitzen and Mermelstein, 2011), however only in female hippocampal neurons are mER functionally coupled to mGluR (Boulware *et al*.,

2005, 2007). Specifically rapid E2-induced CREB phosphorylation via ERα-mGluR1a signalling is observed only in hippocampal cultures from female pups and not in cultures from male pups or in female pups which have been masculinised (Meitzen *et al*., 2012). Moreover, Hunag and Woolley (2010) demonstrate that E2-induced reduction of pre-synaptic GABA release at CA1 neurons occurs via ERα-mGluR1a signalling, and is only observed in slices from female rodents (Huang and Woolley, 2012). As all experiments here were conducted using male hippocampal slices, it is unlikely that ERα-mGluR signalling would account for the observed E2-induced LTD. Although, it is not known whether GPR30 can associate with mGluR's, GPR30 does have the capacity to associate with other GPCRs at CA1 synapses (Akama *et al*., 2013), moreover it has also been speculated that G1 directly stimulates mGluR1a in hypothalamic astrocytes (Kuo *et al*., 2010). Although unlikely, currently we cannot conclusively rule out the possibility that components of the G1- and E2- induced LTD are mediated via mGluRs.

5.4: Conclusion

Overall, this chapter has characterised the E2- and G1- induced long-lasting depression of hippocampal synaptic transmission. Here we find that in the adult hippocampus E2- and G1- induce a novel form of LTD which is likely to be expressed post-synaptically and may be attributed to a reduction in synaptic GluA1-containing AMPAR. Furthermore, this data supports the hypothesis that GPR30 may be (at least in part) contributing to these E2 induced effects. In order to fully establish a role for GPR30 in E2 mediated physiology, a pharmacological evaluation of the G1-induced effects is necessary (see Chapter 6).

-

Chapter 6

Establishing a mechanism for the G1-mediated LTD

6.1: Introduction

The previous chapter describes the properties of acute exposure of E2 and the GRP30 agonist (G1) on basal excitatory hippocampal synaptic transmission and surface AMPAR expression in neurons.

Although widely used as a selective GPR30 agonist, the findings of Kang *et al,* (2010) suggest that G1-induced effects are mediated by an estrogen receptor splice variant (ERα-36). Another complexity to GPR30 pharmacology arises from the recent evidence which suggests that the steroid aldosterone can also activate GPR30, at least in vasculature (Gros *et al*., 2011, 2013; Batenburg *et al*., 2012), in addition to the known capacity of this steroid hormone to modulate hippocampal synaptic function (Pavlides and McEwen, 1999; Maggio and Segal, 2009, 2012). Thus, it is important to characterise the pharmacology fully, in order to establish whether GPR30 mediates the observed effects of G1 in this study.

In order to explore further the target for G1 action in hippocampal neurons, the use of selective GPR30 and estrogen receptor antagonists needs to be employed. In 2009, Dennis and colleagues described a putative GPR30 selective antagonist (G15), that competes with E2 at GPR30 with a K_i of approximately 0.3 – 0.5nM and has a binding affinity for GPR30 of approximately 20 nM (Dennis *et al.*, 2009). G15 can block GPR30 mediated effects in heterologous over expression systems and endogenously expressing cancer cell lines (Dennis *et al*., 2009, 2011; Notas *et al*., 2012).

Importantly, *in vivo* effects of G1 in rodents can be blocked by G15 for example; in a mouse model of depression G15 blocked the G1-induced decrease in immobility time in the tail suspension test (Dennis *et al*., 2009), moreover G1-induced pain-related behaviour in mice (licking, biting and scratching) are blocked by G15 (Deliu *et al*., 2012).

Therefore the aim of this series of experiments was to establish using pharmacological approaches whether the G1-induced effects on hippocampal synaptic transmission and AMPAR expression are mediated by GPR30 or another estrogen-sensitive receptor, and also to investigate potential down-stream signalling pathways involved.

6.2: Results

6.2.1: GPR30 antagonists do not block the G1-induced effects on hippocampal synaptic transmission and AMPAR trafficking.

Previous studies have demonstrated the ability of G15 to block E2-mediated effects in hippocampal neurons. For example, G15 can inhibit E2-mediated protection against glutamate-induced neurotoxicity in immortalised hippocampal cell lines (Gingerich *et al*., 2010). Chronic treatment with G15 also blocks the effect of E2 in hippocampal dependent learning tasks (delayed matching-to-position acquisition) in OVX rats (Hammond *et al*., 2012). Therefore, in order to establish whether the G1-induced effects on excitatory hippocampal synaptic transmission are sensitive to the GPR30 antagonist, G15 (200 nM) was bath applied to adult male (12 – 16 weeks) hippocampal slices for 20min before co-application with G1 (10 nM).

Application of G15 (200nM; 20 min) had no significant effect on baseline transmission (100 ± 1.1 % of baseline; $p > 0.05$; n = 8). In the presence of G15 (200 nM), the G1-induced (10 nM; 20 min) LTD is still observed (to 87 ± 3.2 % of baseline; $F[3,30] = 17.6$; $p < 0.001$ vs. baseline; n = 8). Subsequent stratification revealed that out of the eight slices exposed to these conditions, four elicited a bi-phasic response profile in response to G1 (Fig 6.1 B) such that G1 induced a significant potentiation of synaptic transmission (to 108 ± 2 % of baseline; $F[3,15] = 22.4$; $p < 0.05$; n = 4) followed by a slow-onset depression of synaptic transmission after G1 washout (to 87 ± 6.7 % of baseline; $F[3,15] = 22.4$; $p < 0.05$; n = 4). In the other four slices exposed to G15, G1 depressed synaptic transmission without a preceding potentiation (Fig 6.1 C). Thus, during G1 application no effect on baseline transmission was observed (to 99 ± 1.0 % of baseline; $p > 0.05$; n = 4), however following washout of G1 and in the continued presence of G15, synaptic transmission was significantly reduced (to 87 ± 2.2 % of baseline; $F[3,14] = 21.2$; $p < 0.05$; n = 4). In control slices, G15 was applied for an extended period of time (up to 100 min) to ensure the induction of long-lasting depression of synaptic transmission was not attributed to an extended application of G15 (Fig 6.1 D). Long duration exposure to G15 failed to alter the magnitude of synaptic transmission (to 98 ± 2.2% of baseline at 115 – 120 min; n = 4; $p > 0.05$), suggesting that G15 does not contribute to LTD.

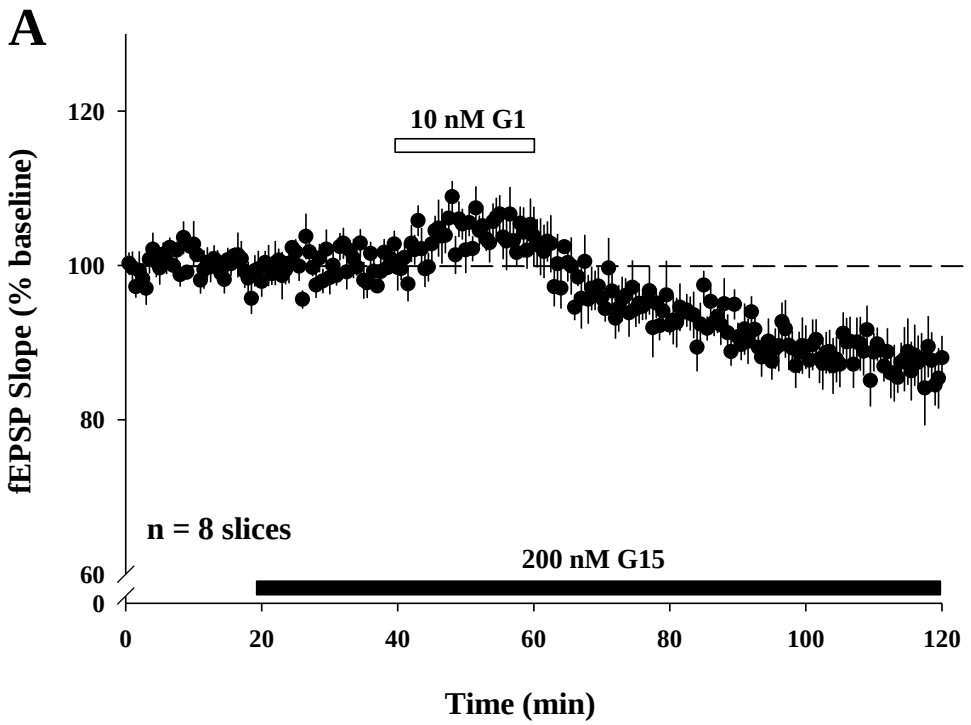
A
10 nM G1
fEPSP Slope (% baseline)
120
100
80
60
0
n = 8 slices
200 nM G15
0
20
40
60
80
100
120
Time (min)

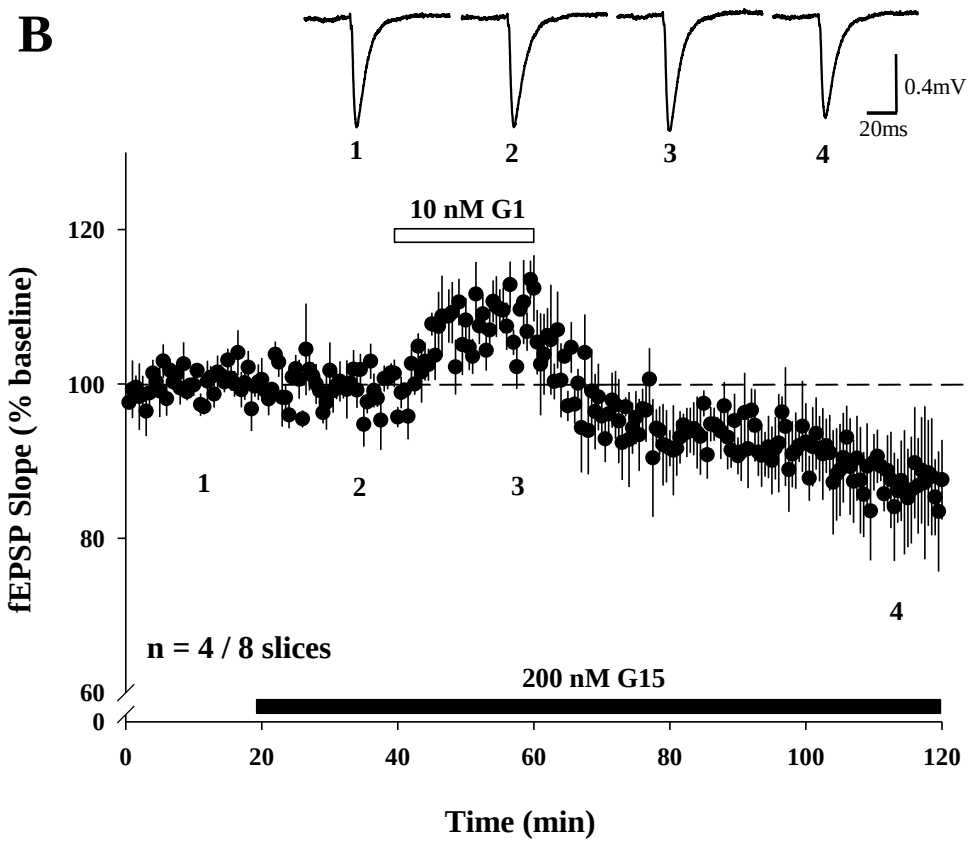
B
0.4mV
20ms
1
2
3
4
10 nM G1
fEPSP Slope (% baseline)
120
100
80
60
0
1
2
3
4
n = 4 / 8 slices
200 nM G15
0
20
40
60
80
100
120
Time (min)

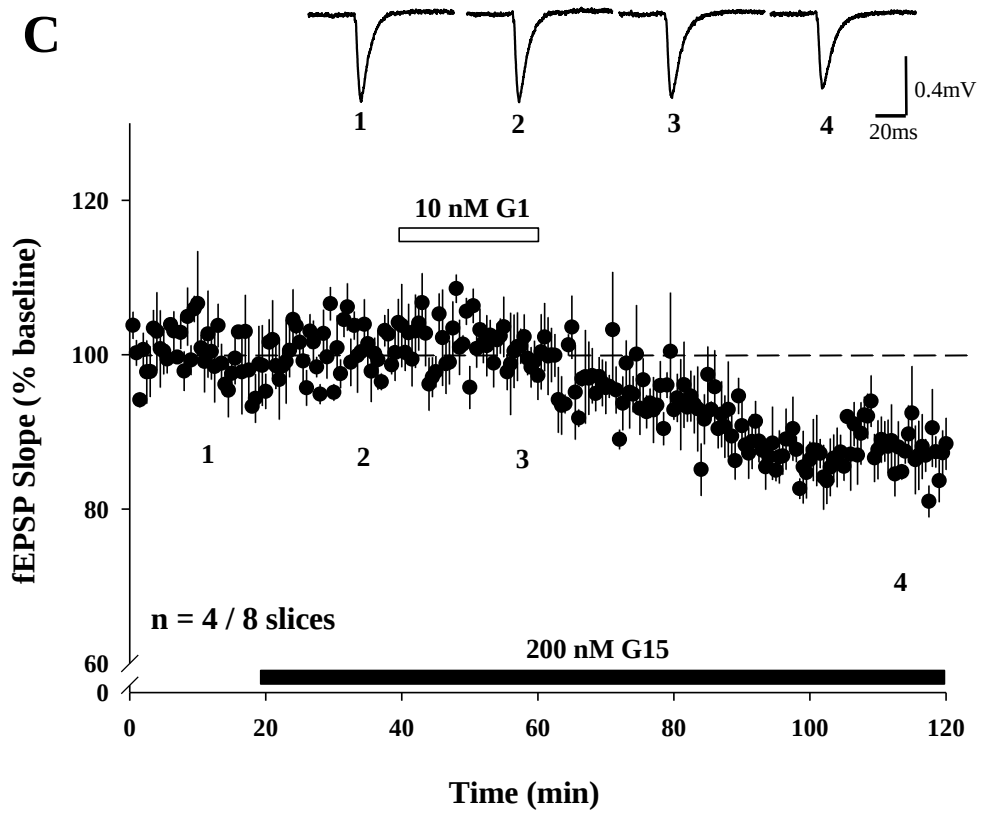
C
0.4mV
20ms
1
2
3
4
10 nM G1
fEPSP Slope (% baseline)
120
100
80
60
0
n = 4 / 8 slices
200 nM G15
0
20
40
60
80
100
120
Time (min)

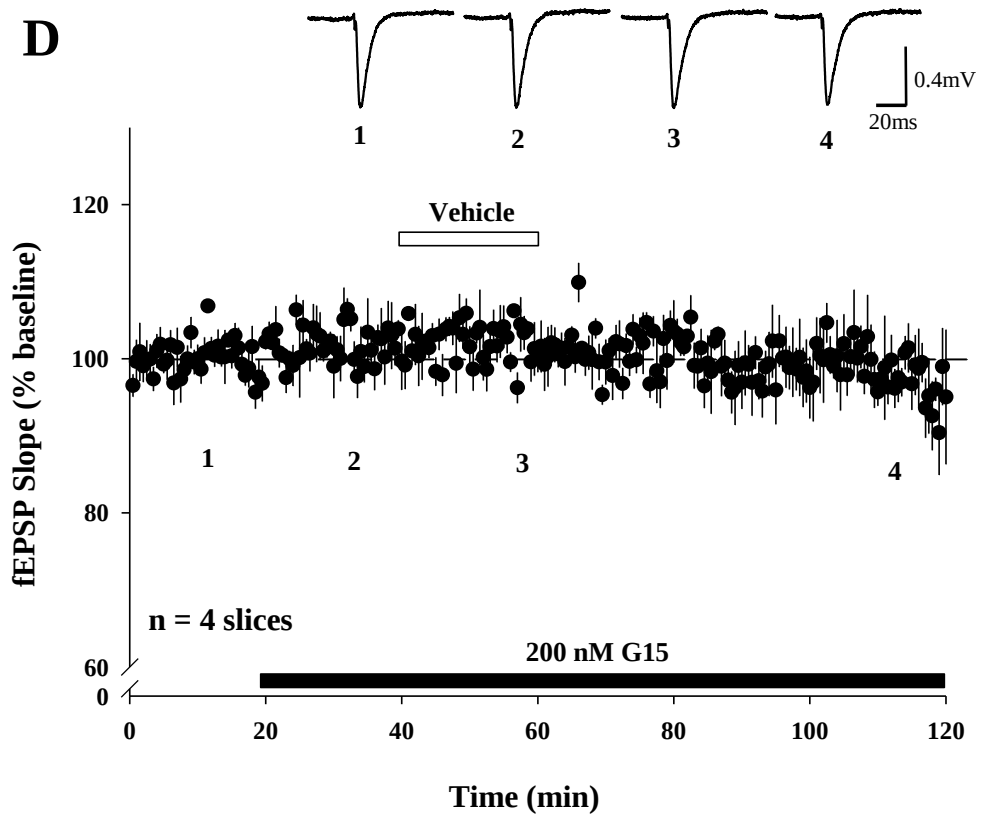
D
0.4mV
20ms
1
2
3
4
Vehicle
fEPSP Slope (% baseline)
120
100
80
60
0
n = 4 slices
200 nM G15
0
20
40
60
80
100
120
Time (min)

Figure 6.1: G15 does not block the G1-induced effects on basal synaptic transmission in adult male hippocampal slices. ***A,*** Pooled data (n = 8 slices) illustrating that in the presence of G15 (200 nM), the G1-induced (10 nM) depression of synaptic transmission is still observed. ***B,*** stratification reveals a bi-phasic response profile of G1 in the presence of G15 in 4 out of 8 slices ***C,*** a depression only response profile is observed in the other 4 out of 8 slices. ***D,*** Pooled data illustrating that G15 (200 nM) in combination with vehicle treatment (0.01% DMSO, 20 min, open bar) had no effect on synaptic transmission (n = 4). Example traces from a representative experiment from each data set are shown at the time points indicated. Data are normalised with respect to baseline and are expressed as mean ± SEM.

In parallel immunocytochemistry studies, exposure of primary hippocampal cultures (DIV 8 – 16) to G15 (200 nM; 45 min) also failed to inhibit the G1-induced effects on surface GluA1 staining (Fig 6.2). Specifically, in the presence of G15 (200 nM) application of G1 (10 nM) significantly reduced surface GluA1 staining (to 86 ± 1.6 % of vehicle; n = 48; H = 60.9 with 3 degrees of freedom; $p < 0.05$ vs. vehicle treatment), which was not significantly different from the reduction induced by G1 alone (to 79 ± 2.2% of vehicle treated cultures; n = 48; $p < 0.05$ vs. vehicle treatment; $p > 0.05$ vs. G15 + G1 treatment).

Recently, another compound, G36 was developed as an antagonist for GPR30, with improved selectivity and less off target effects compared to G15 (Dennis *et al*., 2011). We obtained G36 from Dr. Arterburn and assessed its effects in the AMPAR trafficking assay. Here we find that exposure of hippocampal neurons to G36 (1 µM; 45 min) was also unable to inhibit the G1-induced reduction in surface AMPAR expression (Fig 6.3). Thus application of G1 (10 nM), in combination with G36 significantly reduced surface GluA1 staining (to 85 ± 3.0 % of vehicle; n = 36; H = 20.7 with 3 degrees of freedom; $p < 0.05$ vs. vehicle treatment;); the magnitude of which was not significantly different to that induced by G1 alone (84 ± 2.7%; n = 36; $p < 0.05$ vs. vehicle treated cultures; $p > 0.05$ vs. G36 + G1 treatment). Although there was a slight reduction in surface GluA1 staining with G36 alone, this effect was not significantly different from vehicle treated cultures (to 92 ± 3.3%; $p > 0.05$ vs. vehicle treatment; n = 36).

Taken together, these results suggest that GPR30 antagonists are unable to inhibit the effects of G1 on hippocampal excitatory synaptic transmission and surface AMPAR expression.

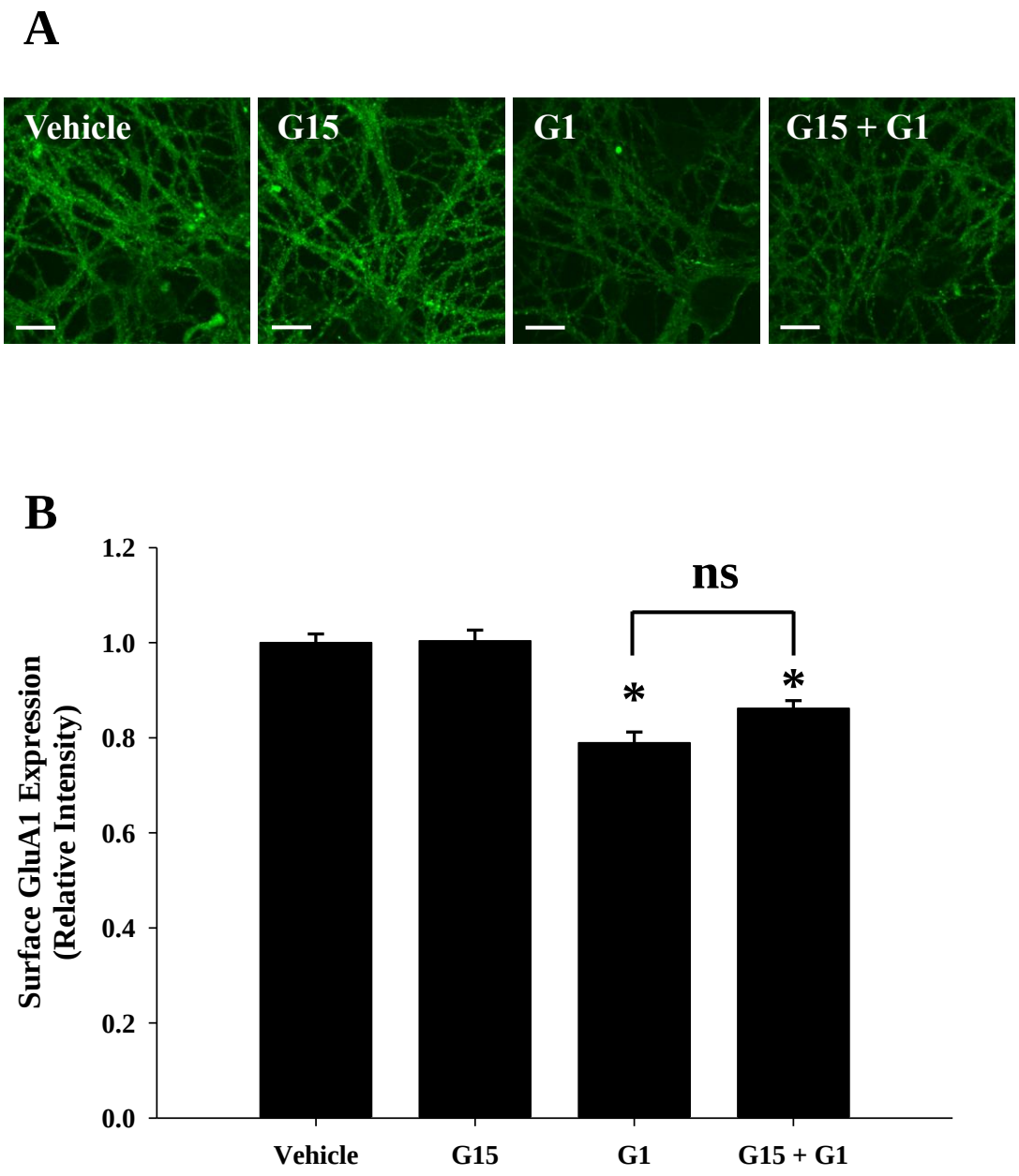

Figure 6.2: G15 does not inhibit the G1-induced reduction in surface AMPAR expression. *Neurons were pre-treated with vehicle (0.01% DMSO) or G15 (200 nM; 15 min) and then G1 (10 nM) or vehicle, or in combination with G15 (30 min).* ***A,*** representative confocal images of surface GluA1 staining in hippocampal cultures. ***B,*** pooled data showing relative changes in surface GluA1 expression after exposure to G15 alone and in the presence of G1. Scale bars, 20 µm. A Kruskal-Wallis one way ANOVA on ranks followed by Dunn's *post-hoc* analysis was performed. * represents $p < 0.05$ vs. vehicle treatment; ns represents $p > 0.05$ between the indicated treatments; n = 48 from 4 individual cultures from different animals.

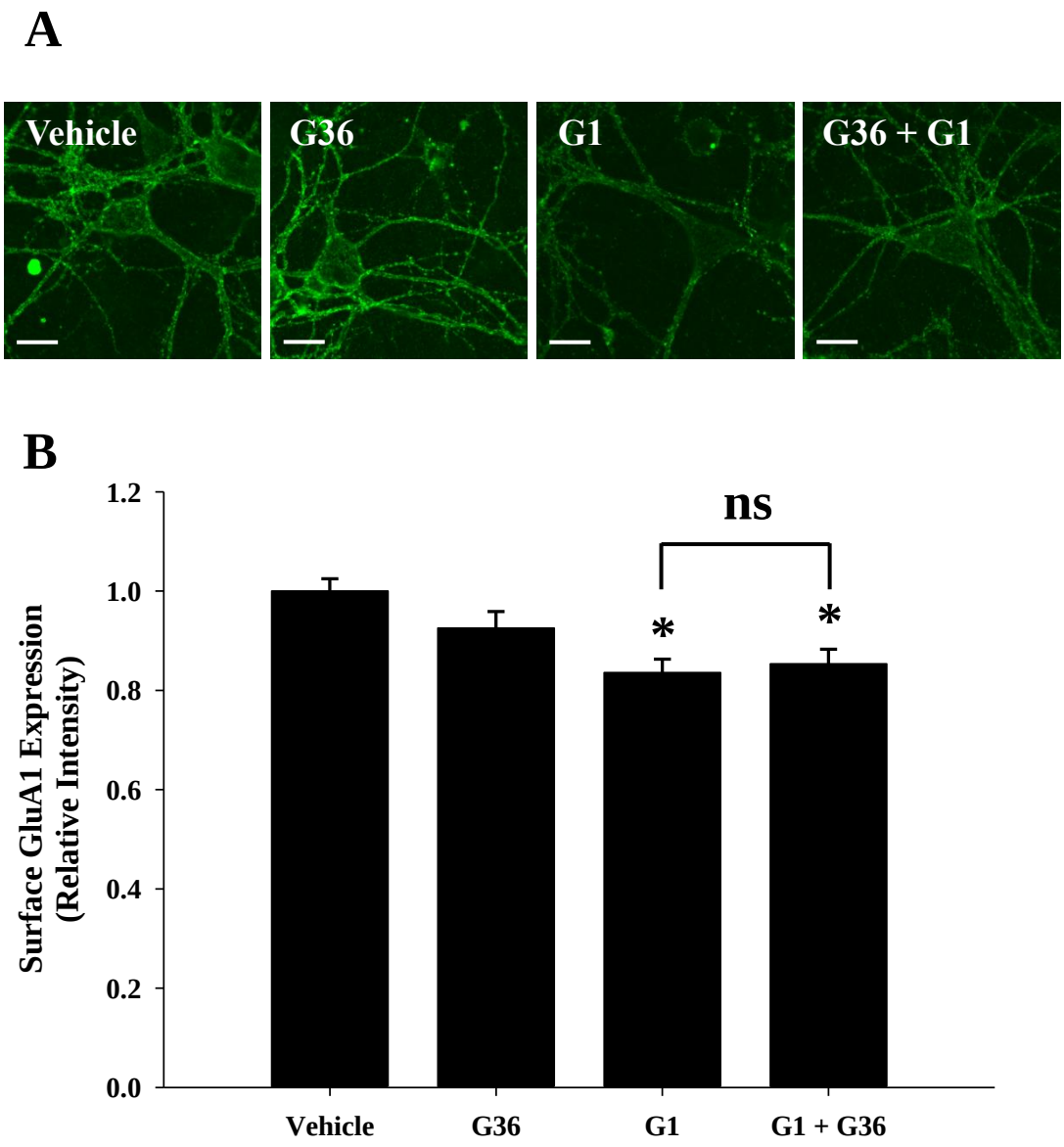

Figure 6.3: The GPR30 antagonist (G36) does not block the G1-induced reduction in surface AMPAR expression. *Neurons were pre-treated with vehicle (0.01 % DMSO) or G36 (1 µM; 15 min) and then G1 (10 nM) or vehicle, or in combination with G36 (30 min).* ***A,*** representative confocal images of surface GluA1 expression. ***B,*** pooled data showing relative changes in surface GluA1 after exposure to G36 alone and in the presence of G1. Scale bars, 20 µm. A Kruskill-Wallis one way ANOVA on ranks followed by Dunn's *post-hoc* analysis was performed. * represents $p < 0.05$ vs. vehicle treatment and ns represents $p > 0.05$ between the indicated treatments; n = 36 neurites from 3 individual cultures from different animals.

6.2.2: The Estrogen Receptor α antagonist does not attenuate the G1-induced effects on hippocampal synaptic transmission and AMPAR trafficking.

It has been suggested that G1 binds to and activates a 36kDa ERα splice variant (ERα-36; Kang *et al*., 2010), which may provide an explanation as to why the GPR30 antagonist (G15) failed to block the G1-induced effects. Moreover, it has been suggested that signalling via GPR30 may require association with mERα (Albanito *et al*., 2007; Levin, 2009a; Notas *et al*., 2012), in support of this idea a direct interaction between GPR30 and ERα has been observed in breast cancer cells (Vivacqua *et al*., 2009). Thus, in order to examine whether G1-mediated effects on excitatory synaptic transmission involve ERα or its variant ERα-36, MPP dihydrochloride (MPP) was utilised. This compound was developed as a selective antagonist against nuclear ERα (ERα-66), with a K_i of 2.7nM and over 200-fold selectivity over ERβ (Sun *et al.*, 2002). Although it is not known if MPP can bind to and inhibit ERα-36, there is evidence to suggest that this compound can inhibit non-genomic effects of E2 via inhibition of membrane associated ERα (Lin *et al*., 2011; Tuo *et al*., 2012; Zárate *et al*., 2012).

Thus, MPP (1 µM) was applied to slices for 20 – 35 min prior to G1 (10 nM; 20 min) administration. In these conditions, the G1-induced LTD was still observed (to 86 ± 2.8 % of baseline; $F[2,17] = 23.8$; $p < 0.001$ vs. MPP baseline; n = 6; Fig 6.4 A). Subsequent stratification revealed that three out of the six slices exhibited a bi-phasic response profile in response to G1 (Fig 6.4 B). G1 induced a significant potentiation of synaptic transmission (to 110 ± 3.4 % of baseline; $F[2,8] = 27.3$; $p < 0.05$; n = 3) that was followed by a slow-onset significant depression of synaptic transmission after G1 washout (to 90 ± 3.8 % of baseline; $F[2,8] = 27.3$; $p < 0.05$; n = 3). In the other three slices, a persistent depression of synaptic transmission was induced by G1 without a preceding potentiation (Fig 6.4 C). Specifically, in the presence of MPP, G1 had no significant effect on basal excitatory synaptic transmission (100 ± 3.9 % of baseline; $p > 0.05$; n = 3), however following washout a significant reduction in transmission was observed (to 83 ± 3.1 % of baseline; $F[2,8] = 8.6$; $p < 0.05$; n = 3). In control experiments, exposure of slices to MPP for extended periods of time (100 min) had no significant effect on basal synaptic transmission ($p > 0.05$; n = 4; Fig 6.4 D).

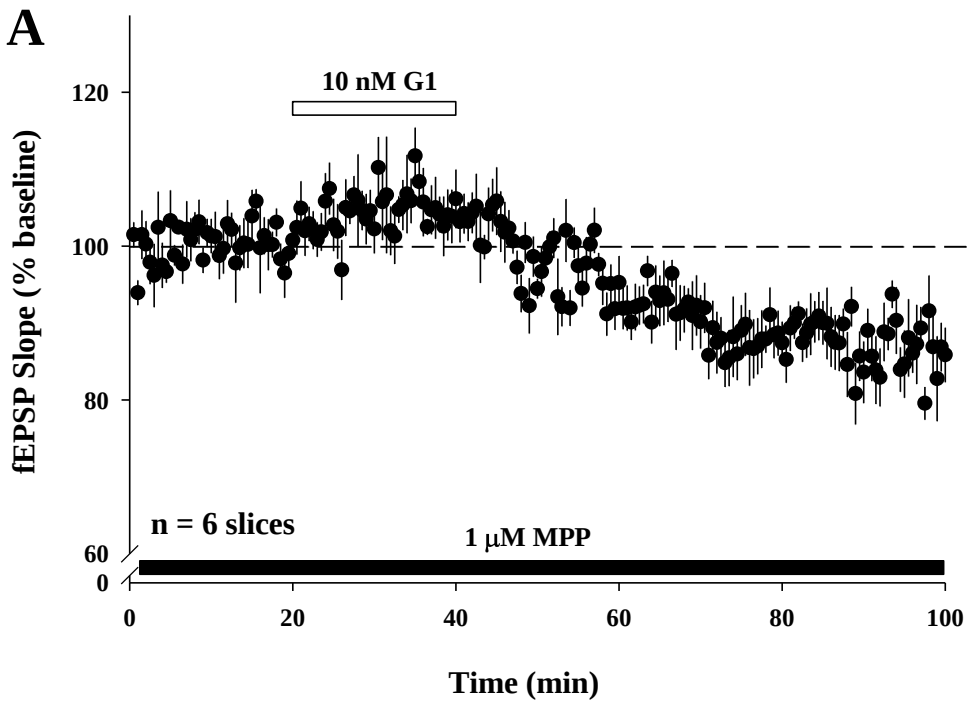
A
10 nM G1
fEPSP Slope (% baseline)
120
100
80
60
0
n = 6 slices
1 μM MPP
0
20
40
60
80
100
Time (min)

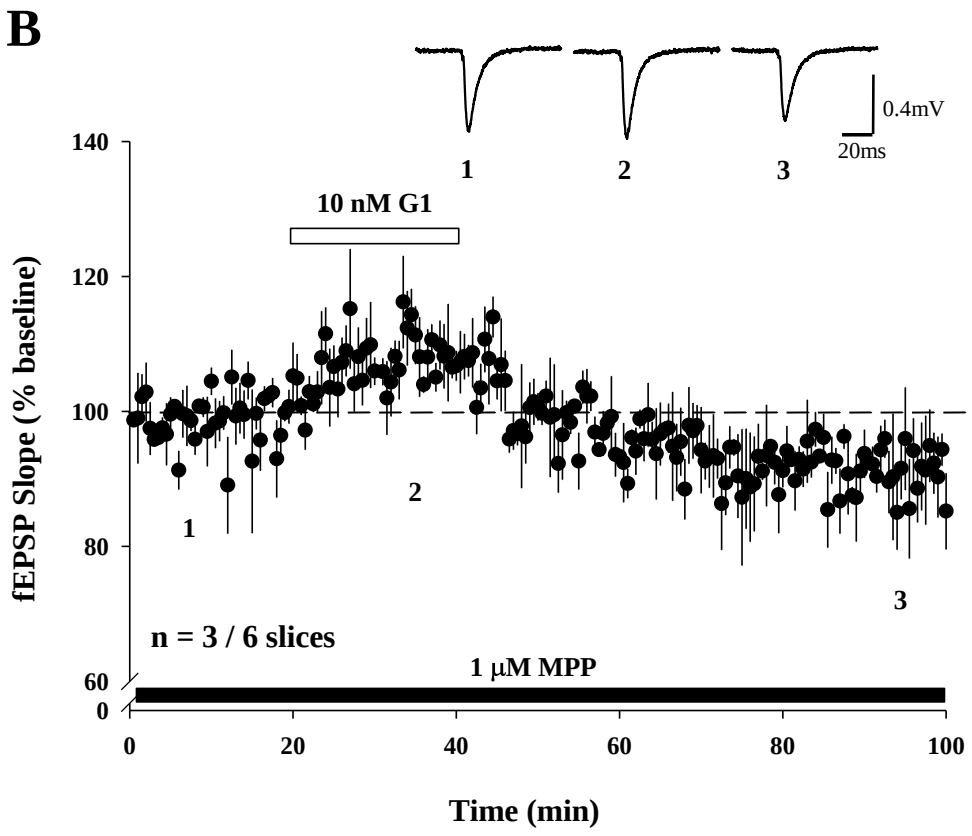
B
0.4mV
20ms
1
2
3
10 nM G1
fEPSP Slope (% baseline)
140
120
100
80
60
0
n = 3 / 6 slices
1 μM MPP
0
20
40
60
80
100
Time (min)

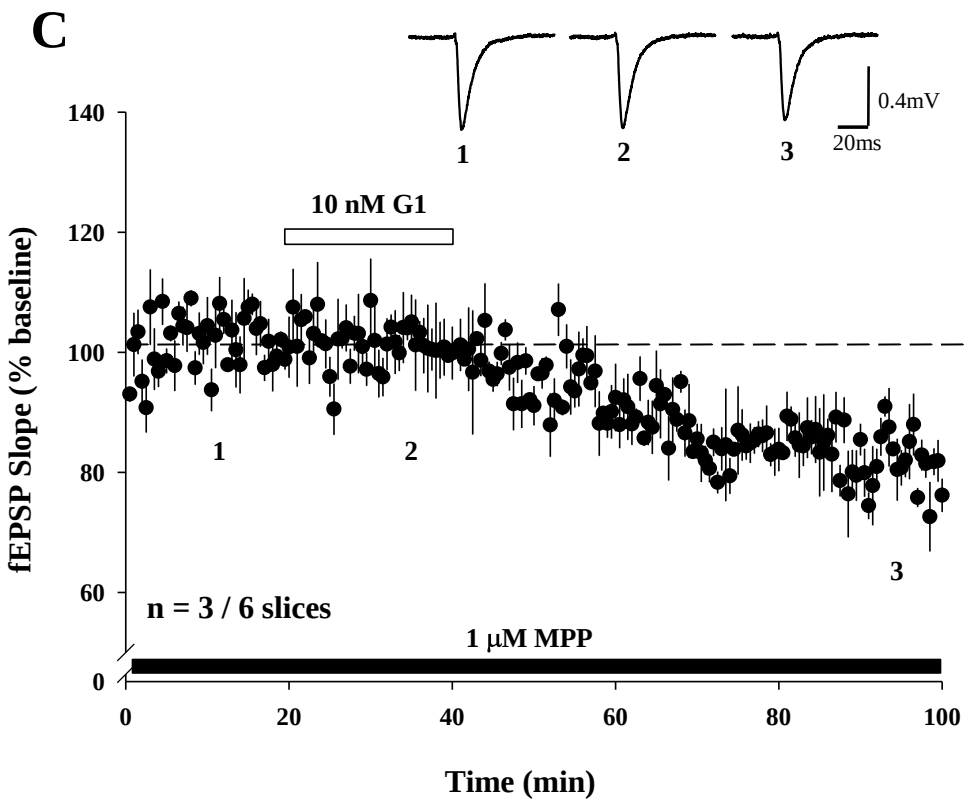
C
0.4mV
20ms
1
2
3
10 nM G1
fEPSP Slope (% baseline)
140
120
100
80
60
0
1
2
3
n = 3 / 6 slices
1 μM MPP
0
20
40
60
80
100
Time (min)

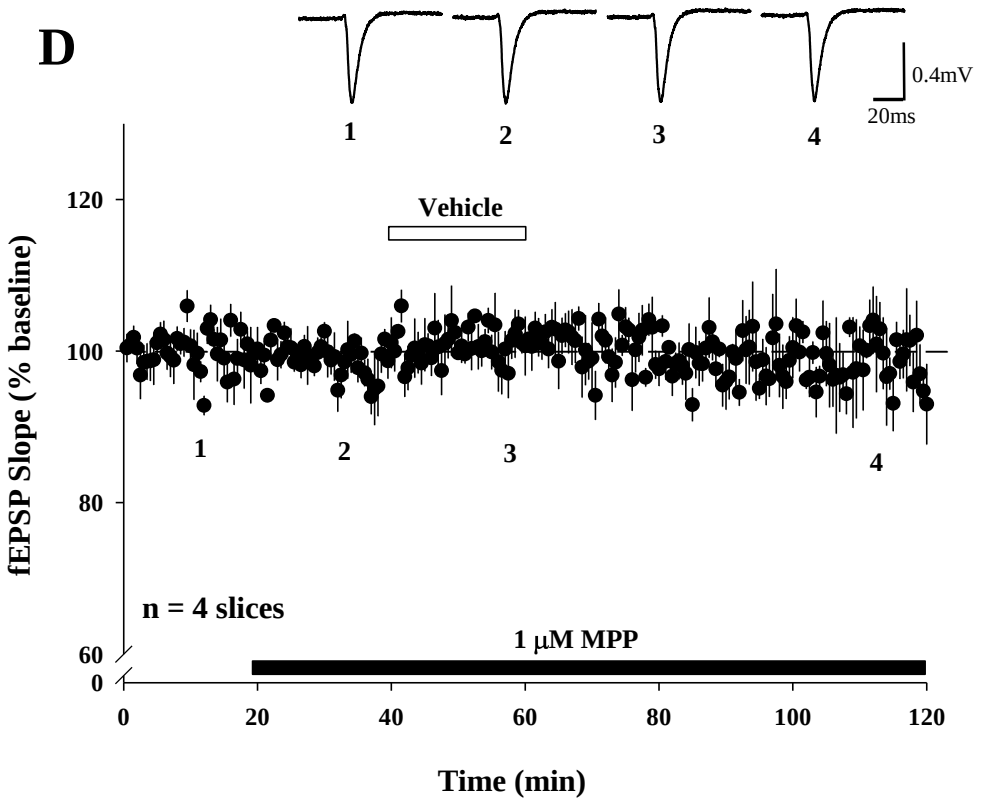
D
0.4mV
20ms
1
2
3
4
Vehicle
fEPSP Slope (% baseline)
120
100
80
60
0
1
2
3
4
n = 4 slices
1 μM MPP
0
20
40
60
80
100
120
Time (min)

Figure 6.4: A selective ERα antagonist (MPP) does not block the G1-induced effects on basal synaptic transmission in adult male hippocampal slices. ***A,*** Pooled data (n = 6 slices) illustrating that in the presence of MPP (1 µM), the G1-induced (10 nM) depression of synaptic transmission is still observed. ***B,*** stratification reveals a bi-phasic response profile of G1 in the presence of MPP in 3 out of 6 slices**.** ***C,*** a depression only response is observed in the other 3 (out of 6) slices. ***D,*** pooled data illustrating MPP (1 µM) in combination with a vehicle treatment (0.01% DMSO; 20 min; open bar) had no effect on basal excitatory synaptic transmission (n = 4). Example traces from a representative experiment from each data set are shown at the time points indicated. Data are normalised with respect to baseline and are expressed as mean ± SEM.

The effects of MPP on surface AMPAR expression were also examined in hippocampal cultures (Fig 6.5). Addition of MPP (1 µM; 45 min) had no effect on surface AMPAR expression (99 ± 2% of vehicle; $p > 0.05$ vs. vehicle treatment; n = 36), moreover MPP failed to block the G1-induced reduction in surface GluA1 staining as there was no significant difference between G1 treatment (10 nM; 88 ± 2% of vehicle; $F[3,143] = 12.9$; $p < 0.001$ vs. vehicle treatment) and co-treatment with MPP (86 ± 2% of vehicle; $F[3,143] = 12.9$; $p < 0.001$ vs. vehicle treatment; $p > 0.05$ vs. G1 alone;). Taken together these data suggest that in the presence of an ERα antagonist, the ability of G1 to reduce surface GluA1-containing AMPAR expression and induce LTD in hippocampal slices is retained.

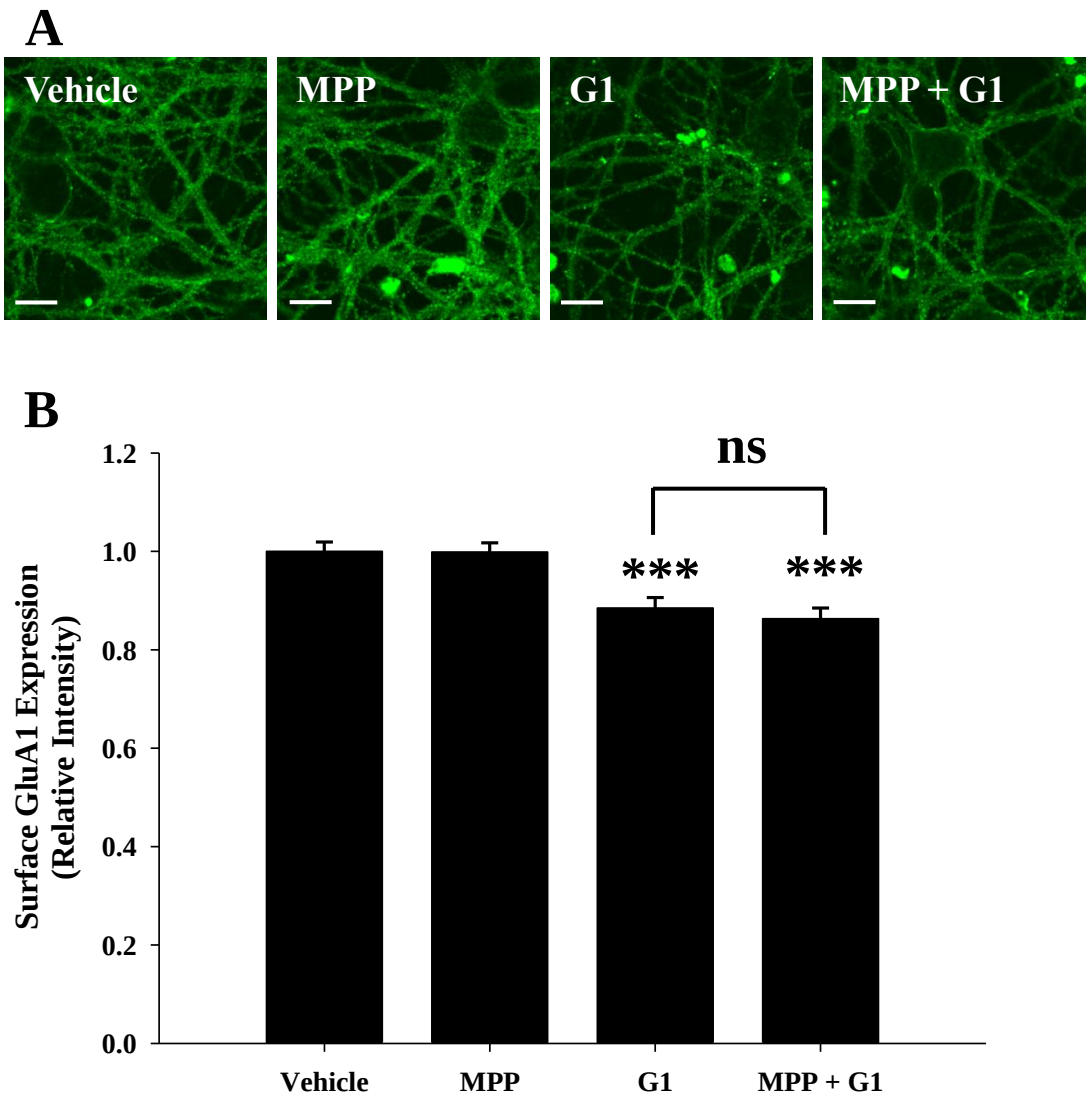

Figure 6.5: MPP does not block the G1-induced effects on surface AMPAR expression. *Neurons were pre-treated with vehicle (0.01 % DMSO) or MPP (1 µM; 15 min) and then G1 (10 nM) or vehicle, or in combination with MPP (30 min).* ***A,*** representative confocal images of surface GluA1 staining. ***B,*** pooled data showing relative changes in surface GluA1 after exposure to MPP alone and in the presence of G1. Scale bars, 20 µm. A one way ANOVA, followed by Tukey *post-hoc* anlaysis was performed. *** represents $p < 0.001$ vs. vehicle treatment, and ns represents $p > 0.05$ between the indicated treatments; n = 36 neurites from 3 individual cultures from different animals.

6.2.3: The Estrogen Receptor β antagonist does not block the G1-induced effects on hippocampal synaptic transmission and AMPAR trafficking.

ERβ has been implicated as being an important modulator of hippocampal LTP (Day *et al*., 2005; Kramár *et al*., 2009) and estradiol-induced alterations in hippocampal excitatory synaptic transmission (Smejkalova and Woolley, 2010). Moreover, application of ERβ agonists regulate the expression of synaptic proteins important for plasticity (Spencer-Segal *et al*., 2012) and disruption of the ERβ gene impairs hippocampal dependant spatial learning (Rissman *et al*., 2002). In addition it has been recently demonstrated that both ERβ and GPR30 are implicated in the neuroprotective effects of the phytoestrogen, daidzen (Kajta *et al*., 2013). Thus, a possible interaction between GPR30 and ERβ cannot be overlooked. In order to test this, we utilised a selective ERβ antagonist (PHTPP), a compound which selectively binds to and competes with E2 at nuclear ERβ to inhibit ERβ-mediated gene transcription (Compton *et al*., 2004). Currently, there is no direct evidence to suggest that this compound does not inhibit non-genomic effects of E2.

It was observed that PHTPP administration (1 μM) potentiated basal synaptic transmission in a proportion of slices (50%, 7 out of 14 slices; from 11 animals; Fig 6.6). The mean magnitude after 20 min PHTPP exposure in this group was significantly larger than baseline transmission (to 108 ± 2.3 % of baseline; $p < 0.05$). Therefore, in the slices that were exposed to G1 in the presence of PHTPP, the data were normalised to the magnitude of synaptic transmission 15 min prior to G1 administration (Fig 6.7 A, B and C). In the presence of PHTPP, exposure to G1 (10 nM; 20 min) still induced a significant depression of synaptic transmission after G1 washout (to 90 ± 2.3 % of PHTPP baseline; n = 8; $F[2,23] = 29.2$; $p < 0.001$ vs. PHTPP baseline). Subsequent stratification of response profiles revealed that in the eight slices that were exposed to G1 in the presence of PHTPP, four slices elicited a bi-phasic response profile in response to G1 (Fig 6.7 B). Specifically, a significant potentiation (to 105 ± 1.0 % of PHTPP baseline; n = 4; $F[2,11] = 55.7$; $p < 0.05$) and depression (to 91 ± 1.4 % of PHTPP baseline; n = 4; $F[2,11] = 55.7$; $p < 0.05$) was observed. Three out of eight slices elicited a depression only profile in response to G1 (Fig 5.7 C). Specifically, G1 exposure did not significantly potentiate synaptic transmission (101 ± 1.0 % of PHTPP baseline; n = 3; $p > 0.05$), however following G1 washout, a significant depression of synaptic transmission was still observed (to 85 ± 2.9 % of PHTPP baseline; n = 3;

F[2,8] = 26.3; $p < 0.01$). In one slice, in the presence of PHTPP, administration of G1 resulted in a sustained increase in synaptic transmission (data not shown). PHTPP controls were run to ensure the depression of synaptic transmission was not an artefact of extended PHTPP administration (Fig 6.7 D). At the end of 100 min PHTPP exposure, the magnitude of synaptic transmission was not significantly different from baseline (102 ± 1.3 % of baseline; n = 5; $p > 0.05$).

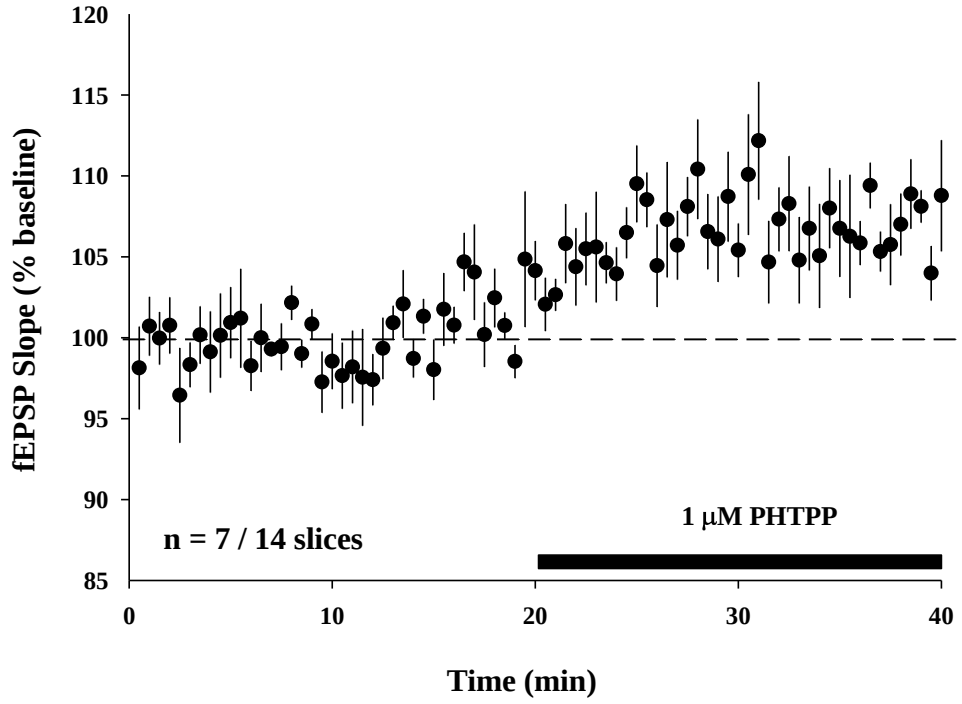

Figure 6.6: The selective ERβ antagonist (PHTPP) can potentiate synaptic transmission in a proportion of slices. Pooled data (n = 7 / 14 slices) illustrating that PHTPP can rapidly potentiate synaptic transmission in a proportion of adult hippocampal slices. Data are normalised with respect to baseline and are expressed as mean ± SEM.

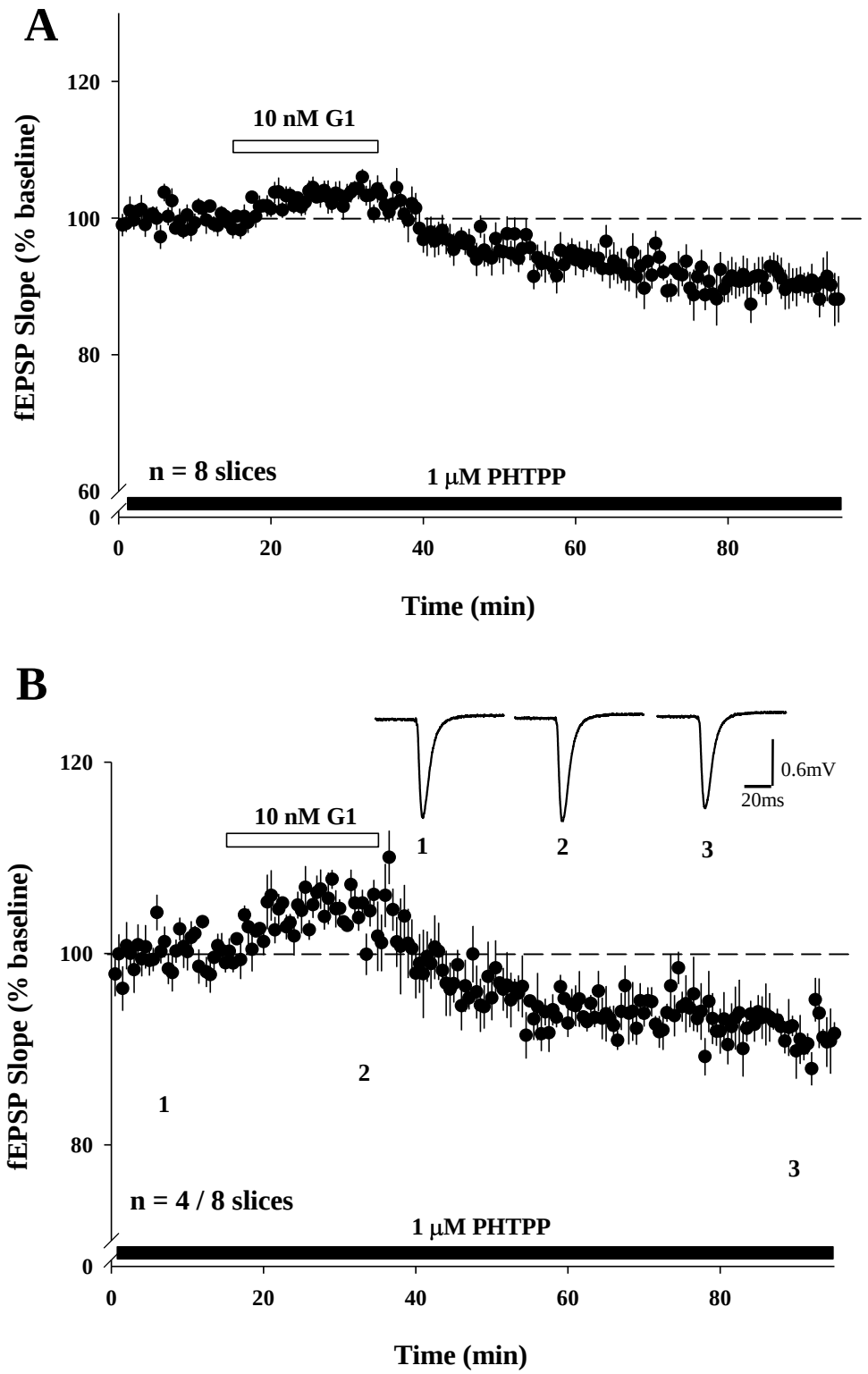
A
120
100
80
60
0
fEPSP Slope (% baseline)
10 nM G1
n = 8 slices
1 μM PHTPP
0
20
40
60
80
Time (min)
B
120
100
80
0
fEPSP Slope (% baseline)
10 nM G1
1
2
3
0.6mV
20ms
n = 4 / 8 slices
1 μM PHTPP
0
20
40
60
80
Time (min)

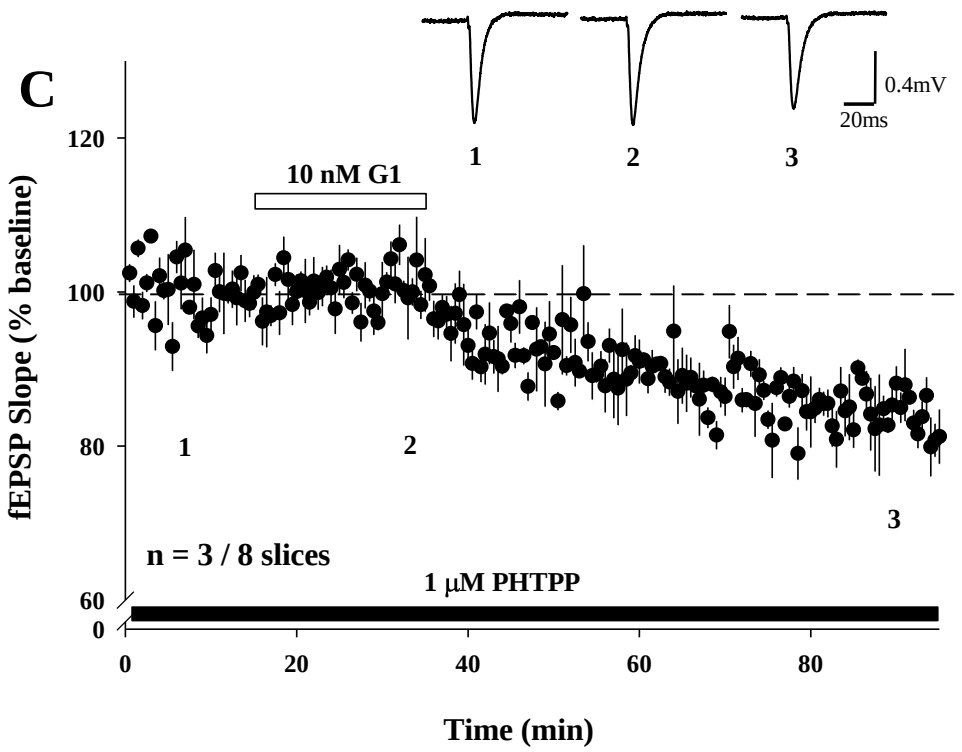
C
0.4mV
20ms
1
2
3
10 nM G1
fEPSP Slope (% baseline)
120
100
80
60
0
1
2
3
n = 3 / 8 slices
1 μM PHTPP
0
20
40
60
80
Time (min)

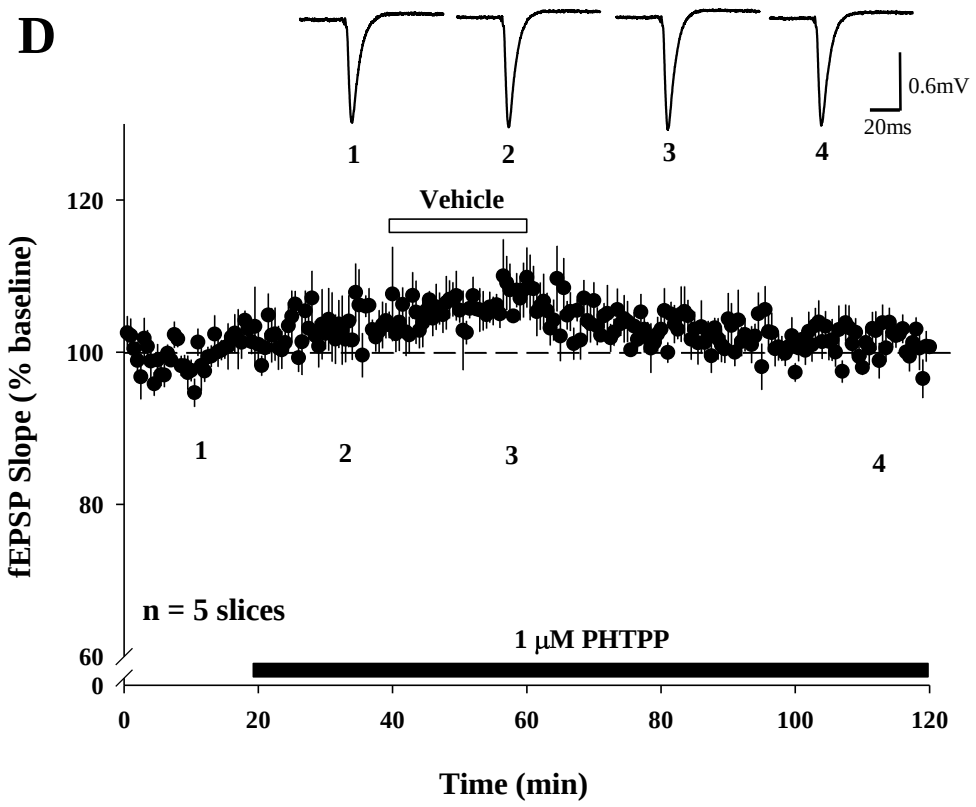
D
0.6mV
20ms
1
2
3
4
Vehicle
fEPSP Slope (% baseline)
120
100
80
60
0
1
2
3
4
n = 5 slices
1 μM PHTPP
0
20
40
60
80
100
120
Time (min)

Figure 6.7: The selective ERβ antagonist, PHTPP does not inhibit the G1-induced effects on basal synaptic transmission in adult male hippocampal slices. ***A,*** Pooled data (n = 8 slices) illustrating that in the presence of PHTPP (1 µM), the G1-induced (10 nM) depression of synaptic transmission is still observed. ***B,*** stratification reveals a bi-phasic response profile of G1 in the presence of PHTPP in 4 out of 8 slices***. C,*** a depression only response is observed in another other 3 (out of 8) slices. ***D,*** pooled data illustrating PHTPP (1 µM) in combination with a vehicle treatment (0.01% DMSO; 20 min; open bar) did not induce a depression of synaptic transmission (n = 5). Example traces from a representative experiment from each data set are shown at the time points indicated. Data are normalised with respect to baseline and are expressed as mean ± SEM.

Despite having an effect on synaptic transmission in a proportion of slices, PHTPP (1 µM; 45 min) did not affect surface GluA1 expression (98 ± 2.2 % of vehicle; $p > 0.05$ vs. vehicle treatment; n = 48; Fig 6.8), moreover PHTPP was unable to block the G1-induced reduction in surface AMPAR expression (G1: 84 ± 1.6 % of vehicle, $p < 0.05$ vs. vehicle; G1 + PHTPP: 80 ± 1.3 % of vehicle, $p < 0.05$ vs. vehicle, $p > 0.05$ vs. G1 alone; n = 48; H = 65.5 with 3 degrees of freedom). Together, these results suggest that a selective ERβ antagonist does not block the G1-induced effects on synaptic transmission and surface GluA1 expression.

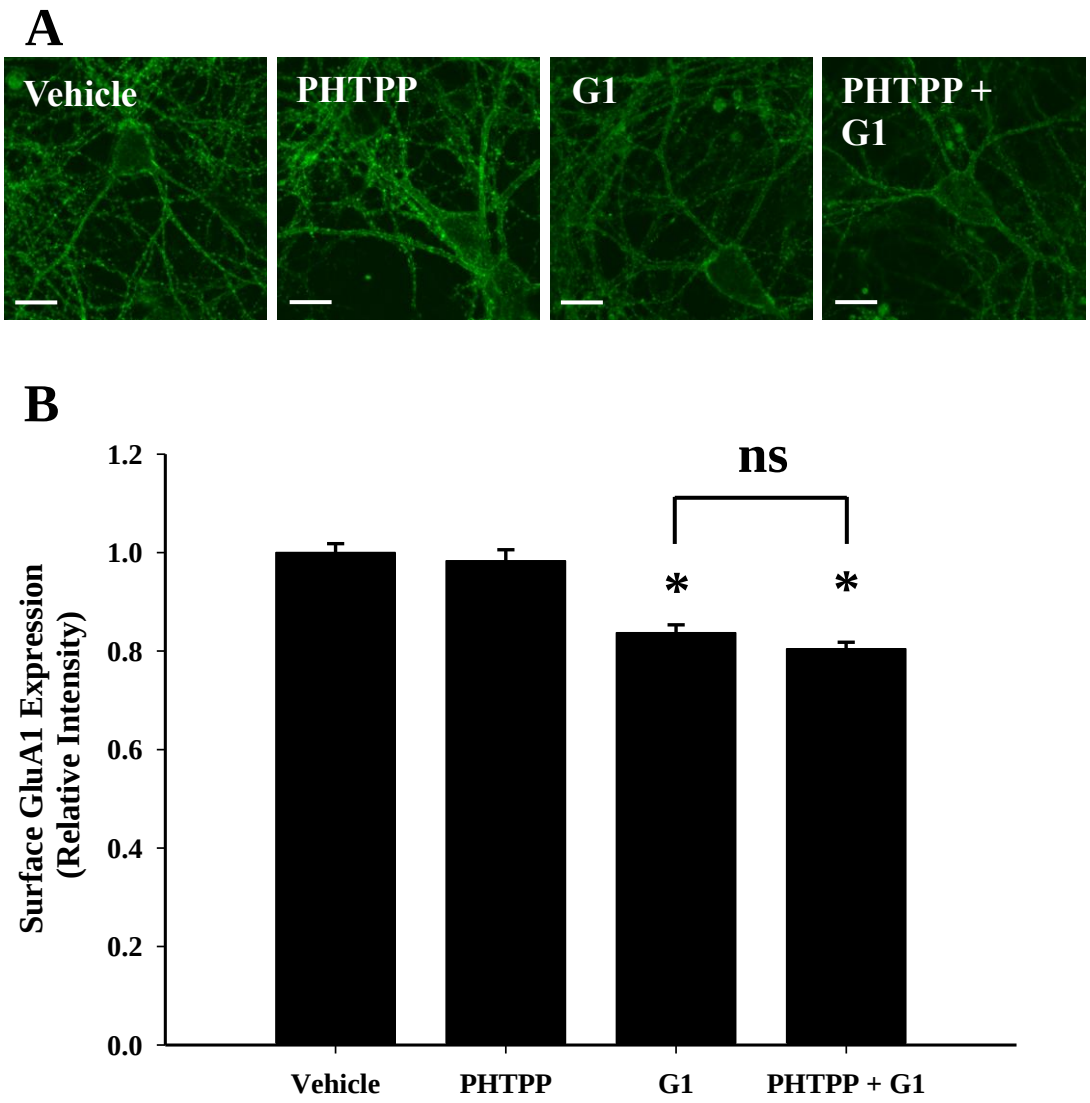

Figure 6.8: PHTPP does not inhibit the G1-induced reduction in surface AMPAR expression. *Neurons were pre-treated with vehicle (0.1 % DMSO) or PHTPP (1 μM; 15 min) and then G1 (10 nM) or vehicle, or in combination with PHTPP (30 min).* ***A,*** representative confocal images of surface GluA1 staining. ***B,*** pooled data showing relative changes in surface GluA1 after exposure to PHTPP alone and in the presence of G1. Scale bars, 20 μm. A Kruskal-Wallis one way ANOVA on Ranks was performed, followed by Dunn's *post-hoc* analysis. * represents $p < 0.05$ vs. vehicle treatment and ns represents $p > 0.05$ between the indicated treatments; n = 48 neurites from 4 individual cultures from different animals.

6.2.4: ICI has no effect on basal synaptic transmission in adult hippocampal slices.

As the selective ER antagonists failed to inhibit the effects of G1, another approach is to establish if another compound capable of selectively activating GPR30, without any known agonist activity at other receptors, can mimic the effects of G1. Previous studies indicate that selective estrogen receptor downregulator (SERD) ICI 182,780 (ICI) can mimic the non-genomic effects of E2 in heterologous and breast cancer cell based-assays (Aronica *et al*., 1994; Filardo *et al.*, 2002; Thomas *et al*., 2005). Moreover, ICI can displace E2 in binding assays for GPR30 (Thomas *et al*., 2005), suggesting that it is a potential GPR30 agonist. In addition, ICI can mimic non-genomic effects of E2 in hippocampal neurons (Zhao *et al*., 2006; Smejkalova and Woolley, 2010). This compound classically acts as a competitive antagonist of the genomic mechanism of action of E2. ICI prevents E2 binding to both intracellular ERα and ERβ, prevents receptor dimerization and nucleo-cytoplasmic shuffling and ultimately increases the degradation of these receptors (Wakeling *et al*., 1991; Dauvois *et al*., 1993; Bemd and Kuiper, 1999).

Therefore, we utilised ICI in order to test whether it would mimic the effects of G1 in our system. However, in adult hippocampal slices, application of ICI (100 nM; 20 min) had no significant effect on basal excitatory synaptic transmission during application, or after a 30min washout period (Fig 6.9 A). Specifically, during ICI application baseline transmission was unchanged (to 101 ± 2.7 % of baseline; n = 4; $p > 0.05$), moreover baseline transmission was unaffected after the 30 min ICI washout (to 104 ± 1.5 % of baseline; n = 4; $p > 0.05$).

In contrast, however, our preliminary data in juvenile hippocampal slices (P16 – P17) illustrates that application of 500 nM ICI can mimic the effects of G1 in low Mg^{2+} aCSF (0.1 mM; Fig 6.9 B). Specifically, in one slice, ICI application rapidly (within 10 min) potentiated synaptic transmission (to > 10 %). However in the other slice ICI had no potentiating effect. Importantly, after ICI washout, a slow onset depression of synaptic transmission was observed in both slices, reaching maximum magnitude approximately 60 min after washout (to 76 ± 2.9 % of baseline; n = 2; Fig 6.9 B). These data suggest that under certain conditions and at specific stages of postnatal development, ICI can induce a persistent depression of excitatory synaptic transmission. However as these data are only preliminary, further examination into the effect of ICI in the juvenile model needs to be conducted.

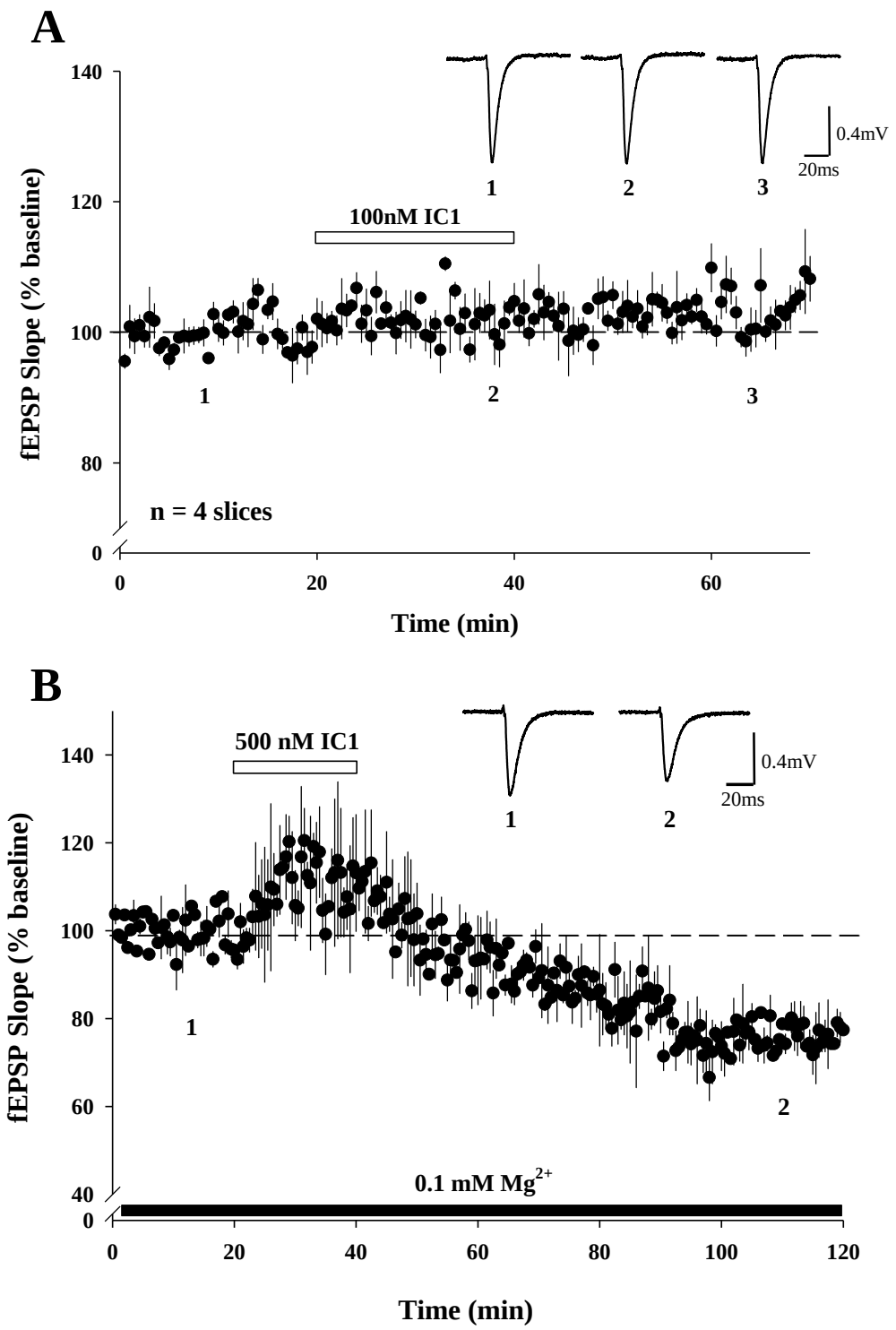

Figure 6.9: ICI 182,780 (ICI) has no effect on baseline transmission in adult slices, however induces a large depression of synaptic transmission in hyper-excitable juvenile slices. ***A,*** Pooled data (n = 4) illustrating no change in baseline transmission or washout after ICI (100 nM; 20 min) exposure in adult slices. ***B,*** Preliminary pooled data (n =2) illustrating that ICI (500 nM; 20min) can induce a significant slow-onset but sustained depression of synaptic transmission in juvenile slices bathed in aCSF containing 0.1 mM Mg^{2+}. Example traces from a representative experiment from each data set are shown at the time points indicated. Data are normalised with respect to baseline and are expressed as mean ± SEM

6.2.5: ICI reduces GluA1 surface expression and can attenuate G1-induced effects in primary hippocampal cultures.

As ICI was unable to mimic the effects of G1 on basal excitatory synaptic transmission in adult hippocampal slices but induced a significant depression in juvenile tissue, we explored the actions of ICI further by evaluating its effects on surface GluA1 staining in primary hippocampal cultures.

Application of ICI (1 µM; 45 min) resulted in a significant reduction in surface GluA1-staining (to 90 ± 1.9 % of vehicle treated neurons; $F[3,143] = 30.1$; $p < 0.01$ vs. vehicle treatment; n = 36; Fig 6.10). Moreover, the magnitude of the G1 induced reduction in surface GluA1 was significantly different from ICI alone (G1: 74 ± 2.4% of vehicle treated neurons; $F[3,143] = 30.1$; $p < 0.001$ vs. vehicle treatment; $p < 0.001$ vs. ICI alone). However, in combination with ICI, the magnitude of the G1 induced reduction of surface GluA1 was significantly attenuated, and this was not significantly different from ICI alone (ICI + G1: 93 ± 2.0 % of vehicle; $F[3,143] = 30.1$; $p < 0.001$ vs. G1 treatment and $p > 0.05$ vs. ICI alone). These data suggest that in this assay, the ICI compound can reduce surface GluA1-trafficking, however not to the same magnitude that which G1 can elicit. Importantly, ICI treatment in combination with G1 can attenuate G1-induced effects in this assay.

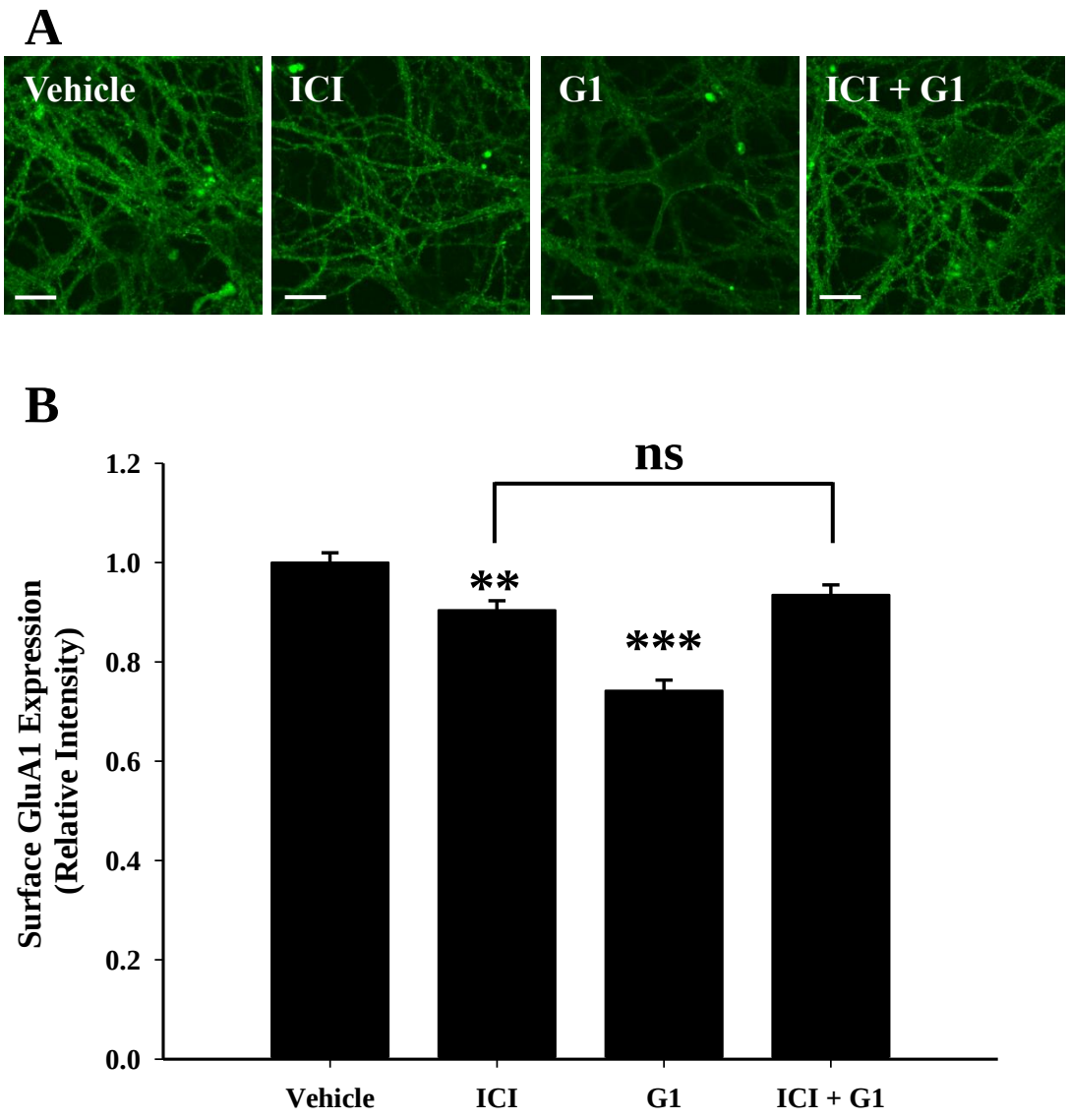

Figure 6.10: ICI can reduce surface AMPAR expression and attenuate the G1-induced effects in primary hippocampal cultures. *Primary cultured hippocampal neurons were pre-treated with vehicle (0.01% DMSO) or ICI (1 µM; 15 min) and then G1 (10 nM) or vehicle, or in combination with ICI (30 min).* ***A,*** representative confocal images of surface GluA1 staining. ***B,*** pooled data showing relative changes in surface GluA1 immunostaining after exposure to ICI, G1 and in combined presence of ICI and G1. Scale bars, 20µm. A one way ANOVA followed by Tukey *post-hoc* analysis was performed. ** and *** represent $p < 0.01$ and $p < 0.001$ vs. vehicle respectively, and ns represents $p > 0.05$ between the indicated treatments; n = 36 neurites from 3 individual cultures from different animals.

6.2.6: ICI can attenuate the magnitude of the G1-induced depression of synaptic transmission.

As exposure to ICI attenuates the effects of G1 in the surface AMPAR expression assay, in the next series of experiments we examined if ICI also attenuated effects of G1 in adult hippocampal slices. Thus, ICI (1 μM) was applied to adult hippocampal slices 20 min before co-application with G1 (10 nM). Application of ICI had no effect on basal synaptic transmission (100 ± 1.0 %; n = 6; $p > 0.05$, Fig 6.11 A). However in slices exposed to ICI, the magnitude of the G1-induced LTD was significantly attenuated (from 87 ± 2.4% of baseline in G1 treated slices, $F[2,17] = 19.2$; $p < 0.01$ vs. baseline; n = 6; to 96 ± 3.0 % of baseline in ICI treated slices, $p > 0.05$ vs. baseline; $F[6,41] = 7.2$; $p < 0.05$ vs. G1 treated; Fig 6.11 B). Moreover, an extended application of ICI 182,780 (1 μM; 100 min) had no significant effect on basal synaptic transmission ($p > 0.05$; n = 4; Fig 6.11 C)

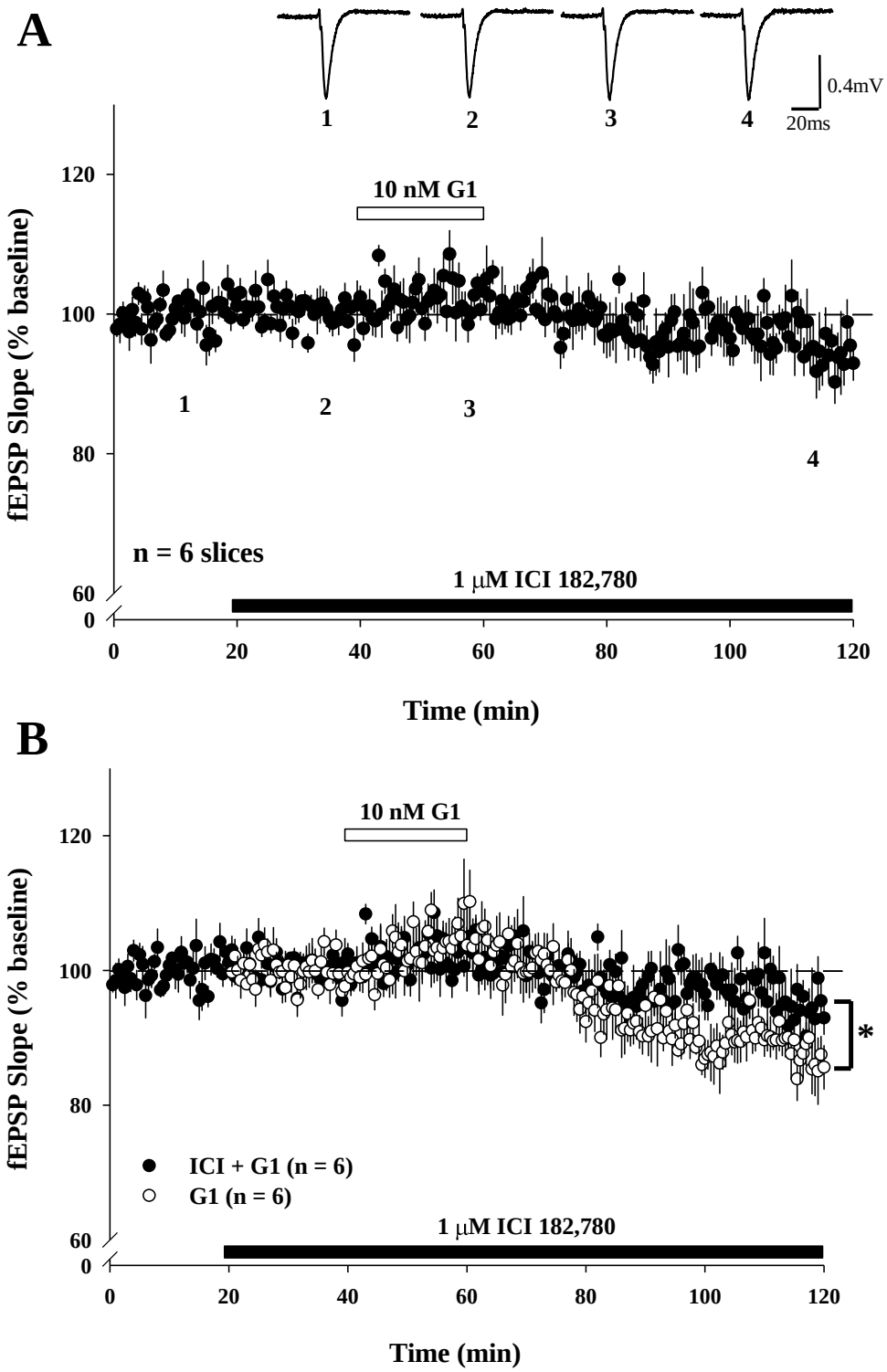
A
0.4mV
20ms
1
2
3
4
10 nM G1
fEPSP Slope (% baseline)
120
100
80
60
0
n = 6 slices
1 μM ICI 182,780
0
20
40
60
80
100
120
Time (min)
B
10 nM G1
fEPSP Slope (% baseline)
120
100
80
60
0
*
ICI + G1 (n = 6)
G1 (n = 6)
1 μM ICI 182,780
0
20
40
60
80
100
120
Time (min)

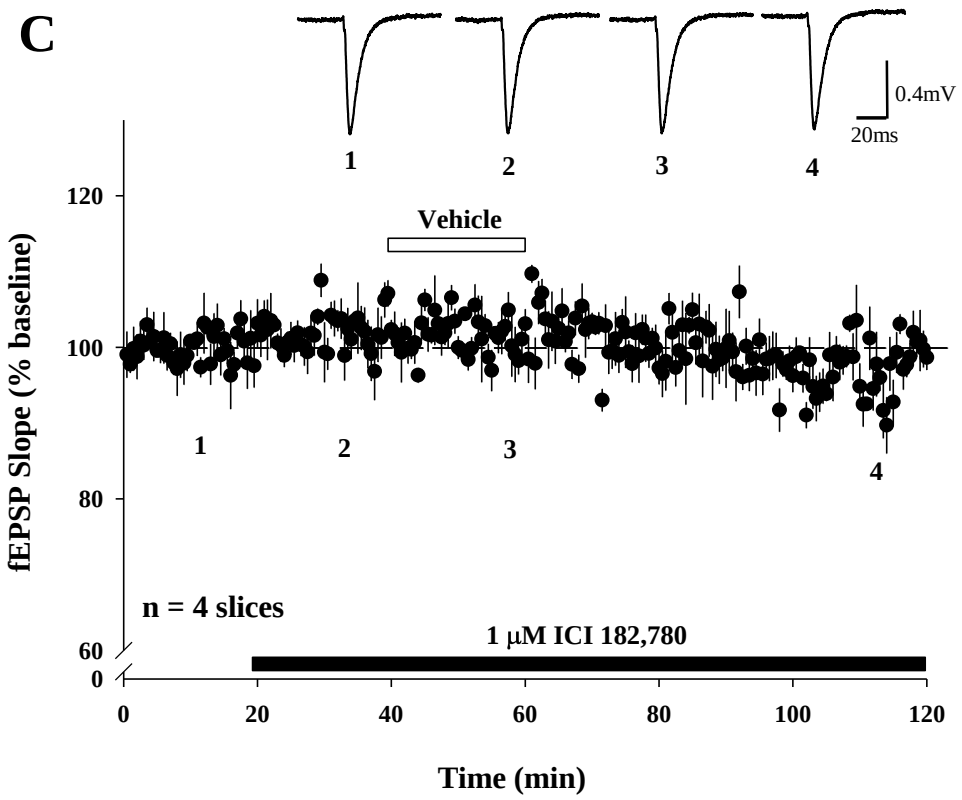

Figure 6.11: ICI attenuates the G1-induced LTD in adult hippocampal slices. ***A,*** Pooled data (n = 6 slices) illustrating that in the presence of ICI (1 μM), the magnitude of LTD induced by G1 (10 nM) is attenuated. ***B,*** Pooled data illustrating that there is a significant difference between the magnitude of LTD induced by G1 slices (n =5) and with G1 in combination with ICI (n = 6). ***C,*** Pooled data illustrating that an extended application of ICI (1 μM; n = 5 slices) in combination with vehicle treatment (0.01 % DMSO; 20 min; open bar) does not cause a significant depression of synaptic transmission. Example traces from a representative experiment from each data set are shown at the time points indicated. Data are normalised with respect to baseline and are expressed as mean ± SEM.

6.2.7: Selective ER antagonists do not inhibit the G1-induced LTD or reduction of surface AMPAR expression.

Although G1-induced effects were not inhibited by individual application of either ER antagonists, it is feasible that the observed effects of G1 are due to the activation of both ERα or ERβ, rather than GPR30. In order to explore this possibility, the effects of PHTPP and MPP in combination were examined. In these studies a combination of PHTPP (1 µM) and MPP (1µM) were applied to adult hippocampal slices 20 min prior to G1 (10 nM; 20 min) application. Considering the variable effects of PHTPP on baseline transmission (Fig 6.6 and Fig 6.7 C), data were normalised to the mean values of fEPSP slope measurements 15 min prior to G1 application.

Out of the 6 slices that were treated in these conditions, only one slice elicited a bi-phasic response profile in response to G1, however a significant G1-induced reduction in synaptic transmission was observed in all 6 slices (to 89 ± 4.2 %; $F[2,17] = 7.8$; $p < 0.05$; n = 6; Fig 6.12 A). Moreover, the magnitude of this effect was not-significantly different from control slices treated with G1 alone (88 ± 2.8 %; $F[2,14] = 39.4$; $p < 0.05$ vs. baseline; $p > 0.05$ vs. PHTPP + MPP + G1; n = 5; Fig 6.12 B). It should be worth noting that a G1-induced transient increase in synaptic transmission was observed in 4 of the 5 control slices. Considering the variable nature of the G1-induced transient increase in synaptic transmission and considering that G1-induced biphasic effects were observed when the antagonists were administered alone (Fig 6.7 A/B and Fig 6.4 A/B), it is likely that a combination of the antagonists does not block the G1-induced transient increase.

In immunocytochemistry studies in hippocampal cultures, a combination of MPP and PHTPP (1 µM for each; 45 min) had no effect on the relative intensity of surface GluA1-staining (to 98 ± 1.9 % of vehicle; $p > 0.05$ vs. vehicle treatment; n = 36). Furthermore, the ability of G1 to reduce surface GluA1 expression was unaffected by ERα and ERβ inhibition, as the relative intensity of surface GluA1-staining was not significantly different between neurons treated with G1 and those treated with G1 in combination with the two antagonists (G1: 82 ± 1.8 % of vehicle; $p < 0.05$ vs. vehicle; MPP + PHTPP + G1: 74 ± 2.2 % of vehicle; $p < 0.05$ vs. vehicle; $p > 0.05$ vs. G1 alone; n = 36; H = 71.0 with 3 degrees of freedom; Fig 6.13). Thus these data indicate that the G1-induced LTD and decrease in surface AMPAR expression are not attenuated when in the presence of a combination of ER antagonists.

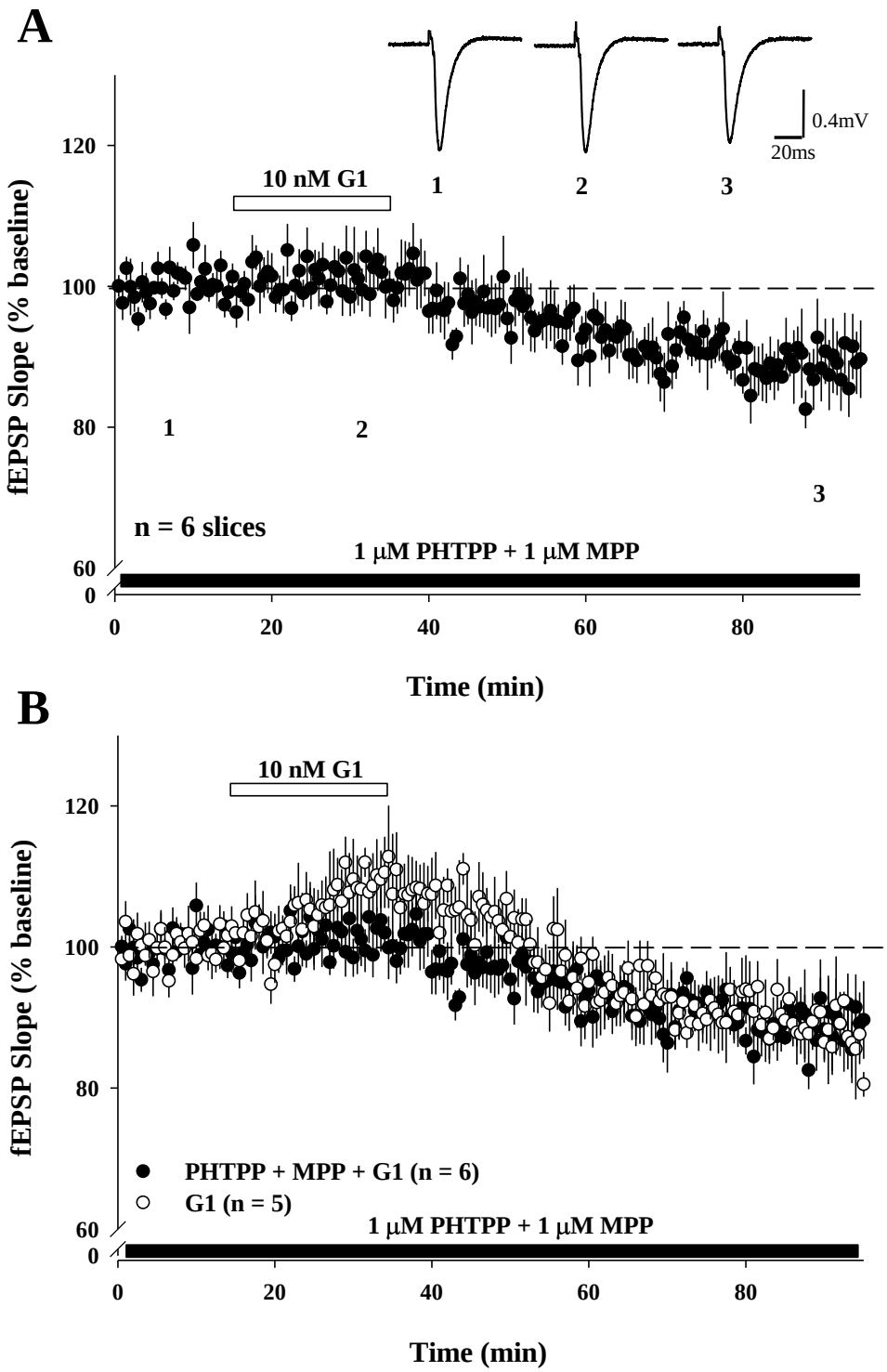

Figure 6.12: A combination of PHTPP and MPP does not block the G1-induced effects on basal synaptic transmission in adult hippocampal slices. ***A,*** Pooled data (n = 6 slices) illustrating that in the presence of MPP and PHTPP (1 μM), application of G1 (10 nM) induces LTD. .***B,*** Pooled data illustrating that there is no difference in the magnitude of the synaptic depression induced by G1 (n =5) and slices treated with G1 in combination with the antagonists. Example traces from a representative experiment are shown at the time points indicated. Data are normalised with respect to baseline (as indicated in text) and are expressed as mean ± SEM.

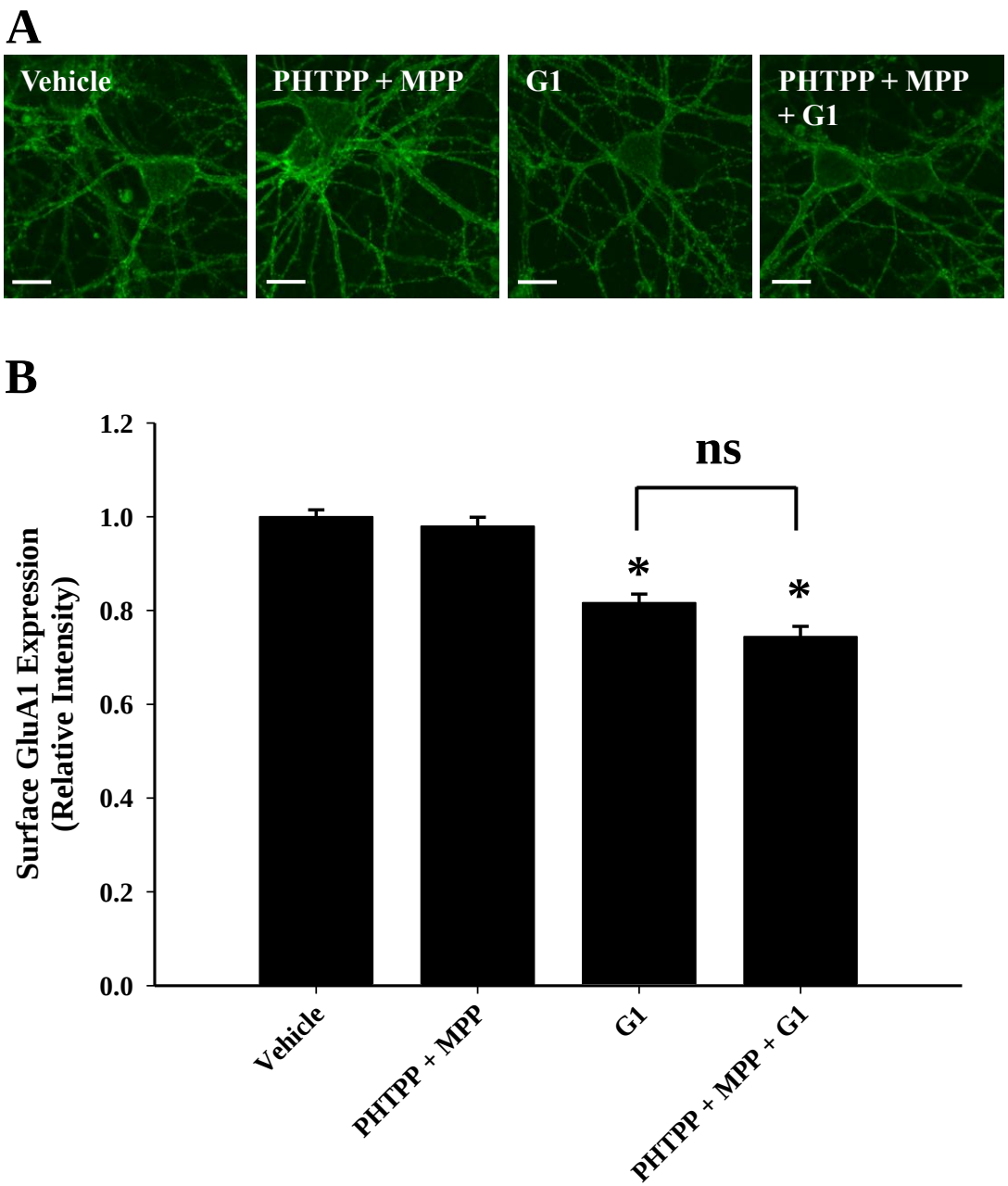

Figure 6.13: A combination of PHTPP and MPP fails to inhibit the G1-induced effects on surface GluA1-staining. *Div 8 – 16 cultured hippocampal neurons were pre-treated with vehicle (0.1% DMSO) or PHTPP and MPP in combination (1 µM; 15 min) and then G1 (10 nM) or vehicle, or in combination with the antagonists (30 min).* ***A,*** representative confocal images of surface GluA1 staining. ***B,*** pooled data showing relative changes in surface GluA1 after exposure to the combination of antagonists, G1 alone and G1 in the presence of both antagonists. Scale bars, 20 µm. A Kruskal-Wallis one way ANOVA on Ranks was performed, followed by Dunn's *post-hoc* analysis. * represents $p < 0.05$ vs. vehicle treatment and ns represents $p > 0.05$ between the indicated treatments; n = 36 neurites from 3 individual cultures from different animals.

6.2.8: siRNA against rGPR30 does not affect GPR30 staining in primary hippocampal cultures

Considering the interesting pharmacology of our G1-induced effects, it was worth establishing whether selective knockdown of GPR30 expression in hippocampal cultures would abolish the G1- or E2-induced effects on surface GluA1 staining. It is known that delivery of genetic material into post-mitotic cells is notoriously difficult (Karra and Dahm, 2010). The use of cationic-lipid based transfection reagents (such as DharmaFECT), although reliable in easy to transfect cell lines (such as HEK-293 cells), often has low efficiency in neurons. As a positive control, we confirmed protein knockdown of hGPR55 in hGPR55-HEK-293 cells using Dharmafect 1 and SMARTpool siRNA (see section 2.2.2.3 of methods). Thus, in order to establish whether efficient protein knockdown in primary hippocampal neurons could be achieved using this protocol, we transfected DIV 5 neurons for 48, 72 or 96 hours with siRNA against rGria-1, the gene for which encodes rat GluA1.

Using immunofluorescence, preliminary results suggest that significant knockdown of GluA1 expression could be achieved in primary hippocampal neurons after 72 and 96 hours of siRNA treatment (Fig 6.14). Specifically, 46 hours of siRNA treatment reduced relative total GluA1 expression to 84 ± 5.5 % of total GluA1 expression in control neurons, however this reduction was not significant ($p > 0.05$ vs. untreated; n = 20 cells;). After 72 and 96 hours of siRNA treatment, relative total GluA1 expression was significantly reduced to 66 ± 10 % and 73 ± 6.9 % of control levels, respectively ($p < 0.05$ vs. untreated; n = 20 cells; H = 25.2 with 5 degrees of freedom). It is worth noting that after 96 hours in siRNA, the viability of some neurons became impaired.

Considering we were able to achieve a significant knockdown of GluA1 expression, an attempt was made to knockdown GPR30 protein expression. DIV 5 hippocampal cultures were treated with rGPR30 siRNA, hGPR55 siRNA or were left untreated for 46, 72 or 96 hours. hGPR55 siRNA was utilised as a negative control. Relative GPR30 expression was examined using the GPR30 antibody previously described in Chapter 3 (see figures 3.5 and 3.6), and quantified as relative corrected fluorescence intensity (see section 2.2.5.3 of methods). Fig 6.15 illustrates that relative fluorescence intensity of GPR30 staining in primary hippocampal cultures is not significantly altered after 46, 72 or 96 hours of siRNA treatment when compared with untreated neurons, suggesting that

GPR30 staining is unaffected in primary hippocampal neurons after treatment with siRNA against rGPR30.

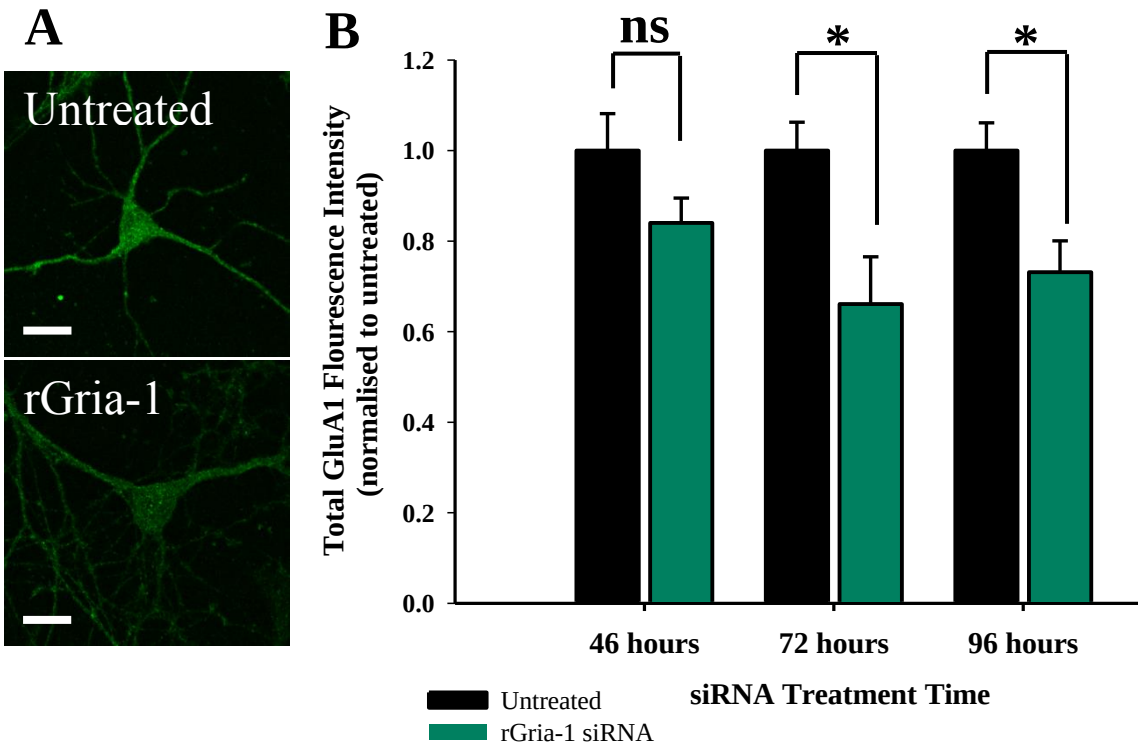

Figure 6.14: siRNA against rGria-1 reduces total GluA1 expression in primary rat hippocampal cultures. *Relative total GluA1 expression after DIV 5 hippocampal cultures were treated with rGria-1 siRNA for 46, 72 or 96 hours, or left untreated for the indicated times.* ***A,*** representative confocal images of total GluA1 staining after 72 hours siRNA treatment. ***B,*** pooled data illustrating relative total GluA1 expression after siRNA treatment for the indicated time periods. A Kruskal-Wallis one way ANOVA on Ranks was performed followed by Dunn's *post-hoc* analysis. n = 20 cells from two individual cultures from different animals. * represents $p < 0.05$ between the indicated groups and ns represents $p > 0.05$ between the indicated groups. Scale bars, 20µm.

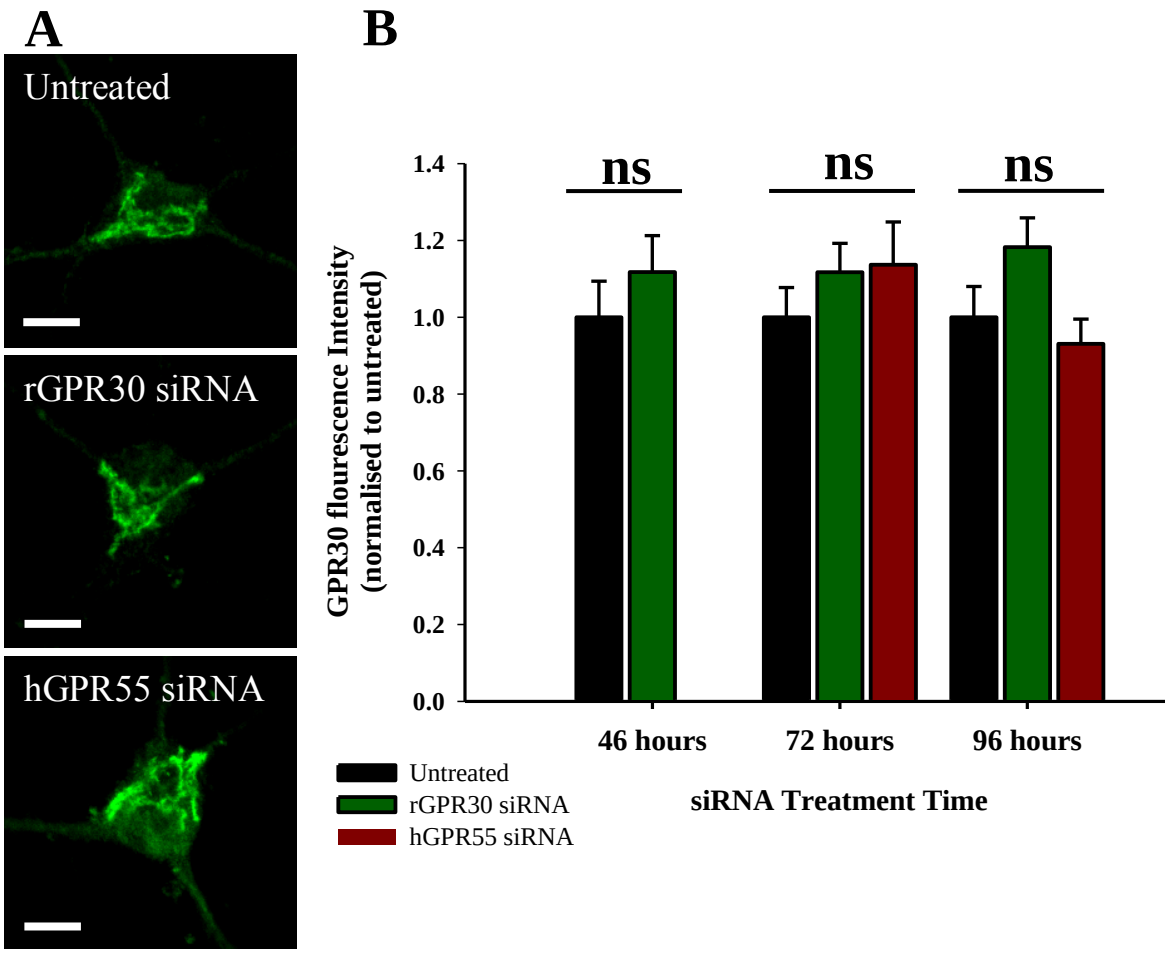

Figure 6.15: siRNA against rGPR30 does not alter relative levels of GPR30 staining in primary rat hippocampal cultures. *Relative GPR30 fluorescence intensity expression after DIV 5 hippocampal cultures were treated with rGPR30 or hGPR55 siRNA for 46, 72 or 96 hours, or left untreated for the indicated times.* ***A,*** representative confocal images of GPR30 staining after 72 hours siRNA treatment. ***B,*** pooled data illustrating relative GPR30 immunofluorescence after siRNA treatment for the indicated time periods. A one way ANOVA was performed. n = 20 cells from two individual cultures from different animals. ns represents $p > 0.05$, a non-significant ANOVA. Scale bars, 10µm.

6.2.9: siRNA against rGPR30 does not inhibit the E2- or G1 –induced reduction of surface AMPAR expression in primary hippocampal cultures

As alluded to in Chapter 3, there is the possibility that the antibody used here may not be recognising functional GPR30, and without confirmation of gene knockdown by quantification of mRNA expression, we cannot conclusively rule out the possibility that expression of GPR30 is attenuated after siRNA treatment. Moreover, others have established that functional effects of E2 and G1 can be mitigated by GPR30 gene silencing in primary cultures of developing rat hippocampal neurons (Ruiz-Palmero *et al*., 2013) and mature cortical neurons (Liu *et al*., 2012).

Therefore we tested whether siRNA treatment (72 hours) against GPR30 could attenuate the effects of E2 and G1, using the surface AMPAR expression assay (Fig 6.16). In this set of experiments, surface GluA1 staining was normalised to vehicle (0.01 % DMSO) treated neurons which were not subjected to siRNA treatment. Treatment with hGPR55 siRNA was utilised as a negative control.

As shown previously, E2 and G1 (10 nM; 30 min) significantly reduced surface GluA1 expression in neurons which were not treated with siRNA (to 85 ± 1.9 % and 80 ± 2.4 % of vehicle, respectively; $p < 0.05$ vs. vehicle treated neurons not subjected to siRNA treatment; n = 36; H = 84.6 with 8 degrees of freedom). Relative surface GluA1 staining of vehicle controls was not significantly altered in neurons subjected to either rGPR30 or hGPR55 siRNA (to 94 ± 1.7 % and 99 ± 2.3 % of untreated vehicle, respectively; $p > 0.05$ vs. vehicle treated neurons not subjected to siRNA treatment; n = 36), suggesting that treating cultures with siRNA does not compromise surface GluA1-expression. In cultures subjected to rGPR30 siRNA, E2 and G1 treatment still significantly reduced surface GluA1 staining in neurons (to 80 ± 2.3 % and 80 ± 2.0 % of untreated vehicle, respectively; H = 84.6 with 8 degrees of freedom; $p < 0.05$ vs. rGPR30 siRNA treated vehicle controls; n = 36). Moreover, there was no significant difference in the magnitudes of the E2- or G1-induced reduction of surface GluA1 expression between neurons which were treated with siRNA against rGPR30 or hGPR55 or neurons which were left untreated ($p > 0.05$).

Therefore, these results demonstrate that the effects of E2 and G1 on surface AMPAR expression could not be mitigated in neurons which were treated with siRNA against rGPR30.

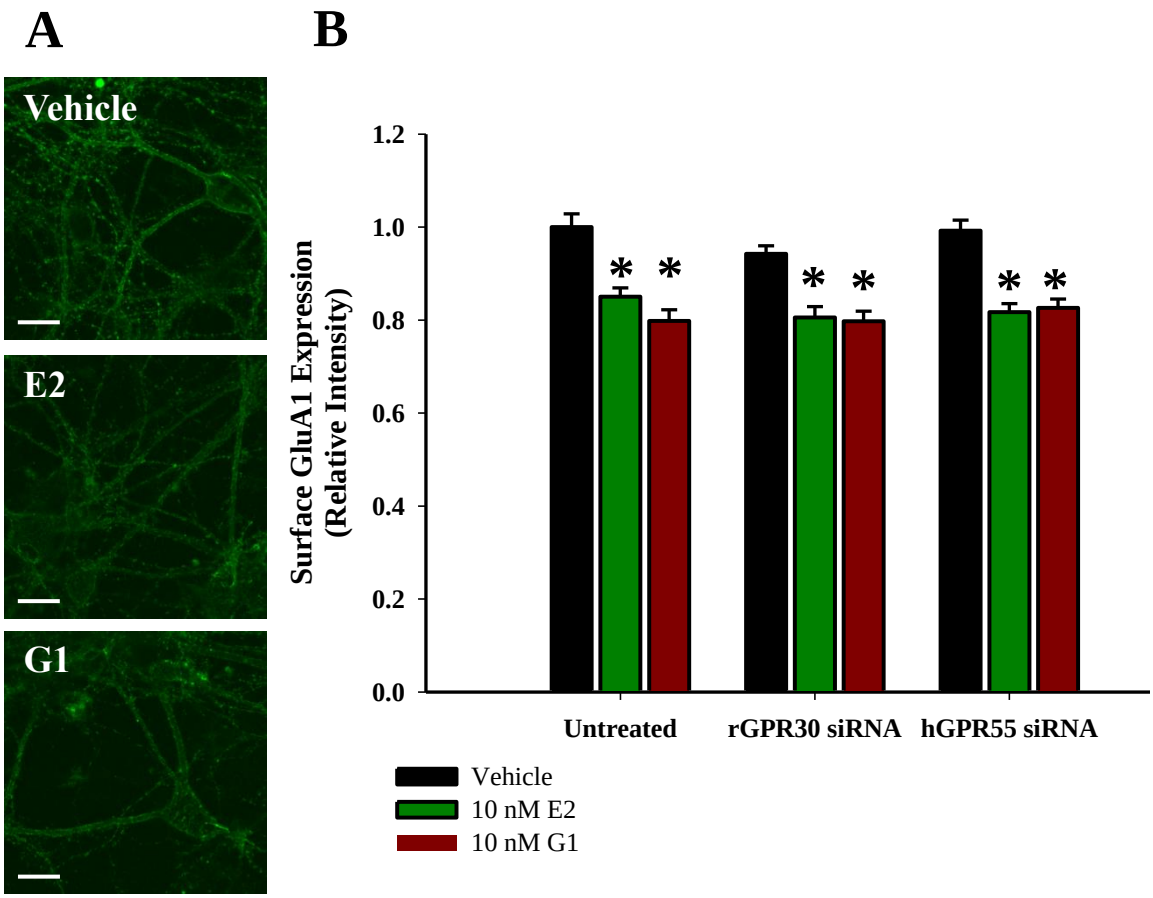

Figure 6.16: siRNA against rGPR30 does not inhibit the ability of E2 or G1 to reduce surface GluA1-expression. *Relative surface GluA1 expression after DIV 5 - 6 hippocampal cultures were treated with rGPR30 or hGPR55 siRNA, or left untreated for 72 hours.* ***A,*** representative confocal images of surface GluA1 staining after 72 hours GPR30 siRNA exposure illustrating a reduction in surface GluA1 expression after E2 or G1 (10 nM) treatment (30 min) . ***B****,* pooled data illustrating relative surface GluA1 expression after ligand treatment in hippocampal cultures treated with siRNA against rGPR30. A Kruskal-Wallis one way ANOVA on Ranks was performed followed by Dunn's *post-hoc* analysis. n = 36 neurites from two individual cultures from different animals. * represents $p < 0.05$ vs. respective vehicle treatment. Scale bars, 20µm.

6.2.10: G1-induced effects are likely to be mediated via the MAPK signalling pathway.

Early evidence from breast cancer cell lines suggested that E2-induced activation of GPR30 can stimulate ERK1/2 signalling via a mechanism involving transactivation of EGFR (Filardo *et al*., 2000, 2002; Maggiolini *et al*., 2004). Moreover, it is known that acute effects of E2 on hippocampal synaptic architecture are mediated via ERK 1/2 signalling (Mukai *et al*., 2007; Srivastava *et al*., 2008; Zadran *et al*., 2009). In addition, in cortical neurons, G1 mediated depression of NMDA induced currents and inhibition of NR2B phosphorylation is sensitive to MEK inhibition (Liu *et al*., 2012). In view of this evidence, we utilised the MEK inhibitor PD 98059 (25 μM), to determine whether G1-induced LTD involves ERK1/2 signalling. It is worth noting here that PD 98059 inhibits ERK 1/2 signalling by preventing activation of MEK by upstream kinases (Dudley *et al*., 1995; Davies *et al.*, 2000).

It was observed (post-hoc) that basal synaptic transmission was transiently altered during bath administration of PD 98059 (25 μM; 100 min; Fig 6.17 A; n = 3). Though, after 100 min PD 98059 exposure, synaptic transmission was not significantly different from baseline (to 96 ± 2.5 % of baseline; $p > 0.05$; n = 3). Although application of this compound has previously been shown to have no effect on CA3 – CA1 basal excitatory synaptic transmission (English and Sweatt, 1997) on close examination of their published data it would appear that there is an effect of PD 98059 similar to the effect observed here.

Importantly, the ability for G1 (10 nM; 20 min) to induce a depression of synaptic transmission was inhibited when co-applied with PD 98059 (25 μM; Fig 6.18 A). Specifically, by the end of G1 washout (100 min; in the presence of PD 98059) the mean magnitude of synaptic transmission was above but not significantly different from baseline (106 ± 6.4 % of baseline; $p > 0.05$; n = 6). Moreover, there was no significant difference in the mean magnitude of synaptic transmission between the PD 98059 control slices and the slices treated with PD 98059 and G1 ($p > 0.05$) at the conclusion of the experiments. In control slices treated with G1 (10 nM; 20 min) alone, a bi-phasic profile was exhibited in 2 of the 5 slices, and in 3 of the 5 slices a depression only profile was observed. For clarity, all 5 slices were pooled (Fig 6.18 B), and a significant depression of synaptic transmission was observed after 60 min washout of G1 (to 89 ± 2.5 % of baseline; $F[2,14] = 12.1$; $p < 0.05$; n = 5). In combination with a MEK

inhibitor, it would appear that the ability of G1 to induce a depression of synaptic transmission may be blocked. However, due to the large between slice variability in the magnitude of the fEPSP responses during the washout phase in these conditions and the small number of replicates in the extended MEK inhibitor only controls, a conclusive statement regarding whether the G1-induced LTD involves ERK1/2 activation cannot be made, and further investigation is require.

In parallel immunocytochemistry studies, the G1-induced reduction in surface GluA1 staining was blocked by both of the two structurally diverse inhibitors PD 98059 (25 µM) and U0126 (5 µM). Neither of the MEK inhibitors had any significant effect on surface GluA1 expression (PD 98059: 97 ± 1.8 % of vehicle, n = 48; $p > 0.05$ vs. vehicle treatment; U0126: 97 ± 2.1 % of vehicle; n = 36; $p > 0.05$ vs. vehicle treatment). Moreover, there was no significant difference between the PD and U0126 compounds alone and in combination with G1 (97 ± 1.6 % of vehicle, n = 48, and 96 ± 2.2 % of vehicle, n = 36, respectively, $p > 0.05$ vs. PD or U0126 alone, $F[5,335] = 20.9$; $p < 0.05$ vs. G1 alone). Further supporting the evidence that MEK signalling is involved in the G1-mediated effects on surface GluA-1 expression, co-administration of the inactive analogue for U0126 (U0124; 5 µM), did not affect the ability of G1 (10 nM) to reduce surface AMPAR expression (to 86 ± 3.0 % of U0124 alone, n = 36, H = 10.9 with 1 degree of freedom; $p < 0.05$; Fig 6.20).

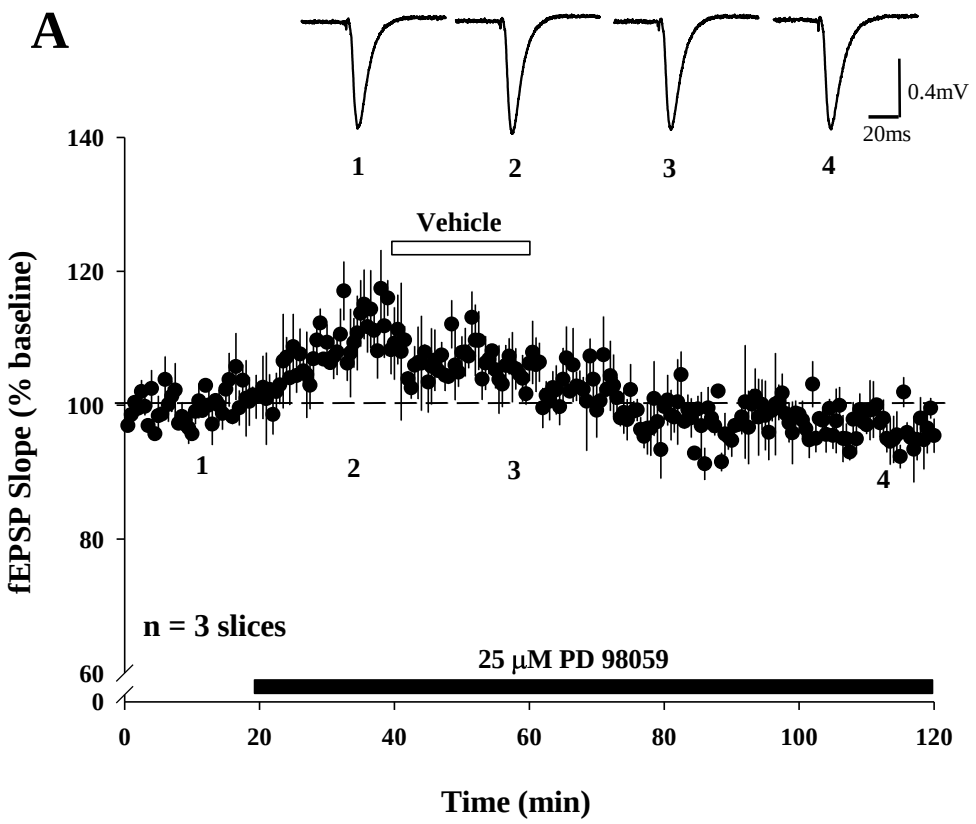

Figure 6.17: The MEK inhibitor PD 98059 has a variable effect on synaptic transmission. ***A,*** Pooled data (n = 3 slices) illustrating that an extended application of PD 98059 (25 μM) can firstly rapidly potentiate synaptic transmission followed by a reduction in synaptic transmission in adult hippocampal slices. Example traces from a representative experiment are shown at the time points indicated. Data are normalised with respect to baseline and are expressed as mean ± SEM.

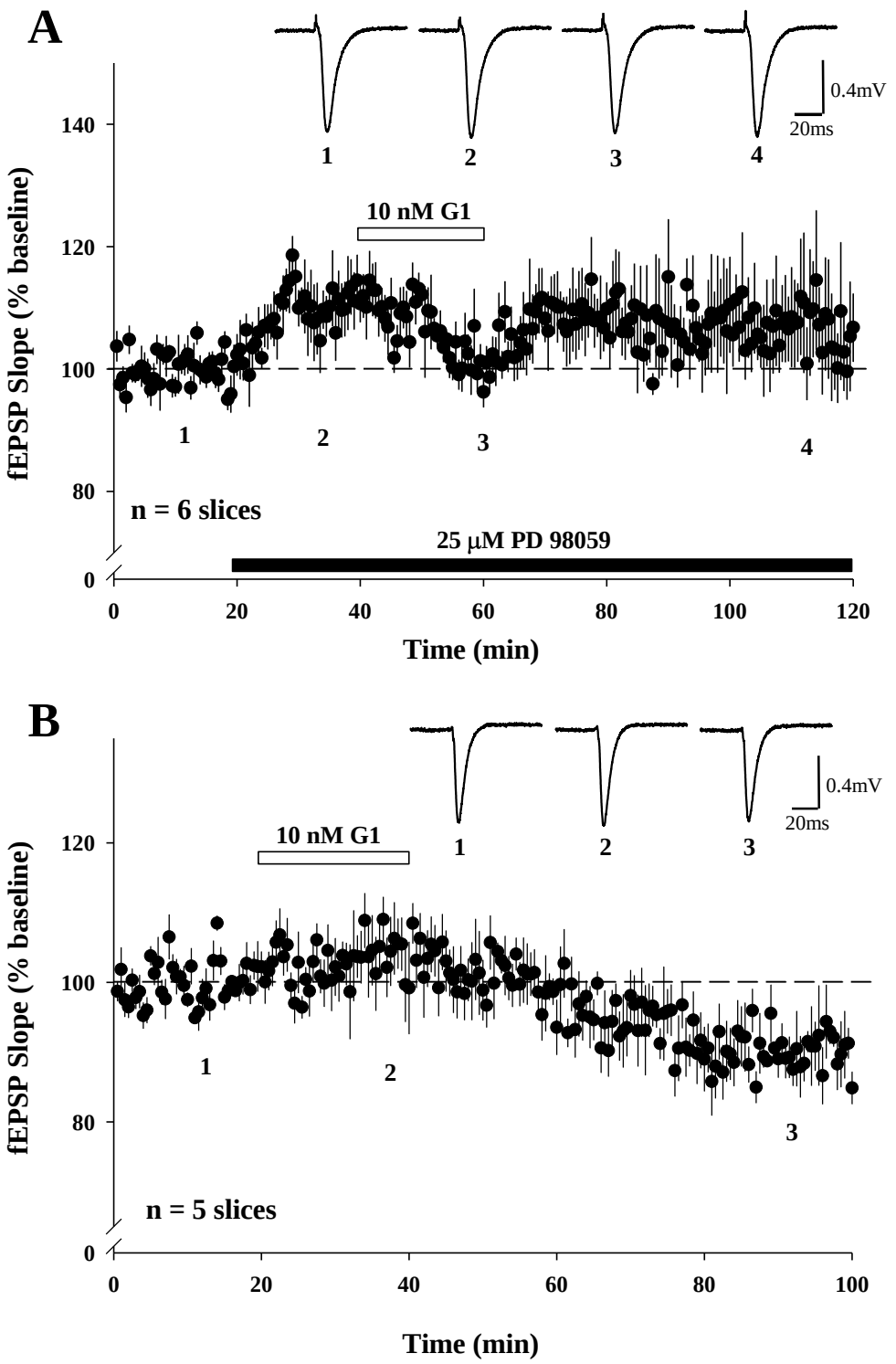

Figure 6.18: PD 98059 blocks the G1-induced depression of synaptic transmission. ***A,*** Pooled data (n = 6 slices) illustrating that in the presence of PD98059 (25 μM), a depression of synaptic transmission is not observed following G1 (10 nM) washout. ***B,*** Pooled data from control slices (n =5) illustrating a G1-induced depression. Example traces from a representative experiment are shown at the time points indicated. Data are normalised with respect to baseline and are expressed as mean ± SEM.

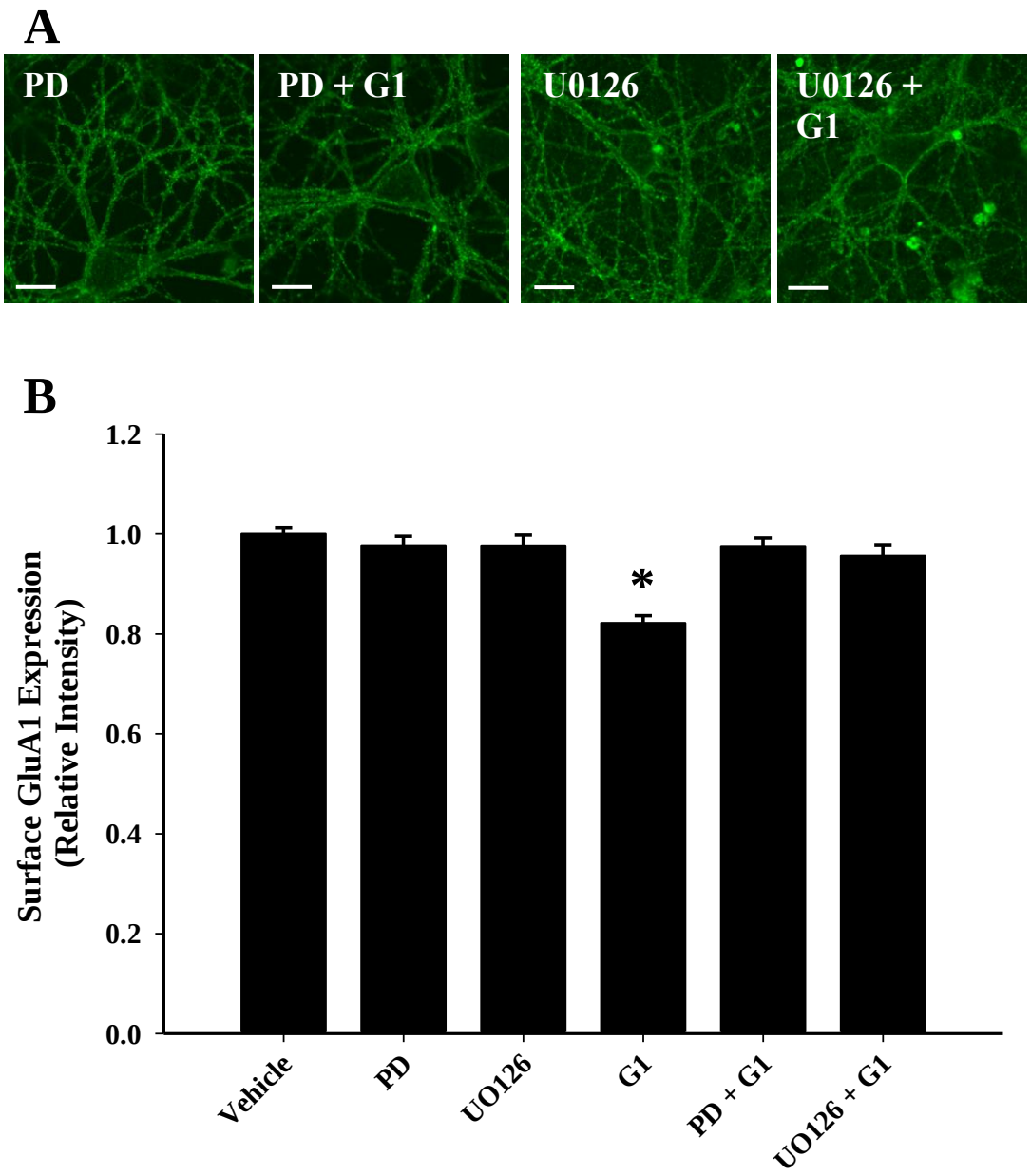

Figure 6.19: Inhibitors of the MEK signalling pathway block the G1-induced reduction in surface AMPAR expression. *Div 8 – 16 cultured hippocampal neurons were pre-treated with vehicle (0.1% DMSO), PD 98059 (25 µM) or U0126 (5 µM) for 30 min and then G1 (10 nM) or vehicle, or in combination with inhibitors (30 min).* ***A,*** representative confocal images of surface GluA1 staining. ***B,*** pooled data showing relative changes in surface GluA1 after exposure to the MEK inhibitors alone and in the presence of G1. Scale bars, 20 µm. A one way ANOVA was performed, followed by Tukey *post-hoc* analysis. * represents $p < 0.05$ vs. vehicle treatment; n = 36 neurites from 3 individual cultures from different animals.

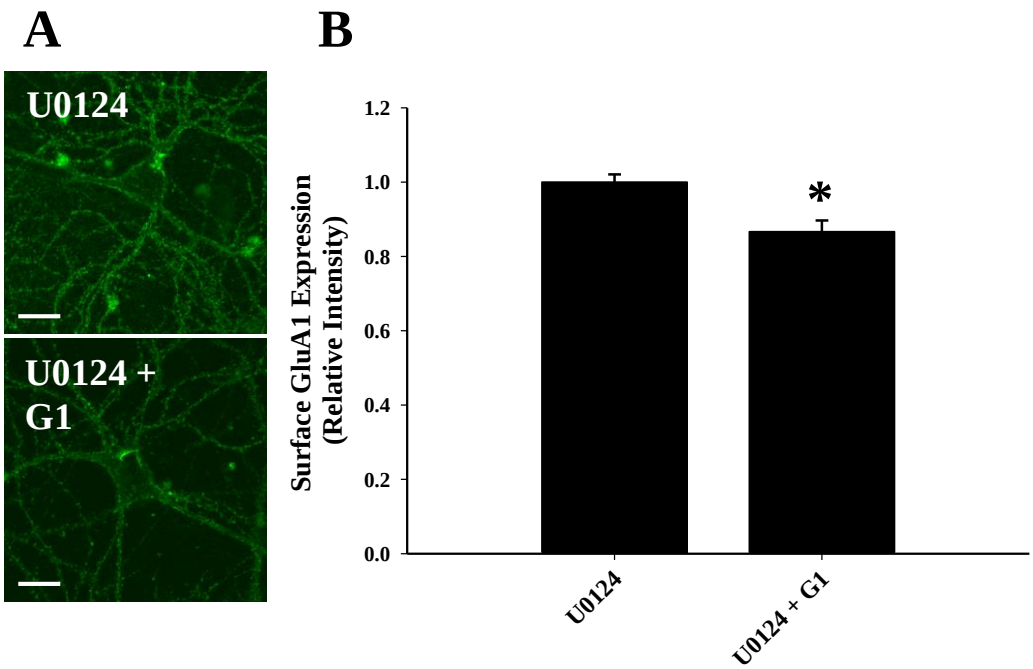

Figure 6.20: An inactive analogue for U0126 does not inhibit the G1-induced reduction in surface AMPAR expression. *Div 8 – 16 cultured hippocampal neurons were pre-treated with U0124 (5 µM) for 30 min and then G1 (10 nM) in combination with U0124 (30 min).* ***A,*** representative confocal images of surface GluA1 staining. ***B,*** pooled data showing relative changes in surface GluA1 after exposure to U0124 alone or in the presence of G1. Scale bars, 20 µm. A Kruskal-Wallis one way ANOVA on Ranks was performed, followed by Dunn's *post-hoc* analysis. * represents $p < 0.05$ vs. U0124 treatment; n = 36 neurites from 3 individual cultures from different animals.

6.2.11: An inhibitor of PI3K activity does not block the G1-induced effects on surface AMPAR expression

In breast cancer cell lines, GPR30 activation can increase PIP_3 accumulation via PI3K activity (Revankar *et al*., 2005). Activation of the PI3K/Akt pathway is also thought to mediate GPR30-induced neuroprotection in immortalised hippocampal cell lines (Gingerich *et al*., 2010) and neuritogenesis in primary hippocampal cultures (Ruiz-Palmero *et al*., 2013). Moreover, activation of PI3K/Akt signalling cascade is implicated in various forms of hippocampal LTD, for example inhibitors of PI3K signalling attenuates NMDAR dependent HFS-LTD in juvenile rodents (Daw *et al*., 2002), DHPG-induced LTD in adult mice (Hou and Klann, 2004) and insulin-induced LTD in juvenile rodents (van der Heide *et al*., 2005). Moreover, genetic deletion of PI3Kγ impairs NMDAR mediated LTD in juvenile mice (Kim *et al*., 2011). Therefore, it is feasible that PI3K signalling plays a role in the G1-induced effects on AMPAR trafficking. In order to examine the potential role of PI3K signalling, wortmannin, a metabolite found in fungal species, was utilised to inhibit PI3K activity (Arcaro and Wymann, 1993; Powis *et al*., 1994).

Application of wortmannin (50 nM; Fig 6.21) to hippocampal cultures caused a small but non-significant increase in surface GluA1-staining (to 109 ± 4.0 % of vehicle; $p > 0.05$ vs. vehicle treatment; n = 36). Moreover, co-treatment of hippocampal neurons with G1 (10 nM) and wortmannin (50 nM) did not inhibit the ability of G1 to reduce GluA1-surface staining (to 88 ± 3.2 % of vehicle; H = 44.5 with 3 degrees of freedom; $p > 0.05$ vs. Gl alone; $p < 0.05$ vs. vehicle; n = 36). Therefore these results suggest that it is likely that PI3K signalling is not required for the reduction in surface AMPAR expression induced by G1.

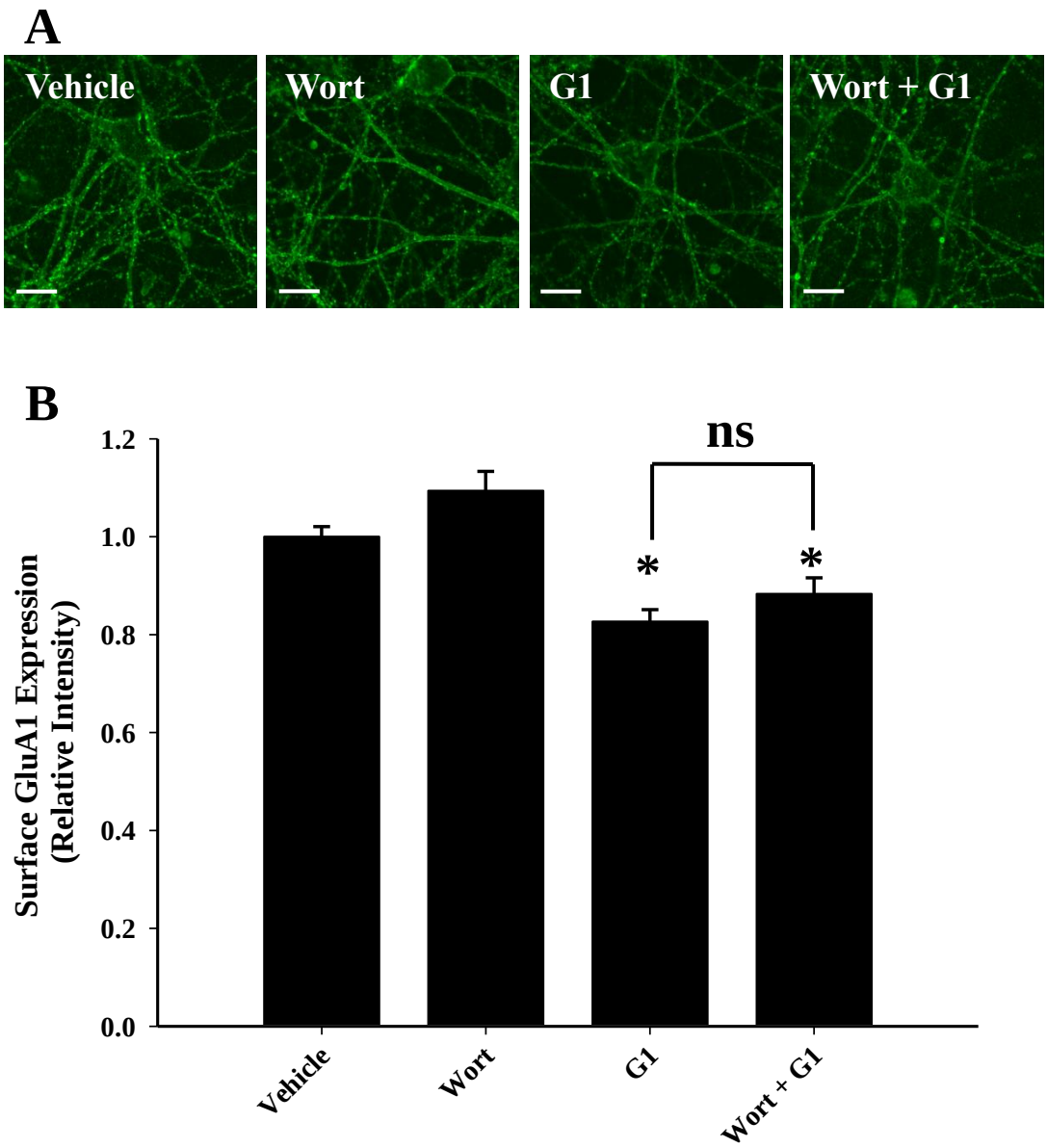

Figure 6.21: PI3K signalling does not underlie the G1-induced reduction in surface AMPAR expression. *DIV (8 – 16) hippocampal neurons were pre-treated with vehicle (0.01% DMSO) or wortmannin (50 nM; 30 min) and then G1 (10 nM) or vehicle, or in combination with wortmannin (30 min).* ***A,*** representative confocal images of surface GluA1 staining. ***B,*** pooled data illustrating relative changes in surface GluA1 after exposure to wortmannin, G1 alone and in the presence of wortmannin. Scale bars, 20 µm. A Kruskal-Wallis one way ANOVA on Ranks followed by Dunn's *post-hoc* analysis was performed. * represents $p < 0.05$ vs. vehicle treatment, ns represents $p > 0.05$ between the indicated treatments; n = 36 neurites from 3 individual cultures from different animals.

Summary of findings from Chapter 6:

1) G1-induced effects on hippocampal synaptic transmission and AMPAR trafficking are not blocked by antagonists for GPR30, ERα or ERβ
2) The SERD and putative agonist for GPR30, ICI had no effect on excitatory synaptic transmission in adult hippocampal slices, but preliminary data suggests that it mimics the effects of G1 in hyper-excitable hippocampal slices from juvenile rodents.
3) Application of ICI attenuated both the G1-induced LTD in adult hippocampal slices and the reduction of surface AMPAR expression in cultured hippocampal neurons.
4) siRNA against GPR30 did not affect relative GPR30 staining or inhibit G1- and E2-induced effects on surface AMPAR expression in cultured hippocampal neurons.
5) The G1-induced effects may involve signalling via ERK 1/2, however further investigation into this signalling mechanism is required.

6.3: Discussion

6.3.1: Lack of inhibition of G1- induced effects from selective GPR30, ER α or ER β antagonists

The data presented here indicates that the ability of G1 to induce LTD in adult hippocampal slices is not blocked by the putative GPR30 antagonist, G15. Moreover, treatment of hippocampal neurons with G15 or another putative GPR30 antagonist, G36 also failed to prevent G1-induced reduction of surface AMPAR expression.

These findings are in contrast to recent reports, suggesting that G15 is a selective antagonist for GPR30. For example, G15 is reported to block G1- and E2- induced intracellular Ca^{2+} mobilization and PIP_3 accumulation in a human breast cancer cell line, SKBr3 cells, which express GPR30 and ERα-36, but which do not express classical ERα or ERβ (Dennis *et al*., 2009). One possibility for the lack of observed effects of G15 in this study could be due to species differences in the selectivity of this

compound, as differing pharmacological profiles of synthetic compounds between human and rodent GPCRs has been observed (Jenkins *et al.*, 2010). However, this is unlikely as G15 is reported to block G1-induced membrane depolarization and intracellular Ca^{2+} mobilization in rat spinal sensory neurons (Deliu *et al*., 2012). Thus the results presented in this thesis would suggest that in our assays, either G1 is acting at another receptor, the potency of G15 at GPR30 differs markedly between different neuronal populations or rat hippocampal GPR30 is insensitive to G15.

Evidence contrary to the latter hypothesis has been recently reported (Ruiz-Palmero *et al*., 2013). In their report, G15 was able to completely inhibit G1-, ICI- and E2-induced neuritogenesis in developing hippocampal neurons, suggesting GPR30 is the sole receptor responsible for this E2-mediated effect in hippocampal neurons and that GPR30 expressed in developing hippocampal neurons is sensitive to G15 (Ruiz-Palmero *et al*., 2013). However, in an earlier report of similar design, the effects of E2 on neurite outgrowth were inhibited by ICI (von Schassen *et al.*, 2006). Thus, the picture for GPR30 pharmacology and the selectivity of the compounds used to probe for GPR30 function is not clear, particularly in native tissue. In addition, the specificity of G15 has come into question due to the ability of this compound to induce low levels of estrogen-responsive gene transcription via classical estrogen-receptors in MCF-7 cells, hence the generation of G36, a proposed GPR30 antagonist with less off-target effects (Dennis *et al*., 2011).

Moreover, there is evidence which suggests that not all G1- or E2-induced effects, thought to be mediated via GPR30, are inhibited by G15. For example, in embryonic zebrafish, G15 was unable to inhibit G1-induced cAMP accumulation (Jayasinghe and Volz, 2012). In the same model, despite GPR30 knockdown inducing morphological changes in embryogenesis (suggesting a critical role for GPR30 in development), G15 failed to induce similar effects (Shi *et al*., 2013). The inability of G15 to block G1 effects has also been reported in *in vivo* models for pain-related behaviours, where only very low concentrations of G1 (0.1 nmol) could be blocked by G15 (Deliu *et al*., 2012). Interestingly, in two immortalised embryonic hippocampal cell lines which express GPR30, E2 protects against glutamate-induced neurotoxicity, an effect which is although reproduced by G1, was only antagonised by G15 in one of the cell lines (Gingerich *et al*., 2010). In the same study the authors not only failed to examine whether G15 blocked the effects of G1, but also suggested that E2-inudced

neuroprotection was mediated via activation of GPR30, even though G15 failed to inhibit the effects of E2 in one of the GPR30 expressing cell lines (Gingerich *et al*., 2010). Interestingly, both immortalised hippocampal cell lines expressed similar levels of ERα, ERβ and GPR30, however they differed in their expression of another steroid-sensing receptor, the androgen receptor (Gingerich *et al*., 2010). Thus it is tempting to speculate that an interaction between GPR30 and androgen receptors contributes to the different pharmacological profiles observed in their study (Gingerich *et al*., 2010).

Thus, it is plausible that heterodimerization of GPR30 with other receptors (either GPCRs or membrane bound steroid receptors) within hippocampal neurons, influences the pharmacology and signalling capacity of GPR30. This notion is supported by recent evidence which suggests that GPR30 can interact with other GPCRs, specifically corticotrophin releasing hormone receptor-1 (CRHR1), progestin membrane receptor-β (PMRβ), and the 5-HT1a receptor (Akama *et al*., 2013). Expression of these receptors is observed within the rodent CNS, and specifically hippocampal expression of the 5-HT1aR (Zavitsanou *et al*., 2010) and CHCR1 (Williams *et al*., 2011) has been reported. Moreover, accumulating evidence suggests that GPCR oligomerization may be an important feature of GPCR signalling in the CNS allowing for fine-tuning and functional diversity in response to a single neurotransmitter or neuromodulator (as reviewed in Franco, 2009; González-Maeso, 2011).

Thus, in a few reported contexts in native tissue, this GPR30 antagonist fails to inhibit GPR30-mediated signalling. It would appear that the working hypothesis by numerous groups suggests that GPR30 may be interacting with other receptors (such as those mentioned above) in a cell specific manner, which may result in diverse pharmacological and signalling profile of this receptor (as reviewed in Srivastava and Evans, 2013).

Previous reports suggest that effects of G1 in GPR30-recombinant and human breast cancer cell lines may be attributed to the ERα splice variant, ERα-36 (Kang *et al*., 2010). Thus we hypothesised that if the G1-induced effects were mediated via this receptor, then competitive inhibition by an ERα antagonist (MPP) may inhibit the G1-induced effect; however this antagonist failed to block the G1-induced LTD and reduction of surface AMPAR expression. It must be emphasised that these results do not exclude the possibility that G1 may still be exerting its actions via this ERα splice

variant, particularly as there is recent evidence suggesting that ERα-36 is expressed in pyramidal neurons of the adult rodent hippocampus (Liu *et al*., 2013). As this variant possesses a truncated ligand binding domain suggestive of a different ligand binding spectrum from classical ERα-66 (Wang *et al*., 2006), there is the possibility that MPP has no affinity for ERα-36, and thus no antagonist action.

In addition we show that the SERD, ICI was able to attenuate G1-induced LTD in adult slices, however application of ICI mimicked the effects of G1 on synaptic transmission in juvenile slices. Treatment of hippocampal cultures with ICI also mirrored the actions of G1 as the ICI compound promoted a modest but significant reduction of surface GluA1-staining. Thus our data suggest that the ICI compound possesses agonist or antagonist activity depending on the model system or age of tissue examined.

Previous reports have shown that ICI can mimic the rapid non-genomic effects of E2 and G1 in hippocampal neurons. For example, in DIV 7 primary hippocampal cultures, ICI induces rapid intracellular Ca^{2+} mobilization, ERK 1/2 and Akt phosphorylation and protects against glutamate and amyloid β toxicity in a manner similar to E2 (Zhao *et al*., 2006). Moreover, in adult hippocampal slices from OVX rats, ICI potentiates synaptically evoked EPSCs and importantly can occlude any further potentiation elicited by E2 (Smejkalova and Woolley, 2010). The results from these reports suggest that the effects of ICI are likely to be mediated via a membrane-associated estrogen sensitive receptor, and are in agreement with the effects of ICI observed in juvenile tissue and in hippocampal cultures in this study. Although this is the first reported evidence for antagonistic activity of ICI for G1-induced effects, it is generally accepted that ICI inhibits genomic actions of E2 within the hippocampus (Zurkovsky *et al.*, 2006; Jelks *et al.*, 2007). This intriguing finding may be explained by the ability for ICI to inhibit the physical interaction between GPR30 and ERα, as has been observed in the Ishikawa human breast cancer cell line (Vivacqua *et al*., 2009), and for ICI to inhibit membrane associated E2 signalling in a breast cancer cell line only expressing GPR30 and the ERα variant, ERα-36 (Notas *et al*., 2012). Thus, if the G1-induced effects in our assays are mediated by GPR30 (or specifically an interaction between GPR30 and another receptor), then the ICI compound may be preventing receptor-receptor interaction, thereby inhibiting G1-induced effects. There is also the possibility that ICI may be acting on another, unidentified receptor in these assays, which has opposing

signalling mechanisms in adult hippocampal tissue thereby preventing G1-induced LTD.

Nevertheless, despite failure to block G1-induced effects with selective GPR30 antagonists, occluding the effects with a ligand for GPR30 suggests the involvement of this receptor. Whether GPR30-initiated signalling occurs independently or via association with another receptor within the hippocampus is an important avenue worth exploring in the future.

6.3.2: Inability to inhibit G1- and E2- induced effects with siRNA against rGPR30

Here we have demonstrated that we were unable to inhibit the effects of G1 and E2 on surface AMPAR expression in cells which were treated with siRNA against rGPR30. Bearing in mind that knockdown of GluA1 expression was only modest (Fig 6.14) and GPR30 staining was unchanged after siRNA treatment (Fig 6.15), it is likely that this protocol has failed to inhibit the expression of a significant proportion of GPR30. Considering the likely possibility that surface GPR30 expression is very low (Cheng *et al*., 2011a, 2011b), physiological effects in response to GPR30 agonists may only require a small number of activated receptors. This concept is supported by the inverted-U shaped concentration response relationship of G1 on surface AMPAR expression (Fig 5.7), where low nanomolar concentrations of G1 were able to illicit significant effects. Thus it may be very difficult to discern the contribution of GPR30 to G1 and E2 mediated responses without a significantly large knockdown of protein expression.

Another concept which cannot be ignored is that G1 may be a promiscuous ligand. Although G1 is reported to have no binding affinity to a panel of 25 well established GPCR's (Blasko *et al*., 2009), the possibility that G1 may have activity at other GPCRs or other targets in neurons (for example, ion channels) cannot be excluded. This is a reasonable possibility as the structure of G1 is modelled on a steroid backbone and steroids are well known modulators of ligand gated ion-channel function (Majewska, 2007; Cameron *et al*., 2012). Moreover, preliminary data in our laboratory suggests that G1 can stimulate the release of intracellular calcium in hGPR55-HEK-293 cells, albeit only at very high concentrations, EC_{50} ~ 1 -2 µM (*Unpublished findings from Henstridge, 2009 and Alexander, 2011;* see appendix), supporting the notion that G1 may have off-target effects.

6.3.3: Potential downstream signalling pathways associated with G1-induced effects

Although further investigation is required to determine whether the G1-induced LTD requires ERK1/2 activity, G1-induced reduction in surface AMPAR expression is blocked when an inhibitor of MEK signalling is present. ERK 1/2 kinases are serine / threonine kinases (also known as p44 and p42 MAPK, respectively) which within hippocampal neurons have a multitude of targets; including transcription factors, cytoskeletal proteins and other kinases (as reviewed in Thomas and Huganir, 2004). ERK signalling was first implicated in hippocampal plasticity in the late 1990's, when it was found that induction of LTP increased ERK 2 phosphorylation (English and Sweatt, 1996), and inhibition of ERK1/2 signalling abrogated LTP induction at CA3 – CA1 synapses, thus implying signalling via ERK critical for hippocampal LTP (English and Sweatt, 1997; Zhu *et al*., 2002; Selcher *et al*., 2003). Activation of the ERK 2 signalling cascade is also implicated in hippocampal LTD as Thiels and colleagues have demonstrated significant ERK 2 phosphorylation after induction of NMDAR-dependent LTD in the CA1 region of adult hippocampus, moreover this form of LTD is blocked with MEK inhibitors (Thiels *et al*., 2002).

Interestingly, the ability of mGluRs to induce LTD in the juvenile hippocampus (DHPG-induced) is also blocked by inhibitors of the MEK pathway (Gallagher *et al*., 2004), whereas in adult slices synaptically-induced mGluR-dependent LTD involves p38 MAPK signalling (Moult *et al*., 2008). Considering the G1-induced LTD is independent of NMDAR activation in adult hippocampal slices, this may illustrate a novel form of LTD in adult rodents which may involve ERK 1/2 signalling.

In further support of a role for ERK 1/2 signalling is that the ability of G1 to reduce the surface expression of AMPARs is blocked when either of the two structurally distinct MEK-inhibitors (PD 98059 or U0126) are present, but unaffected by inhibition of PI3K signalling. These results parallel those from Srivastava and colleagues' (2008), who illustrate that E2-induced reduction of surface GluA1 and E2-induced ERK 1/2 phosphorylation in cultured cortical neurons, occurs on the same time scale, where significant effects are observed after 30 min E2 treatment (Srivastava *et al*., 2008). Although in their study a direct link was not examined, rapid modulation of dendritic spine stability via ERK 1/2 signalling was hypothesised to be a mechanism by which E2 reduces surface GluA1 (Srivastava *et al*., 2008).

A number of different signalling mechanisms underlying the removal of AMPAR from hippocampal synapses has been described (Lin *et al.*, *2000;* Man *et al*., 2000; Moult *et al*., 2006; Casimiro *et al*., 2011; Henley *et al*., 2011). The phosphorylation states of specific regions at the C-terminal domains of GluA1 or GluA2 subunits, phosphorylation states of associated proteins (PSD-95), or the ability of interacting proteins (TARPs) to associate with endosomal transport and machinery, have all been reported to influence AMPAR endocytosis or retention of constitutively recycling AMPAR (as reviewed in Santos *et al*., 2009; Henley *et al.*, 2011; Anggono and Huganir, 2012). Thus, it may be feasible that G1 mediated signalling via ERK1/2 could lead to the modulation of the activity of phosphatases or other kinases, thus altering the phosphorylation states of target proteins mentioned above and hence leading to the reduction in synaptic GluA1-containig AMPAR.

Indeed, Liu and colleagues (2012) recently demonstrated G1-induced ERK 1/2 signalling can modulate the phosphorylation state of ionotropic glutamate receptors. This group observed rapid (within 30 min) ERK 1/2 phosphorylation in pre-frontal cortical neurons treated with G1. The authors found that this G1-mediated ERK 1/2 activity supressed dephosphorylation of death associated protein kinase-1 (DAPK-1), thus resulting in an inhibition of DAPK-1 mediated Ser-1303 phosphorylation of NR2B subunits (Liu *et al*., 2012). If GPR30 is responsible for the effects described in this thesis, a similar convoluted mechanism may be involved in the G1-induced reduction of surface AMPAR expression (*ie:* activity of ERK 1/2 may modulate (indirectly) the phosphorylation state of AMPAR subunits or their associated proteins and thus induce the removal of; or inhibit the insertion of; GluA1 containing AMPAR). Indeed, protein phosphatase 1 (PP1) mediated dephosphorylation of Ser 845 on GluA1-containig subunits has been implicated in hippocampal LTD (as reviewed in Collingridge *et al*., 2010), and there is evidence to suggest (albeit in human aveola macrohpages) that activity of ERK 1/2 influences PP1 activation (Monick *et al*., 2006). Thus, it may be feasible that G1 induced activation of ERK 1/2 promotes dephospohrylation and internalization of GluA1-containing AMPAR via activation of PP1. However, this signalling scenario is purely speculative and the exact mechanisms as to how G1-induced signalling mediated via ERK 1/2 converges to regulate surface AMPAR expression and the expression of long-term depression of synaptic transmission, is yet to be determined.

6.4: Conclusion

Through the use of a variety of pharmacological tools and siRNA gene silencing approaches, the potential mechanisms underlying G1-induced LTD and reduction of surface AMPAR expression were examined. A definitive conclusion as to the target for G1 action cannot be made, however our data indicate that the likeliest targets for G1 in the hippocampus are either GPR30 and/or ERα-36. Moreover, we examined downstream signalling mechanisms that may be initiated upon G1 application. We find here that the G1-induced reduction in surface AMPAR expression is likely to involve the ERK1/2 MAPK signalling pathway; however whether the G1-induced LTD of synaptic transmission involves the activation of ERK-mediated signalling requires further investigation.

Chapter Seven

Summary and Future Directions

7.1: Summary of Principal Findings:

- Expression of GPR30 within hippocampal neurons and glia is located primarily in an intracellular, peri-nuclear compartment.
- E2 can bi-directionally influence glutamatergic synaptic transmission; effects which are mimicked by the GPR30 agonist, G1.
- E2 and G1 can induce LTD in adult hippocampal slices; effects which are likely to be post-synaptically expressed, do not require afferent stimulation and are likely to involve a reduction in the surface expression of post-synaptic AMPARs.
- G1-induced LTD cannot be attenuated by antagonists for GPR30 (G15) ERα (MPP) or ERβ (PHTPP), however can be attenuated by the selective estrogen receptor downregulator and putative GPR30 ligand, ICI.
- G1-induced effects on hippocampal synaptic transmission and surface AMPAR expression may involve ERK1/2 mediated signalling, however further investigation of this signalling mechanism is required.

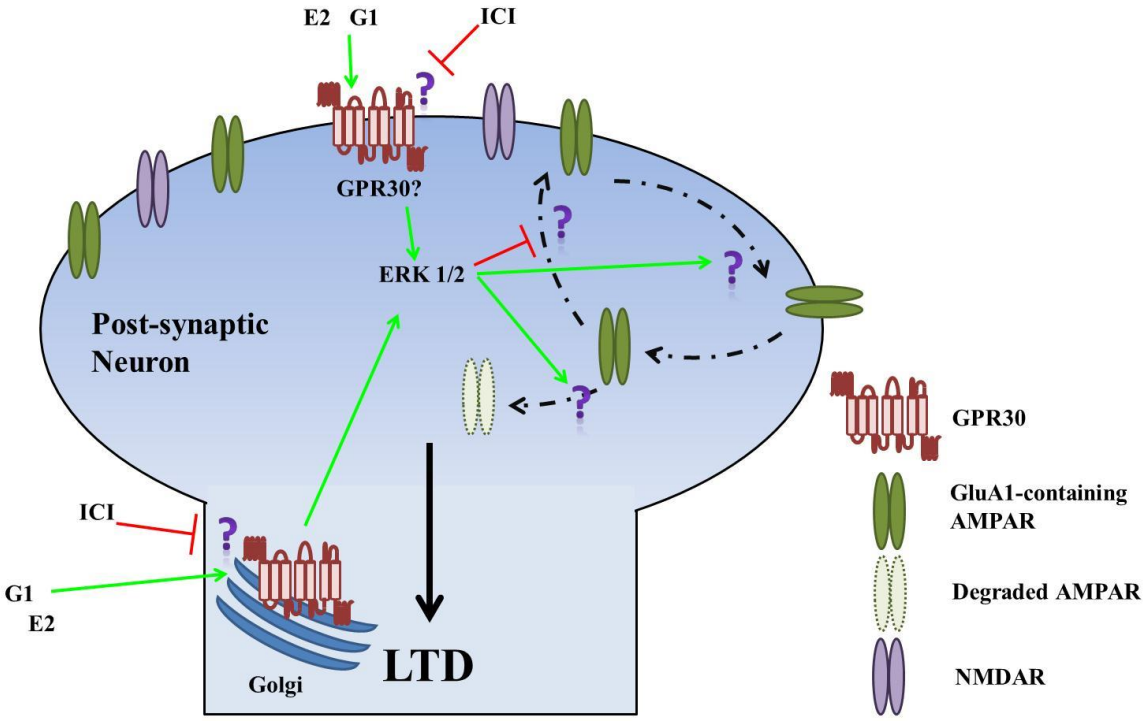

Figure 7.1: Proposed mechanism by which E2 and G1 induce hippocampal LTD. GPR30, located within the Golgi or associated with synapses in adult hippocampal neurons, enhances the removal of synaptic GluA1-containing AMPAR expression potentially via an ERK1/2-dependent pathway which may underlie the expression of LTD of glutamatergic synaptic transmission. Whether modulation of ERK1/2 facilitates the internalisation and degradation of GluA1-contining AMPAR or inhibits the surface expression of recycling AMPAR is yet to be determined. It is not clear if ICI is acting as an antagonist at GPR30, or is functioning as a partial agonist thereby competing with GPR30 in hippocampal slices, and thus is yet to be determined.

7.2: Implications for current hormone therapy

There are currently many pharmaceutical products on the market which target estrogen receptors and the synthesis of estradiol for the treatment of hormone-responsive breast cancer (eg: Tamoxifen, Raloxifene and aromatase inhibitors such as Letrozol and Anastrozole). Moreover, in June of this year (2013) both Tamoxifen and Raloxifen were approved in the UK (under the National Institute for Clinical Care and Excellence guideline 164) to be used as chemopreventatives for postmenopausal woman with a high risk of familiar breast cancer. Although these hormone treatments have unarguably beneficial effects in this highly prevalent disease, some clinical trial data would suggest that women using these endocrine therapies have increased cognitive deficits (Agrawal *et al*., 2010).

E2 is an important modulator of excitatory synaptic transmission in the adult hippocampus, and the data presented in this thesis support this. Moreover, the data presented here suggest that at nano-molar concentrations both E2 and the GPR30 agonist (G1) induce a novel form of LTD. Tamoxifen (specifically, its' metabolite 4-OH Tamoxifen) is a proposed GPR30 agonist (Revankar *et al*., 2005; Thomas *et al*., 2005) and there is evidence to suggest that it can cross the blood brain barrier (Biegon *et al*., 1996). Moreover, it has recently been demonstrated that the induction of hippocampal LTP is abolished in female rodents after chronic intraperitoneal treatment with the aromatase inhibitor Letrozol (Vierk *et al*., 2012) and the magnitude of hippocampal LTP is impaired in male rodents after acute treatment with Letrozol (Grassi *et al*., 2011). Therefore, interference of the neuro-estrogen system by these marketed pharmaceutical products may underlie the cognitive deficits reported in clinical trials. Thus, further investigation into the molecular mechanisms by which E2,

potentially via GPR30, modulates hippocampal transmission is necessary, such that in the future, drug design for estrogen-responsive diseases would involve limiting potentially detrimental off-target CNS side effects. Or conversely, with a greater understanding of the involvement of estrogens in the aging brain, selectively targeting novel estrogen-sensing receptors within in the CNS could be utilized as cognitive enhancers in age-related cognitive decline and age-related pathologies such as Alzheimer's disease.

7.3: Future Directions:

7.3.1: *GPR30 or not GPR30?*

Although we cannot conclusively identify GPR30 as the receptor responsible for mediating E2-induced effects, the possibility that GPR30 may be involved cannot be excluded, particularly as the ICI compound (proposed GPR30 ligand) inhibited G1-induced effects on hippocampal synaptic transmission and surface AMPAR expression. However, due to the potential off target effects of G1 (such as ERα-36 (Kang *et al.*, 2010) and GPR55 (see section A.2 and A.3 of appendix)) this may be a limiting factor in truly establishing GPR30 involvement.

Based on the tools currently available, the ideal experiment to conclusively determine whether the G1- and E2-induced LTD are mediated by GPR30 would involve culturing organotypic adult hippocampal slices. Subsequently, ensuring LTD is generated after E2 and G1 administration in this model and with the use of siRNA against GPR30, optimize a protocol whereby GPR30 gene expression is knocked down, without affecting expression of other estrogen receptors, specifically ERα-36. Thus this would allow one to test whether G1 and E2 mediated LTD are ameliorated in these slices, without the requirement for knockout mice.

7.3.2: *A bottom up approach?*

Whether GPR30 truly is an estrogen-sensing receptor is still currently a matter of debate (Levin, 2009a; Langer *et al*., 2010; Srivastava and Evans, 2013). Moreover, evidence for GPR30 interacting with other receptors such as GPCRs (e.g.: CRHR1, PMRβ and 5-HT1aR; Akama *et al*., 2013) and ER's (e.g.: ERα66; Notas *et al.*, (2012), and

associating proteins (e.g.: RAMP3; Lenhart *et al.*, (2013) and PSD-95; Akama *et al*., (2013)) is beginning to emerge. Thus, it would be worth initiating a "bottom-up" approach to test for GPR30 interacting partners, and whether these partners are necessary for efficient surface expression of GPR30, and E2-mediated signal transduction.

An approach could involve first screening for GPR30 interacting proteins in a native GPR30-expressing cell type of interest using co-immunoprecipitation techniques. Following this, developing chimeric constructs of GPR30 and putative interacting proteins, which would utilize fluorescence resonance energy transfer (FRET) technology. This sensitive technique is useful for detecting whether two proteins interact, as a FRET signal is emitted when the donor fluorophore and acceptor fluorophore are in close proximity to each other. Importantly this technique can also be employed in living cells which enables users to examine the effects of ligands on protein-protein interactions (Comps-Agrar *et al*., 2011). This approach would be coupled with downstream signalling assays which would test functionality and pharmacology for GPR30 and its potential interacting partners. With respect to native tissue, FRET-based technology to test for GPR30 interactions can be employed through the development of fluorescent ligands.

7.4: Concluding Remarks

In summary, the data presented here suggests that E2 is an important regulator of hippocampal excitatory synaptic transmission, eliciting bi-directional effects on glutatmatergic neurotransmission and surface AMPAR expression, and importantly inducing (in most cases) a novel form of LTD at CA3 to CA1 synapses. Moreover, investigation into whether the putative estrogen-sensing GPCR (GPR30) has a role in these E2 mediated effects, although not conclusive as we were unable to successfully knockdown GPR30, has provided evidence implicating this GPCR in E2-mediated effects as the G1-induced LTD and E2-induced LTD share common mechanisms.

The bi-directionality of the E2 and G1 responses on glutamatergic synaptic transmission could implicate estrogen receptors as important physiological targets which may contribute to the modulation of synaptic tone. This reasoning emanates from evidence suggesting that E2 can facilitate the induction, and enhance the magnitude of both LTP

(Córdoba Montoya and Carrer, 1997; Foy *et al*., 1999) and LTD (Zamani *et al*., 2000; Mukai *et al*., 2007), coupled with the data suggesting that estradiol is synthesised within the hippocampus (Hojo *et al*., 2004), potentially in response to afferent activity (Balthazart *et al*., 2003). Such that E2-induced effects may be mediated by the frequency and timing of incoming afferent stimuli. Moreover, the ability of estrogen receptor agonists to influence the expression of surface AMPAR may provide a molecular mechanism whereby levels of post-synaptic excitation could be dynamically controlled in response to locally produced E2. In addition, it is well established that estradiol has the capacity to modulate GABAergic transmission in the adult hippocampus via transiently suppressing GABA synthesis (Rudick and Woolley, 2003) and acutely inhibiting pre-synaptic GABA release (Huang and Woolley, 2012), thereby influencing the balance between excitation and inhibition of principal neurons. The physiological implications for these effects on glutamatergic synaptic transmission and AMPAR trafficking in the hippocampus and the exact molecular mechanisms involved remain to be determined.

Moreover, it is unlikely that the estrogen system will be functioning independently, and rapid cross-talk with other hormonal systems will influence glutamatergic synaptic transmission together with memory formation and consolidation *in vivo*. Indeed, there is already evidence to suggest that estradiol and glucocorticoid interactions have opposing influences on hippocampal excitatory synaptic transmission (Ooishi *et al*., 2012b). Furthermore, the relative responsiveness of estrogen-sensitive neurons from extra-hippocampal regions which send afferents to hippocampal regions (such as cholinergic neurons in the basal forebrain (as reviewed in (Gibbs, 2010)) may contribute to the overall effect estradiol has on hippocampal function *in vivo.*

With the addition of GPR30 to the ever growing list of estrogen-sensing receptors and functional estrogen receptor splice variants, it is vital that there is development of more selective pharmacological tools with less potential off-target effects in order to fully elucidate the role of individual estrogen receptor subtypes within the CNS.

Appendix

TABLE A1: COMPARISON OF LITERATURE REGARDING THE FREQUENCY OF CELLS OR SLICES WHICH RESPOND TO E2 AND G1 BY EXHIBITING AN ENHANCEMENT IN GLUTAMATERGIC SYNAPTIC TRANSMISSION.

Reference	*Sex (if OVX; primed or unprimed)*	*Synaptically evoked EPSCs / EPSPs or fEPSP recordings from CA1*	*% slices or cells exhibiting an **enhancement** of synaptic transmission*
(Foy *et al*., 1999)	Adult male gonadally intact rats	Synaptically evoked and pharmacologically isolated AMPA and NMDA EPSPs from CA1 pyramidal neurons (bath application of 1nM E2)	NMDA-mediated: 9 / 13 cells (69%) AMPA-mediated: 5 / 14 cells (36%)
(Fugger *et al*., 2001)	Adult (1 ½ month +) castrated male and OVX female (unprimed) C57 mice	fEPSP recordings from stratum radiutum of CA1 (bath application of 100pM E2)	Male: 7 / 10 slices (70%) Female: 6/10 slices (60%)
(Sharrow *et al*., 2002)	Adult (3 month) OVX female rats (unprimed)	fEPSP recordings from stratum radiatum of CA1 (bath application of 100pM E2)	14 / 21 slices (67%)
(Rudick and Woolley, 2003)	Adult female rats (OVX and estrogen primed or gonadally intact)	Synaptically evoked EPSCs from CA1 pyramidal neurons (bath application of 100pM E2)	34 / 55 cells (62%) (estradiol priming of OVX rats increased response rate from 33% to 73%)

(Kramár *et al*., 2009)	Young Adult (1 – 1 ½ month) gonadally intact male rats	fEPSP recordings from stratum radiutum of CA1 (Bath application of 1nM E2)	Did not state rate of response: "*highly reproducible responses"*
(Zadran *et al.*, 2009)	Adult (2-4 month) gonadally intact male rats	fEPSP recordings from stratum radiutum of CA1 (Bath application of 10nM E2)	Did not state rate of response *i.e.* all 10 slices responded to estradiol treatment (100%)
(Lebesgue *et al*., 2009)	Adult (~ 2month) OVX female rats (unprimed)	Synaptically evoked EPSCs from CA1 pyramidal neurons (bath application of 100nM G1 or E2)	G1: 4 / 7 cells (57%) E2: 3 / 5 cells (60%)
(Lebesgue *et al*., 2010)	Adult (~ 2month) OVX female rats (unprimed)	fEPSP recordings from Stratum Radiutum of CA1 (bath application of 10nM G1 or E2)	G1: 9 / 14 slices (64%) E2: 8 / 9 slices (89%)
(Smejkalova and Woolley, 2010)	Adult female (2 ½ - 3 month) OVX rats (E2 primed)	Synaptically evoked EPSCs from CA1 pyramidal neurons (Bath application of 100pM - 100nM E2 and 100nM G1)	100pM E2: 6 / 14 cells (43%) 1nM E2: 9 / 22 cells (41%) 10nM E2: 8 / 17 cells (47%) 100nM E2: 18 / 28 cells (64%) 100nM G1: 2 / 15 cells (13%)
(Alexander, 2013 (*unpublished*))	Adult (3 – 5 month) gonadally intact male rats	fEPSP recordings from stratum radiutum of CA1 (bath application of 1 – 100nM G1 or 10nM E2)	1nM G1: 0 / 5 slices (0%) 10nM G1: 15 / 27 slices (55%) 100nM G1: 5 / 6 slices (83%) 10nM E2: 16 / 22 slices (72%)

A.2: PROMISCUITY OF THE GPR30 AGONIST, G1

Follow up experiments from the unpublished observations by Chris Henstridge (2009), suggest that the GPR30 agonist (G1) can activate hGPR55 and regulate intracellular calcium levels in hGPR55-HEK-293 cells. A brief (5 min) exposure of G1 to hGPR55-HEK-293 cells produced a concentration-dependent increase in peak Ca^{2+} transients, with an EC_{50} of 1.18 ± 0.05 µM (Fig A.1).

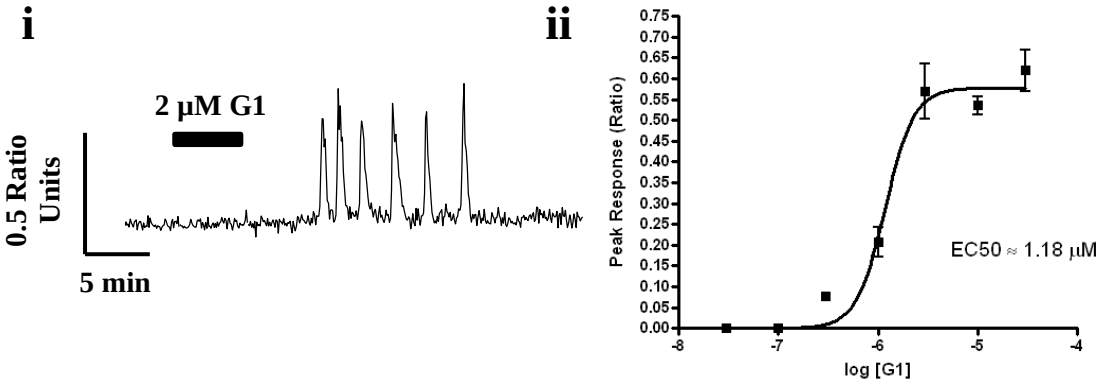

Figure A.1: The GPR30 agonist G1 induces intracellular Ca^{2+} responses in hGPR55-HEK 293 cells. ***i,*** Representative calcium transients induced by G1 (2 µM; 5 min) induces in an individual cell. Calcium transients are expressed as a change in the fluorescence ratio of the Ca^{2+} sensitive dye, Fura-2 AM. ***ii***, Concentration-response curve of the mean peak values of Ca^{2+} transients. Data are mean ± SEM from a total of 30 cells for each concentration, from two individual experiments.

A.3: OTHER PROPOSED GPR30 LIGANDS DO NOT ACTIVATE HGPR55

Preliminary studies with other proposed structurally similar GPR30 ligands (E2, ICI, G15) were conducted in order to test if activation of hGPR55 was specific for G1. In these studies, application of E2 (3 µM; 5 min) ICI (10 µM; 5 min) or G15 (10 µM; 10 min) were able to induce Ca^{2+} transients in hGPR55-HEK-293 cells (Fig A.2). Furthermore, the ability for G1 (2 µM) to activate hGPR55 was not inhibited by co-application of either ICI (10 µM), a compound which can inhibit G1-induced modulation of excitatory synaptic transmission in adult slices or the proposed GPR30 antagonist, G15 (10 µM). The finding that G15 does not stimulate or inhibit G1-induced

Ca^{2+} transients in these cells is interesting, considering that the only difference in the two structures is the presence of an ethanone moiety in G1 (Fig 1.5).

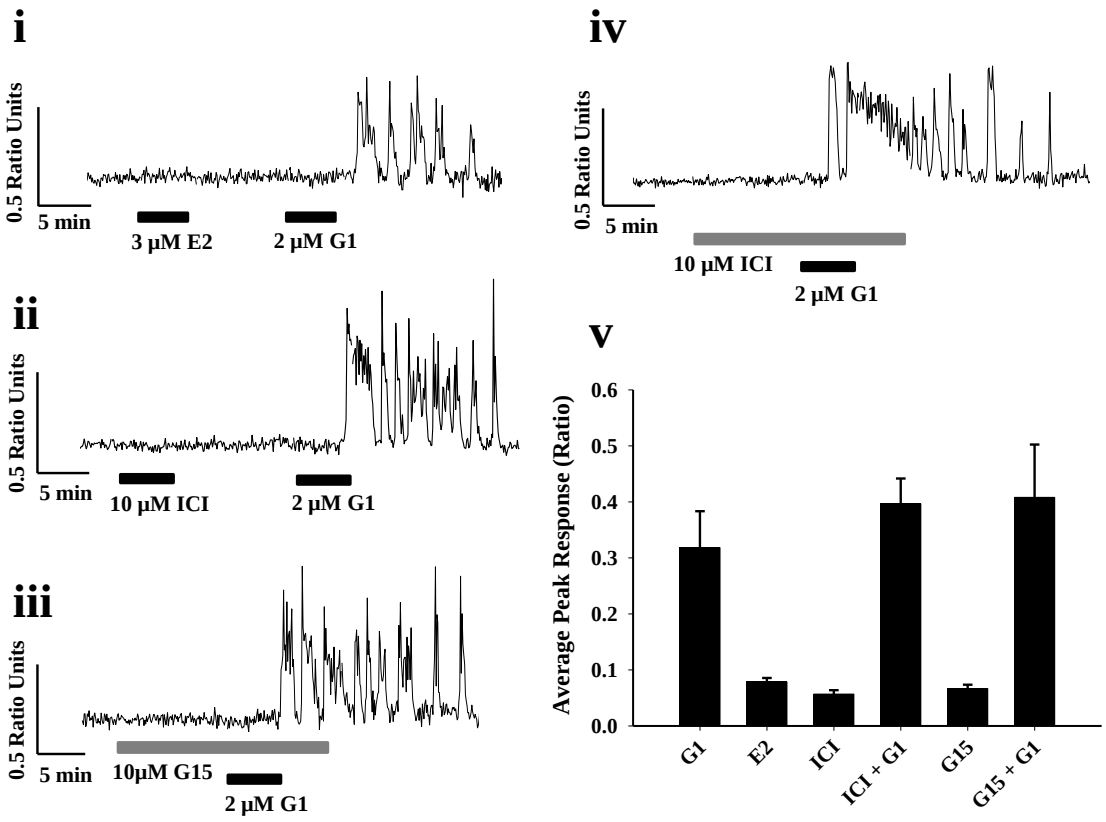

Figure A.2: Other proposed GPR30 ligands do not activate hGPR55.

Representative calcium traces from individual cells illustrating that **i)** E2 (3 µM; 5min), **ii)** ICI (10 µM; 5 min) and **iii)** G15 (10 µM; 10 min) do not induce Ca^{2+} transients. Co-application of **iii)** G15 (10 µM) or **iv)** ICI (10 µM), with G1 (2 µM) does not inhibit the G1-induced Ca^{2+} responses. **v)** Histogram representing the mean peak Ca^{2+} responses after ligand application, data are mean ± SEM from a total of 15 cells for each treatment group, from an individual experiment.

References

Acharya, K.D., and Veney, S.L. (2012). Characterization of the G-protein-coupled membrane-bound estrogen receptor GPR30 in the zebra finch brain reveals a sex difference in gene and protein expression. Dev. Neurobiol. *72*: 1433–46.

Adams, M.M., Fink, S.E., Shah, R. a, Janssen, W.G.M., Hayashi, S., Milner, T. a, et al. (2002). Estrogen and aging affect the subcellular distribution of estrogen receptor-alpha in the hippocampus of female rats. J. Neurosci. *22*: 3608–14.

Agrawal, K., Onami, S., Mortimer, J.E., and Pal, S.K. (2010). Cognitive changes associated with endocrine therapy for breast cancer. Maturitas *67*: 209–14.

Akama, K.T., and McEwen, B.S. (2003). Estrogen stimulates postsynaptic density-95 rapid protein synthesis via the Akt/protein kinase B pathway. J. Neurosci. *23*: 2333–9.

Akama, K.T., Thompson, L.I., Milner, T. a, and McEwen, B.S. (2013). Post-synaptic Density-95 (PSD-95) Binding Capacity of G-protein-coupled Receptor 30 (GPR30), an Estrogen Receptor That Can Be Identified in Hippocampal Dendritic Spines. J. Biol. Chem. *288*: 6438–50.

Albanito, L., Madeo, A., Lappano, R., Vivacqua, A., Rago, V., Carpino, A., et al. (2007). G protein-coupled receptor 30 (GPR30) mediates gene expression changes and growth response to 17beta-estradiol and selective GPR30 ligand G-1 in ovarian cancer cells. Cancer Res. *67*: 1859–66.

Anderson, W.W., and Collingridge, G.L. (2001). The LTP Program: a data acquisition program for on-line analysis of long-term potentiation and other synaptic events. J. Neurosci. Methods *108*: 71–83.

Anggono, V., and Huganir, R.L. (2012). Regulation of AMPA receptor trafficking and synaptic plasticity. Curr. Opin. Neurobiol. *22*: 461–9.

Arcaro, A., and Wymann, M.P. (1993). Wortmannin is a potent phosphatidylinositol 3-kinase inhibitor: the role of phosphatidylinositol 3,4,5-trisphosphate in neutrophil responses. Biochem. J. *296*: 297–301.

Ariazi, E. a, Brailoiu, E., Yerrum, S., Shupp, H. a, Slifker, M.J., Cunliffe, H.E., et al. (2010). The G protein-coupled receptor GPR30 inhibits proliferation of estrogen receptor-positive breast cancer cells. Cancer Res. *70*: 1184–94.

Aronica, S.M., Kraus, W.L., and Katzenellenbogen, B.S. (1994). Estrogen action via the cAMP signaling pathway: stimulation of adenylate cyclase and cAMP-regulated gene transcription. Proc. Natl. Acad. Sci. U. S. A. *91*: 8517–21.

Ascher, P., Bregestovski, P., and Nowak, L. (1988). N-methyl-D-aspartate-activated channels of mouse central neurones in magnesium-free solutions. J. Physiol. *399*: 207–26.

Balthazart, J., Baillien, M., Charlier, T.D., and Ball, G.F. (2003). Calcium-dependent phosphorylation processes control brain aromatase in quail. Eur. J. Neurosci. *17*: 1591–1606.

Balthazart, J., and Ball, G.F. (2006). Is brain estradiol a hormone or a neurotransmitter? Trends Neurosci. *29*: 241–9.

Balthazart, J., Stoop, R., Foidart, A., Granneman, J.C., and Lambert, J.G. (1994). Distribution and regulation of estrogen-2-hydroxylase in the quail brain. Brain Res. Bull. *35*: 339–345.

Barton, M. (2012). Position paper: The membrane estrogen receptor GPER--Clues and questions. Steroids *77*: 935–42.

Batenburg, W.W., Jansen, P.M., Bogaerdt, A.J. van den, and J Danser, A.H. (2012). Angiotensin II-aldosterone interaction in human coronary microarteries involves GPR30, EGFR, and endothelial NO synthase. Cardiovasc. Res. *94*: 136–43.

Baulieu, E.E. (1998). Neurosteroids: a novel function of the brain. Psychoneuroendocrinology *23*: 963–87.

Beattie, E.C., Carroll, R.C., Yu, X., Morishita, W., Yasuda, H., Zastrow, M. von, et al. (2000). Regulation of AMPA receptor endocytosis by a signaling mechanism shared with LTD. Nat. Neurosci. *3*: 1291–300.

Bemd, G. Van Den, and Kuiper, G. (1999). Distinct effects on the conformation of estrogen receptor α and β by both the antiestrogens ICI 164,384 and ICI 182,780 leading to opposite effects on receptor stability. Biochem. … *261*: 1–5.

Bi, R., Broutman, G., Foy, M.R., Thompson, R.F., and Baudry, M. (2000). The tyrosine kinase and mitogen-activated protein kinase pathways mediate multiple effects of estrogen in hippocampus. Proc. Natl. Acad. Sci. U. S. A. *97*: 3602–7.

Bi, R., Foy, M.R., Thompson, R.F., and Baudry, M. (2003). Effects of estrogen, age, and calpain on MAP kinase and NMDA receptors in female rat brain. Neurobiol. Aging *24*: 977–983.

Bi, R., Foy, M.R., Vouimba, R.M., Thompson, R.F., and Baudry, M. (2001). Cyclic changes in estradiol regulate synaptic plasticity through the MAP kinase pathway. Proc. Natl. Acad. Sci. U. S. A. *98*: 13391–5.

Biegon, A., Brewster, M., Degani, H., Pop, E., Somjen, D., and Kaye, A.M. (1996). A permanently charged tamoxifen derivative displays anticancer activity and improved tissue selectivity in rodents. Cancer Res. *56*: 4328–4331.

Blasko, E., Haskell, C.A., Leung, S., Gualtieri, G., Halks-Miller, M., Mahmoudi, M., et al. (2009). Beneficial role of the GPR30 agonist G-1 in an animal model of multiple sclerosis. J. Neuroimmunol. *214*: 67–77.

Bliss, T. V, and Collingridge, G.L. (1993). A synaptic model of memory: long-term potentiation in the hippocampus. Nature *361*: 31–9.

Bliss, T. V, and Lomo, T. (1973). Long-lasting potentiation of synaptic transmission in the dentate area of the anaesthetized rabbit following stimulation of the perforant path. J. Physiol. *232*: 331–56.

Boehm, J., and Malinow, R. (2005). AMPA receptor phosphorylation during synaptic plasticity. Biochem. Soc. Trans. *33*: 1354–6.

Boivin, B., Vaniotis, G., Allen, B.G., and Hébert, T.E. (2008). G protein-coupled receptors in and on the cell nucleus: a new signaling paradigm? J. Recept. Signal Transduct. Res. *28*: 15–28.

Bologa, C.G., Revankar, C.M., Young, S.M., Edwards, B.S., Arterburn, J.B., Kiselyov, A.S., et al. (2006). Virtual and biomolecular screening converge on a selective agonist for GPR30. Nat. Chem. Biol. *2*: 207–212.

Bolshakov, V.Y., and Siegelbaum, S. a (1995). Regulation of hippocampal transmitter release during development and long-term potentiation. Science *269*: 1730–4.

Boulware, M.I., Kordasiewicz, H., and Mermelstein, P.G. (2007). Caveolin proteins are essential for distinct effects of membrane estrogen receptors in neurons. J. Neurosci. *27*: 9941–50.

Boulware, M.I., and Mermelstein, P.G. (2009). Membrane estrogen receptors activate metabotropic glutamate receptors to influence nervous system physiology. Steroids *74*: 608–13.

Boulware, M.I., Weick, J.P., Becklund, B.R., Kuo, S.P., Groth, R.D., and Mermelstein, P.G. (2005). Estradiol activates group I and II metabotropic glutamate receptor signaling, leading to opposing influences on cAMP response element-binding protein. J. Neurosci. *25*: 5066–78.

Brailoiu, E., Dun, S.L., Brailoiu, G.C., Mizuo, K., Sklar, L. a, Oprea, T.I., et al. (2007). Distribution and characterization of estrogen receptor G protein-coupled receptor 30 in the rat central nervous system. J. Endocrinol. *193*: 311–21.

Brewer, G.J., Torricelli, J.R., Evege, E.K., and Price, P.J. (1993). Optimized survival of hippocampal neurons in B27-supplemented Neurobasal, a new serum-free medium combination. J. Neurosci. Res. *35*: 567–76.

Brothers, S.P., Janovick, J.A., and Conn, P.M. (2003). Unexpected effects of epitope and chimeric tags on gonadotropin-releasing hormone receptors: implications for understanding the molecular etiology of hypogonadotropic hypogonadism. J. Clin. Endocrinol. Metab. *88*: 6107–12.

Bryant, D.N., and Dorsa, D.M. (2010). Roles of estrogen receptors alpha and beta in sexually dimorphic neuroprotection against glutamate toxicity. Neuroscience *170*: 1261–9.

Burgess, A., Vigneron, S., Brioudes, E., Labbé, J., Lorca, T., and Castro, A. (2010). Loss of human Greatwall results in G2 arrest and multiple mitotic defects due to deregulation of the cyclin B-Cdc2/PP2A balance. Proc. Natl. Acad. Sci. U. S. A. *107*: 12564–9.

Cameron, K., Bartle, E., Roark, R., Fanelli, D., Pham, M., Pollard, B., et al. (2012). Neurosteroid binding to the amino terminal and glutamate binding domains of ionotropic glutamate receptors. Steroids *77*: 774–9.

Carmeci, C., Thompson, D. a, Ring, H.Z., Francke, U., and Weigel, R.J. (1997). Identification of a gene (GPR30) with homology to the G-protein-coupled receptor superfamily associated with estrogen receptor expression in breast cancer. Genomics *45*: 607–17.

Casimiro, T.M., Sossa, K.G., Uzunova, G., Beattie, J.B., Marsden, K.C., and Carroll, R.C. (2011). mGluR and NMDAR activation internalize distinct populations of AMPARs. Mol. Cell. Neurosci. *48*: 161–70.

Cerqueira, J.J., Mailliet, F., Almeida, O.F.X., Jay, T.M., and Sousa, N. (2007). The prefrontal cortex as a key target of the maladaptive response to stress. J. Neurosci. *27*: 2781–7.

Champagne, F. a, Weaver, I.C.G., Diorio, J., Sharma, S., and Meaney, M.J. (2003). Natural variations in maternal care are associated with estrogen receptor alpha expression and estrogen sensitivity in the medial preoptic area. Endocrinology *144*: 4720–4.

Chaouloff, F., Hémar, A., and Manzoni, O. (2008). Local facilitation of hippocampal metabotropic glutamate receptor-dependent long-term depression by corticosterone and dexamethasone. Psychoneuroendocrinology *33*: 686–91.

Cheng, S.-B., Graeber, C.T., Quinn, J. a, and Filardo, E.J. (2011a). Retrograde transport of the transmembrane estrogen receptor, G-protein-coupled-receptor-30 (GPR30/GPER) from the plasma membrane towards the nucleus. Steroids *76*: 892–6.

Cheng, S.-B., Quinn, J. a, Graeber, C.T., and Filardo, E.J. (2011b). Down-modulation of the G-protein-coupled estrogen receptor, GPER, from the cell surface occurs via a trans-Golgi-proteasome pathway. J. Biol. Chem. *286*: 22441–55.

Clark, B.J., Wells, J., King, S.R., and Stocco, D.M. (1994). The purification, cloning, and expression of a novel luteinizing hormone-induced mitochondrial protein in MA-10 mouse Leydig tumor cells. Characterization of the steroidogenic acute regulatory protein (StAR). J. Biol. Chem. *269*: 28314–22.

Collingridge, G.L., Peineau, S., Howland, J.G., and Wang, Y.T. (2010). Long-term depression in the CNS. Nat. Rev. Neurosci. *11*: 459–73.

Comps-Agrar, L., Maurel, D., Rondard, P., Pin, J.-P., Trinquet, E., and Prézeau, L. (2011). Cell-Surface Protein-Protein Interaction Analysis with Time-Resolved FRET and Snap-Tag Technologies: Application to G Protein-Coupled Receptor Oligomerization. Methods Mol. Biol. Clift. Nj *756*: 201–214.

Compton, D.R., Sheng, S., Carlson, K.E., Rebacz, N.A., Lee, I.Y., Katzenellenbogen, B.S., et al. (2004). Pyrazolo[1,5-a]pyrimidines: estrogen receptor ligands possessing estrogen receptor beta antagonist activity. J. Med. Chem. *47*: 5872–93.

Córdoba Montoya, D. a, and Carrer, H.F. (1997). Estrogen facilitates induction of long term potentiation in the hippocampus of awake rats. Brain Res. *778*: 430–8.

Corpéchot, C., Robel, P., Axelson, M., Sjövall, J., and Baulieu, E.E. (1981). Characterization and measurement of dehydroepiandrosterone sulfate in rat brain. Proc. Natl. Acad. Sci. U. S. A. *78*: 4704–7.

Creager, R., Dunwiddie, T., and Lynch, G. (1980). Paired-pulse and frequency facilitation in the CA1 region of the in vitro rat hippocampus. J. Physiol. *299*: 409–24.

Cull-Candy, S.G., and Leszkiewicz, D.N. (2004). Role of distinct NMDA receptor subtypes at central synapses. Sci. STKE *2004*: re16.

Dauvois, S., White, R., and Parker, M.G. (1993). The antiestrogen ICI 182780 disrupts estrogen receptor nucleocytoplasmic shuttling. J. Cell Sci. *106 (Pt 4*: 1377–88.

Davies, S.P., Reddy, H., Caivano, M., and Cohen, P. (2000). Specificity and mechanism of action of some commonly used protein kinase inhibitors. Biochem. J. *351*: 95–105.

Daw, M.I., Bortolotto, Z. a, Saulle, E., Zaman, S., Collingridge, G.L., and Isaac, J.T.R. (2002). Phosphatidylinositol 3 kinase regulates synapse specificity of hippocampal long-term depression. Nat. Neurosci. *5*: 835–6.

Day, M., Sung, A., Logue, S., Bowlby, M., and Arias, R. (2005). Beta estrogen receptor knockout (BERKO) mice present attenuated hippocampal CA1 long-term potentiation and related memory deficits in contextual fear conditioning. Behav. Brain Res. *164*: 128–31.

Dehmelt, L., and Halpain, S. (2005). The MAP2/Tau family of microtubule-associated proteins. Genome Biol. *6*: 204.

Deliu, E., Brailoiu, G.C., Arterburn, J.B., Oprea, T.I., Benamar, K., Dun, N.J., et al. (2012). Mechanisms of G protein-coupled estrogen receptor-mediated spinal nociception. J. Pain *13*: 742–54.

Dennis, M.K., Burai, R., Ramesh, C., Petrie, W.K., Alcon, S.N., Nayak, T.K., et al. (2009). In vivo effects of a GPR30 antagonist. Nat. Chem. Biol. *5*: 421–7.

Dennis, M.K., Field, A.S., Burai, R., Ramesh, C., Petrie, W.K., Bologa, C.G., et al. (2011). Identification of a GPER/GPR30 antagonist with improved estrogen receptor counterselectivity. J. Steroid Biochem. Mol. Biol. *127*: 358–66.

Dingledine, R., Borges, K., Bowie, D., and Traynelis, S.F. (1999). The glutamate receptor ion channels. Pharmacol. Rev. *51*: 7–61.

Doherty, G.H., Beccano-Kelly, D., Yan, S. Du, Gunn-Moore, F.J., and Harvey, J. (2013). Leptin prevents hippocampal synaptic disruption and neuronal cell death induced by amyloid β. Neurobiol. Aging *34*: 226–37.

Dong, C., Filipeanu, C.M., Duvernay, M.T., and Wu, G. (2007). Regulation of G protein-coupled receptor export trafficking. Biochim. Biophys. Acta *1768*: 853–70.

Dong, S., Terasaka, S., and Kiyama, R. (2011). Bisphenol A induces a rapid activation of Erk1/2 through GPR30 in human breast cancer cells. Environ. Pollut. *159*: 212–8.

Dudek, S.M., and Bear, M.F. (1993). Bidirectional long-term modification of synaptic effectiveness in the adult and immature hippocampus. J. Neurosci. *13*: 2910–8.

Dudley, D.T., Pang, L., Decker, S.J., Bridges, a J., and Saltiel, a R. (1995). A synthetic inhibitor of the mitogen-activated protein kinase cascade. Proc. Natl. Acad. Sci. U. S. A. *92*: 7686–9.

Dun, S.L., Brailoiu, G.C., Gao, X., Brailoiu, E., Arterburn, J.B., Prossnitz, E.R., et al. (2009). Expression of estrogen receptor GPR30 in the rat spinal cord and in autonomic and sensory ganglia. J. Neurosci. Res. *87*: 1610–9.

Durakoglugil, M., Irving, A.J., and Harvey, J. (2005). Leptin induces a novel form of NMDA receptor-dependent long-term depression. J. Neurochem. *95*: 396–405.

Ehlers, M.D. (2000). Reinsertion or degradation of AMPA receptors determined by activity-dependent endocytic sorting. Neuron *28*: 511–25.

Ellis, J., Pediani, J.D., Canals, M., Milasta, S., and Milligan, G. (2006). Orexin-1 receptor-cannabinoid CB1 receptor heterodimerization results in both ligand-dependent and -independent coordinated alterations of receptor localization and function. J. Biol. Chem. *281*: 38812–24.

English, J.D., and Sweatt, J.D. (1996). Activation of p42 mitogen-activated protein kinase in hippocampal long term potentiation. J. Biol. Chem. *271*: 24329–32.

English, J.D., and Sweatt, J.D. (1997). A requirement for the mitogen-activated protein kinase cascade in hippocampal long term potentiation. J. Biol. Chem. *272*: 19103–6.

Espeland, M.A., Shumaker, S.A., Limacher, M., Rapp, S.R., Bevers, T.B., Barad, D.H., et al. (2010). Relative effects of tamoxifen, raloxifene, and conjugated equine estrogens on cognition. J. Womens. Health (Larchmt). *19*: 371–9.

Etgen, A.M., Jover-Mengual, T., and Zukin, R.S. (2011). Neuroprotective actions of estradiol and novel estrogen analogs in ischemia: translational implications. Front. Neuroendocrinol. *32*: 336–52.

Feng, Y., and Gregor, P. (1997). Cloning of a novel member of the G protein-coupled receptor family related to peptide receptors. Biochem. Biophys. Res. Commun. *231*: 651–4.

Ferreira, A., and Rapoport, M. (2002). The synapsins: beyond the regulation of neurotransmitter release. Cell. Mol. Life Sci. *59*: 589–95.

Filardo, E., Quinn, J., Pang, Y., Graeber, C., Shaw, S., Dong, J., et al. (2007). Activation of the novel estrogen receptor G protein-coupled receptor 30 (GPR30) at the plasma membrane. Endocrinology *148*: 3236–45.

Filardo, E.J., Graeber, C.T., Quinn, J. a, Resnick, M.B., Giri, D., DeLellis, R. a, et al. (2006). Distribution of GPR30, a seven membrane-spanning estrogen receptor, in primary breast cancer and its association with clinicopathologic determinants of tumor progression. Clin. Cancer Res. *12*: 6359–66.

Filardo, E.J., Quinn, J. a, Bland, K.I., and Frackelton, a R. (2000). Estrogen-induced activation of Erk-1 and Erk-2 requires the G protein-coupled receptor homolog, GPR30, and occurs via trans-activation of the epidermal growth factor receptor through release of HB-EGF. Mol. Endocrinol. *14*: 1649–60.

Filardo, E.J., Quinn, J. a, Frackelton, a R., and Bland, K.I. (2002). Estrogen action via the G protein-coupled receptor, GPR30: stimulation of adenylyl cyclase and cAMP-mediated attenuation of the epidermal growth factor receptor-to-MAPK signaling axis. Mol. Endocrinol. *16*: 70–84.

Filardo, E.J., and Thomas, P. (2012). Minireview: G protein-coupled estrogen receptor-1, GPER-1: its mechanism of action and role in female reproductive cancer, renal and vascular physiology. Endocrinology *153*: 2953–62.

Fitzjohn, S.M., Bortolotto, Z. a, Palmer, M.J., Doherty, a J., Ornstein, P.L., Schoepp, D.D., et al. (1998). The potent mGlu receptor antagonist LY341495 identifies roles for both cloned and novel mGlu receptors in hippocampal synaptic plasticity. Neuropharmacology *37*: 1445–58.

Fitzjohn, S.M., Kingston, a E., Lodge, D., and Collingridge, G.L. (1999). DHPG-induced LTD in area CA1 of juvenile rat hippocampus; characterisation and sensitivity to novel mGlu receptor antagonists. Neuropharmacology *38*: 1577–83.

Fitzjohn, S.M., Palmer, M.J., May, J.E.R., Neeson, A., Morris, S.A.C., and Collingridge, G.L. (2001). A characterisation of long-term depression induced by metabotropic glutamate receptor activation in the rat hippocampus in vitro. 421–430.

Foster, T.C. (2012). Role of estrogen receptor alpha and beta expression and signaling on cognitive function during aging. Hippocampus *22*: 656–69.

Foster, T.C., Rani, A., Kumar, A., Cui, L., and Semple-Rowland, S.L. (2008). Viral vector-mediated delivery of estrogen receptor-alpha to the hippocampus improves spatial learning in estrogen receptor-alpha knockout mice. Mol. Ther. *16*: 1587–93.

Foy, M.R. (2001). 17beta-estradiol: effect on CA1 hippocampal synaptic plasticity. Neurobiol. Learn. Mem. *76*: 239–52.

Foy, M.R. (2011). Ovarian hormones, aging and stress on hippocampal synaptic plasticity. Neurobiol. Learn. Mem. *95*: 134–44.

Foy, M.R., Baudry, M., Diaz Brinton, R., and Thompson, R.F. (2008). Estrogen and hippocampal plasticity in rodent models. J. Alzheimers. Dis. *15*: 589–603.

Foy, M.R., Xu, J., Xie, X., Brinton, R.D., Thompson, R.F., and Berger, T.W. (1999). 17beta-estradiol enhances NMDA receptor-mediated EPSPs and long-term potentiation. J. Neurophysiol. *81*: 925–9.

Franco, R. (2009). G-protein-coupled receptor heteromers or how neurons can display differently flavoured patterns in response to the same neurotransmitter. Br. J. Pharmacol. *158*: 23–31.

Frick, K.M. (2012). Building a better hormone therapy? How understanding the rapid effects of sex steroid hormones could lead to new therapeutics for age-related memory decline. Behav. Neurosci. *126*: 29–53.

Frick, K.M. (2013). Epigenetics, estradiol, and hippocampal memory consolidation. J. Neuroendocrinol.

Fugger, H.N., Kumar, a, Lubahn, D.B., Korach, K.S., and Foster, T.C. (2001). Examination of estradiol effects on the rapid estradiol mediated increase in hippocampal synaptic transmission in estrogen receptor alpha knockout mice. Neurosci. Lett. *309*: 207–9.

Funakoshi, T., Yanai, A., Shinoda, K., Kawano, M.M., and Mizukami, Y. (2006). G protein-coupled receptor 30 is an estrogen receptor in the plasma membrane. Biochem. Biophys. Res. Commun. *346*: 904–10.

Gallagher, S.M., Daly, C. a, Bear, M.F., and Huber, K.M. (2004). Extracellular signal-regulated protein kinase activation is required for metabotropic glutamate receptor-dependent long-term depression in hippocampal area CA1. J. Neurosci. *24*: 4859–64.

Gao, F., Ma, X., Ostmann, A.B., and Das, S.K. (2011). GPR30 activation opposes estrogen-dependent uterine growth via inhibition of stromal ERK1/2 and estrogen receptor alpha (ERα) phosphorylation signals. Endocrinology *152*: 1434–47.

Gao, S., Hendrie, H.C., Hall, K.S., and Hui, S. (1998). The relationships between age, sex, and the incidence of dementia and Alzheimer disease: a meta-analysis. Arch. Gen. Psychiatry *55*: 809–15.

Gassmann, M., Haller, C., Stoll, Y., Abdel Aziz, S., Biermann, B., Mosbacher, J., et al. (2005). The RXR-type endoplasmic reticulum-retention/retrieval signal of GABAB1 requires distant spacing from the membrane to function. Mol. Pharmacol. *68*: 137–44.

Gavet, O., and Pines, J. (2010). Progressive activation of CyclinB1-Cdk1 coordinates entry to mitosis. Dev. Cell *18*: 533–43.

Gibbs, R.B. (2010). Estrogen therapy and cognition: a review of the cholinergic hypothesis. Endocr. Rev. *31*: 224–53.

Gingerich, S., Kim, G.L., Chalmers, J. a, Koletar, M.M., Wang, X., Wang, Y., et al. (2010). Estrogen receptor α and G-protein coupled receptor 30 mediate the neuroprotective effects of 17β-estradiol in novel murine hippocampal cell models. Neuroscience *170*: 54–66.

Gobeil, F., Fortier, A., Zhu, T., Bossolasco, M., Leduc, M., Grandbois, M., et al. (2006). G-protein-coupled receptors signalling at the cell nucleus: an emerging paradigm. Can. J. Physiol. Pharmacol. *84*: 287–297.

González-Burgos, I., Alejandre-Gómez, M., and Cervantes, M. (2005). Spine-type densities of hippocampal CA1 neurons vary in proestrus and estrus rats. Neurosci. Lett. *379*: 52–4.

González-Maeso, J. (2011). GPCR oligomers in pharmacology and signaling. Mol. Brain *4*: 20.

Gould, E., Woolley, C.S., Frankfurt, M., and McEwen, B.S. (1990). Gonadal steroids regulate dendritic spine density in hippocampal pyramidal cells in adulthood. J. Neurosci. *10*: 1286–91.

Graham, F.L., Smiley, J., Russell, W.C., and Nairn, R. (1977). Characteristics of a human cell line transformed by DNA from human adenovirus type 5. J. Gen. Virol. *36*: 59–74.

Grassi, S., Tozzi, a, Costa, C., Tantucci, M., Colcelli, E., Scarduzio, M., et al. (2011). Neural 17β-estradiol facilitates long-term potentiation in the hippocampal CA1 region. Neuroscience *192*: 67–73.

Greger, I.H., Khatri, L., Kong, X., and Ziff, E.B. (2003). AMPA receptor tetramerization is mediated by Q/R editing. Neuron *40*: 763–74.

Greger, I.H., Khatri, L., and Ziff, E.B. (2002). RNA editing at arg607 controls AMPA receptor exit from the endoplasmic reticulum. Neuron *34*: 759–72.

Groc, L., Bard, L., and Choquet, D. (2009). Surface trafficking of N-methyl-D-aspartate receptors: physiological and pathological perspectives. Neuroscience *158*: 4–18.

Groc, L., Choquet, D., and Chaouloff, F. (2008). The stress hormone corticosterone conditions AMPAR surface trafficking and synaptic potentiation. Nat. Neurosci. *11*: 868–70.

Gros, R., Ding, Q., Liu, B., Chorazyczewski, J., and Feldman, R.D. (2013). Aldosterone mediates its rapid effects in vascular endothelial cells through GPER activation. Am. J. Physiol. Cell Physiol. *304*: C532–40.

Gros, R., Ding, Q., Sklar, L. a, Prossnitz, E.E., Arterburn, J.B., Chorazyczewski, J., et al. (2011). GPR30 expression is required for the mineralocorticoid receptor-independent rapid vascular effects of aldosterone. Hypertension *57*: 442–51.

Gu, Q., Korach, K.S., and Moss, R.L. (1999). Rapid action of 17beta-estradiol on kainate-induced currents in hippocampal neurons lacking intracellular estrogen receptors. Endocrinology *140*: 660–6.

Gu, Q., and Moss, R.L. (1996). 17 beta-Estradiol potentiates kainate-induced currents via activation of the cAMP cascade. J. Neurosci. *16*: 3620–9.

Gu, Q., and Moss, R.L. (1998). Novel mechanism for non-genomic action of 17 beta-oestradiol on kainate-induced currents in isolated rat CA1 hippocampal neurones. J. Physiol. *506 (Pt 3*: 745–54.

Hammond, R., Mauk, R., Ninaci, D., Nelson, D., and Gibbs, R.B. (2009). Chronic treatment with estrogen receptor agonists restores acquisition of a spatial learning task in young ovariectomized rats. Horm. Behav. *56*: 309–14.

Hammond, R., Nelson, D., and Gibbs, R.B. (2011). GPR30 co-localizes with cholinergic neurons in the basal forebrain and enhances potassium-stimulated acetylcholine release in the hippocampus. Psychoneuroendocrinology *36*: 182–92.

Hammond, R., Nelson, D., Kline, E., and Gibbs, R.B. (2012). Chronic treatment with a GPR30 antagonist impairs acquisition of a spatial learning task in young female rats. Horm. Behav. *62*: 367–74.

Hanley, J.G. (2008). AMPA receptor trafficking pathways and links to dendritic spine morphogenesis. Cell Adh. Migr. *2*: 276–82.

Hazell, G.G.J., Yao, S.T., Roper, J. a, Prossnitz, E.R., O'Carroll, A.-M., and Lolait, S.J. (2009). Localisation of GPR30, a novel G protein-coupled oestrogen receptor, suggests multiple functions in rodent brain and peripheral tissues. J. Endocrinol. *202*: 223–36.

Hebb, D.O. (1949). The Organization of Behavior: A Neuropsychological Theory (New York, NY: John Wiley & Sons).

Heide, L.P. van der, Kamal, A., Artola, A., Gispen, W.H., and Ramakers, G.M.J. (2005). Insulin modulates hippocampal activity-dependent synaptic plasticity in a N-methyl-d-aspartate receptor and phosphatidyl-inositol-3-kinase-dependent manner. J. Neurochem. *94*: 1158–66.

Henley, J.M., Barker, E. a, and Glebov, O.O. (2011). Routes, destinations and delays: recent advances in AMPA receptor trafficking. Trends Neurosci. *34*: 258–68.

Henson, M.A., Roberts, A.C., Pérez-Otaño, I., and Philpot, B.D. (2010). Influence of the NR3A subunit on NMDA receptor functions. Prog. Neurobiol. *91*: 23–37.

Henstridge, C.M., Balenga, N. a B., Ford, L. a, Ross, R. a, Waldhoer, M., and Irving, A.J. (2009). The GPR55 ligand L-alpha-lysophosphatidylinositol promotes RhoA-dependent Ca2+ signaling and NFAT activation. FASEB J. *23*: 183–93.

Higo, S., Hojo, Y., Ishii, H., Kominami, T., Nakajima, K., Poirier, D., et al. (2009). Comparison of sex-steroid synthesis between neonatal and adult rat hippocampus. Biochem. Biophys. Res. Commun. *385*: 62–6.

Hirahara, Y., Matsuda, K.I., Yamada, H., Saitou, A., Morisaki, S., Takanami, K., et al. (2013). G protein-coupled receptor 30 contributes to improved remyelination after cuprizone-induced demyelination. Glia *61*: 420–31.

Hojo, Y., Hattori, T.-A., Enami, T., Furukawa, A., Suzuki, K., Ishii, H.-T., et al. (2004). Adult male rat hippocampus synthesizes estradiol from pregnenolone by cytochromes P45017alpha and P450 aromatase localized in neurons. Proc. Natl. Acad. Sci. U. S. A. *101*: 865–70.

Hojo, Y., Higo, S., Ishii, H., Ooishi, Y., Mukai, H., Murakami, G., et al. (2009). Comparison between hippocampus-synthesized and circulation-derived sex steroids in the hippocampus. Endocrinology *150*: 5106–12.

Hojo, Y., Higo, S., Kawato, S., Hatanaka, Y., Ooishi, Y., Murakami, G., et al. (2011). Hippocampal synthesis of sex steroids and corticosteroids: essential for modulation of synaptic plasticity. Front. Endocrinol. (Lausanne). *2*: 43.

Hojo, Y., Murakami, G., Mukai, H., Higo, S., Hatanaka, Y., Ogiue-Ikeda, M., et al. (2008). Estrogen synthesis in the brain--role in synaptic plasticity and memory. Mol. Cell. Endocrinol. *290*: 31–43.

Hollmann, M., Hartley, M., and Heinemann, S. (1991). Ca2+ permeability of KA-AMPA--gated glutamate receptor channels depends on subunit composition. Science *252*: 851–3.

Hou, L., and Klann, E. (2004). Activation of the phosphoinositide 3-kinase-Akt-mammalian target of rapamycin signaling pathway is required for metabotropic glutamate receptor-dependent long-term depression. J. Neurosci. *24*: 6352–61.

Huang, C.-C., Chen, J.-P., Yeh, C.-M., and Hsu, K.-S. (2012). Sex difference in stress-induced enhancement of hippocampal CA1 long-term depression during puberty. Hippocampus *22*: 1622–34.

Huang, C.-C., Lee, C.-C., and Hsu, K.-S. (2004). An investigation into signal transduction mechanisms involved in insulin-induced long-term depression in the CA1 region of the hippocampus. J. Neurochem. *89*: 217–31.

Huang, G.Z., and Woolley, C.S. (2012). Estradiol acutely suppresses inhibition in the hippocampus through a sex-specific endocannabinoid and mGluR-dependent mechanism. Neuron *74*: 801–8.

Huber, K.M., Kayser, M.S., and Bear, M.F. (2000). Role for rapid dendritic protein synthesis in hippocampal mGluR-dependent long-term depression. Science *288*: 1254–7.

Huber, K.M., Roder, J.C., and Bear, M.F. (2001). Chemical induction of mGluR5- and protein synthesis--dependent long-term depression in hippocampal area CA1. J. Neurophysiol. *86*: 321–5.

Isensee, J., Meoli, L., Zazzu, V., Nabzdyk, C., Witt, H., Soewarto, D., et al. (2009). Expression pattern of G protein-coupled receptor 30 in LacZ reporter mice. Endocrinology *150*: 1722–30.

Izant, J.G., and McIntosh, J.R. (1980). Microtubule-associated proteins: a monoclonal antibody to MAP2 binds to differentiated neurons. Proc. Natl. Acad. Sci. U. S. A. *77*: 4741–5.

Jackson, A.C., and Nicoll, R. a (2011). The expanding social network of ionotropic glutamate receptors: TARPs and other transmembrane auxiliary subunits. Neuron *70*: 178–99.

Jayasinghe, B.S., and Volz, D.C. (2012). Aberrant ligand-induced activation of G protein-coupled estrogen receptor 1 (GPER) results in developmental malformations during vertebrate embryogenesis. Toxicol. Sci. *125*: 262–73.

Jelks, K.B., Wylie, R., Floyd, C.L., McAllister, a K., and Wise, P. (2007). Estradiol targets synaptic proteins to induce glutamatergic synapse formation in cultured hippocampal neurons: critical role of estrogen receptor-alpha. J. Neurosci. *27*: 6903–13.

Jenkins, L., Brea, J., Smith, N.J., Hudson, B.D., Reilly, G., Bryant, N.J., et al. (2010). Identification of novel species-selective agonists of the G-protein-coupled receptor GPR35 that promote recruitment of β-arrestin-2 and activate Gα13. Biochem. J. *432*: 451–9.

Jiang, L., Teng, G.M.K., Chan, E.Y.M., Au, S.W.N., Wise, H., Lee, S.S.T., et al. (2012). Impact of cell type and epitope tagging on heterologous expression of G protein-coupled receptor: a systematic study on angiotensin type II receptor. PLoS One *7*: e47016.

Joffe, H., and Cohen, L.S. (1998). Estrogen, serotonin, and mood disturbance: where is the therapeutic bridge? Biol. Psychiatry *44*: 798–811.

Jonas, P., and Burnashev, N. (1995). Molecular mechanisms controlling calcium entry through AMPA-type glutamate receptor channels. Neuron *15*: 987–90.

Kajta, M., Rzemieniec, J., Litwa, E., Lason, W., Lenartowicz, M., Krzeptowski, W., et al. (2013). The key involvement of estrogen receptor β and G-protein-coupled receptor 30 in the neuroprotective action of daidzein. Neuroscience *238*: 345–60.

Kang, L., Zhang, X., Xie, Y., Tu, Y., Wang, D., Liu, Z., et al. (2010). Involvement of estrogen receptor variant ER-alpha36, not GPR30, in nongenomic estrogen signaling. Mol. Endocrinol. *24*: 709–21.

Karra, D., and Dahm, R. (2010). Transfection techniques for neuronal cells. J. Neurosci. *30*: 6171–7.

Karst, H., Berger, S., Turiault, M., Tronche, F., Schütz, G., and Joëls, M. (2005). Mineralocorticoid receptors are indispensable for nongenomic modulation of hippocampal glutamate transmission by corticosterone. Proc. Natl. Acad. Sci. U. S. A. *102*: 19204–7.

Katz, B., and Miledi, R. (1968). The role of calcium in neuromuscular facilitation. J. Physiol. *195*: 481–92.

Kerchner, G.A., and Nicoll, R.A. (2008). Silent synapses and the emergence of a postsynaptic mechanism for LTP. Nat. Rev. Neurosci. *9*: 813–25.

Kessels, H.W., and Malinow, R. (2009). Synaptic AMPA receptor plasticity and behavior. Neuron *61*: 340–50.

Kim, C.H., Chung, H.J., Lee, H.K., and Huganir, R.L. (2001). Interaction of the AMPA receptor subunit GluR2/3 with PDZ domains regulates hippocampal long-term depression. Proc. Natl. Acad. Sci. U. S. A. *98*: 11725–30.

Kim, H.J., Park, C.H., Roh, G.S., Kang, S.S., Cho, G.J., and Choi, W.S. (2002). Changes of steroidogenic acute regulatory protein mRNA expression in postnatal rat development. Dev. Brain Res. *139*: 247–54.

Kim, J.-I., Lee, H.-R., Sim, S., Baek, J., Yu, N.-K., Choi, J.-H., et al. (2011). PI3Kγ is required for NMDA receptor-dependent long-term depression and behavioral flexibility. Nat. Neurosci. *14*: 1447–54.

Kim, M.T., Soussou, W., Gholmieh, G., Ahuja, a, Tanguay, a, Berger, T.W., et al. (2006). 17beta-Estradiol potentiates field excitatory postsynaptic potentials within each subfield of the hippocampus with greatest potentiation of the associational/commissural afferents of CA3. Neuroscience *141*: 391–406.

Kimoto, T., Ishii, H., Higo, S., Hojo, Y., and Kawato, S. (2010). Semicomprehensive analysis of the postnatal age-related changes in the mRNA expression of sex steroidogenic enzymes and sex steroid receptors in the male rat hippocampus. Endocrinology *151*: 5795–806.

Kingston, A.E., Ornstein, P.L., Wright, R.A., Johnson, B.G., Mayne, N.G., Burnett, J.P., et al. (1998). LY341495 is a nanomolar potent and selective antagonist of group II metabotropic glutamate receptors. Neuropharmacology *37*: 1–12.

Klausberger, T., and Somogyi, P. (2008). Neuronal diversity and temporal dynamics: the unity of hippocampal circuit operations. Science *321*: 53–7.

Konkle, A.T.M., and McCarthy, M.M. (2011). Developmental time course of estradiol, testosterone, and dihydrotestosterone levels in discrete regions of male and female rat brain. Endocrinology *152*: 223–35.

Kosaka, Y., Quillinan, N., Bond, C., Traystman, R., Hurn, P., and Herson, P. (2012). GPER1/GPR30 activation improves neuronal survival following global cerebral ischemia induced by cardiac arrest in mice. Transl. Stroke Res. *3*: 500–507.

Kramár, E. a, Chen, L.Y., Brandon, N.J., Rex, C.S., Liu, F., Gall, C.M., et al. (2009). Cytoskeletal changes underlie estrogen's acute effects on synaptic transmission and plasticity. J. Neurosci. *29*: 12982–93.

Kretz, O., Fester, L., Wehrenberg, U., Zhou, L., Brauckmann, S., Zhao, S., et al. (2004). Hippocampal synapses depend on hippocampal estrogen synthesis. J. Neurosci. *24*: 5913–21.

Kristensen, A.S., Jenkins, M. a, Banke, T.G., Schousboe, A., Makino, Y., Johnson, R.C., et al. (2011). Mechanism of Ca2+/calmodulin-dependent kinase II regulation of AMPA receptor gating. Nat. Neurosci. *14*: 727–35.

Kuhn, J., Dina, O. a, Goswami, C., Suckow, V., Levine, J.D., and Hucho, T. (2008). GPR30 estrogen receptor agonists induce mechanical hyperalgesia in the rat. Eur. J. Neurosci. *27*: 1700–9.

Kuiper, G.G., Enmark, E., Pelto-Huikko, M., Nilsson, S., and Gustafsson, J.A. (1996). Cloning of a novel receptor expressed in rat prostate and ovary. Proc. Natl. Acad. Sci. U. S. A. *93*: 5925–30.

Kumar, A. (2010). Carbachol-induced long-term synaptic depression is enhanced during senescence at hippocampal CA3-CA1 synapses. J. Neurophysiol. *104*: 607–16.

Kuo, J., Hamid, N., Bondar, G., Prossnitz, E.R., and Micevych, P. (2010). Membrane estrogen receptors stimulate intracellular calcium release and progesterone synthesis in hypothalamic astrocytes. J. Neurosci. *30*: 12950–7.

Langer, G., Bader, B., Meoli, L., Isensee, J., Delbeck, M., Noppinger, P.R., et al. (2010). A critical review of fundamental controversies in the field of GPR30 research. Steroids *75*: 603–10.

Lappano, R., Rosano, C., Marco, P. De, Francesco, E.M. De, Pezzi, V., and Maggiolini, M. (2010). Estriol acts as a GPR30 antagonist in estrogen receptor-negative breast cancer cells. Mol. Cell. Endocrinol. *320*: 162–70.

Lebesgue, D., Chevaleyre, V., Zukin, R.S., and Etgen, A.M. (2009). Estradiol rescues neurons from global ischemia-induced cell death: multiple cellular pathways of neuroprotection. Steroids *74*: 555–61.

Lebesgue, D., Traub, M., Butte-Smith, M. De, Chen, C., Zukin, R.S., Kelly, M.J., et al. (2010). Acute administration of non-classical estrogen receptor agonists attenuates ischemia-induced hippocampal neuron loss in middle-aged female rats. PLoS One *5*: e8642.

Lee, H. (2006). AMPA Receptor Phosphorylation in Synaptic Plasticity: Insights from Knockin Mice. In The Dynamic Synapse: Molecular Methods in Ionotropic Receptor Biology, J. Kittler, and S. Moss, eds. (Boca Raton (FL): CRC Press),.

Lee, H.K., Kameyama, K., Huganir, R.L., and Bear, M.F. (1998). NMDA induces long-term synaptic depression and dephosphorylation of the GluR1 subunit of AMPA receptors in hippocampus. Neuron *21*: 1151–62.

Lee, S.J., Romeo, R.D., Svenningsson, P., Campomanes, C.R., Allen, P.B., Greengard, P., et al. (2004). Estradiol affects spinophilin protein differently in gonadectomized males and females. Neuroscience *127*: 983–8.

Lenhart, P.M., Broselid, S., Barrick, C.J., Leeb-Lundberg, L.F., and Caron, K.M. (2013). GPR30 Interacts with RAMP3 and Confers Sex-Dependent Cardioprotection. J. Mol. Endocrinol. 1–33.

Leskelä, T.T., Markkanen, P.M.H., Pietilä, E.M., Tuusa, J.T., and Petäjä-Repo, U.E. (2007). Opioid receptor pharmacological chaperones act by binding and stabilizing newly synthesized receptors in the endoplasmic reticulum. J. Biol. Chem. *282*: 23171–83.

Levin, E.R. (2009a). G protein-coupled receptor 30: estrogen receptor or collaborator? Endocrinology *150*: 1563–5.

Levin, E.R. (2009b). Plasma membrane estrogen receptors. Trends Endocrinol. Metab. *20*: 477–82.

Levin, E.R. (2011). Minireview: Extranuclear steroid receptors: roles in modulation of cell functions. Mol. Endocrinol. *25*: 377–84.

Liao, D., Hessler, N.A., and Malinow, R. (1995). Activation of postsynaptically silent synapses during pairing-induced LTP in CA1 region of hippocampal slice. Nature *375*: 400–404.

Lin, A.H.Y., Leung, G.P.H., Leung, S.W.S., Vanhoutte, P.M., and Man, R.Y.K. (2011). Genistein enhances relaxation of the spontaneously hypertensive rat aorta by transactivation of epidermal growth factor receptor following binding to membrane estrogen receptors-α and activation of a G protein-coupled, endothelial nitric oxide synthase-de. Pharmacol. Res. *63*: 181–9.

Lin, B.C., Suzawa, M., Blind, R.D., Tobias, S.C., Bulun, S.E., Scanlan, T.S., et al. (2009). Stimulating the GPR30 estrogen receptor with a novel tamoxifen analogue activates SF-1 and promotes endometrial cell proliferation. Cancer Res. *69*: 5415–23.

Lin, J.W., Ju, W., Foster, K., Lee, S.H., Ahmadian, G., Wyszynski, M., et al. (2000). Distinct molecular mechanisms and divergent endocytotic pathways of AMPA receptor internalization. Nat. Neurosci. *3*: 1282–90.

Lindsey, S.H., and Chappell, M.C. (2011). Evidence that the G protein-coupled membrane receptor GPR30 contributes to the cardiovascular actions of estrogen. Gend. Med. *8*: 343–54.

Lindsey, S.H., Yamaleyeva, L.M., Brosnihan, K.B., Gallagher, P.E., and Chappell, M.C. (2011). Estrogen receptor GPR30 reduces oxidative stress and proteinuria in the salt-sensitive female mRen2.Lewis rat. Hypertension *58*: 665–71.

Liston, C., and Gan, W. (2011). Glucocorticoids are critical regulators of dendritic spine development and plasticity in vivo. Proc. Natl. Acad. Sci. U. S. A. *108*: 16074–9.

Liu, F., Day, M., Muñiz, L.C., Bitran, D., Arias, R., Revilla-Sanchez, R., et al. (2008). Activation of estrogen receptor-beta regulates hippocampal synaptic plasticity and improves memory. Nat. Neurosci. *11*: 334–43.

Liu, S., Zhang, N., Guo, Y., Zhao, R., Shi, T., Feng, S., et al. (2012). G-protein-coupled receptor 30 mediates rapid neuroprotective effects of estrogen via depression of NR2B-containing NMDA receptors. J. Neurosci. *32*: 4887–900.

Liu, Y., Fang, C., Zou, P., Ma, Y.-N., Han, D.-N., Ji, Z.-H., et al. (2013). [Diverse expression of ER-α36, a novel variant of ER-α, in hippocampus and cortex of neonatal and adult rats.]. Sheng Li Xue Bao *65*: 263–268.

Lledo, P.M., Zhang, X., Südhof, T.C., Malenka, R.C., and Nicoll, R.A. (1998). Postsynaptic membrane fusion and long-term potentiation. Science *279*: 399–403.

Lu, W., Man, H., Ju, W., Trimble, W.S., MacDonald, J.F., and Wang, Y.T. (2001). Activation of synaptic NMDA receptors induces membrane insertion of new AMPA receptors and LTP in cultured hippocampal neurons. Neuron *29*: 243–54.

Lu, W., Shi, Y., Jackson, A.C., Bjorgan, K., During, M.J., Sprengel, R., et al. (2009). Subunit composition of synaptic AMPA receptors revealed by a single-cell genetic approach. Neuron *62*: 254–68.

Luine, V.N., and Frankfurt, M. (2012). Estrogens facilitate memory processing through membrane mediated mechanisms and alterations in spine density. Front. Neuroendocrinol. *33*: 388–402.

Luine, V.N., Jacome, L.F., and Maclusky, N.J. (2003). Rapid enhancement of visual and place memory by estrogens in rats. Endocrinology *144*: 2836–44.

Lüscher, C., Xia, H., Beattie, E.C., Carroll, R.C., Zastrow, M. von, Malenka, R.C., et al. (1999). Role of AMPA receptor cycling in synaptic transmission and plasticity. Neuron *24*: 649–58.

Madak-Erdogan, Z., Kieser, K.J., Kim, S.H., Komm, B., Katzenellenbogen, J. a, and Katzenellenbogen, B.S. (2008). Nuclear and extranuclear pathway inputs in the regulation of global gene expression by estrogen receptors. Mol. Endocrinol. *22*: 2116–27.

Magalhaes, A.C., Dunn, H., and Ferguson, S.S.G. (2012). Regulation of GPCR activity, trafficking and localization by GPCR-interacting proteins. Br. J. Pharmacol. *165*: 1717–36.

Magariños, a M., Li, C.J., Gal Toth, J., Bath, K.G., Jing, D., Lee, F.S., et al. (2011). Effect of brain-derived neurotrophic factor haploinsufficiency on stress-induced remodeling of hippocampal neurons. Hippocampus *21*: 253–64.

Maggio, N., and Segal, M. (2009). Differential modulation of long-term depression by acute stress in the rat dorsal and ventral hippocampus. J. Neurosci. *29*: 8633–8.

Maggio, N., and Segal, M. (2012). Cellular basis of a rapid effect of mineralocorticosteroid receptors activation on LTP in ventral hippocampal slices. Hippocampus *22*: 267–75.

Maggiolini, M., and Picard, D. (2010). The unfolding stories of GPR30, a new membrane-bound estrogen receptor. J. Endocrinol. *204*: 105–14.

Maggiolini, M., Vivacqua, A., Fasanella, G., Recchia, A.G., Sisci, D., Pezzi, V., et al. (2004). The G protein-coupled receptor GPR30 mediates c-fos up-regulation by 17beta-estradiol and phytoestrogens in breast cancer cells. J. Biol. Chem. *279*: 27008–16.

Maiti, K., Paul, J.W., Read, M., Chan, E.C., Riley, S.C., Nahar, P., et al. (2011). G-1-activated membrane estrogen receptors mediate increased contractility of the human myometrium. Endocrinology *152*: 2448–55.

Majewska, M.D. (2007). Steroids and ion channels in evolution: from bacteria to synapses and mind. Evolutionary role of steroid regulation of GABA(A) receptors. Acta Neurobiol. Exp. (Wars). *67*: 219–33.

Malenka, R.C. (2003). Synaptic plasticity and AMPA receptor trafficking. Ann. N. Y. Acad. Sci. *1003*: 1–11.

Malenka, R.C., and Bear, M.F. (2004). LTP and LTD: an embarrassment of riches. Neuron *44*: 5–21.

Malinow, R., and Malenka, R.C. (2002). AMPA receptor trafficking and synaptic plasticity. Annu. Rev. Neurosci. *25*: 103–26.

Man, H.Y., Lin, J.W., Ju, W.H., Ahmadian, G., Liu, L., Becker, L.E., et al. (2000). Regulation of AMPA receptor-mediated synaptic transmission by clathrin-dependent receptor internalization. Neuron *25*: 649–662.

Man, H.-Y., Sekine-Aizawa, Y., and Huganir, R.L. (2007). Regulation of {alpha}-amino-3-hydroxy-5-methyl-4-isoxazolepropionic acid receptor trafficking through PKA phosphorylation of the Glu receptor 1 subunit. Proc. Natl. Acad. Sci. U. S. A. *104*: 3579–84.

Mårtensson, U.E. a, Salehi, S.A., Windahl, S., Gomez, M.F., Swärd, K., Daszkiewicz-Nilsson, J., et al. (2009). Deletion of the G protein-coupled receptor 30 impairs glucose tolerance, reduces bone growth, increases blood pressure, and eliminates estradiol-stimulated insulin release in female mice. Endocrinology *150*: 687–98.

Martin, S., Henley, J.M., Holman, D., Zhou, M., Wiegert, O., Spronsen, M. van, et al. (2009). Corticosterone alters AMPAR mobility and facilitates bidirectional synaptic plasticity. PLoS One *4*: e4714.

Matsuda, K., Sakamoto, H., Mori, H., Hosokawa, K., Kawamura, A., Itose, M., et al. (2008). Expression and intracellular distribution of the G protein-coupled receptor 30 in rat hippocampal formation. Neurosci. Lett. *441*: 94–9.

Mayer, M.L., Westbrook, G.L., and Guthrie, P.B. (1984). Voltage-dependent block by Mg2+ of NMDA responses in spinal cord neurones. Nature *309*: 261–263.

McAllister, C.E., Creech, R.D., Kimball, P. a, Muma, N. a, and Li, Q. (2012). GPR30 is necessary for estradiol-induced desensitization of 5-HT1A receptor signaling in the paraventricular nucleus of the rat hypothalamus. Psychoneuroendocrinology *37*: 1248–60.

McCarthy, M.M. (2008). Estradiol and the developing brain. Physiol. Rev. *88*: 91–124.

McDonald, N. a, Henstridge, C.M., Connolly, C.N., and Irving, A.J. (2007a). Generation and functional characterization of fluorescent, N-terminally tagged CB1 receptor chimeras for live-cell imaging. Mol. Cell. Neurosci. *35*: 237–48.

McDonald, N.A., Henstridge, C.M., Connolly, C.N., and Irving, A.J. (2007b). An essential role for constitutive endocytosis, but not activity, in the axonal targeting of the CB1 cannabinoid receptor. Mol. Pharmacol. *71*: 976–84.

McEwen, B.S. (2001). Invited review: Estrogens effects on the brain: multiple sites and molecular mechanisms. J. Appl. Physiol. *91*: 2785–801.

Megías, M., Emri, Z., Freund, T.F., and Gulyás, A.I. (2001). Total number and distribution of inhibitory and excitatory synapses on hippocampal CA1 pyramidal cells. Neuroscience *102*: 527–40.

Meitzen, J., Grove, D.D., and Mermelstein, P.G. (2012). The organizational and aromatization hypotheses apply to rapid, nonclassical hormone action: neonatal masculinization eliminates rapid estradiol action in female hippocampal neurons. Endocrinology *153*: 4616–21.

Meitzen, J., and Mermelstein, P.G. (2011). Estrogen receptors stimulate brain region specific metabotropic glutamate receptors to rapidly initiate signal transduction pathways. J. Chem. Neuroanat. *42*: 236–41.

Milner, A.J., Cummings, D.M., Spencer, J.P., and Murphy, K.P.S.J. (2004). Bi-directional plasticity and age-dependent long-term depression at mouse CA3-CA1 hippocampal synapses. Neurosci. Lett. *367*: 1–5.

Milner, T. a, Ayoola, K., Drake, C.T., Herrick, S.P., Tabori, N.E., McEwen, B.S., et al. (2005). Ultrastructural localization of estrogen receptor beta immunoreactivity in the rat hippocampal formation. J. Comp. Neurol. *491*: 81–95.

Milner, T. a, McEwen, B.S., Hayashi, S., Li, C.J., Reagan, L.P., and Alves, S.E. (2001). Ultrastructural evidence that hippocampal alpha estrogen receptors are located at extranuclear sites. J. Comp. Neurol. *429*: 355–71.

Mitra, S.W. (2003). Immunolocalization of Estrogen Receptor beta in the Mouse Brain: Comparison with Estrogen Receptor alpha. Endocrinology *144*: 2055–2067.

Monick, M.M., Powers, L.S., Gross, T.J., Flaherty, D.M., Barrett, C.W., and Hunninghake, G.W. (2006). Active ERK contributes to protein translation by preventing JNK-dependent inhibition of protein phosphatase 1. J. Immunol. *177*: 1636–45.

Monyer, H., Burnashev, N., Laurie, D.J., Sakmann, B., and Seeburg, P.H. (1994). Developmental and regional expression in the rat brain and functional properties of four NMDA receptors. Neuron *12*: 529–40.

Monyer, H., Sprengel, R., Schoepfer, R., Herb, A., Higuchi, M., Lomeli, H., et al. (1992). Heteromeric NMDA receptors: molecular and functional distinction of subtypes. Science *256*: 1217–21.

Mosbacher, J., Schoepfer, R., Monyer, H., Burnashev, N., Seeburg, P.H., and Ruppersberg, J.P. (1994). A molecular determinant for submillisecond desensitization in glutamate receptors. Science *266*: 1059–62.

Moult, P.R., Corrêa, S. a L., Collingridge, G.L., Fitzjohn, S.M., and Bashir, Z.I. (2008). Co-activation of p38 mitogen-activated protein kinase and protein tyrosine phosphatase underlies metabotropic glutamate receptor-dependent long-term depression. J. Physiol. *586*: 2499–510.

Moult, P.R., Cross, A., Santos, S.D., Carvalho, A.-L., Lindsay, Y., Connolly, C.N., et al. (2010). Leptin regulates AMPA receptor trafficking via PTEN inhibition. J. Neurosci. *30*: 4088–101.

Moult, P.R., Gladding, C.M., Sanderson, T.M., Fitzjohn, S.M., Bashir, Z.I., Molnar, E., et al. (2006). Tyrosine phosphatases regulate AMPA receptor trafficking during metabotropic glutamate receptor-mediated long-term depression. J. Neurosci. *26*: 2544–54.

Moult, P.R., and Harvey, J. (2011). NMDA receptor subunit composition determines the polarity of leptin-induced synaptic plasticity. Neuropharmacology *61*: 924–36.

Mukai, H., Tsurugizawa, T., Murakami, G., Kominami, S., Ishii, H., Ogiue-Ikeda, M., et al. (2007). Rapid modulation of long-term depression and spinogenesis via synaptic estrogen receptors in hippocampal principal neurons. J. Neurochem. *100*: 950–67.

Muller, R.E., Johnston, T.C., Traish, A.M., and Wotiz, H.H. (1979). Studies on the mechanism of estradiol uptake by rat uterine cells and on estradiol binding to uterine plasma membranes. Adv. Exp. Med. Biol. *117*: 401–421.

Munro, S., and Pelham, H.R.B. (1987). A C-terminal signal prevents secretion of luminal ER proteinsMunro. Cell *48*: 899–907.

Murphy, D.D., and Segal, M. (1996). Regulation of dendritic spine density in cultured rat hippocampal neurons by steroid hormones. J. Neurosci. *16*: 4059–68.

Nilsson, B.-O., Olde, B., and Leeb-Lundberg, L.M.F. (2011). G protein-coupled oestrogen receptor 1 (GPER1)/GPR30: a new player in cardiovascular and metabolic oestrogenic signalling. Br. J. Pharmacol. *163*: 1131–9.

Nishikawa, K., and MacIver, M.B. (2000). Excitatory synaptic transmission mediated by NMDA receptors is more sensitive to isoflurane than are non-NMDA receptor-mediated responses. Anesthesiology *92*: 228–36.

Niswender, C.M., and Conn, P.J. (2010). Metabotropic glutamate receptors: physiology, pharmacology, and disease. Annu. Rev. Pharmacol. Toxicol. *50*: 295–322.

Noel, S.D., Keen, K.L., Baumann, D.I., Filardo, E.J., and Terasawa, E. (2009). Involvement of G protein-coupled receptor 30 (GPR30) in rapid action of estrogen in primate LHRH neurons. Mol. Endocrinol. *23*: 349–59.

Nosyreva, E.D., and Huber, K.M. (2005). Developmental switch in synaptic mechanisms of hippocampal metabotropic glutamate receptor-dependent long-term depression. J. Neurosci. *25*: 2992–3001.

Notas, G., Kampa, M., Pelekanou, V., and Castanas, E. (2012). Interplay of estrogen receptors and GPR30 for the regulation of early membrane initiated transcriptional effects: A pharmacological approach. Steroids *77*: 943–50.

O'Dowd, B.F., Nguyen, T., Marchese, a, Cheng, R., Lynch, K.R., Heng, H.H., et al. (1998). Discovery of three novel G-protein-coupled receptor genes. Genomics *47*: 310–3.

O'Keefe, J. a, Li, Y., Burgess, L.H., and Handa, R.J. (1995). Estrogen receptor mRNA alterations in the developing rat hippocampus. Brain Res. Mol. Brain Res. *30*: 115–24.

Ogiue-Ikeda, M., Tanabe, N., Mukai, H., Hojo, Y., Murakami, G., Tsurugizawa, T., et al. (2008). Rapid modulation of synaptic plasticity by estrogens as well as endocrine disrupters in hippocampal neurons. Brain Res. Rev. *57*: 363–75.

Olde, B., and Leeb-Lundberg, L.M.F. (2009). GPR30/GPER1: searching for a role in estrogen physiology. Trends Endocrinol. Metab. *20*: 409–16.

Ooishi, Y., Kawato, S., Hojo, Y., Hatanaka, Y., Higo, S., Murakami, G., et al. (2012a). Modulation of synaptic plasticity in the hippocampus by hippocampus-derived estrogen and androgen. J. Steroid Biochem. Mol. Biol. *131*: 37–51.

Ooishi, Y., Mukai, H., Hojo, Y., Murakami, G., Hasegawa, Y., Shindo, T., et al. (2012b). Estradiol rapidly rescues synaptic transmission from corticosterone-induced suppression via synaptic/extranuclear steroid receptors in the hippocampus. Cereb. Cortex *22*: 926–36.

Osborne, C.K., Wakeling, a, and Nicholson, R.I. (2004). Fulvestrant: an oestrogen receptor antagonist with a novel mechanism of action. Br. J. Cancer *90 Suppl 1*: S2–6.

Otto, C., Fuchs, I., Kauselmann, G., Kern, H., Zevnik, B., Andreasen, P., et al. (2009). GPR30 does not mediate estrogenic responses in reproductive organs in mice. Biol. Reprod. *80*: 34–41.

Otto, C., Rohde-Schulz, B., Schwarz, G., Fuchs, I., Klewer, M., Brittain, D., et al. (2008). G protein-coupled receptor 30 localizes to the endoplasmic reticulum and is not activated by estradiol. Endocrinology *149*: 4846–56.

Owman, C., Blay, P., Nilsson, C., and Lolait, S.J. (1996). Cloning of human cDNA encoding a novel heptahelix receptor expressed in Burkitt's lymphoma and widely distributed in brain and peripheral tissues. Biochem. Biophys. Res. Commun. *228*: 285–92.

Pagano, a, Rovelli, G., Mosbacher, J., Lohmann, T., Duthey, B., Stauffer, D., et al. (2001). C-terminal interaction is essential for surface trafficking but not for heteromeric assembly of GABA(b) receptors. J. Neurosci. *21*: 1189–202.

Palmer, M.J., Irving, a J., Seabrook, G.R., Jane, D.E., and Collingridge, G.L. (1998). The group I mGlu receptor agonist DHPG induces a novel form of LTD in the CA1 region of the hippocampus. Neuropharmacology *36*: 1517–32.

Pang, Y., Dong, J., and Thomas, P. (2008). Estrogen signaling characteristics of Atlantic croaker G protein-coupled receptor 30 (GPR30) and evidence it is involved in maintenance of oocyte meiotic arrest. Endocrinology *149*: 3410–26.

Park, M., Penick, E.C., Edwards, J.G., Kauer, J. a, and Ehlers, M.D. (2004). Recycling endosomes supply AMPA receptors for LTP. Science *305*: 1972–5.

Pavlides, C., and McEwen, B.S. (1999). Effects of mineralocorticoid and glucocorticoid receptors on long-term potentiation in the CA3 hippocampal field. Brain Res. *851*: 204–14.

Pawlak, R., Rao, B.S.S., Melchor, J.P., Chattarji, S., McEwen, B., and Strickland, S. (2005). Tissue plasminogen activator and plasminogen mediate stress-induced decline of neuronal and cognitive functions in the mouse hippocampus. Proc. Natl. Acad. Sci. U. S. A. *102*: 18201–6.

Pedram, A., Razandi, M., and Levin, E.R. (2006). Nature of functional estrogen receptors at the plasma membrane. Mol. Endocrinol. *20*: 1996–2009.

Petäjä-Repo, U.E., Hogue, M., Bhalla, S., Laperrière, A., Morello, J.-P., and Bouvier, M. (2002). Ligands act as pharmacological chaperones and increase the efficiency of delta opioid receptor maturation. EMBO J. *21*: 1628–37.

Péterfi, Z., Urbán, G.M., Papp, O.I., Németh, B., Monyer, H., Szabó, G., et al. (2012). Endocannabinoid-mediated long-term depression of afferent excitatory synapses in hippocampal pyramidal cells and GABAergic interneurons. J. Neurosci. *32*: 14448–63.

Peyton, C., and Thomas, P. (2011). Involvement of epidermal growth factor receptor signaling in estrogen inhibition of oocyte maturation mediated through the G protein-coupled estrogen receptor (Gper) in zebrafish (Danio rerio). Biol. Reprod. *85*: 42–50.

Pickard, L., Noël, J., Duckworth, J.K., Fitzjohn, S.M., Henley, J.M., Collingridge, G.L., et al. (2001). Transient synaptic activation of NMDA receptors leads to the insertion of native AMPA receptors at hippocampal neuronal plasma membranes. Neuropharmacology *41*: 700–13.

Pickard, L., Noël, J., Henley, J.M., Collingridge, G.L., and Molnar, E. (2000). Developmental changes in synaptic AMPA and NMDA receptor distribution and AMPA receptor subunit composition in living hippocampal neurons. J. Neurosci. *20*: 7922–31.

Plassart-Schiess, E., and Baulieu, E.E. (2001). Neurosteroids: recent findings. Brain Res. Brain Res. Rev. *37*: 133–40.

Plath, N., Ohana, O., Dammermann, B., Errington, M.L., Schmitz, D., Gross, C., et al. (2006). Arc/Arg3.1 is essential for the consolidation of synaptic plasticity and memories. Neuron *52*: 437–44.

Popoli, M., Yan, Z., McEwen, B.S., and Sanacora, G. (2012). The stressed synapse: the impact of stress and glucocorticoids on glutamate transmission. Nat. Rev. Neurosci. *13*: 22–37.

Potapova, T. a, Sivakumar, S., Flynn, J.N., Li, R., and Gorbsky, G.J. (2011). Mitotic progression becomes irreversible in prometaphase and collapses when Wee1 and Cdc25 are inhibited. Mol. Biol. Cell *22*: 1191–206.

Powis, G., Bonjouklian, R., Berggren, M.M., Gallegos, A., Abraham, R., Ashendel, C., et al. (1994). Wortmannin, a potent and selective inhibitor of phosphatidylinositol-3-kinase. Cancer Res. *54*: 2419–23.

Prange-Kiel, J., Wehrenberg, U., Jarry, H., and Rune, G.M. (2003). Para/autocrine regulation of estrogen receptors in hippocampal neurons. Hippocampus *13*: 226–34.

Prossnitz, E.R., Arterburn, J.B., Smith, H.O., Oprea, T.I., Sklar, L. a, and Hathaway, H.J. (2008a). Estrogen signaling through the transmembrane G protein-coupled receptor GPR30. Annu. Rev. Physiol. *70*: 165–90.

Prossnitz, E.R., and Barton, M. (2011). The G-protein-coupled estrogen receptor GPER in health and disease. Nat. Rev. Endocrinol. *7*: 715–26.

Prossnitz, E.R., Oprea, T.I., Sklar, L.A., and Arterburn, J.B. (2008b). The ins and outs of GPR30: a transmembrane estrogen receptor. J. Steroid Biochem. Mol. Biol. *109*: 350–3.

Quinn, J. a, Graeber, C.T., Frackelton, a R., Kim, M., Schwarzbauer, J.E., and Filardo, E.J. (2009). Coordinate regulation of estrogen-mediated fibronectin matrix assembly and epidermal growth factor receptor transactivation by the G protein-coupled receptor, GPR30. Mol. Endocrinol. *23*: 1052–64.

Rego, J.L. Do, Seong, J.Y., Burel, D., Leprince, J., Luu-The, V., Tsutsui, K., et al. (2009). Neurosteroid biosynthesis: enzymatic pathways and neuroendocrine regulation by neurotransmitters and neuropeptides. Front. Neuroendocrinol. *30*: 259–301.

Revankar, C.M., Cimino, D.F., Sklar, L. a, Arterburn, J.B., and Prossnitz, E.R. (2005). A transmembrane intracellular estrogen receptor mediates rapid cell signaling. Science *307*: 1625–30.

Revankar, C.M., Mitchell, H.D., Field, A.S., Burai, R., Corona, C., Ramesh, C., et al. (2007). Synthetic estrogen derivatives demonstrate the functionality of intracellular GPR30. ACS Chem. Biol. *2*: 536–44.

Reyes-Harde, M., Potter, B. V, Galione, A., and Stanton, P.K. (1999). Induction of hippocampal LTD requires nitric-oxide-stimulated PKG activity and Ca2+ release from cyclic ADP-ribose-sensitive stores. J. Neurophysiol. *82*: 1569–76.

Rissman, E.F., Heck, A.L., Leonard, J.E., Shupnik, M.A., and Gustafsson, J.-A. (2002). Disruption of estrogen receptor beta gene impairs spatial learning in female mice. Proc. Natl. Acad. Sci. U. S. A. *99*: 3996–4001.

Roepke, T. a, Qiu, J., Bosch, M. a, Rønnekleiv, O.K., and Kelly, M.J. (2009). Cross-talk between membrane-initiated and nuclear-initiated oestrogen signalling in the hypothalamus. J. Neuroendocrinol. *21*: 263–70.

Rosenbaum, D.M., Rasmussen, S.G.F., and Kobilka, B.K. (2009). The structure and function of G-protein-coupled receptors. Nature *459*: 356–63.

Rossi, D. V, Dai, Y., Thomas, P., Carrasco, G. a, DonCarlos, L.L., Muma, N. a, et al. (2010). Estradiol-induced desensitization of 5-HT1A receptor signaling in the paraventricular nucleus of the hypothalamus is independent of estrogen receptor-beta. Psychoneuroendocrinology *35*: 1023–33.

Rousseaux, C.G., Starling, E.H., Dale, H., and Elliot, T.R. (2008). A Review of Glutamate Receptors I: Current Understanding of Their Biology. J. Toxicol. Pathol. *21*: 25–51.

Rovati, G.E., Capra, V., and Neubig, R.R. (2007). The highly conserved DRY motif of class A G protein-coupled receptors: beyond the ground state. Mol. Pharmacol. *71*: 959–64.

Rozov, A., Sprengel, R., and Seeburg, P.H. (2012). GluA2-lacking AMPA receptors in hippocampal CA1 cell synapses: evidence from gene-targeted mice. Front. Mol. Neurosci. *5*: 22.

Rudick, C.N., and Woolley, C.S. (2003). Selective estrogen receptor modulators regulate phasic activation of hippocampal CA1 pyramidal cells by estrogen. Endocrinology *144*: 179–87.

Ruiz-Palmero, I., Hernando, M., Garcia-Segura, L.M., and Arevalo, M.-A. (2013). G protein-coupled estrogen receptor is required for the neuritogenic mechanism of 17β-estradiol in developing hippocampal neurons. Mol. Cell. Endocrinol. *372*: 105–15.

Sakamoto, H., Matsuda, K., Hosokawa, K., Nishi, M., Morris, J.F., Prossnitz, E.R., et al. (2007). Expression of G protein-coupled receptor-30, a G protein-coupled membrane estrogen receptor, in oxytocin neurons of the rat paraventricular and supraoptic nuclei. Endocrinology *148*: 5842–50.

Sandén, C., Broselid, S., Cornmark, L., Andersson, K., Daszkiewicz-Nilsson, J., Mårtensson, U.E.A., et al. (2011). G protein-coupled estrogen receptor 1/G protein-coupled receptor 30 localizes in the plasma membrane and traffics intracellularly on cytokeratin intermediate filaments. Mol. Pharmacol. *79*: 400–10.

Sandstrom, N.J., and Williams, C.L. (2004). Spatial memory retention is enhanced by acute and continuous estradiol replacement. Horm. Behav. *45*: 128–35.

Santos, S.D., Carvalho, a L., Caldeira, M. V, and Duarte, C.B. (2009). Regulation of AMPA receptors and synaptic plasticity. Neuroscience *158*: 105–25.

Sanz-Clemente, A., Nicoll, R. a, and Roche, K.W. (2013). Diversity in NMDA receptor composition: many regulators, many consequences. Neuroscientist *19*: 62–75.

Schassen, C. von, Fester, L., Prange-Kiel, J., Lohse, C., Huber, C., Böttner, M., et al. (2006). Oestrogen synthesis in the hippocampus: role in axon outgrowth. J. Neuroendocrinol. *18*: 847–56.

Scoville, W.B., and Milner, B. (1957). LOSS OF RECENT MEMORY AFTER BILATERAL HIPPOCAMPAL LESIONS. J. Neurol. Neurosurg. Psychiatry *20*: 11–21.

Selcher, J.C., Weeber, E.J., Christian, J., Nekrasova, T., Landreth, G.E., and Sweatt, J.D. (2003). A role for ERK MAP kinase in physiologic temporal integration in hippocampal area CA1. Learn. Mem. *10*: 26–39.

Shankar, G.M., Bloodgood, B.L., Townsend, M., Walsh, D.M., Selkoe, D.J., and Sabatini, B.L. (2007). Natural oligomers of the Alzheimer amyloid-beta protein induce reversible synapse loss by modulating an NMDA-type glutamate receptor-dependent signaling pathway. J. Neurosci. *27*: 2866–75.

Shanley, L.J., O'Malley, D., Irving, a J., Ashford, M.L., and Harvey, J. (2002). Leptin inhibits epileptiform-like activity in rat hippocampal neurones via PI 3-kinase-driven activation of BK channels. J. Physiol. *545*: 933–944.

Shansky, R.M., and Lipps, J. (2013). Stress-induced cognitive dysfunction: hormone-neurotransmitter interactions in the prefrontal cortex. Front. Hum. Neurosci. *7*: 123.

Sharrow, K.M., Kumar, A., and Foster, T.C. (2002). Calcineurin as a potential contributor in estradiol regulation of hippocampal synaptic function. Neuroscience *113*: 89–97.

Sheng, M., Cummings, J., Roldan, L.A., Jan, Y.N., and Jan, L.Y. (1994). Changing subunit composition of heteromeric NMDA receptors during development of rat cortex. Nature *368*: 144–7.

Shepherd, J.D., and Huganir, R.L. (2007). The cell biology of synaptic plasticity: AMPA receptor trafficking. Annu. Rev. Cell Dev. Biol. *23*: 613–43.

Shi, Y., Liu, X., Zhu, P., Li, J., Sham, K.W.Y., Cheng, S.H., et al. (2013). G-protein-coupled estrogen receptor 1 is involved in brain development during zebrafish (Danio rerio) embryogenesis. Biochem. Biophys. Res. Commun.

Shiau, a K., Barstad, D., Loria, P.M., Cheng, L., Kushner, P.J., Agard, D. a, et al. (1998). The structural basis of estrogen receptor/coactivator recognition and the antagonism of this interaction by tamoxifen. Cell *95*: 927–37.

Shikano, S., and Li, M. (2003). Membrane receptor trafficking: evidence of proximal and distal zones conferred by two independent endoplasmic reticulum localization signals. Proc. Natl. Acad. Sci. U. S. A. *100*: 5783–8.

Shinoda, Y., Tanaka, T., Tominaga-Yoshino, K., and Ogura, A. (2010). Persistent synapse loss induced by repetitive LTD in developing rat hippocampal neurons. PLoS One *5*: e10390.

Shiroma, S., Yamaguchi, T., and Kometani, K. (2005). Effects of 17beta-estradiol on chemically induced long-term depression. Neuropharmacology *49*: 97–102.

Shughrue, P.J., Lane, M. V, and Merchenthaler, I. (1997). Comparative distribution of estrogen receptor-alpha and -beta mRNA in the rat central nervous system. J. Comp. Neurol. *388*: 507–25.

Shumaker, S. a, Legault, C., Kuller, L., Rapp, S.R., Thal, L., Lane, D.S., et al. (2004). Conjugated equine estrogens and incidence of probable dementia and mild cognitive impairment in postmenopausal women: Women's Health Initiative Memory Study. JAMA *291*: 2947–58.

Sierra, A., Lavaque, E., Perez-Martin, M., Azcoitia, I., Hales, D.B., and Garcia-Segura, L.M. (2003). Steroidogenic acute regulatory protein in the rat brain: cellular distribution, developmental regulation and overexpression after injury. Eur. J. Neurosci. *18*: 1458–1467.

Sinchak, K., and Wagner, E.J. (2012). Estradiol signaling in the regulation of reproduction and energy balance. Front. Neuroendocrinol. *33*: 342–63.

Smejkalova, T., and Woolley, C.S. (2010). Estradiol acutely potentiates hippocampal excitatory synaptic transmission through a presynaptic mechanism. J. Neurosci. *30*: 16137–48.

Smith, M.S., Freeman, M.E., and Neill, J.D. (1975). The Control of Progesterone Secretion During the Estrous Cycle and Early Pseudopregnancy in the Rat: Prolactin, Gonadotropin and Steroid Levels Associated with Rescue of the Corpus Luteum of Pseudopregnancy. Endocrinology *96*: 219–226.

Snyder, E.M., Philpot, B.D., Huber, K.M., Dong, X., Fallon, J.R., and Bear, M.F. (2001). Internalization of ionotropic glutamate receptors in response to mGluR activation. Nat. Neurosci. *4*: 1079–85.

Solum, D.T., and Handa, R.J. (2001). Localization of estrogen receptor alpha (ER alpha) in pyramidal neurons of the developing rat hippocampus. Brain Res. Dev. Brain Res. *128*: 165–75.

Sommer, B., Keinänen, K., Verdoorn, T. a, Wisden, W., Burnashev, N., Herb, a, et al. (1990). Flip and flop: a cell-specific functional switch in glutamate-operated channels of the CNS. Science *249*: 1580–5.

Sommer, B., Köhler, M., Sprengel, R., and Seeburg, P.H. (1991). RNA editing in brain controls a determinant of ion flow in glutamate-gated channels. Cell *67*: 11–9.

Spencer-Segal, J.L., Tsuda, M.C., Mattei, L., Waters, E.M., Romeo, R.D., Milner, T. a, et al. (2012). Estradiol acts via estrogen receptors alpha and beta on pathways important for synaptic plasticity in the mouse hippocampal formation. Neuroscience *202*: 131–46.

Srivastava, D.P., and Evans, P.D. (2013). GPER 1: trials and tribulations of a Membrane Oestrogen Receptor. J. Neuroendocrinol.

Srivastava, D.P., Waters, E.M., Mermelstein, P.G., Kramár, E. a, Shors, T.J., and Liu, F. (2011). Rapid estrogen signaling in the brain: implications for the fine-tuning of neuronal circuitry. J. Neurosci. *31*: 16056–63.

Srivastava, D.P., Woolfrey, K.M., Woolfrey, K., Jones, K.A., Shum, C.Y., Lash, L.L., et al. (2008). Rapid enhancement of two-step wiring plasticity by estrogen and NMDA receptor activity. Proc. Natl. Acad. Sci. U. S. A. *105*: 14650–5.

Strandberg, J., and Gustafsson, B. (2011). Critical and complex role of N-methyl-D-aspartate receptors in long-term depression at CA3-CA1 synapses in the developing hippocampus. Neuroscience *192*: 54–66.

Strandberg, J., Wasling, P., and Gustafsson, B. (2009). Modulation of low-frequency-induced synaptic depression in the developing CA3-CA1 hippocampal synapses by NMDA and metabotropic glutamate receptor activation. J. Neurophysiol. *101*: 2252–62.

Strasser, A., Wittmann, H.-J., Buschauer, A., Schneider, E.H., and Seifert, R. (2013). Species-dependent activities of G-protein-coupled receptor ligands: lessons from histamine receptor orthologs. Trends Pharmacol. Sci. *34*: 13–32.

Strom, J.O., Theodorsson, A., and Theodorsson, E. (2011). Hormesis and Female Sex Hormones. Pharmaceuticals *4*: 726–740.

Südhof, T.C. (1990). The structure of the human synapsin I gene and protein. J. Biol. Chem. *265*: 7849–52.

Südhof, T.C., and Rothman, J.E. (2009). Membrane fusion: grappling with SNARE and SM proteins. Science *323*: 474–7.

Sun, J., Huang, Y.R., Harrington, W.R., Sheng, S., Katzenellenbogen, J.A., and Katzenellenbogen, B.S. (2002). Antagonists selective for estrogen receptor alpha. Endocrinology *143*: 941–7.

Tadevosyan, A., Vaniotis, G., Allen, B.G., Hébert, T.E., and Nattel, S. (2012). G protein-coupled receptor signalling in the cardiac nuclear membrane: evidence and possible roles in physiological and pathophysiological function. J. Physiol. *590*: 1313–30.

Takada, Y., Kato, C., Kondo, S., Korenaga, R., and Ando, J. (1997). Cloning of cDNAs encoding G protein-coupled receptor expressed in human endothelial cells exposed to fluid shear stress. Biochem. Biophys. Res. Commun. *240*: 737–741.

Takanami, K., Sakamoto, H., Matsuda, K.-I., Hosokawa, K., Nishi, M., Prossnitz, E.R., et al. (2010). Expression of G protein-coupled receptor 30 in the spinal somatosensory system. Brain Res. *1310*: 17–28.

Terasawa, E., and Kenealy, B.P. (2012). Neuroestrogen, rapid action of estradiol, and GnRH neurons. Front. Neuroendocrinol. *33*: 364–75.

Teyler, T.J., Vardaris, R.M., Lewis, D., and Rawitch, A.B. (1980). Gonadal steroids: effects on excitability of hippocampal pyramidal cells. Science *209*: 1017–8.

Thiels, E., Kanterewicz, B.I., Norman, E.D., Trzaskos, J.M., and Klann, E. (2002). Long-term depression in the adult hippocampus in vivo involves activation of extracellular signal-regulated kinase and phosphorylation of Elk-1. J. Neurosci. *22*: 2054–62.

Thomas, G.M., and Huganir, R.L. (2004). MAPK cascade signalling and synaptic plasticity. Nat. Rev. Neurosci. *5*: 173–83.

Thomas, P., and Dong, J. (2006). Binding and activation of the seven-transmembrane estrogen receptor GPR30 by environmental estrogens: a potential novel mechanism of endocrine disruption. J. Steroid Biochem. Mol. Biol. *102*: 175–9.

Thomas, P., Pang, Y., Filardo, E.J., and Dong, J. (2005). Identity of an estrogen membrane receptor coupled to a G protein in human breast cancer cells. Endocrinology *146*: 624–32.

Tiano, J.P., and Mauvais-Jarvis, F. (2012). Importance of oestrogen receptors to preserve functional β-cell mass in diabetes. Nat. Rev. Endocrinol. *8*: 342–51.

Timmers, R.J., Granneman, J.C., Lambert, J.G., and Oordt, P.G. Van (1988). Estrogen-2-hydroxylase in the brain of the male African catfish, Clarias gariepinus. Gen. Comp. Endocrinol. *72*: 190–203.

Toran-Allerand, C.D. (2005). Estrogen and the brain: beyond ER-alpha, ER-beta, and 17beta-estradiol. Ann. N. Y. Acad. Sci. *1052*: 136–44.

Towart, L. a, Alves, S.E., Znamensky, V., Hayashi, S., McEwen, B.S., and Milner, T. a (2003). Subcellular relationships between cholinergic terminals and estrogen receptor-alpha in the dorsal hippocampus. J. Comp. Neurol. *463*: 390–401.

Traynelis, S.F., Wollmuth, L.P., McBain, C.J., Menniti, F.S., Vance, K.M., Ogden, K.K., et al. (2010). Glutamate receptor ion channels: structure, regulation, and function. Pharmacol. Rev. *62*: 405–96.

Tuo, B., Wen, G., Wang, X., Xu, J., Xie, R., Liu, X., et al. (2012). Estrogen potentiates prostaglandin E_2-stimulated duodenal mucosal HCO_3^- secretion in mice. Am. J. Physiol. Endocrinol. Metab. *303*: E111–21.

Vasudevan, N., and Pfaff, D.W. (2007). Membrane-initiated actions of estrogens in neuroendocrinology: emerging principles. Endocr. Rev. *28*: 1–19.

Vierk, R., Glassmeier, G., Zhou, L., Brandt, N., Fester, L., Dudzinski, D., et al. (2012). Aromatase inhibition abolishes LTP generation in female but not in male mice. J. Neurosci. *32*: 8116–26.

Vischer, H.F., Watts, A.O., Nijmeijer, S., and Leurs, R. (2011). G protein-coupled receptors: walking hand-in-hand, talking hand-in-hand? Br. J. Pharmacol. *163*: 246–60.

Vivacqua, A., Bonofiglio, D., Recchia, A.G., Musti, A.M., Picard, D., Andò, S., et al. (2006). The G protein-coupled receptor GPR30 mediates the proliferative effects induced by 17beta-estradiol and hydroxytamoxifen in endometrial cancer cells. Mol. Endocrinol. *20*: 631–46.

Vivacqua, A., Lappano, R., Marco, P. De, Sisci, D., Aquila, S., Amicis, F. De, et al. (2009). G protein-coupled receptor 30 expression is up-regulated by EGF and TGF alpha in estrogen receptor alpha-positive cancer cells. Mol. Endocrinol. *23*: 1815–26.

Vogel, R., Mahalingam, M., Lüdeke, S., Huber, T., Siebert, F., and Sakmar, T.P. (2008). Functional role of the "ionic lock"--an interhelical hydrogen-bond network in family A heptahelical receptors. J. Mol. Biol. *380*: 648–55.

Wakeling, A.E., Dukes, M., and Bowler, J. (1991). A potent specific pure antiestrogen with clinical potential. Cancer Res. *51*: 3867–73.

Wallace, M., Luine, V., Arellanos, a, and Frankfurt, M. (2006). Ovariectomized rats show decreased recognition memory and spine density in the hippocampus and prefrontal cortex. Brain Res. *1126*: 176–82.

Wang, C., Dehghani, B., Magrisso, I.J., Rick, E. a, Bonhomme, E., Cody, D.B., et al. (2008). GPR30 contributes to estrogen-induced thymic atrophy. Mol. Endocrinol. *22*: 636–48.

Wang, H., Meyer, K., and Korz, V. (2013). Stress induced hippocampal mineralocorticoid and estrogen receptor β gene expression and long-term potentiation in male adult rats is sensitive to early-life stress experience. Psychoneuroendocrinology *38*: 250–62.

Wang, Z., Zhang, X., Shen, P., Loggie, B.W., Chang, Y., and Deuel, T.F. (2005). Identification, cloning, and expression of human estrogen receptor-alpha36, a novel variant of human estrogen receptor-alpha66. Biochem. Biophys. Res. Commun. *336*: 1023–7.

Wang, Z., Zhang, X., Shen, P., Loggie, B.W., Chang, Y., and Deuel, T.F. (2006). A variant of estrogen receptor-{alpha}, hER-{alpha}36: transduction of estrogen- and antiestrogen-dependent membrane-initiated mitogenic signaling. Proc. Natl. Acad. Sci. U. S. A. *103*: 9063–8.

Wasling, P., Hanse, E., and Gustafsson, B. (2004). Developmental changes in release properties of the CA3-CA1 glutamate synapse in rat hippocampus. J. Neurophysiol. *92*: 2714–24.

Wehrenberg, U., Prange-Kiel, J., and Rune, G.M. (2001). Steroidogenic factor-1 expression in marmoset and rat hippocampus: co-localization with StAR and aromatase. J. Neurochem. *76*: 1879–86.

Wei, W., Nguyen, L.N., Kessels, H.W., Hagiwara, H., Sisodia, S., and Malinow, R. (2010). Amyloid beta from axons and dendrites reduces local spine number and plasticity. Nat. Neurosci. *13*: 190–6.

Weiland, N.G., Orikasa, C., Hayashi, S., and McEwen, B.S. (1997). Distribution and hormone regulation of estrogen receptor immunoreactive cells in the hippocampus of male and female rats. J. Comp. Neurol. *388*: 603–12.

Welshons, W. V, Wolf, M.F., Murphy, C.S., and Jordan, V.C. (1988). Estrogenic activity of phenol red. Mol. Cell. Endocrinol. *57*: 169–78.

Wheatley, M., Wootten, D., Conner, M.T., Simms, J., Kendrick, R., Logan, R.T., et al. (2012). Lifting the lid on GPCRs: the role of extracellular loops. Br. J. Pharmacol. *165*: 1688–703.

White, R., Lees, J.A., Needham, M., Ham, J., and Parker, M. (1987). Structural organization and expression of the mouse estrogen receptor. Mol. Endocrinol. Balt. Md *1*: 735–744.

Williams, T.J., Akama, K.T., Knudsen, M.G., McEwen, B.S., and Milner, T.A. (2011). Ovarian hormones influence corticotropin releasing factor receptor colocalization with delta opioid receptors in CA1 pyramidal cell dendrites. Exp. Neurol. *230*: 186–196.

Wilson, M.E., Westberry, J.M., and Trout, A.L. (2011). Estrogen receptor-alpha gene expression in the cortex: sex differences during development and in adulthood. Horm. Behav. *59*: 353–7.

Wong, M., and Moss, R.L. (1992). Long-term and short-term electrophysiological effects of estrogen on the synaptic properties of hippocampal CA1 neurons. J. Neurosci. *12*: 3217–25.

Woolley, C.S. (2007). Acute effects of estrogen on neuronal physiology. Annu. Rev. Pharmacol. Toxicol. *47*: 657–80.

Woolley, C.S., and McEwen, B.S. (1992). Estradiol mediates fluctuation in hippocampal synapse density during the estrous cycle in the adult rat. J. Neurosci. *12*: 2549–54.

Woolley, C.S., and McEwen, B.S. (1994). Estradiol regulates hippocampal dendritic spine density via an N-methyl-D-aspartate receptor-dependent mechanism. J. Neurosci. *14*: 7680–7.

Woolley, C.S., Weiland, N.G., McEwen, B.S., and Schwartzkroin, P. a (1997). Estradiol increases the sensitivity of hippocampal CA1 pyramidal cells to NMDA receptor-mediated synaptic input: correlation with dendritic spine density. J. Neurosci. *17*: 1848–59.

Wu, L.G., and Saggau, P. (1994). Adenosine inhibits evoked synaptic transmission primarily by reducing presynaptic calcium influx in area CA1 of hippocampus. Neuron *12*: 1139–48.

Wu, T.-W., Wang, J.M., Chen, S., and Brinton, R.D. (2005). 17Beta-estradiol induced Ca2+ influx via L-type calcium channels activates the Src/ERK/cyclic-AMP response element binding protein signal pathway and BCL-2 expression in rat hippocampal neurons: a potential initiation mechanism for estrogen-induced neurop. Neuroscience *135*: 59–72.

Xu, H., Qin, S., Carrasco, G. a, Dai, Y., Filardo, E.J., Prossnitz, E.R., et al. (2009). Extra-nuclear estrogen receptor GPR30 regulates serotonin function in rat hypothalamus. Neuroscience *158*: 1599–607.

Zadran, S., Qin, Q., Bi, X., Zadran, H., Kim, Y., Foy, M.R., et al. (2009). 17-Beta-estradiol increases neuronal excitability through MAP kinase-induced calpain activation. Proc. Natl. Acad. Sci. U. S. A. *106*: 21936–41.

Zamani, M.R., Desmond, N.L., Levy, W.B., Reza, M., and Es-, W.B.L. (2000). Estradiol modulates long-term synaptic depression in female rat hippocampus. J. Neurophysiol. *84*: 1800–8.

Zárate, S., Jaita, G., Ferraris, J., Eijo, G., Magri, M.L., Pisera, D., et al. (2012). Estrogens induce expression of membrane-associated estrogen receptor α isoforms in lactotropes. PLoS One *7*: e41299.

Zavitsanou, K., Wang, H., Dalton, V.S., and Nguyen, V. (2010). Cannabinoid administration increases 5HT1A receptor binding and mRNA expression in the hippocampus of adult but not adolescent rats. Neuroscience *169*: 315–324.

Zerangue, N., Schwappach, B., Jan, Y.N., and Jan, L.Y. (1999). A new ER trafficking signal regulates the subunit stoichiometry of plasma membrane K(ATP) channels. Neuron *22*: 537–48.

Zhang, B., Subramanian, S., Dziennis, S., Jia, J., Uchida, M., Akiyoshi, K., et al. (2010). Estradiol and G1 reduce infarct size and improve immunosuppression after experimental stroke. J. Immunol. *184*: 4087–94.

Zhao, L., Chen, S., Ming Wang, J., and Brinton, R.D. (2005). 17beta-estradiol induces Ca2+ influx, dendritic and nuclear Ca2+ rise and subsequent cyclic AMP response element-binding protein activation in hippocampal neurons: a potential initiation mechanism for estrogen neurotrophism. Neuroscience *132*: 299–311.

Zhao, L., O'Neill, K., and Brinton, R.D. (2006). Estrogenic agonist activity of ICI 182,780 (Faslodex) in hippocampal neurons: implications for basic science understanding of estrogen

signaling and development of estrogen modulators with a dual therapeutic profile. J. Pharmacol. Exp. Ther. *319*: 1124–32.

Zhu, B.T., and Conney, a H. (1998). Functional role of estrogen metabolism in target cells: review and perspectives. Carcinogenesis *19*: 1–27.

Zhu, J.J., Qin, Y., Zhao, M., Aelst, L. Van, and Malinow, R. (2002). Ras and Rap control AMPA receptor trafficking during synaptic plasticity. Cell *110*: 443–55.

Zou, Y., Ding, L., Coleman, M., and Wang, Z. (2009). Estrogen receptor-alpha (ER-alpha) suppresses expression of its variant ER-alpha 36. FEBS Lett. *583*: 1368–74.

Zurkovsky, L., Brown, S.L., and Korol, D.L. (2006). Estrogen modulates place learning through estrogen receptors in the hippocampus. Neurobiol. Learn. Mem. *86*: 336–43.